

# **Development of and Mechanistic Insights into Palladium-Catalyzed C–H Arylation Reactions**

by

**Nicholas R. Deprez**

A dissertation submitted in partial fulfillment  
of the requirements for the degree of  
Doctor of Philosophy  
(Chemistry)  
in The University of Michigan  
2010

Doctoral Committee:

Associate Professor Melanie S. Sanford, Chair  
Professor Adam J. Matzger  
Professor David H. Sherman  
Associate Professor John. P. Wolfe

© Nicholas R. Deprez

---

2010

To Mom and Dad

## Acknowledgements

I owe an immense amount of gratitude to many people that helped make graduate school a fantastic experience. Through my time in graduate school I learned that the science you do is very important, but the people around you is what can make it really great.

Melanie, I feel I am very fortunate to have had the opportunity to work in your lab. Your enthusiasm toward chemistry is contagious and inspiring. You are always encouraging, and always see the positive in every result. You have taught me an enormous amount about how to approach problems and think about chemistry. You are a tremendous mentor, and thank you for helping make graduate school the experience that I hoped it would be.

I would like to thank my committee members Drs. Wolfe, Matzger and Sherman. First, Dr. Wolfe, it was a pleasure to have group meetings with your lab for a number of years. Second, Dr. Matzger, I am very glad I had the opportunity to work in your lab for a rotation. I would like to thank each of you for always being helpful whenever I had a question, your insight and perspective is always helpful. Dr. Sherman, I would like to thank you for serving on my committee.

I must thank the department support staff for all of the help they have provided. Drs. Eugenio Alvarado and Chris Kojiro, you have been very helpful and patient in helping me with NMR experiments. Jim Windak, thank you for help with mass spectrometry, even when I wanted to try experiments that you were skeptical of.

I would like to thank Drs. Lopa Desai, Kami Hull, and Dipa Kalyani, who are all wonderful labmates and became the closest thing to sisters I have ever had. Lopa, your enthusiasm and go get 'em attitude toward everything you do is fantastic. Kami, in lab you always had thoughtful suggestions, and interesting ideas to try, and are the best coffee buddy. Dipa, your work ethic and determination are unlike anyone I have ever



met. You are all great friends and mentors, and I feel very fortunate to have had the opportunity to work with all of you.

There are many other Sanford lab members that I came into contact in my time who have all been extremely helpful. Kara, you have always been willing to go out of your way to help me, whether it was to help proof read or to discuss kinetics. Tom, thank you for never providing a dull moment. Sharon, It was a pleasure to work next to you for a number of years. Andrew, you are definitely not a voice of reason. Eric Kalberer, I very much appreciate you showing me the ropes when I began graduate school. Leilani, I had a blast working with you, you are so encouraging and positive. Nick, I have always appreciated the great chemistry conversations we always had. I also appreciate the random, hysterical comments you often make.

There are also numerous people outside of my lab that have been instrumental in helping me through graduate school. Jon, you have been a great friend and roommate. I appreciate that we can have conversations about chemistry and learn from each other. Amy, you have been an incredibly supportive friend through all of the trials and tribulations I have had in grad school. I know I can always count on you. Natalie, I can't thank you enough for your unconditional support, patience, and encouragement you have given me.

Last but certainly not least, I thank my Mom and Dad. In everything I have ever done, you have always been encouraging and supportive. You always told me to set my goals high and never back down. Mom, you are my rock. Through thick and thin I know that you will always be there for me no matter what. Dad, you were always incredibly supportive, and I know you would be just as supportive of me now. I miss you. I am so grateful I have both of you as parents.

# Table of Contents

Dedication .....	ii
Acknowledgements .....	iii
List of Tables .....	viii
List of Schemes .....	x
List of Figures .....	xv
Abstract .....	xviii
<b>Chapter 1</b>	
Introduction.....	1
1.1 References .....	10
<b>Chapter 2</b>	
Scope and Development of Palladium-Catalyzed C–H Arylation.....	13
3.1 Background and Significance.....	13
2.2 Phenylation Development.....	16
2.3 Arylation Development.....	20
2.4 Alternative I <sup>III</sup> Reagents.....	28
2.5 In situ Oxidant Generation.....	29
2.6 Subsequent Examples of C–H Arylation Methodology .....	38
2.7 Conclusions .....	41
2.8 General Procedures and Materials and Methods.....	41
2.9 References.....	77

### Chapter 3

#### Mechanistic Investigations of Ligand Directed C–H Activation/Arylation Reactions...81

3.1 Background and Significance .....	81
3.2 Preliminary Mechanistic Experiments.....	83
3.3 Kinetic Orders .....	85
3.4 Catalyst Resting State .....	92
3.5 Oxidant Resting State .....	95
3.6 Hammett Studies .....	99
3.7 Oxidant Counterion Effect.....	102
3.8 Kinetic Isotope Effect Studies.....	104
3.9 Summary of the Mechanistic Data .....	105
3.10 Mechanistic Implications .....	108
3.11 Investigations Towards New Catalysts.....	111
3.13 Preliminary Investigations of the Generality of the Mechanism.....	113
3.13 Conclusions .....	122
3.14 General Procedures and Materials and Methods.....	122
3.15 References .....	142

### Chapter 4

#### Development of Direct C–H Arylation Reactions of Heterocycles and Simple

Arenes .....	145
4.1 Background and Significance .....	145
4.2 Our Development of Indole Phenylation .....	147
4.3 Scope of Indole Phenylation .....	149
4.4 Scope of Indole Arylation.....	152
4.5 In Situ Oxidant Generation for Pd-Catalyzed Indole Arylation.....	154
4.6 Expansion to Other Heterocycles .....	158
4.7 Expansion to Non-Heterocyclic Substrates.....	161
4.8 Synthesis of the IMePd(OAc) <sub>2</sub> •H <sub>2</sub> O Ligand .....	168

4.9 Subsequent Examples of Direct C–H Arylation .....	173
4.10 Conclusions .....	175
4.11 General Procedures and Materials and Methods .....	175
4.12 References .....	193

## Chapter 5

Initial Mechanistic Investigations of Palladium-Catalyzed C–H Arylation of Indole .	196
---	-----

5.1 Background and Significance.....	196
5.2 Development of Collection Method .....	197
5.3 Mechanistic Investigations with Pd(OAc) <sub>2</sub> .....	202
5.4 Mechanistic Investigations with IMesPd(OAc) <sub>2</sub> •H <sub>2</sub> O.....	207
5.5 Comparison of Pd(OAc) <sub>2</sub> and IMesPd(OAc) <sub>2</sub> •H <sub>2</sub> O .....	208
5.6 Possible Mechanisms for Indole Arylation.....	210
5.7 Conclusions .....	215
5.8 General Procedures and Materials and Methods.....	215
5.9 References .....	219

## List of Tables

### Chapter 2

#### Scope and Development of Palladium-Catalyzed C–H Activation/Arylation

<b>Table 2.1:</b> Substrate Scope of C–H Phenylation Reactions .....	18
<b>Table 2.2:</b> Synthesis of Electron Neutral and Poor Arene Oxidants .....	22
<b>Table 2.3:</b> Synthesis of [Ph–I <sup>III</sup> –( <i>p</i> -MeOC <sub>6</sub> H <sub>4</sub> )]BF <sub>4</sub> .....	22
<b>Table 2.4:</b> Scope of Arylation with [Mes–I <sup>III</sup> –Ar]BF <sub>4</sub> Oxidants.....	25
<b>Table 2.5:</b> Arylation of <b>72</b> with [Mes–I <sup>III</sup> –Ar]BF <sub>4</sub> Oxidants .....	26
<b>Table 2.6:</b> Arylation of Pyrrolidinone Substrates with [Ar–I <sup>III</sup> –Ar]BF <sub>4</sub> .....	28

### Chapter 3

#### Mechanistic Investigations of Ligand Directed C–H Activation/Arylation Reactions

<b>Table 3.1:</b> [Ph–I <sup>III</sup> –Ph]X Oxidants.....	103
<b>Table 3.2:</b> Initial Reaction Rates for Each [3] Conducted at 80 °C.....	128
<b>Table 3.3:</b> Initial Reaction Rates for Each [3] Conducted at 110 °C.....	129
<b>Table 3.4:</b> Initial Reaction Rates for Each [6] Conducted at 110 °C.....	130
<b>Table 3.5:</b> Initial Reaction Rates for each [Pd] with Pd(OAc) <sub>2</sub> and <b>35</b> at 100 °C.....	131
<b>Table 3.6:</b> Reaction Rate for Oxidants used in the Hammett Studies .....	132
<b>Table 3.7:</b> Reaction Rate for Substrates Used in the Hammett Studies.....	133
<b>Table 3.8:</b> <sup>1</sup> H NMR chemical shift data for Job plot at 110 °C.....	134
<b>Table 3.9:</b> <sup>1</sup> H NMR chemical shift data for Job plot at 80 °C.....	135
<b>Table 3.10:</b> <sup>1</sup> H NMR Chemical Shift Data for Equilibrium Determination at 110 °C.	136
<b>Table 3.11:</b> <sup>1</sup> H NMR Chemical Shift Data for Equilibrium Determination at 110 °C.	136

## Chapter 4

### Development of Direct C–H Arylation Reactions of Heterocycles and Simple Arenes

<b>Table 4.1:</b> Catalyst Screening for Pd-Catalyzed Phenylation of Indole.....	149
<b>Table 4.2:</b> Scope of Pd-Catalyzed Phenylation of Indoles .....	150
<b>Table 4.3:</b> Scope of Pd–Catalyzed Indole Arylation.....	153
<b>Table 4.4:</b> Screen of I <sup>III</sup> Regents for <i>in situ</i> Oxidant Generation Employing Heteroarenes .....	156
<b>Table 4.5:</b> Screen of Temperature for <i>in situ</i> Oxidant Employing Heteroarenes.....	157
<b>Table 4.6:</b> Solvent Effects on the Arylation of Benzofuran .....	158
<b>Table 4.7:</b> Catalyst Effects on the Arylation of Benzofuran.....	159
<b>Table 4.8:</b> Solvent Effects for the Pd-Catalyzed Arylation of Benzothiophene .....	160
<b>Table 4.9:</b> Substrates Unsuccessful in Pd-Catalyzed C–H Phenylation.....	161
<b>Table 4.10:</b> Naphthalene Phenylation Equivalents Study.....	163
<b>Table 4.11:</b> Catalyst Screen for Naphthalene Phenylation .....	164
<b>Table 4.12:</b> Solvent Screen for Naphthalene Phenylation .....	165
<b>Table 4.13:</b> Catalyst Loading Study for Naphthalene Phenylation.....	166
<b>Table 4.14:</b> Catalyst Loading Study for Naphthalene Phenylation.....	167
<b>Table 4.15:</b> Phenylation of <i>p</i> -Xylene.....	168

## Chapter 5

### Initial Mechanistic Investigations of Palladium-Catalyzed C–H Arylation of Indole

<b>Table 5.1:</b> Kinetic Order in Pd(OAc) <sub>2</sub> .....	203
<b>Table 5.2:</b> Order in Substrate <b>4</b> with Pd(OAc) <sub>2</sub> .....	205
<b>Table 5.3:</b> Order in Oxidant with IMesPd(OAc) <sub>2</sub> •H <sub>2</sub> O .....	207
<b>Table 5.4:</b> Rate Data for [Pd] Order Study with Pd(OAc) <sub>2</sub> .....	216
<b>Table 5.5:</b> Rate Data for Substrate Order Study with Pd(OAc) <sub>2</sub> .....	217
<b>Table 5.6:</b> Rate Data for Oxidant Order Study with IMesPd(OAc) <sub>2</sub> •H <sub>2</sub> O.....	218

## List of Schemes

### Chapter 1

#### Introduction

<b>Scheme 1.1:</b> Palladium Catalyzed Cross Coupling Chemistry .....	1
<b>Scheme 1.2:</b> C–H Activation Approach to Biaryl Formation. ....	2
<b>Scheme 1.3:</b> Miura’s Directed Phenylation of Phenols .....	2
<b>Scheme 1.4:</b> Fagnou’s Intramolecular Direct Arylation .....	3
<b>Scheme 1.5:</b> Ligand Directed C–H Acetoxylation .....	4
<b>Scheme 1.6:</b> Mechanistic Pathways for C–H activation/Functionalization .....	4
<b>Scheme 1.7:</b> Stoichiometric oxidation of a palladacycle by [Ph–I <sup>III</sup> –Ph]OTf.....	5
<b>Scheme 1.8:</b> Palladium Catalyzed C–H Arylation Reactions .....	6
<b>Scheme 1.9:</b> Pd <sup>II/0</sup> Arylation of Thiazole .....	7
<b>Scheme 1.10:</b> Pd <sup>II/0</sup> Arylation of Indolizine .....	7
<b>Scheme 1.11:</b> Sames’ Precedent for Pd-Catalyzed Direct Arylation of Indole.....	7
<b>Scheme 1.12:</b> Proposed Mechanism of Sames’ Pd-Catalyzed Indole Arylation .....	8
<b>Scheme 1.13:</b> Proposed Mechanism of Pd-Catalyzed Arylation with [Ph–I <sup>III</sup> –Ph]BF <sub>4</sub> .....	8
<b>Scheme 1.14:</b> Site Selective Arylation of Indoles .....	9
<b>Scheme 1.15:</b> Induction Period Suggests the Formation of an ‘Active Intermediate’.....	9

### Chapter 2

#### Scope and Development of Palladium-Catalyzed C–H Activation/Arylation

<b>Scheme 2.1:</b> Ligand Directed C–H Activation/C–O Bond Formation .....	13
--	----

<b>Scheme 2.2:</b> Mechanistic Pathways for C–H Activation/Functionalization .....	14
<b>Scheme 2.3:</b> Stoichiometric Oxidation of a Palladacycle by [Ph–I <sup>III</sup> –Ph]OTf.....	15
<b>Scheme 2.4:</b> Proposed Catalytic Cycle for C–H Arylation .....	15
<b>Scheme 2.5:</b> C–H Phenylation of 3-Methyl-2-Phenylpyridine .....	16
<b>Scheme 2.6:</b> Observed Selectivity of Phenylation for 2-Phenylquinoline.....	19
<b>Scheme 2.7:</b> Trace Products Observed from C–H Arylation of <b>32</b> .....	20
<b>Scheme 2.8:</b> Synthesis of [( <i>p</i> -CF <sub>3</sub> C <sub>6</sub> H <sub>4</sub> ) <sub>2</sub> I <sup>III</sup> ] <sub>2</sub> BF <sub>4</sub> .....	23
<b>Scheme 2.9:</b> Mixtures of Products Obtained Using [Ph–I <sup>III</sup> –Ar]BF <sub>4</sub> Oxidants.....	24
<b>Scheme 2.10:</b> Selective Arylation with [Mes–I <sup>III</sup> –( <i>p</i> -MeOC <sub>6</sub> H <sub>4</sub> )]BF <sub>4</sub> .....	24
<b>Scheme 2.11:</b> Selectivity of Arylation of <b>72</b> with [Mes–I <sup>III</sup> –( <i>p</i> -MeOPh)]BF <sub>4</sub> .....	26
<b>Scheme 2.12:</b> Pd-Catalyzed Reaction of <b>11</b> with [Mes–I–(2-thiophene)]BF <sub>4</sub> ( <b>81</b> ) .....	27
<b>Scheme 2.13:</b> Product Yields with <b>83</b> and [Mes–I–( <i>p</i> -XC <sub>6</sub> H <sub>4</sub> )]BF <sub>4</sub> oxidants	
[Ph–I <sup>III</sup> –Ph]BF <sub>4</sub> .....	27
<b>Scheme 2.14:</b> Stoichiometric Oxidation using a Vinyl–I <sup>III</sup> Oxidant.....	28
<b>Scheme 2.15:</b> General Scheme <i>in situ</i> Oxidant Generation .....	31
<b>Scheme 2.16:</b> Phenylation of 3-Methyl-2-Phenylpyridine by <i>in situ</i> Oxidant	
Generation.....	30
<b>Scheme 2.17:</b> Heteroarylation of 3-Methyl-2-Phenylpyridine by <i>in situ</i> Oxidant	
Generation.....	31
<b>Scheme 2.18:</b> Optimizations for <i>in situ</i> C–H Activation/Heteroarylation .....	32
<b>Scheme 2.19:</b> Generation of [Mes–I <sup>III</sup> –(2-thiophene)] <sup>+</sup> <i>in situ</i> .....	32
<b>Scheme 2.20:</b> <i>in situ</i> C–H Arylation with 3-Thiopheneboronic Acid .....	33
<b>Scheme 2.21:</b> <i>in situ</i> C–H Arylation with 2-Furylboronic Acid.....	34
<b>Scheme 2.22:</b> <i>in situ</i> C–H Arylation with 3-Furylboronic Acid.....	34
<b>Scheme 2.23:</b> Control of Oxidant Counterion by the Addition of Additives.....	35
<b>Scheme 2.24:</b> Control of Oxidant Counterion by Variation of I <sup>III</sup> Ligands .....	35
<b>Scheme 2.25:</b> Variation of ArI <sup>III</sup> (OAc) <sub>2</sub> for <i>in situ</i> Oxidant Generation .....	36
<b>Scheme 2.26:</b> Coupling Aryltrimethylsilanes with PhI <sup>III</sup> (OAc) <sub>2</sub> .....	36
<b>Scheme 2.27:</b> Coupling of PhSiMe <sub>3</sub> with PhI <sup>III</sup> (OAc) <sub>2</sub> .....	37
<b>Scheme 2.28:</b> <i>In situ</i> Oxidant Generation with PhSiMe <sub>3</sub> and PhI <sup>III</sup> (OAc) <sub>2</sub> .....	37
<b>Scheme 2.29:</b> <i>Meta</i> C–H Arylation Using a Copper Catalyst.....	38



<b>Scheme 2.30:</b> C–H Arylation Employing Ar–I and Stoichiometric AgOAc .....	39
<b>Scheme 2.31:</b> General Mechanism of Miura’s C–H Arylation .....	39
<b>Scheme 2.32:</b> General Mechanism of C–H Arylation using a Transmetallating Reagent .....	40
<b>Scheme 2.33:</b> C–H Arylation through Oxidative Coupling .....	40

### Chapter 3

#### Mechanistic Investigations of Ligand Directed C–H Activation/Arylation Reactions

<b>Scheme 3.1:</b> Initially Proposed Catalytic Cycle for C–H Arylation.....	82
<b>Scheme 3.2:</b> Replacement of [Ph–I <sup>III</sup> –Ph]BF <sub>4</sub> with Ph–I and Ph–OTf.....	84
<b>Scheme 3.3:</b> Addition of Hg <sup>0</sup> to the Standard C–H Arylation Reaction.....	84
<b>Scheme 3.4:</b> Stoichiometric Reaction of <b>5</b> with [Ph <sub>2</sub> I <sup>III</sup> ]BF <sub>4</sub> .....	85
<b>Scheme 3.5:</b> Replacement of Pd(OAc) <sub>2</sub> with <b>5</b> .....	85
<b>Scheme 3.6:</b> Rybov’s Example of the Monomer Dimer Equilibrium .....	94
<b>Scheme 3.7:</b> Observation of the <b>9</b> Under the Reaction Conditions.....	94
<b>Scheme 3.8:</b> Equilibrium Between the I <sup>III</sup> Reagent and Pyridine.....	95
<b>Scheme 3.9:</b> Equilibrium Between [Mes–I <sup>III</sup> –Ph]BF <sub>4</sub> <b>6</b> and <b>3</b> .....	96
<b>Scheme 3.10:</b> Synthesis of [Ph–I <sup>III</sup> –Ph]X Oxidants.....	103
<b>Scheme 3.11:</b> Study of Counterion Effects on the Reaction Rate .....	104
<b>Scheme 3.12:</b> Intramolecular Kinetic Isotope Effect Study of <b>22</b> .....	105
<b>Scheme 3.13:</b> Intermolecular Kinetic Isotope Effect Study of <b>3</b> .....	105
<b>Scheme 3.14:</b> Intermolecular Kinetic Isotope Effect Study of <b>23</b> .....	105
<b>Scheme 3.15:</b> The Final Proposed Mechanism of C–H Activation/Arylation.....	106
<b>Scheme 3.16:</b> Synthesis of the esp Tethered Complex <b>35</b> .....	111
<b>Scheme 3.17:</b> Alternative C–H Activation/Arylation Mechanism.....	117

### Chapter 4

#### Development of Direct C–H Arylation Reactions of Heterocycles and Simple Arenes

<b>Scheme 4.1:</b> Sames' Precedent for C–H Arylation of Indole.....	146
<b>Scheme 4.2:</b> Proposed Mechanism of Sames' Indole Arylation.....	146
<b>Scheme 4.3:</b> Proposed Mechanism of Indole Arylation with [Ph–I <sup>III</sup> –Ph]BF <sub>4</sub> .....	147
<b>Scheme 4.4:</b> Pd(OAc) <sub>2</sub> –Catalyzed Phenylation of <i>N</i> -Methylindole.....	148
<b>Scheme 4.5:</b> Pd-Catalyzed Phenylation of Pyrroles.....	151
<b>Scheme 4.6:</b> Comparison of I <sup>III</sup> Oxidants for Pd-Catalyzed Indole Phenylation.....	152
<b>Scheme 4.7:</b> C2/C3 Selectivity for Installation of <i>o</i> -Tolyl Group Using Pd <sup>0/II</sup> Catalysis.....	154
<b>Scheme 4.8:</b> Strategy for <i>in situ</i> Oxidant Generation/C–H Arylation.....	154
<b>Scheme 4.9:</b> <i>In situ</i> Oxidant Generation/C–H Arylation with Substituted Arenes.....	155
<b>Scheme 4.10:</b> <i>In situ</i> Oxidant Employing Heteroarenes.....	155
<b>Scheme 4.11:</b> <i>in situ</i> Arylation with 3-Thiophene Boronic Acid.....	157
<b>Scheme 4.12:</b> Pd-Catalyzed Arylation of Benzofuran.....	159
<b>Scheme 4.13:</b> Pd-Catalyzed Arylation of Benzothiophene.....	160
<b>Scheme 4.14:</b> Crabtree's Acetoxylation of Naphthalene.....	162
<b>Scheme 4.15:</b> Synthesis of IMesPd(OAc)•H <sub>2</sub> O.....	169
<b>Scheme 4.16:</b> Reported Synthesis of IMesPd(OAc) <sub>2</sub> .....	170
<b>Scheme 4.17:</b> Synthesis of IMes <sub>2</sub> Pd(OAc) <sub>2</sub> .....	172
<b>Scheme 4.18:</b> Utilization of the Products from Synthesis of <b>50</b> for Indole Arylation.....	172
<b>Scheme 4.19:</b> Utilization of IMes <sub>2</sub> Pd(OAc) <sub>2</sub> in Catalysis.....	172
<b>Scheme 4.20:</b> C3 Indole Arylation with a Cu Catalyst and [Ar–I <sup>III</sup> –Ar]OTf.....	173
<b>Scheme 4.21:</b> C2 Indole Arylation with a Cu Catalyst and [Ar–I <sup>III</sup> –Ar]OTf.....	173
<b>Scheme 4.22:</b> C3 Indole Arylation Through Oxidative Coupling.....	174
<b>Scheme 4.23:</b> C2 Indole Arylation Through Oxidative Coupling.....	174
<b>Scheme 4.24:</b> C2 Indole Arylation Using Ag <sup>+</sup> and Ar–I.....	175

## Chapter 5

### Initial Mechanistic Investigations of Palladium-Catalyzed C–H Arylation of Indole

<b>Scheme 5.1:</b> Proposed Mechanism of Non-Directed Arylation with [Ph–I <sup>III</sup> –Ph]BF <sub>4</sub> .....	197
<b>Scheme 5.2:</b> Strategy for Eliminating the Induction Period Using a Sacrificial.....	

Substrate .....	201
<b>Scheme 5.3:</b> Proposed Palladation Mechanism for a Pd <sup>0/II</sup> C–H Arylation.....	211
<b>Scheme 5.4:</b> Proposed Palladation Mechanism for a Pd <sup>II/IV</sup> C–H Arylation.....	212
<b>Scheme 5.5:</b> Pd <sup>II/IV</sup> Direct C2 Metallation Mechanism for Arylation. ....	213
<b>Scheme 5.6:</b> Pd <sup>II/IV</sup> Olefin Insertion Mechanism for Arylation .....	213
<b>Scheme 5.7:</b> Pd <sup>0/II</sup> Direct C2 Metallation Mechanism for Arylation.....	214
<b>Scheme 5.8:</b> Pd <sup>0/II</sup> Olefin Insertion Mechanism for Arylation.....	214

## List of Figures

### Chapter 1

#### Introduction

**Figure 1.1:** High Oxidation Palladium Dimer Intermediate .....6

### Chapter 2

#### Scope and Development of Palladium-Catalyzed C–H Activation/Arylation

**Figure 2.1:** Problematic Substrates for C–H Arylation .....20

**Figure 2.2:** Alternative I<sup>III</sup> Oxidants Attempted for C–H Arylation.....29

### Chapter 3

#### Mechanistic Investigations of Ligand Directed C–H Activation/Arylation Reactions

**Figure 3.1:** Kinetic Order in Substrate at 80 °C .....86

**Figure 3.2:** Plot of Initial Rate ( $\Delta[4]/\Delta t$ ) versus  $[3]^{-3}$  in Regime II.....87

**Figure 3.3:** Data Fit of Initial Rate ( $\Delta[4]/\Delta t$ ) versus  $[4]$  in Regime II.....87

**Figure 3.4:** Plot of Initial Rate ( $\Delta[4]/\Delta t$ ) versus  $[3]$  .....88

**Figure 3.5:** Plot of Initial Rate ( $\Delta[4]/\Delta t$ ) versus  $[3]^{-3}$  .....89

**Figure 3.6:** Data Fit of Initial Rate ( $\Delta[4]/\Delta t$ ) versus  $[3]$ .....89

**Figure 3.7:** Initial Rate ( $\Delta[4]/\Delta t$ ) versus  $[I^{III}]$ .....90

**Figure 3.8:** Data Fit of Initial Rate ( $\Delta[4]/\Delta t$ ) versus  $[I^{III}]$ .....90

**Figure 3.9:** Plot of Initial Rate ( $\Delta[4]/\Delta t$ ) versus  $[Pd]$  .....91

**Figure 3.10:** Plot of Initial Rate ( $\Delta[4]/\Delta t$ ) versus  $[Pd]^2$  .....92

**Figure 3.11:** Data Fit of Initial Rate ( $\Delta[4]/\Delta t$ ) versus  $[Pd]$ .....92

<b>Figure 3.13:</b> $^1\text{H}$ NMR Experiments to Observe the Catalyst Resting State .....	93
<b>Figure 3.14:</b> Job Plot of $\Delta\delta\cdot\chi$ versus $\chi$ at 110 °C.....	96
<b>Figure 3.15:</b> Job Plot of $\Delta\delta\cdot\chi$ versus $\chi$ at 80 °C.....	97
<b>Figure 3.16:</b> $\delta_{\text{H}(4)}$ as a Function of $[\text{I}^{\text{III}}]$ at 110 °C .....	98
<b>Figure 3.17:</b> $\delta_{\text{H}(4)}$ as a Function of $[\text{I}^{\text{III}}]$ at 80 °C .....	98
<b>Figure 3.18:</b> Competition Study with $[\text{Mes-I}^{\text{III}}\text{-Ph}]\text{BF}_4$ and $[\text{Mes-I}^{\text{III}}\text{-Ar}]\text{BF}_4$ .....	99
<b>Figure 3.19:</b> Competition Study with $[\text{Ph-I}^{\text{III}}\text{-Ph}]\text{BF}_4$ and $[\text{Ar-I}^{\text{III}}\text{-Ar}]\text{BF}_4$ .....	100
<b>Figure 3.20:</b> Initial Rate Hammett Plot with $[\text{Mes-I}^{\text{III}}\text{-Ar}]\text{BF}_4$ Oxidants.....	101
<b>Figure 3.21:</b> Initial Rate Directing Group Hammett Study with $[\text{Mes-I}^{\text{III}}\text{-Ph}]\text{BF}_4$ .....	102
<b>Figure 3.22:</b> Structure of <b>5</b> , and the Two Limiting Structures of <b>25</b> .....	109
<b>Figure 3.23:</b> Examples of Palladium and Platinum $\text{M}^{\text{III}}\text{-M}^{\text{III}}$ Bonds .....	110
<b>Figure 3.24:</b> Oxidation of the Pt Complex X to the $\text{Pt}^{\text{III}}\text{-Pt}^{\text{III}}$ Dimer <b>31</b> .....	110
<b>Figure 3.25:</b> Initial Rate ( $\Delta[\mathbf{4}]/\Delta t$ ) versus $[\text{Pd}]$ for $\text{Pd}(\text{OAc})_2$ and Complex <b>35</b> .....	112
<b>Figure 3.26:</b> Plot of initial rate ( $\Delta[\mathbf{4}]/\Delta t$ ) versus $[\text{Pd}]^2$ using complex <b>35</b> as the catalyst.....	113
<b>Figure 3.27:</b> Data Fit of Initial Rate ( $\Delta[\mathbf{4}]/\Delta t$ ) versus $[\text{Pd}]$ for Complex <b>35</b> .....	113
<b>Figure 3.28:</b> Competition Study of <b>3</b> with Mesityl Oxidants in $\text{CHCl}_3$ .....	115
<b>Figure 3.29:</b> Competition Study of <b>36</b> with Mesityl Oxidants in $\text{CHCl}_3$ .....	115
<b>Figure 3.30:</b> Competition Study of <b>37</b> with Mesityl Oxidants in $\text{CHCl}_3$ .....	117
<b>Figure 3.31:</b> Competition Study of <b>38</b> with Mesityl Oxidants in $\text{CHCl}_3$ .....	118
<b>Figure 3.32:</b> Competition Study of <b>3</b> with Symmetric Oxidants in $\text{CHCl}_3$ .....	119
<b>Figure 3.33:</b> Competition Study of <b>36</b> with Symmetric Oxidants in $\text{CHCl}_3$ .....	120
<b>Figure 3.34:</b> Competition Study of <b>37</b> with Symmetric Oxidants in $\text{CHCl}_3$ .....	121
<b>Figure 3.35:</b> Competition Study of <b>38</b> with Symmetric Oxidants in $\text{CHCl}_3$ .....	121
<b>Figure 3.36:</b> A Representative Kinetic Plot .....	127

## Chapter 4

### Development of Direct C–H Arylation Reactions of Heterocycles and Simple Arenes

<b>Figure 4.1:</b> Indoles Unsuccessful for C–H Phenylation .....	151
<b>Figure 4.2:</b> $\text{Pd}(\text{OAc})_2$ Complexes Bearing IMes Ligands .....	169

<b>Figure 4.3:</b> $^1\text{H}$ NMR Spectra of the Product Obtained in the Synthesis of <b>50</b> and <b>51</b> in $\text{CDCl}_3$ .....	171
---	-----

## Chapter 5

### Initial Mechanistic Investigations of Palladium-Catalyzed C–H Arylation of Indole

<b>Figure 5.1:</b> $\text{IMesPd}(\text{OAc})_2 \cdot \text{H}_2\text{O}$ Catalyst .....	197
<b>Figure 5.2:</b> Arrayed $^{19}\text{F}$ NMR Spectra of Indole Arylation.....	199
<b>Figure 5.3:</b> Induction Period Based on Product Appearance.....	200
<b>Figure 5.4:</b> Induction Period Based on Starting Material Disappearance .....	200
<b>Figure 5.5:</b> Product Appearance After Eliminating the Induction Period .....	201
<b>Figure 5.6:</b> Starting Material Disappearance After Eliminating the Induction Period.....	202
<b>Figure 5.7:</b> Kinetic Order in $\text{Pd}(\text{OAc})_2$ Based on Product Appearance .....	203
<b>Figure 5.8:</b> Kinetic Order in $\text{Pd}(\text{OAc})_2$ Based on Starting Material Disappearance....	203
<b>Figure 5.9:</b> Order in <b>4</b> with $\text{Pd}(\text{OAc})_2$ based on Product Appearance .....	205
<b>Figure 5.10:</b> Order in <b>4</b> with $\text{Pd}(\text{OAc})_2$ based on Starting Material Disappearance ....	206
<b>Figure 5.11:</b> Oxidant Order with $\text{IMesPd}(\text{OAc})_2 \cdot \text{H}_2\text{O}$ based on Product Appearance .....	208
<b>Figure 5.12:</b> Oxidant order with $\text{Pd}(\text{OAc})_2$ based on Starting Material Disappearance.....	208
<b>Figure 5.13:</b> Example $^{19}\text{F}$ NMR Spectra of Indole Arylation Kinetics with $\text{IMesPd}(\text{OAc})_2 \cdot \text{H}_2\text{O}$ .....	209

## Abstract

Biaryls are important targets for numerous applications in organic synthesis. As a result, the development of metal-mediated aryl cross-coupling has been extensively studied. The disadvantage of this approach is the requirement for each coupling partner to be prefunctionalized. To address this challenge, our studies focused on the development of direct, site selective C–H arylation.

We developed a Pd<sup>II</sup>-catalyzed, ligand-directed C–H arylation reaction, that employs [Ar–I<sup>III</sup>–Ar]<sup>+</sup> reagents as terminal oxidants. High site-selectivity was achieved by employing substrates containing either oxygen or nitrogen-directing groups for functionalization of a specific C–H bond. This approach led to the installation of both electron rich and electron poor aryl groups. Additionally, excellent functional group tolerance was observed. Finally, investigations found that the generation of [Ar–I<sup>III</sup>–Ar]<sup>+</sup> *in situ* were feasible for subsequent C–H functionalization.

Mechanistic investigations of directed C–H arylation elucidated the catalytic cycle. This represents the first thorough investigation of a ligand-directed, palladium-catalyzed C–H arylation. These studies implicated a high-oxidation state dimeric palladium species as a catalytic intermediate. Furthermore, oxidation was found to be rate-limiting, unlike most C–H functionalization reactions.

We also extended this methodology to the C–H arylation of substrates lacking a directing group. We demonstrated that palladium catalysts and [Ar–I<sup>III</sup>–Ar]<sup>+</sup> oxidants afford site selective C2 arylation of indoles at room temperature, with excellent functional group tolerance. The installation of both electron rich and electron poor indoles, with electronically diverse of aryl groups was achieved. The viability of *in situ* oxidant generation, followed by indole arylation also was shown. Preliminary mechanistic investigations of indole arylation implicated the formation of an active catalyst prior to arylation.

This dissertation describes the development of site selective C–H arylation reactions using palladium catalysis. These transformations are general with respect to aryl group and substrate, and are complimentary to Pd<sup>0/II</sup> catalytic cycles. The functional group tolerance, broad substrate scope, and variety of installed aryl groups, make this methodology attractive for biaryl synthesis.

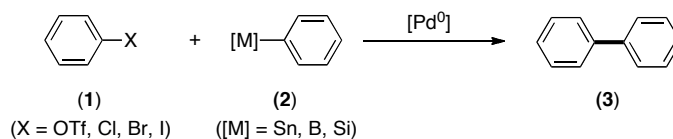


# Chapter 1

## Introduction

Biarayls are prevalent structures in many different natural products, pharmaceuticals, agrochemicals, and conjugated materials. This has led to significant interest in the development of new reactions to efficiently construct Ar–Ar bonds. The most extensively developed methodologies are palladium-catalyzed cross-coupling reactions, which include: Stille, Suzuki–Miyaura, Sonogashira, Hiyama, and Negishi couplings.<sup>1-9</sup> These methods generally involve a Pd<sup>0/II</sup> catalytic cycle and result in the coupling of an aryl halide **1** with an organometallic component **2** (X = Sn, B, Si, etc, **Scheme 1.1**). Such approaches suffer from two significant disadvantages. First, the requirement that each coupling partner be prefunctionalized prior to coupling can be problematic because sensitive functional groups must be maintained through several synthetic steps in lengthy synthesis. Second, the byproducts of these reactions are undesirable inorganic salts that must be removed and can be problematic for large-scale reactions.

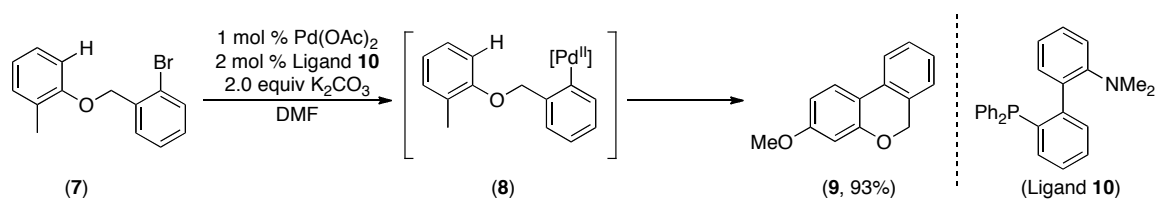
**Scheme 1.1:** Palladium Catalyzed Cross Coupling Chemistry.



A potential alternative to traditional metal-catalyzed cross-coupling chemistry, would be the employment of metal mediated C–H activation chemistry to ultimately afford functionalization. This approach addresses some of the challenges associated with



**Scheme 1.4:** Fagnou's Intramolecular Direct Arylation.<sup>35</sup>



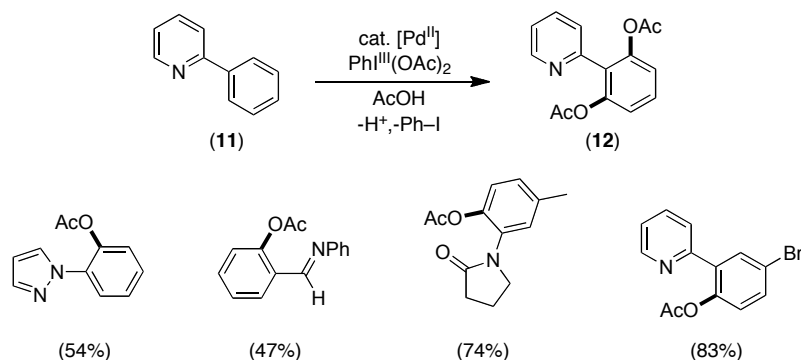
Importantly, a number of other transition metals are viable catalysts for directed C–H arylation reactions, including Ru, Rh, Ir, and Pt.<sup>19,22</sup> However palladium offers several advantages over these metals making it more attractive for further development.<sup>22</sup> First, palladacycles have been demonstrated to be compatible with oxidants. Second, palladacyclic intermediates can be selectively functionalized. Each of these points can be problematic with the previously mentioned metals due to stability or the unreactive nature of the respective metallacycles. Thirdly, a broad range of directing groups are known to facilitate cyclopalladation, including amides, pyridines, pyrazoles, isoxazolines and oximes. Finally, palladium is known to undergo cyclometallation with both  $sp^2$  and  $sp^3$  C–H bonds, providing the opportunity to afford several combinations of C–C bond formations.

The previously reported metal-mediated C–H functionalization methodologies demonstrated the viability of a C–H arylation transformation. However, to be more broadly applicable several additional challenges needed to be addressed. First, an increased scope of directing groups viable for C–H activation is necessary. Second, a more expansive functional group tolerance would make this methodology more appealing for general use. Specifically, it would be desirable if a transformation could be developed that was tolerant of aryl halides, which are often reactive with the low valent metals used for C–H arylation. Additionally, enolizable ketones can be problematic due to the often-necessary requirement for strong bases. Thus the development of a C–H arylation methodology to address these challenges would be of great interest.

Previously, our laboratory had used a palladium-catalyzed, ligand-directed approach to afford C–H acetoxylation products.<sup>36-40</sup> This was accomplished utilizing substrates such as **11** with Pd(OAc)<sub>2</sub> and the hypervalent iodide reagent PhI<sup>III</sup>(OAc)<sub>2</sub> as the terminal oxidant to afford product **12** (Scheme 1.5). This transformation was

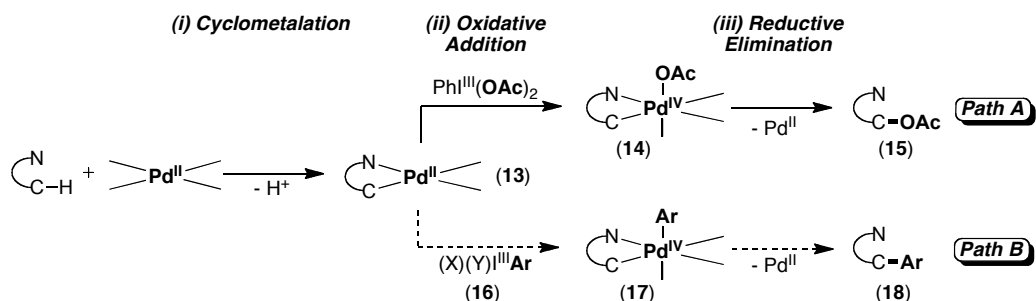
demonstrated to be general with respect to directing groups and functional group compatibility (**Scheme 1.5**).

**Scheme 1.5:** Ligand Directed C–H Acetoxylation.<sup>36-40</sup>



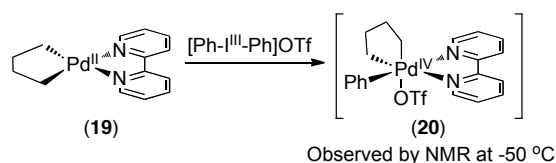
The mechanism for C–H acetoxylation is believed to proceed through (**Scheme 1.6**, Path A): (i) coordination of palladium followed by C–H activation, (ii) two electron oxidation of the Pd<sup>II</sup> intermediate **13** to the key Pd<sup>IV</sup> intermediate **14**, and (iii) C–O bond forming reductive elimination to provide the product **15** and regenerate Pd<sup>II</sup>. The approach we took to achieve C–H arylation stems from insight gained from the proposed mechanism of C–H acetoxylation. It was reasoned that an analogous mechanistic manifold could be employed to achieve C–H arylation by considering alternative I<sup>III</sup> reagents (**16**), that could oxidize the Pd<sup>II</sup> intermediate **13** and give access to an Ar–Pd<sup>IV</sup> species **17** (**Scheme 1.6**, Path B). Subsequent C–C bond forming reductive elimination from **17** would provide the desired C–H arylation product.

**Scheme 1.6:** Mechanistic Pathways for C–H activation/Functionalization.



Extensive research has been conducted on  $I^{III}$  reagents to allow us to identify the appropriate oxidant (**16**).<sup>41-43</sup> Literature reports have provided examples that support the oxidation of  $Pd^{II}$  to  $Ar-Pd^{IV}$  employing oxidants  $(X)(Y)I^{III}Ar$  to generate intermediates related to **17**.<sup>44-54</sup> Specifically, Canty has demonstrated the oxidation of the cyclometallated complex **19** to the observable  $Ar-Pd^{IV}$  adduct **20** using the hypervalent iodine oxidant  $[Ph-I^{III}-Ph]OTf$  (**Scheme 1.7**).<sup>44,45</sup> This provides key precedent for the viability of the proposed oxidation step to yield intermediate **17** within the catalytic cycle (**Scheme 1.6**, Path B).

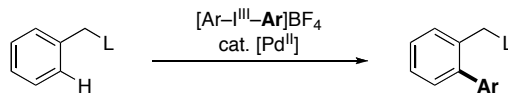
**Scheme 1.7:** Stoichiometric oxidation of a palladacycle by  $[Ph-I^{III}-Ph]OTf$ .<sup>44</sup>



Employing a reaction that proceeds through a  $Pd^{II/IV}$  mechanistic pathway offers several advantages over traditional cross coupling and C–H arylation reactions (which involve a  $Pd^{0/II}$  mechanism). First, high oxidation state palladium species are known to be stable to ambient air and moisture, making this transformation amenable to bench top chemistry and avoiding the requirement for dry solvents and specialized glassware.<sup>44-49,51-54</sup> Second, the unreactive nature of high oxidation palladium with aryl halides highlights the complementarity of the proposed methodology to traditional  $Pd^{0/II}$  methodology.<sup>36-40</sup>

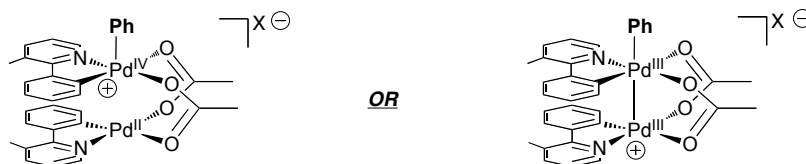
Our efforts toward the development of a  $Pd^{II/IV}$  C–H arylation transformation employing  $[Ar-I^{III}-Ar]^+$  oxidants is outlined in *Chapter 2* (**Scheme 1.8**).<sup>38,55</sup> This reaction was explored with a variety of directing groups for the site selective installation of phenyl groups. Additionally, the implementation of  $I^{III}$  reagents to afford C–H arylation with diverse aryl groups will be discussed. This transformation demonstrates a broad functional group tolerance, including orthogonal reactivity to  $Pd^{0/II}$  cross coupling chemistry. Finally, initial results exploring the *in situ* formation of the  $I^{III}$  reagents to increase the practical utility of this methodology is described.

**Scheme 1.8:** Palladium Catalyzed C–H Arylation Reactions.



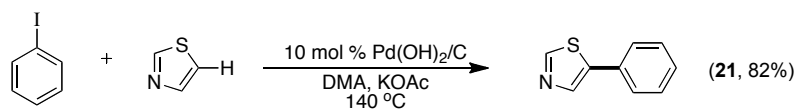
As described above this reaction is proposed to proceed through a high oxidation palladium intermediate. This led us to complete the detailed mechanistic studies discussed in *Chapter 3*.<sup>55</sup> Experiments included the determination of kinetic order in each reaction component, kinetic isotope effect studies, and Hammett studies. These investigations allowed for elucidation of the rate law, determination that oxidation is the rate-limiting step of the catalytic cycle, and identification of the resting state of the catalyst and oxidant. Through these studies, evidence was provided to support a unique high oxidation palladium dimer as a key intermediate in the catalytic cycle (**Figure 1.1**). Preliminary investigations regarding the generality of this mechanism amongst several directing groups will also be discussed.

**Figure 1.1:** High Oxidation Palladium Dimer Intermediate.

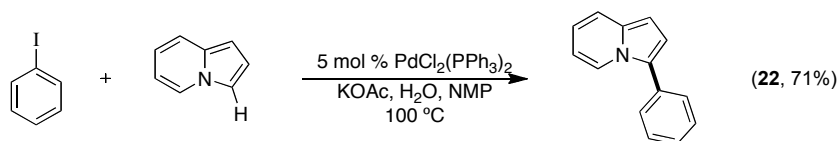


Our next goal was to expand this unique palladium-catalyzed C–H arylation methodology to substrates that do not contain directing groups. Numerous examples of direct C–H arylation employing Pd<sup>II/0</sup> catalytic cycles have been developed for a variety of different nitrogen, oxygen and sulfur containing heterocycles.<sup>10-24</sup> For example Fagnou has demonstrated the C–H arylation of thiazole to selectively yield product **21** (**Scheme 1.9**). Similarly, Gevorgyan has reported the site-selective, direct arylation of indolizine to afford **22** (**Scheme 1.10**)<sup>56</sup>

**Scheme 1.9:** Pd<sup>II/0</sup> Arylation of Thiazole.<sup>56</sup>

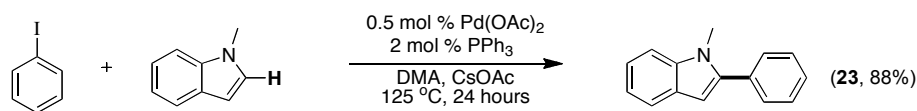


**Scheme 1.10:** Pd<sup>II/0</sup> Arylation of Indolizine.<sup>57</sup>



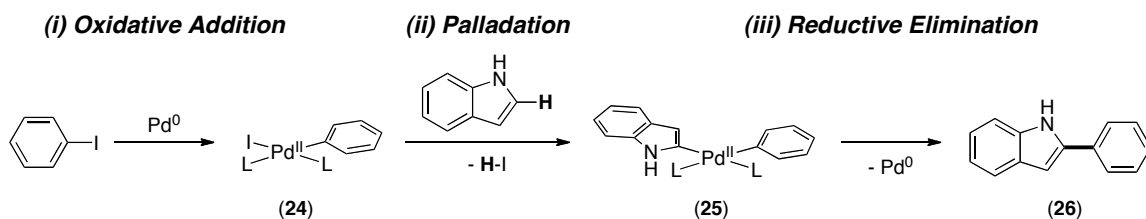
A particularly interesting report by Sames describes the site selective C2 arylation of indoles, such as **23** (**Scheme 1.11**).<sup>58-60</sup> This methodology proved to be general with respect to a variety of indole substrates and for a range of aryl iodides. However, this reaction suffered from several drawbacks: (1) forcing reaction conditions (>125 °C) were required for effective C–H arylation, (2) additives were necessary to arylate free N–H indoles, and (3) the reactions were not compatible with aryl halides due to the intermediacy of low valent palladium species.

**Scheme 1.11:** Sames' Precedent for Pd-Catalyzed Direct Arylation of Indole.<sup>58-60</sup>



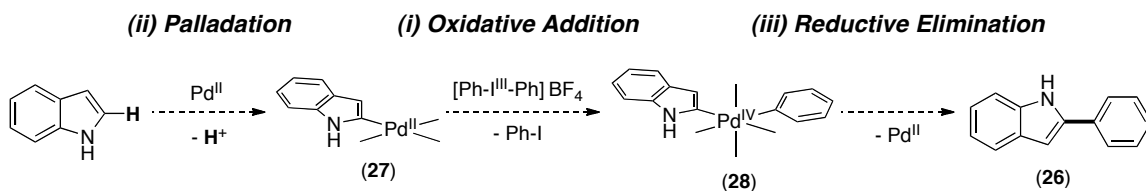
At the onset of our investigations into direct C–H arylation chemistry, we reasoned a Pd<sup>II/IV</sup> reaction pathway could address the challenges associated with Sames' methodology based on the analysis of his mechanistic proposal. His Pd<sup>II/0</sup> mechanism is believed to proceed through (**Scheme 1.12**): (i) oxidative addition of Pd<sup>0</sup> to Ar–I to yield intermediate **24**, (ii) C–H palladation to provide intermediate **25**, and (iii) C–C bond forming reductive elimination to release the C2 arylation product **26** and regenerate Pd<sup>0</sup>.

**Scheme 1.12:** Proposed Mechanism of Sames' Pd-Catalyzed Indole Arylation.<sup>58-60</sup>



Alternatively, a mechanism involving a Pd<sup>II/IV</sup> catalytic cycle (**Scheme 1.13**) employing I<sup>III</sup> oxidants would proceed through: (i) C–H palladation to afford intermediate **27**, (ii) oxidation of Pd<sup>II</sup> by [Ar–I<sup>III</sup>–Ar]<sup>+</sup> to generate Ar–Pd<sup>IV</sup> intermediate **28**, and (iii) C–C bond forming reductive elimination to provide product **26**. It was reasoned that indole palladation with a more electrophilic Pd<sup>II</sup> catalyst, along with the employment of a stronger I<sup>III</sup> oxidant, would address the challenges with Pd<sup>0/II</sup> chemistry by allowing milder reaction conditions and increased functional group tolerance.

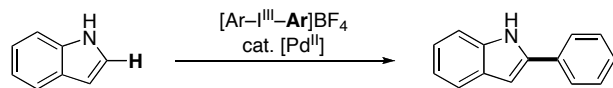
**Scheme 1.13:** Proposed Mechanism of Pd-Catalyzed Arylation with [Ph–I<sup>III</sup>–Ph]BF<sub>4</sub>.



The application of the Pd<sup>II/IV</sup> C–H arylation chemistry using a variety of substrates will be discussed in *Chapter 4*.<sup>61</sup> Initial investigations focused on the room temperature phenylation of indoles at the C2 position with high site selectivity (**Scheme 1.14**). In addition, modification of the I<sup>III</sup> oxidant allowed for the installation of diverse aryl groups. As previously demonstrated, reactivity complimentary to Pd<sup>0/II</sup> catalytic cycles was observed. In addition to indoles, this methodology was also extended to several other heterocycles, and initial investigations for the C–H arylation of simple unactivated arenes are also detailed. Preliminary investigations exploring the generation of the I<sup>III</sup> reagent *in situ* are also discussed.



**Scheme 1.14:** Site Selective Arylation of Indoles.



Initial studies to understand the mechanism of this transformation are outlined in *Chapter 5*. The strategy employed to study this reaction is discussed and involves labeling the substrate and oxidant with fluorine for monitoring by  $^{19}\text{F}$  NMR spectroscopy. Kinetic studies implicate an induction period, often associated with the formation of an active catalyst prior to the reaction that affords the desired product (**Scheme 1.15**). With the method developed, the kinetic order of several reaction components, with two catalysts are discussed.

**Scheme 1.15:** Induction Period Suggests the Formation of an ‘Active Intermediate’.



In conclusion, this dissertation describes efforts toward the development and mechanistic investigations of both ligand directed C–H arylation and direct C–H arylation. Each of these methodologies are general with respect to substrate scope and the installation of diverse sets of aryl groups. A broad range of functional group compatibility has been observed, including complementary reactivity to  $\text{Pd}^{0/\text{II}}$  chemistry. Thorough mechanistic studies have been completed for directed C–H arylation and have provided evidence for a unique high oxidation-state palladium intermediate. Additionally, preliminary experiments have been initiated to probe the detailed mechanism of the direct C–H arylation. These efforts have provided synthetically useful C–H arylation reactions, which are primed for further development due to the mechanistic understanding achieved.

## 1.1 References

1. Stille, J. K. *Angew. Chem., Int. Ed.* **1986**, *25*, 508-524.
2. Farina, V.; Krishnamurthy, V.; Scott, W. J. *Org. React. (N. Y.)* **1997**, *50*, 1-652.
3. Miyaura, N.; Suzuki, A. *Chem. Rev.* **1995**, *95*, 2457-2483.
4. Suzuki, A. *J. Organomet. Chem.* **1999**, *576*, 147-168.
5. Beletskaya, I. P.; Cheprakov, A. V. *Chem. Rev.* **2000**, *100*, 3009-3066.
6. Kotha, S.; Lahiri, K.; Kashinath, D. *Tetrahedron* **2002**, *58*, 9633-9695.
7. Denmark, S. E.; Sweis, R. F. *Acc. Chem. Res.* **2002**, *35*, 835-846.
8. Muci, A. R.; Buchwald, S. L. *Top. Curr. Chem.* **2002**, *219*, 131-209.
9. Negishi, E.-I.; Anastasia, L. *Chem. Rev.* **2003**, *103*, 1979-2017.
10. Campeau, L.-C.; Fagnou, K. *Chem. Commun.* **2006**, 1253-1264.
11. Daugulis, O.; Zaitsev, V. G.; Shabashov, D.; Pham, Q.-N.; Lazareva, A. *Synlett* **2006**, 3382-3388.
12. Yu, J.-Q.; Giri, R.; Chen, X. *Org. Biomol. Chem.* **2006**, *4*, 4041-4047.
13. Godula, K.; Sames, D. *Science* **2006**, *312*, 67-72.
14. Alberico, D.; Scott, M. E.; Lautens, M. *Chem. Rev.* **2007**, *107*, 174-238.
15. Beccalli, E. M.; Broggini, G.; Martinelli, M.; Sottocornola, S. *Chem. Rev.* **2007**, *107*, 5318-5365.
16. Ackermann, L. *Synlett* **2007**, 507-526.
17. Campeau, L.-C.; Fagnou, K. *Chem. Soc. Rev.* **2007**, *36*, 1058-1068.
18. Catellani, M.; Motti, E.; Della Ca, N. *Acc. Chem. Res.* **2008**, *41*, 1512-1522.
19. Kakiuchi, F.; Kochi, T. *Synthesis* **2008**, 3013-3039.
20. Li, B.-J.; Yang, S.-D.; Shi, Z.-J. *Synlett* **2008**, 949-957.
21. McGlacken, G. P.; Bateman, L. M. *Chem. Soc. Rev.* **2009**, *38*, 2447-2464.
22. Lyons, T. W.; Sanford, M. S. *Chem. Rev.* **in press**.
23. Daugulis, O.; Do, H.-Q.; Shabashov, D. *Acc. Chem. Res.* **2009**, *42*, 1074-1086.
24. Chen, X.; Engle, K. M.; Wang, D.-H.; Yu, J.-Q. *Angew. Chem., Int. Ed.* **2009**, *48*, 5094-5115.
25. Satoh, T.; Kawamura, Y.; Miura, M.; Nomura, M. *Angew. Chem., Int. Ed. Engl.* **1997**, *36*, 1740-1742.

26. Kametani, Y.; Satoh, T.; Miura, M.; Nomura, M. *Tetrahedron Lett.* **2000**, *41*, 2655-2658.
27. Kawamura, Y.; Satoh, T.; Miura, M.; Nomura, M. *Chem. Lett.* **1999**, 961-962.
28. Satoh, T.; Inoh, J.-i.; Kawamura, Y.; Kawamura, Y.; Miura, M.; Nomura, M. *Bull. Chem. Soc. Jpn.* **1998**, *71*, 2239-2246.
29. Terao, Y.; Kametani, Y.; Wakui, H.; Satoh, T.; Miura, M.; Nomura, M. *Tetrahedron* **2001**, *57*, 5967-5974.
30. Wakui, H.; Kawasaki, S.; Satoh, T.; Miura, M.; Nomura, M. *J. Am. Chem. Soc.* **2004**, *126*, 8658-8659.
31. Terao, Y.; Wakui, H.; Satoh, T.; Miura, M.; Nomura, M. *J. Am. Chem. Soc.* **2001**, *123*, 10407-10408.
32. Terao, Y.; Wakui, H.; Nomoto, M.; Satoh, T.; Miura, M.; Nomura, M. *J. Org. Chem.* **2003**, *68*, 5236-5243.
33. Hennings, D. D.; Iwasa, S.; Rawal, V. H. *J. Org. Chem.* **1997**, *62*, 2-3.
34. Campeau, L.-C.; Thansandote, P.; Fagnou, K. *Org. Lett.* **2005**, *7*, 1857-1860.
35. Campeau, L.-C.; Rousseaux, S.; Fagnou, K. *J. Am. Chem. Soc.* **2005**, *127*, 18020-18021.
36. Dick, A. R.; Hull, K. L.; Sanford, M. S. *J. Am. Chem. Soc.* **2004**, *126*, 2300-2301.
37. Desai, L. V.; Hull, K. L.; Sanford, M. S. *J. Am. Chem. Soc.* **2004**, *126*, 9542-9543.
38. Kalyani, D.; Deprez, N. R.; Desai, L. V.; Sanford, M. S. *J. Am. Chem. Soc.* **2005**, *127*, 7330-7331.
39. Desai, L. V.; Malik, H. A.; Sanford, M. S. *Org. Lett.* **2006**, *8*, 1141-1144.
40. Kalberer, E. W.; Whitfield, S. R.; Sanford, M. S. *J. Mol. Catal. A: Chem.* **2006**, *251*, 108-113.
41. Zhdankin, V. V.; Stang, P. J. *Chem. Rev.* **2008**, *108*, 5299-5358.
42. Deprez, N. R.; Sanford, M. S. *Inorg. Chem.* **2007**, *46*, 1924-1935.
43. Zhdankin, V. V.; Stang, P. J. *Chem. Rev.* **2002**, *102*, 2523-2584.
44. Canty, A. J.; Patel, J.; Rodemann, T.; Ryan, J. H.; Skelton, B. W.; White, A. H. *Organometallics* **2004**, *23*, 3466-3473.

45. Bayler, A.; Canty, A. J.; Ryan, J. H.; Skelton, B. W.; White, A. H. *Inorg. Chem. Commun.* **2000**, *3*, 575-578.
46. Canty, A. J.; Rodemann, T. *Inorg. Chem. Commun.* **2003**, *6*, 1382-1384.
47. Canty, A. J.; Rodemann, T.; Skelton, B. W.; White, A. H. *Inorg. Chem. Commun.* **2005**, *8*, 55-57.
48. Canty, A. J.; Rodemann, T.; Skelton, B. W.; White, A. H. *Organometallics* **2006**, *25*, 3996-4001.
49. Chaudhuri, P. D.; Guo, R.; Malinakova, H. C. *J. Organomet. Chem.* **2008**, *693*, 567-573.
50. Canty, A. J.; Gardiner, M. G.; Jones, R. C.; Rodemann, T.; Sharma, M. *J. Am. Chem. Soc.* **2009**, *131*, 7236-7237.
51. Lagunas, M.-C.; Gossage, R. A.; Spek, A. L.; van Koten, G. *Organometallics* **1998**, *17*, 731-741.
52. Dick, A. R.; Kampf, J. W.; Sanford, M. S. *J. Am. Chem. Soc.* **2005**, *127*, 12790-12791.
53. Whitfield, S. R.; Sanford, M. S. *J. Am. Chem. Soc.* **2007**, *129*, 15142-15143.
54. Racowski, J. M.; Dick, A. R.; Sanford, M. S. *J. Am. Chem. Soc.* **2009**, *131*, 10974-10983.
55. Deprez, N. R.; Sanford, M. S. *J. Am. Chem. Soc.* **2009**, *131*, 11234-11241.
56. Parisien, M.; Valette, D.; Fagnou, K. *J. Org. Chem.* **2005**, *70*, 7578-7584.
57. Park, C.-H.; Ryabova, V.; Seregin, I. V.; Sromek, A. W.; Gevorgyan, V. *Org. Lett.* **2004**, *6*, 1159-1162.
58. Lane, B. S.; Sames, D. *Org. Lett.* **2004**, *6*, 2897-2900.
59. Lane, B. S.; Brown, M. A.; Sames, D. *J. Am. Chem. Soc.* **2005**, *127*, 8050-8057.
60. Bellina, F.; Cauteruccio, S.; Rossi, R. *Eur. J. Org. Chem.* **2006**, 1379-1382.
61. Deprez, N. R.; Kalyani, D.; Krause, A.; Sanford, M. S. *J. Am. Chem. Soc.* **2006**, *128*, 4972-4973.

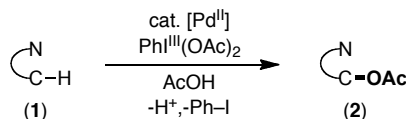
## Chapter 2

### Scope and Development of Palladium-Catalyzed C–H Arylation

#### 2.1 Background and Significance

Previously in our laboratory, Pd<sup>II</sup> catalysts were utilized to perform C–H activations in the presence of PhI<sup>III</sup>(OAc)<sub>2</sub> as a terminal oxidant providing a new C–O bonds.<sup>1-5</sup> Site selectivity was achieved using substrates containing functionality (1) that acts as a ligand for Pd<sup>II</sup> and directs it toward a specific C–H bond for acetoxylation (2, **Scheme 2.1**). This transformation proved to be general with respect to directing groups as well as tolerant of a wide range of functional groups. We envisaged that C–H activation/C–C bond formation could be achieved in a manner analogous to this C–O bond formation by using (Ar)(Ar')I<sup>III</sup>(X) as oxidants.

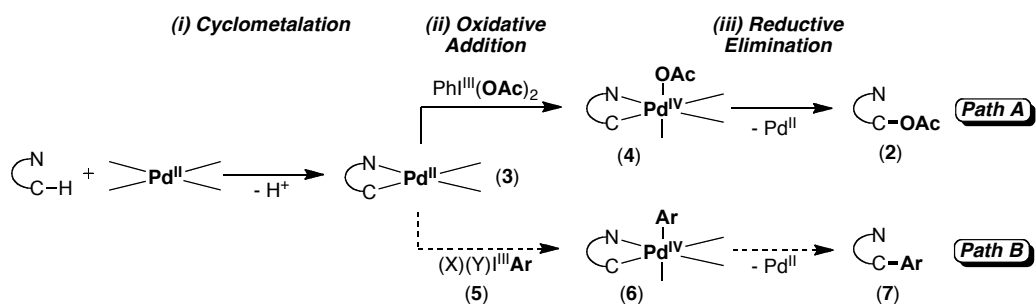
**Scheme 2.1:** Ligand Directed C–H Activation/C–O Bond Formation.<sup>1-5</sup>



The mechanism for C–H activation/C–O bond formation (**Scheme 2.2**, Path A) is believed to proceed through: (i) coordination of palladium to the directing group followed by C–H activation, (ii) subsequent two electron oxidation of palladacycle **3** to the key Pd<sup>IV</sup> intermediate **4**, and (iii) C–O bond forming reductive elimination to provide the product **2** while regenerating the Pd<sup>II</sup> catalyst. It was reasoned that an analogous mechanistic manifold could be employed to achieve C–H arylation by considering alternative I<sup>III</sup> reagents (**5**), that could oxidize palladacycle **3** to an Ar–Pd<sup>IV</sup> species **6**

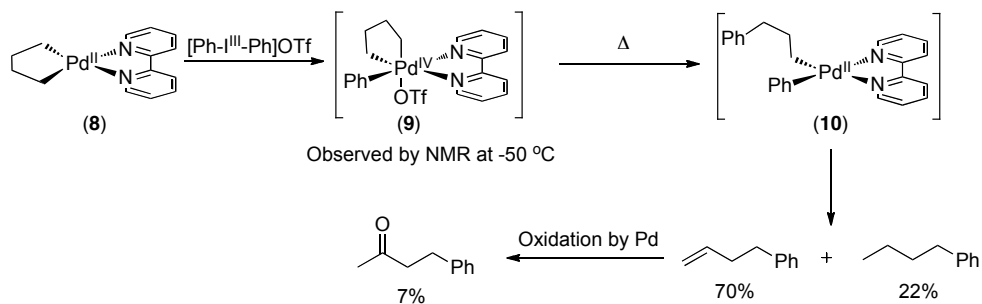
(Scheme 2.2, Path B). Subsequent C–C bond forming reductive elimination of **6** would provide the desired product **7**.

**Scheme 2.2:** Mechanistic Pathways for C–H Activation/Functionalization.



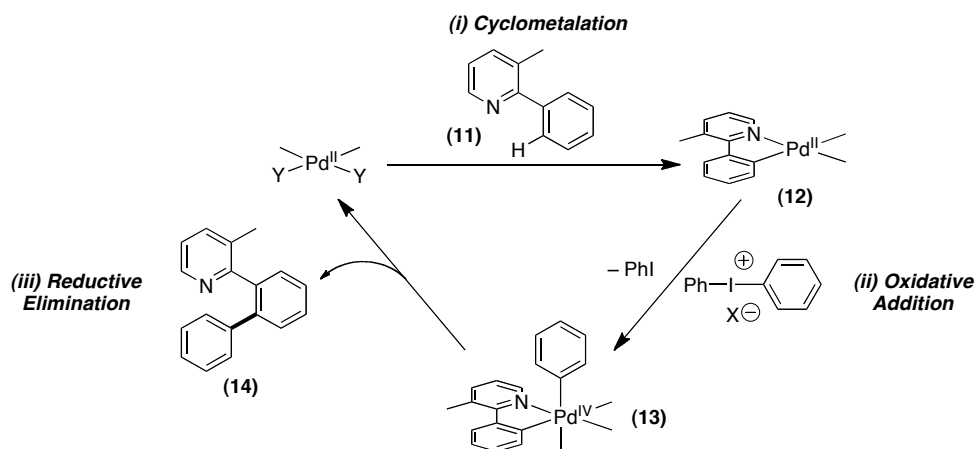
Canty has demonstrated that Ph–Pd<sup>IV</sup> complexes analogous to **6** are accessible via the oxidation of Pd<sup>II</sup> precursors with I<sup>III</sup> reagents. For example, cyclometallated palladium complexes such as **8** were stoichiometrically oxidized with [Ph–I<sup>III</sup>–Ph]OTf to the corresponding Ph–Pd<sup>IV</sup> intermediate **9** at –50 °C as characterized by low temperature <sup>1</sup>H NMR spectroscopy (Scheme 2.3).<sup>6,7</sup> Warming this complex to room temperature led to C–C bond-forming reductive elimination, providing the transient alkyl–Pd<sup>II</sup> species **10** which quickly decomposed to various isolable products resulting from protonolysis, β-hydride elimination, and Wacker oxidation. In addition to utilizing [Ph–I<sup>III</sup>–Ph]<sup>+</sup> as a stoichiometric oxidant, literature examples have demonstrated that [Ph–I<sup>III</sup>–R]<sup>+</sup>, where R is vinyl or alkynyl, can also stoichiometrically oxidize Pd<sup>II</sup> to Pd<sup>IV</sup>. Each of these cases led to R–Pd<sup>IV</sup> with selective transfer of only the alkenyl or alkynyl group in preference to the phenyl group.<sup>8–12</sup> Finally, several other examples have demonstrated the use of I<sup>III</sup> reagents to oxidize Pd<sup>II</sup> to R–Pd<sup>IV</sup> species where R is a heteroatom.<sup>13–16</sup> Together, these examples provide considerable precedent for the viability of the proposed oxidation step of the catalytic cycle (**Path B**).

**Scheme 2.3:** Stoichiometric Oxidation of a Palladacycle by  $[\text{Ph-I}^{\text{III}}\text{-Ph}]\text{OTf}$ .<sup>6</sup>



The precedent provided by both the catalytic C–H activation/C–O bond forming methodology and stoichiometric oxidations of  $\text{Pd}^{\text{II}}$  with  $\text{I}^{\text{III}}$  reagents allowed us to envision the following catalytic cycle for C–H activation/C–C bond forming reactions (**Scheme 2.4**). The catalytic cycle employing **11** would begin by coordination of the pyridine and activation of the proximal C–H bond to give **12** (step ii), followed by oxidative addition of the  $[\text{Ph-I}^{\text{III}}\text{-Ph}]^+$  to the cyclometallated  $\text{Pd}^{\text{II}}$  to give a  $\text{Ph-Pd}^{\text{IV}}$  intermediate (**13**, step ii), and final C–C bond forming reductive elimination would provide the desired product **14** and release  $\text{Pd}^{\text{II}}$  (step iii).

**Scheme 2.4:** Proposed Catalytic Cycle for C–H Arylation.



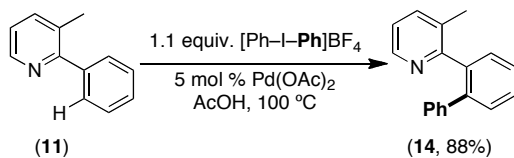
This transformation, which is proposed to proceed through a  $\text{Pd}^{\text{II/IV}}$  manifold, was expected to offer several advantages over existing C–H arylation methods proceeding through  $\text{Pd}^{0/\text{II}}$  catalytic cycles. Typically reactions involving  $\text{Pd}^0$  intermediates are

sensitive to ambient air and moisture, often necessitating the use of special glassware and dry solvents. These precautions should be unnecessary in the proposed methodology, since high oxidation state Pd species are known to be stable to ambient air and moisture.<sup>6-11,13-16</sup> Furthermore, reaction pathways employing high oxidation state palladium should also be tolerant of sensitive functionalities such as aryl halides. These types of compounds are often reactive with Pd<sup>0</sup> or strong bases required in transformations proceeding through a Pd<sup>0/II</sup> pathway. Finally, the inertness of high oxidation palladium toward aryl halides also should result in complementary substrate scope of the proposed methodology versus traditional Pd<sup>0/II</sup> chemistry.

## 2.2 Phenylation Development

Initial efforts to develop palladium catalyzed C–H arylation methodology focused on the substrate 3-methyl-2-phenylpyridine (**11**) using Pd(OAc)<sub>2</sub> as the catalyst and the hypervalent iodine reagent [Ph–I<sup>III</sup>–Ph]BF<sub>4</sub>. This particular substrate was chosen for initial studies based on previous results suggesting that pyridine directing groups were particularly effective for palladium-catalyzed C–H functionalizations, and that a methyl group at the 3-position would prevent overfunctionalization.<sup>1,2,17,18</sup> We were pleased to find that this reaction afforded the desired C–H phenylation product selectively in a variety of organic solvents (AcOH, CH<sub>2</sub>Cl<sub>2</sub>, toluene, benzene). Further screening identified the optimal conditions as 1.1 equiv of [Ph–I<sup>III</sup>–Ph]BF<sub>4</sub> and 5 mol % of Pd(OAc)<sub>2</sub> at 100 °C in AcOH, which afforded **14** in an 88% isolated yield (**Scheme 2.5**). Importantly, this reaction proceeds in the presence of ambient moisture and atmosphere and does not require added base or ligands.

**Scheme 2.5:** C–H Phenylation of 3-Methyl-2-Phenylpyridine.





We next sought to explore the generality of this transformation with respect to directing groups (**Table 2.1**). This reaction provided phenylation products under the optimized conditions for **11** (5 mol % Pd(OAc)<sub>2</sub>, 1.1 equiv [Ph-I<sup>III</sup>-Ph]BF<sub>4</sub>, AcOH, 100 °C) for several different pyridine (**15**, **16**, **17**) and quinoline (**18**, **19**, **20**) substrates in good to excellent yields. The scope was also extended to substrates containing the oxygen-directing groups of pyrrolidinones (**21**, **22**, **23**), oxazolidinones (**24**) and amides (**25**, **26**), which afforded the desired products in good yields. Optimal conditions for these substrates were slightly modified and utilized 5 mol % of Pd(OAc)<sub>2</sub>, 1.5–2.5 equiv of [Ph-I<sup>III</sup>-Ph]BF<sub>4</sub> in toluene with 1.5 equiv of NaHCO<sub>3</sub> at 100 °C. In general, the functionalization of substrates containing oxygen-directing groups proved to be less efficient and required higher oxidant loadings. It is important to note that although optimized conditions utilized added base, this was not always required to achieve high conversions.

These reactions were also tolerant of a variety of functionalities including enolizable ketones (**15**), aldehydes (**17**), ethers (**22**) and amides (**26**). Notably, aryl bromides (**23**) also remained unaffected under the reaction conditions, highlighting the complementarity of this methodology to traditional Pd<sup>0/II</sup> cross coupling chemistry, while also providing evidence that a Pd<sup>0/II</sup> mechanism is unlikely. Finally, successful phenylation of benzylic sp<sup>3</sup> C–H bond was also achieved (**18**, **19**). Importantly, this functionalization occurred only when the benzylic C–H bond was proximal to an appropriate directing group.

**Table 2.1:** Substrate Scope of C–H Phenylation Reactions.

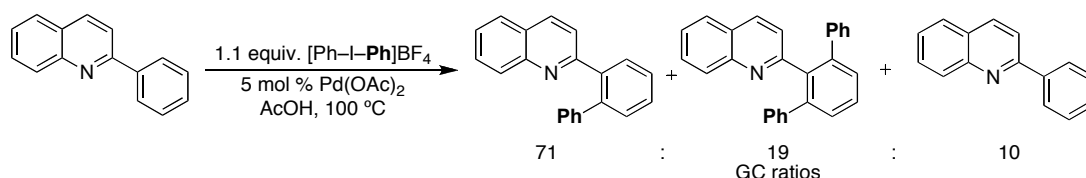
Entry	Product	Yield <sup>a</sup>	Entry	Product	Yield <sup>a</sup>	Entry	Product	Yield <sup>a</sup>
1		(91%) 15	5		(60%) <sup>d</sup> 19	9		(78%) 23
2		(74%) 16	6		(58%) <sup>b</sup> 20	10		(83%) <sup>e</sup> 24
3		(51%) <sup>b</sup> 17	7		(75%) <sup>e</sup> 21	11		(49%) <sup>b</sup> 25
4		(72%) <sup>c</sup> 18	8		(84%) <sup>e</sup> 22	12		(67%) 26

<sup>a</sup> Conditions: 1 equiv of substrate, 1.1–2.5 equiv of [Ph<sub>2</sub>]BF<sub>4</sub>, 5 mol % of Pd(OAc)<sub>2</sub> in AcOH, AcOH/Ac<sub>2</sub>O, benzene, or toluene, 100 °C, 8–24 h. <sup>b</sup> The balance of material was starting material (entry 11) or a mixture of starting material and diarylated product (entries 3 and 6). <sup>c</sup> Conditions: 2 equiv of 8-methylquinoline, 1 equiv of [Ph<sub>2</sub>]BF<sub>4</sub>. <sup>d</sup> Approximately 16% of the product in entry 5 was formed in the absence of Pd(OAc)<sub>2</sub>. <sup>e</sup> 1.2–2 equiv of NaHCO<sub>3</sub> were added.

A potential challenge that can be imagined is the addition of multiple phenyl groups when multiple *ortho* C–H sites are present. However this can be overcome with appropriate choice of oxidant equivalents and substrate. Subjection of substrates with nitrogen directing groups that contain equivalent *ortho* C–H bonds to 1.1 equiv of [Ph–I<sup>III</sup>–Ph]BF<sub>4</sub> afforded mono phenylation in useful yields (**17**, **20**), with the remaining material being diphenylated product and unreacted starting material. For example the reaction to provide **20**, also resulted in diphenylation and starting material in a ratio of 71:19:20 respectively, as determined by gas chromatography (**Scheme 2.6**). Diphenylation with oxygen-containing directing groups proved to be less problematic despite the fact that larger equivalents of oxidant (>1.5 equiv) were used. For example, the phenylation product **21** was obtained in high yield and none of the corresponding diphenylation product was isolated. High selectivity for mono-phenylation was also

observed on arenes *ortho* to a directing group in substrates containing an additional *meta* substituent, such as 3-methyl-2-arylpyridine, or when a *meta* substituent was present on the arene undergoing functionalization (**15**, **16**).

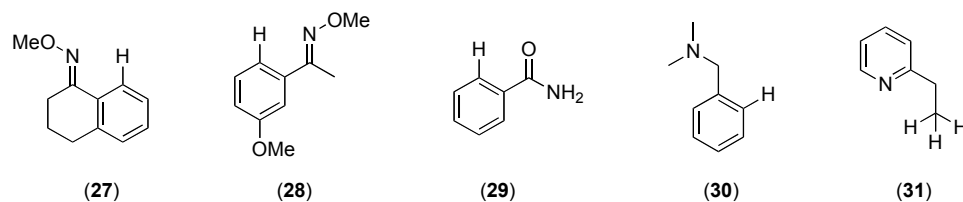
**Scheme 2.6:** Observed Selectivity of Phenylation for 2-Phenylquinoline.



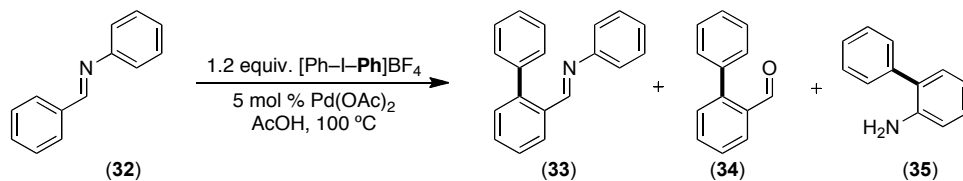
Phenylation of substrates containing *meta* substituents on the arene undergoing functionalization affords exclusively the less hindered regioisomer, with no difunctionalization observed. This suggests that steric control dominates the selectivity for this transformation.<sup>17</sup> In addition, the reactions proceed in good yield and selectivity with both electron withdrawing and donating functionality at the *meta* position. This also demonstrates that activated arenes are not required for this reaction to proceed efficiently. Additionally, high selectivity for the less hindered regioisomer is observed even with substrates containing functional groups with the potential for dual chelation (**15**, **22**, **23**), directing to the more hindered site if operative.

Attempts to implement this chemistry with several other substrates were not all as successful. For example oxime ethers **27** and **28** did not provide detectable C–H arylation products using [Ph–I<sup>III</sup>–Ph]BF<sub>4</sub> (1.2–2.0 equiv) and Pd(OAc)<sub>2</sub> (5 mol %) at 100 °C in a solvent screen (AcOH, benzene, CHCl<sub>3</sub>, CH<sub>3</sub>CN). This is notable given that C–H acetoxylation generally proceeds in high yield with oxime ether directing groups. Interestingly, imine **32** did appear to provide phenylated products upon subjection to [Ph–I<sup>III</sup>–Ph]BF<sub>4</sub> (1.2 equiv) and Pd(OAc)<sub>2</sub> in AcOH at 100 °C for 12 h (**Scheme 2.7**). Masses corresponding to **33**, **34**, and **35** were observable in trace amounts based on analysis by GCMS. However, a screen of solvents failed to increase the amount of products observed, and determination of a yield was difficult due to the decomposition of the starting material and product to other species that could not all be identified.

**Figure 2.1:** Problematic Substrates for C–H Arylation.



**Scheme 2.7:** Trace Products Observed from C–H Arylation of **32**.



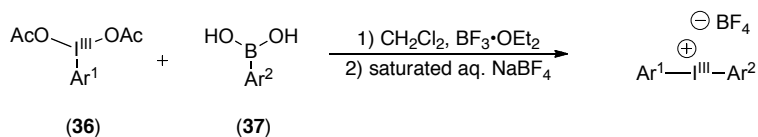
Like imine **32**, several other substrates showed limited success. Amide **29** reacted to form the desired C–H phenylation product in 36% yield when subjected to  $[\text{Ph-I}^{\text{III}}\text{-Ph}]\text{BF}_4$  (1.2. equiv) and  $\text{Pd}(\text{OAc})_2$  (5 mol %) in  $\text{AcOH}$  at  $100^\circ\text{C}$  based on analysis by GCMS. However, further screening of this reaction in the solvents listed above failed to provide better results. Likewise, subsection of benzylamine **30** to two equiv of oxidant provided products with masses corresponding to the mono and diarylated products by GCMS in 11% yield based on uncalibrated GC peak areas. Solvent optimization also did not lead to improvement in yield. Finally, a solvent screen for the substrate **31** provided trace amounts of phenylation products with the correct mass by GCMS using the same conditions as **30**. Notably, none of these substrates were extensively examined, and further optimizations may lead to improved results.

### 2.3 Arylation Development

To expand the utility of this chemistry, focus shifted to achieving selective installation of a variety of aryl groups. This is crucial for a broader applicability of this methodology, especially in the context of late stage diversification of molecules for structure activity relationship studies. For this purpose we sought conditions that would allow installation of both electronically and sterically diverse aryl groups. The challenge associated with varying these electronic and steric factors of the  $\text{I}^{\text{III}}$  reagent is identifying

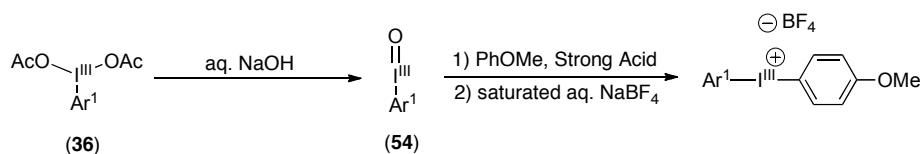
how these factors impact the transfer of the aryl group from the I<sup>III</sup> reagent, and ultimately the functionalization.

To explore these questions, a wide range of [Ar'-I<sup>III</sup>-Ar]BF<sub>4</sub> reagents were required to allow for a systematic study. The majority of these I<sup>III</sup> reagents were easily synthesized from ArI<sup>III</sup>(OAc)<sub>2</sub> (**36**) and the appropriate Ar'B(OH)<sub>2</sub> (**7**) in the presence of BF<sub>3</sub>•Et<sub>2</sub>O, followed by quenching with a saturated aqueous solution of NaBF<sub>4</sub> (**Table 2.2**).<sup>19</sup> Advantageously, these reagents can be purified through simple recrystallization. Further, ArI<sup>III</sup>(OAc)<sub>2</sub> (**36**) reagents that are not commercially available are easily obtained through oxidation of the corresponding Ar-I with NaBO<sub>3</sub>•H<sub>2</sub>O in AcOH.<sup>20</sup> However, this route was not high yielding when Ar<sup>1</sup> or Ar<sup>2</sup> was electron rich, so an alternative synthesis was utilized in these cases. The first step of this alternative approach employed iodosyl arene (**54**) generated by the reaction of ArI<sup>III</sup>(OAc)<sub>2</sub> (**36**) with NaOH (**Table 2.3**).<sup>21</sup> This was then followed by an electrophilic aromatic substitution of the iodosyl arene with anisole under acidic conditions to provide the desired I<sup>III</sup> reagent.<sup>22,23</sup>

**Table 2.2:** Synthesis of Electron Neutral and Poor Arene Oxidants.

Ar <sup>1</sup> =	Ar <sup>2</sup> =	Yield
Mes	<i>p</i> -CF <sub>3</sub> C <sub>6</sub> H <sub>4</sub>	68% ( <b>38</b> )
Mes	<i>p</i> -FC <sub>6</sub> H <sub>4</sub>	58% ( <b>39</b> )
Mes	<i>p</i> -ClC <sub>6</sub> H <sub>4</sub>	53% ( <b>40</b> )
Mes	<i>p</i> -CH <sub>3</sub> C <sub>6</sub> H <sub>4</sub>	85% ( <b>41</b> )
Mes	<i>m</i> -(COMe)C <sub>6</sub> H <sub>4</sub>	nd ( <b>42</b> )
Mes	<i>m</i> -(CHO)C <sub>6</sub> H <sub>4</sub>	72% ( <b>43</b> )
Mes	<i>p</i> -(COMe)C <sub>6</sub> H <sub>4</sub>	25% ( <b>44</b> )
Mes	Ph	81% ( <b>45</b> )
<i>p</i> -ClC <sub>6</sub> H <sub>4</sub>	<i>p</i> -ClC <sub>6</sub> H <sub>4</sub>	93% ( <b>46</b> )
<i>p</i> -CH <sub>3</sub> C <sub>6</sub> H <sub>4</sub>	<i>p</i> -CH <sub>3</sub> C <sub>6</sub> H <sub>4</sub>	63% ( <b>47</b> )
<i>m</i> -CF <sub>3</sub> C <sub>6</sub> H <sub>4</sub>	<i>m</i> -CF <sub>3</sub> C <sub>6</sub> H <sub>4</sub>	50% ( <b>48</b> )
<i>p</i> -FC <sub>6</sub> H <sub>4</sub>	<i>p</i> -FC <sub>6</sub> H <sub>4</sub>	82% ( <b>49</b> )
<i>p</i> -BrC <sub>6</sub> H <sub>4</sub>	<i>p</i> -BrC <sub>6</sub> H <sub>4</sub>	78% ( <b>50</b> )
1-naphthyl	1-naphthyl	70% ( <b>51</b> )
<i>o</i> -CH <sub>3</sub> C <sub>6</sub> H <sub>4</sub>	<i>o</i> -CH <sub>3</sub> C <sub>6</sub> H <sub>4</sub>	82% ( <b>52</b> )
Ph	Ph	78% ( <b>53</b> )

Mes = 2,4,6-trimethylphenyl

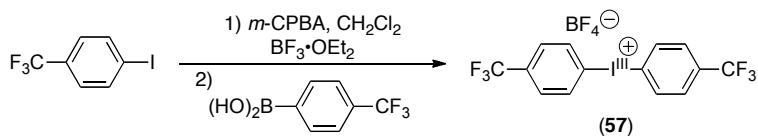
**Table 2.3:** Synthesis of [Ph-I<sup>III</sup>-(*p*-MeOC<sub>6</sub>H<sub>4</sub>)]BF<sub>4</sub>.

Ar <sup>1</sup> =	Yield
Mes	68% ( <b>55</b> )
<i>p</i> -MeOC <sub>6</sub> H <sub>4</sub>	58% ( <b>56</b> )

Subsequent to our investigations Olofsson described an alternative, one-pot synthesis of diaryliodonium salts.<sup>24</sup> This report is potentially very useful because it employs essentially the same procedure for both electron rich and poor oxidants. We found it to be useful for the synthesis of several of the oxidants. In particular we employed it for the synthesis of [(*p*-CF<sub>3</sub>C<sub>6</sub>H<sub>4</sub>)<sub>2</sub>I<sup>III</sup>]<sup>+</sup>BF<sub>4</sub><sup>-</sup>, which proved to be challenging with the above described methods. This was accomplished by combining *p*-CF<sub>3</sub>C<sub>6</sub>H<sub>4</sub>-I

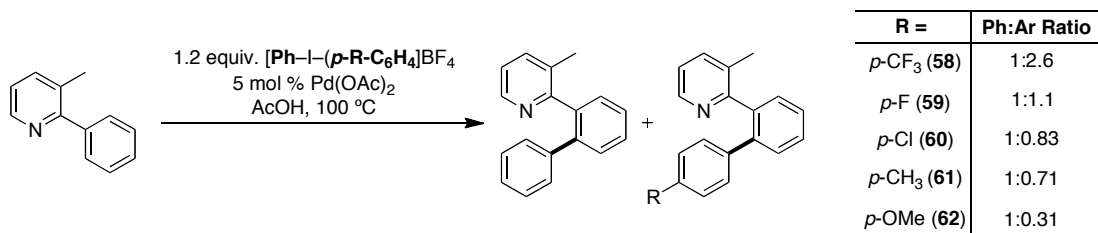
with  $\text{BF}_3 \cdot \text{OEt}_2$  with *m*-CPBA, followed by addition of *p*- $\text{CF}_3\text{C}_6\text{H}_4\text{-B(OH)}_2$  to provide the desired oxidant **57** in 42% yield. The oxidants in the remainder of this dissertation were synthesized using the methods described above.

**Scheme 2.8:** Synthesis of  $[(p\text{-CF}_3\text{C}_6\text{H}_4)_2\text{I}^{\text{III}}]\text{BF}_4$ .



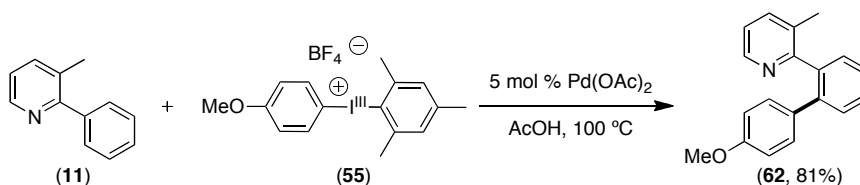
Investigations were initiated by my colleague Dr. Dipannita Kalyani using 3-methyl-2-phenylpyridine (**11**) as the model substrate and the optimal conditions determined for the oxidant  $[\text{Ph-I}^{\text{III}}\text{-Ph}]\text{BF}_4$ . To install different aryl groups, the alternative oxidants  $[\text{Ph-I}^{\text{III}}\text{-Ar}]\text{BF}_4$  were employed. In these cases Ar was substituted at the *para* position with  $\text{CF}_3$ , F, Cl, Me, and OMe. These reactions were analyzed by gas chromatography, which revealed that in all cases the reactions yielded mixtures of products resulting from phenyl addition and substituted aryl group addition (**Scheme 2.9**). Analysis of a calibrated product distribution indicated the preferential transfer of the more electron poor aryl group from the  $\text{I}^{\text{III}}$  reagent. For example, when the oxidant  $[\text{Ph-I}^{\text{III}}\text{-}p\text{-MeOC}_6\text{H}_4]\text{BF}_4$ , (**62**) was employed, preferential transfer of the more electron poor phenyl group was observed over *p*- $\text{MeOC}_6\text{H}_4$  (1 : 0.33). In contrast, utilizing the oxidant containing Ar = *p*- $\text{CF}_3\text{C}_6\text{H}_4$  (**58**) resulted in the preferential transfer of *p*- $\text{CF}_3\text{C}_6\text{H}_4$  (2.6 : 1). Although this reversal in selectivity is interesting, neither of these mixtures of products is synthetically useful, and these experiments demonstrate that electronically differentiating the aryl groups will be problematic. The mechanistic implications of these selectivities will be further discussed (*Chapter 3*).

**Scheme 2.9:** Mixtures of Products Obtained Using [Ph-I<sup>III</sup>-Ar]BF<sub>4</sub> Oxidants.



The second approach taken was to sterically differentiate the aryl groups on the I<sup>III</sup> oxidant to promote preferential transfer of the smaller aryl group. To accomplish this, we designed a set of oxidants of the general formula [Mes-I<sup>III</sup>-Ar]BF<sub>4</sub> (Mes, mesityl = 2,4,6-trimethylbenzene), in which the smaller aryl group would be expected to preferentially transfer rather than the bulky Mes. Gratifyingly, the reaction of **11** with [Mes-I-(*p*-MeOC<sub>6</sub>H<sub>4</sub>)]BF<sub>4</sub> (**55**) under optimized conditions provided exclusive installation of *p*-MeOC<sub>6</sub>H<sub>4</sub> (**62**) as the only detectable product (**Scheme 2.10**). This is in direct contrast to [Ph-I-(*p*-MeOC<sub>6</sub>H<sub>4</sub>)]BF<sub>4</sub> where only a minor amount of *p*-MeOC<sub>6</sub>H<sub>4</sub> was transferred (**Scheme 2.9**).

**Scheme 2.10:** Selective Arylation with [Mes-I<sup>III</sup>-(*p*-MeOC<sub>6</sub>H<sub>4</sub>)]BF<sub>4</sub>.

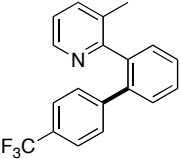
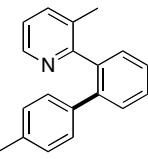
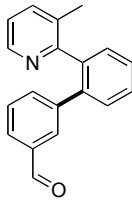
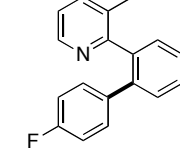
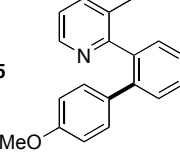
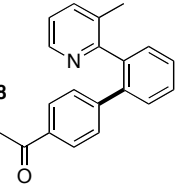
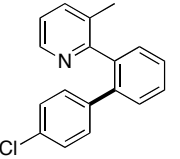
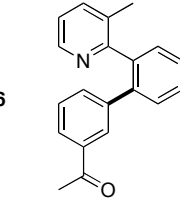
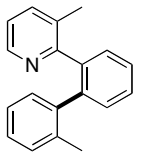


This strategy was expanded to achieve selective transfer of a variety of both electron rich and electron poor aryl groups as the only detectable products (**Table 2.4**). Aryl groups containing functional groups such as enolizable ketones (**68**, **70**), aldehydes (**69**), ethers (**67**), and benzylic hydrogens (**63–71**) were successfully installed. A potential challenge that can be envisioned for this strategy is the transfer of sterically bulky Ar. However, gratifyingly, selective installation of the sterically bulky *o*-tolyl (**71**) was achieved preferentially over the even bulkier mesityl. A further expansion of the utility of this transformation was achieved by the installation of an aryl halide (**64**, **65**). This



functional group can serve as a handle for further manipulations of the product, and again demonstrates the complementarity of this methodology to traditional Pd<sup>0/II</sup> cross coupling chemistry. Finally, the observed regioselectivity and issues related to multiple arylations were analogous to those described in the context of phenylation.

**Table 2.4:** Scope of Arylation with [Mes-I<sup>III</sup>-Ar]BF<sub>4</sub> Oxidants.

Entry	Product	Yield <sup>a</sup>	Entry	Product	Yield <sup>a</sup>	Entry	Product	Yield <sup>a</sup>
1		(87%) 63	4		(84%) 66	7		(88%) 69
2		(88%) 64	5		(81%) <sup>b</sup> 67	8		(81%) 70
3		(83%) 65	6		(81%) 68	9		(72%) 71

<sup>a</sup> 1 equiv of substrate, 1.1–1.3 equiv of [Mes-I<sup>III</sup>-Ar]BF<sub>4</sub>, 5 mol % of Pd(OAc)<sub>2</sub>, AcOH (0.1 M), 100 °C, <sup>b</sup> Reaction carried out at 120 °C.

Interestingly, this strategy was found to be less effective for the arylation of 3-methyl-2-(*o*-methoxyphenyl)pyridine (**72**) with [Mes-I<sup>III</sup>-(*p*-MeOC<sub>6</sub>H<sub>4</sub>)]BF<sub>4</sub> (**55**), which lead to a mixture of both the *p*-MeOC<sub>6</sub>H<sub>4</sub> (**74**) and mesityl (**73**) products (isolated in a 6:1 ratio, **Scheme 2.11**, **Table 2.5**). To further explore the diminished selectivity associated with this substrate, a variety of the other [Mes-I<sup>III</sup>-Ar]BF<sub>4</sub> oxidants were employed (**Scheme 2.11**). In these cases the ratio of the desired aryl addition to mesityl addition increased as the oxidant became more electron deficient (**Table 2.5**). With the exception of [Mes-I<sup>III</sup>-(*p*-MeOC<sub>6</sub>H<sub>4</sub>)]BF<sub>4</sub> (**55**), the asymmetric I<sup>III</sup> oxidants maintained high selectivity (greater than 12:1) for the Ar group transfer. This result is interesting as it

pertains to developing this reaction further for the functionalization of electron rich arenes.

**Scheme 2.11:** Selectivity of Arylation of **72** with [Mes-I<sup>III</sup>-(*p*-MeOPh)]BF<sub>4</sub>.

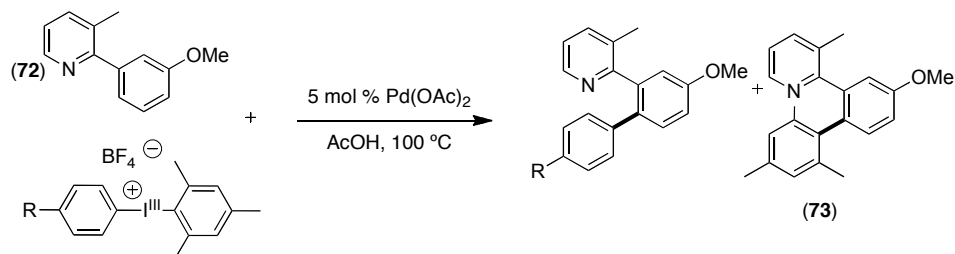


**Table 2.5:** Arylation of **72** with [Mes-I<sup>III</sup>-Ar]BF<sub>4</sub> Oxidants.

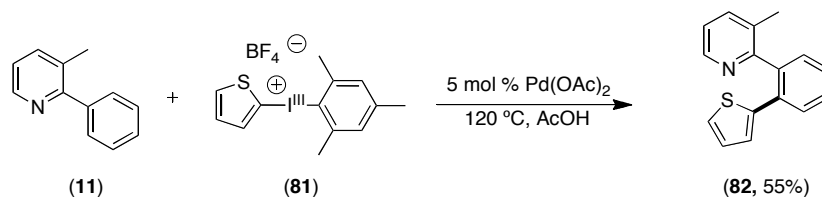
Entry	Product	Yield (Ar:Mes) <sup>a</sup>	Entry	Product	Yield (Ar:Mes) <sup>a</sup>	Entry	Product	Yield (Ar:Mes) <sup>a</sup>
1		(56%) <sup>b</sup> <b>74</b> (6:1)	3		(83%) <b>76</b> (108:1)	5		(85%) <b>78</b> (12:1)
2		(87%) <b>75</b> (58:1)	4		(85%) <b>77</b> (29:1)	6		(71%) <b>79</b> (20:1)

<sup>a</sup> Conditions: 1 equiv of substrate, 1.1 equiv of [Mes-I<sup>III</sup>-Ar]BF<sub>4</sub>, 5 mol % of Pd(OAc)<sub>2</sub>, AcOH (0.1 M) 100 °C, <sup>b</sup> Reaction carried out at 120 °C.

We also wanted to investigate the installation of heteroaryl groups. To accomplish this, the oxidant [Mes-I<sup>III</sup>-(2-thiophene)]OTs (**80**) was synthesized according to a literature procedure, followed by an anion metathesis to give the BF<sub>4</sub><sup>-</sup> salt.<sup>25</sup> The anion exchange resulted in 80% conversion to the BF<sub>4</sub> salt, with 20% of the <sup>-</sup>OTs anion remaining based on <sup>1</sup>H NMR spectroscopy. The C–H arylation was then carried out under similar conditions by combining [Mes-I<sup>III</sup>-(2-thiophene)]BF<sub>4</sub> (**81**) (1.5 equiv) with **11** (1 equiv) using 5 mol % of Pd(tfa)<sub>2</sub> as the catalyst in AcOH at 120 °C (**Scheme 2.12**). This led to a 53% GC yield of product **82**, thereby demonstrating the viability of incorporating

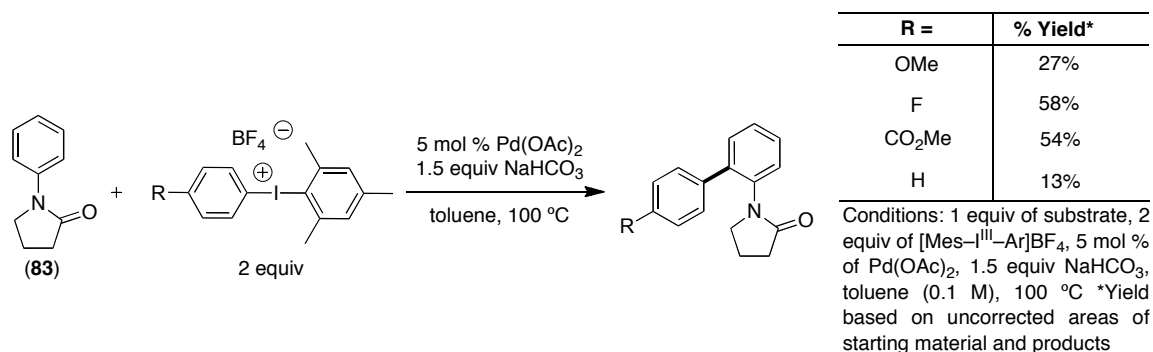
heteroarenes. Interestingly, both Mes-OAc ( $m/z = 178$ ) and Mes-OTs ( $m/z = 290$ ) were observed as byproducts.

**Scheme 2.12:** Pd-Catalyzed Reaction of **11** with [Mes-I-(2-thiophene)]BF<sub>4</sub> (**81**).



In addition to pyridine directing groups, it is desirable to expand the utility of this reaction to the installation of diverse Ar substituents with substrates containing oxygen-directing groups. Initial investigations focused on *N*-phenylpyrrolidinone (**83**) under the optimal conditions demonstrated for phenylation of substrates containing oxygen directing groups, but utilizing [Mes-I<sup>III</sup>-(*p*-XPh)]BF<sub>4</sub> as the oxidant. These attempts led to incomplete conversion of starting material to product based on GC (**Scheme 2.13**).

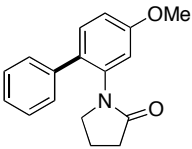
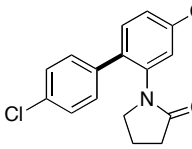
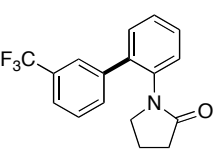
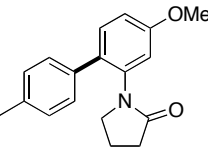
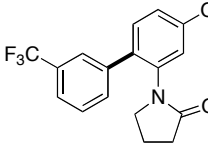
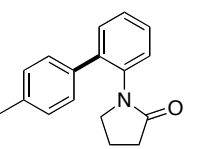
**Scheme 2.13:** Product Yields with **83** and [Mes-I-(*p*-XC<sub>6</sub>H<sub>4</sub>)]BF<sub>4</sub> oxidants.



Upon screening other oxidant variations, it was found that 2.0 equiv of the symmetrical oxidant [Ar-I<sup>III</sup>-Ar]BF<sub>4</sub> provided higher yields. Optimal conditions were determined to be 5 mol % of Pd(OAc)<sub>2</sub>, 2.0 equiv of the symmetric oxidants [Ar-I-Ar]BF<sub>4</sub> and 1.5 equiv of NaHCO<sub>3</sub> in toluene or chloroform at 100 °C. As with the pyridine directing groups, both electron rich (**85**, **89**) and electron poor aryl groups (**86**–**88**) could be successfully installed. Furthermore, tolerance toward aryl halides (**86**),

benzylic C–H bonds (**85**, **89**), and ethers (**84**, **86**, **87**) was demonstrated (Table 2.6). Selective monoarylation was observed in substrates where multiple functionalizations are possible, as was observed in phenylation (*vide supra*).

**Table 2.6:** Arylation of Pyrrolidinone Substrates with  $[\text{Ar-I}^{\text{III}}-\text{Ar}]\text{BF}_4$ .

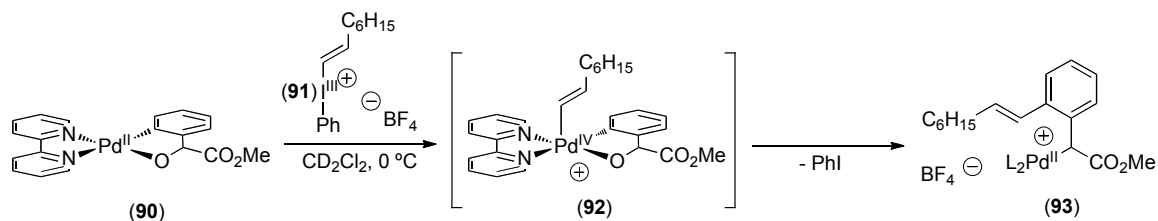
Entry	Product	Yield	Entry	Product	Yield	Entry	Product	Yield
1		(73%) <b>84</b>	3		(66%) <b>86</b>	5		(80%) <b>88</b>
2		(85%) <b>85</b>	4		(87%) <b>87</b>	6		(85%) <b>89</b>

Conditions: 1 equiv of substrate, 2 equiv of  $[\text{Ar-I}^{\text{III}}-\text{Ar}]\text{BF}_4$ , 5 mol % of  $\text{Pd}(\text{OAc})_2$ , 1.5 equiv  $\text{NaHCO}_3$ , toluene (0.1 M), 100 °C

## 2.4 Alternative $\text{I}^{\text{III}}$ Reagents

In addition to employing  $[\text{Ar-I}^{\text{III}}-\text{Ar}]^+$  for the oxidation of  $\text{Pd}^{\text{II}}$  complexes, several literature reports have examined the viability of both  $[\text{Ph-I}^{\text{III}}-\text{vinyl}]^+$  and  $[\text{Ph-I}^{\text{III}}-\text{alkynyl}]^+$  reagents as oxidants. For example, Malinakova achieved the oxidation of  $\text{Pd}^{\text{II}}$  complex **90** to  $\text{Pd}^{\text{IV}}$  complex **92** by utilizing vinyl  $\text{I}^{\text{III}}$  reagent **91**. This complex subsequently underwent C–C bond forming reductive elimination to afford product **93**.<sup>11</sup>

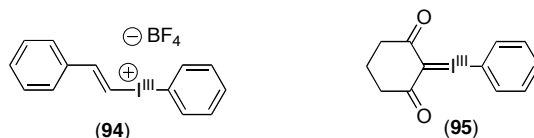
**Scheme 2.14:** Stoichiometric Oxidation using a Vinyl- $\text{I}^{\text{III}}$  Oxidant.



This report provided precedent for the expansion of our methodology to C–H activation/alkenylation. Our brief studies in this area focused on oxidant **94**, which was

synthesized according to literature procedures (**Figure 2.2**).<sup>19</sup> However, a screen of the reaction between 2-phenylpyridine, 1.2 equiv of oxidant **94**, and 5 mol % of Pd(OAc)<sub>2</sub> at 100 °C in numerous solvents (AcOH, CH<sub>3</sub>CN, trifluorotoluene, MeOH, dichloroethane, chlorobenzene, dioxane, trifluoroethanol, benzene and CHCl<sub>3</sub> at 0.1 M) resulted in no reaction based on GC. A temperature study was also undertaken at 60, 80, 100, and 120 °C but provided the same result. The lack of reactivity is likely due to the decomposition of the oxidant **94** under these reaction conditions.<sup>26</sup> The vinylidonium reagent may have undergone hydrolysis with solvent or adventitious water, as has been observed with similar reagents.

**Figure 2.2:** Alternative I<sup>III</sup> Oxidants Attempted for C–H Arylation.



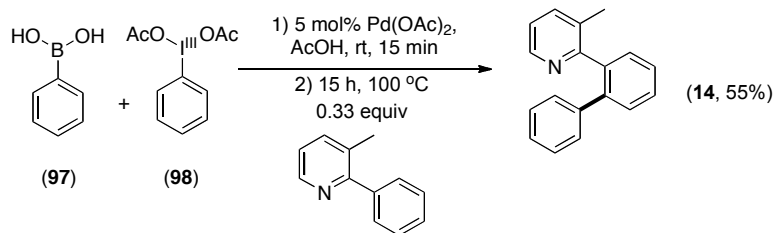
Additionally, I<sup>III</sup> reagent **95** containing a dione was also employed as an alternative oxidant for C–H activation/C–C bond formation.<sup>27</sup> This substrate was screened with 2-phenylpyridine, 1.1 equiv of oxidant **95** and 5 mol % of Pd(OAc)<sub>2</sub> at 100 °C using the same solvents. These reactions also failed to provide any product as determined by GC. This oxidant may not be reactive because of increased stabilization of the positive charge on I<sup>III</sup> due to its ylide nature. This would result in **95** being less electrophilic than the [Ar–I<sup>III</sup>–Ar]BF<sub>4</sub> oxidants and therefore less reactive.

## 2.5 In situ Oxidant Generation

A potential limiting factor for the above-described methodology is the lack of commercially available oxidants. [Ph–I<sup>III</sup>–Ph]<sup>+</sup> salts are available from several commercial sources, but I<sup>III</sup> reagents with diverse aryl substituents are not. While these oxidants are operationally simple to isolate from readily available starting materials, they are limited in their versatility due to the necessity to synthesize them. This becomes limiting especially in the context of screening a large number of Ar groups. Thus, an important advance to this methodology would be the generation of the I<sup>III</sup> oxidant bearing

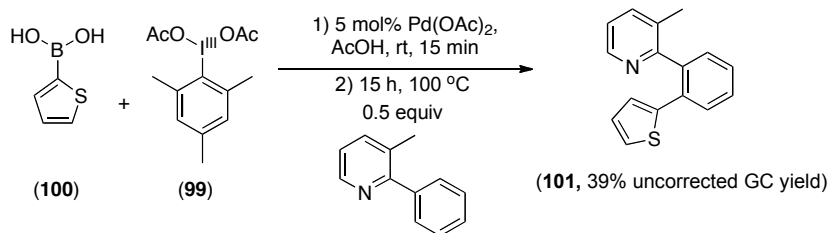


**Scheme 2.16:** Phenylation of 3-Methyl-2-Phenylpyridine by *in situ* Oxidant Generation.



We next sought to extend this system to heteroarylation. This was first explored by using MesI<sup>III</sup>(OAc)<sub>2</sub> (**99**) with 2-thiophene boronic acid (**100**), which would generate [Mes-I<sup>III</sup>-(2-thiophene)]OAc upon coupling. Initial screening began with solvent studies under conditions similar to the phenylation example (5 mol % of Pd(OAc)<sub>2</sub>, 2 equiv of MesI<sup>III</sup>(OAc)<sub>2</sub> (**99**) and 2 equiv of 2-thiophene boronic acid at 100 °C (**Scheme 2.17**). Gratifyingly, these reaction conditions gave the desired product (**101**) as analyzed by GCMS, albeit in low yield (39% based on the uncorrected GC peak areas).

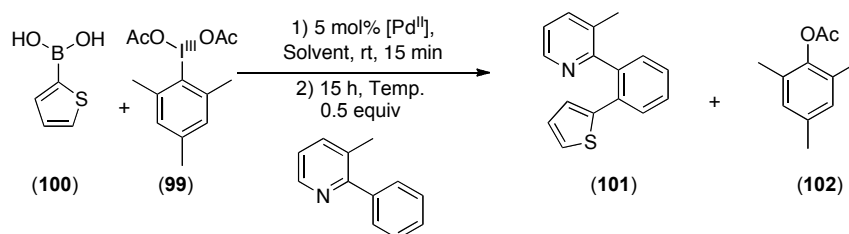
**Scheme 2.17:** Heteroarylation of 3-Methyl-2-Phenylpyridine by *in situ* Oxidant Generation.



We next performed a series of optimization experiments to investigate this reaction further. A study of solvent effects indicated that only reactions completed in acidic solvents afforded the desired product **101**, with AcOH providing the best yield (**Scheme 2.18**). The yields are reported as uncorrected ratios based on the areas of the product and starting material peaks as determined by GC. Investigation of the effect of temperature revealed that higher temperatures provided better yield (56%) with 120 °C being optimal (**Scheme 2.18**). Finally, different catalysts were examined, which revealed that Pd(tfa)<sub>2</sub> provided a similar yield (55%) as that observed with Pd(OAc)<sub>2</sub> (56%) (**Scheme 2.18**). This reaction was then repeated on a larger scale and resulted in the

desired product **101** in a 23% isolated yield. Interestingly, Mes-OAc (**102**) appears to be a significant byproduct in all of the above reaction mixtures, as determined by GC/MS ( $m/z = 178$ ).

**Scheme 2.18:** Optimizations for *in situ* C–H Activation/Heteroarylation.



Solvent Study <sup>a,b,c</sup>			Temperature Study <sup>a,b</sup>			Catalyst Study <sup>a,c,d</sup>		
Entry	Solvent	Yield	Entry	Temperature (°C)	Yield	Entry	Catalyst	Yield
1	AcOH	39%	7	120 °C	41%	13	Pd(OAc) <sub>2</sub>	41%
2	TFA	6%	8	100 °C	56%	14	Pd(tfa) <sub>2</sub>	55%
3	CH <sub>2</sub> Cl <sub>2</sub>	0%	9	80 °C	21%	15	PdCl <sub>2</sub>	54%
4	Dichloroethane	0%	10	70 °C	25%	16	K <sub>2</sub> PdCl <sub>4</sub>	6%
5	CH <sub>3</sub> CN	0%	11	60 °C	8%	17	PdI <sub>2</sub>	14%
6	Toluene	0%	12	50 °C	10%			

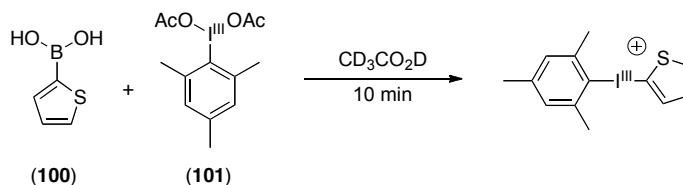
Conditions: 5 mol % of [Pd<sup>II</sup>], solvent (0.1 M), 1 equiv of 2-thiophene boronic acid, 1 equiv of MesI<sup>III</sup>(OAc)<sub>2</sub>, 0.5 equiv of 2-methyl-2-phenylpyridine and yield based on GC peak areas of starting material and product,<sup>a</sup> [Pd<sup>II</sup>] was Pd(OAc)<sub>2</sub>,<sup>b</sup> Reaction solvent was AcOH. <sup>c</sup>Reaction was run at 100 °C. <sup>d</sup>Reaction temp was 120 °C.

Based on the incomplete conversion of starting material to product as well as the observed byproduct, we hypothesized that decomposition of the oxidant to Mes-OAc is competitive with the desired C–H activation/heteroarylation. We next examined if the limitations were a result of incomplete oxidant formation, or of a decomposition process competes with C–H activation/heteroarylation. To accomplish this, two comparisons were made with the independently isolated [Mes–I<sup>III</sup>–(2-thiophene)]BF<sub>4</sub> (**81**). First, it was earlier demonstrated that the reaction of **81** with 3-methyl-2-phenylpyridine (**11**) resulted in a 55% yield based upon GC with the observation of the Mes-OAc and Mes-OTs byproducts (**Scheme 2.12**). This yield is identical to what was observed when the oxidant was generated *in situ* (55%), and has similar byproducts. Second, 2-thiophene boronic acid was combined with MesI<sup>III</sup>(OAc)<sub>2</sub> in CD<sub>3</sub>CO<sub>2</sub>D (**Scheme 2.19**). After 10 minutes, analysis by <sup>1</sup>H NMR showed that resonances associated with starting material had moved to approximately the same chemical shifts of [Mes–I<sup>III</sup>–(2-thiophene)]BF<sub>4</sub> (**81**). This suggested that the oxidant was cleanly being formed, and also that it did not require



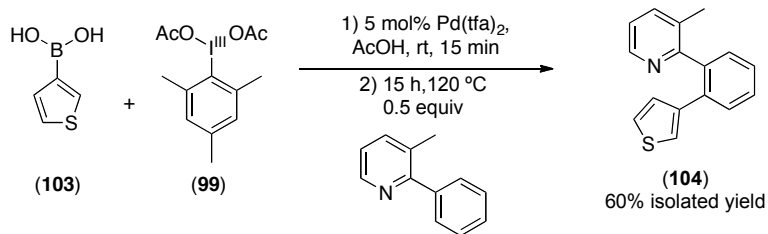
$\text{Pd}(\text{OAc})_2$  for its formation. It appears based on these experiments that the challenge is associated with the C–H activation/heteroarylation reaction, and not the oxidant formation.

**Scheme 2.19:** Generation of  $[\text{Mes-I}^{\text{III}}-(2\text{-thiophene})]^+$  *in situ*.



Efforts next turned to examining 3-thiophene boronic acid, to investigate if the challenges encountered with 2-thiophene boronic acid were general. This was completed by combining 2 equiv  $\text{MesI}^{\text{III}}(\text{OAc})_2$  (99) with 2 equiv of 3-thiophene boronic acid (103) in AcOH and then adding 5 mol % of  $\text{Pd}(\text{tfa})_2$ . This solution was stirred at room temperature for 15 min, then 1 equiv of 3-methyl-2-phenylpyridine was added, and the reaction was heated to 120 °C for 15 h. In contrast to the previous results, the desired product 104 was isolated in 60% yield (87% yield by GC, **Scheme 2.20**). However, it is important to note however, that the same  $\text{MesOAc}$  (102) byproduct described above was present.

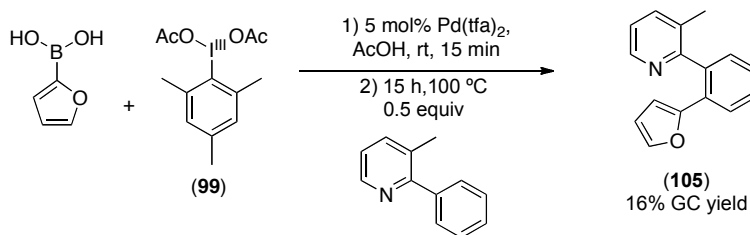
**Scheme 2.20:** *in situ* C–H Arylation with 3-Thiopheneboronic Acid.



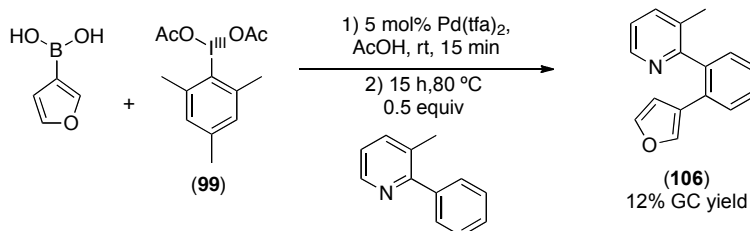
In addition to thiophenes, attempts were also made to generate oxidants *in situ* with furyl boronic acids. Unfortunately the use of 2-furyl boronic acid and 3-furyl boronic acid led to low yields of the desired products based upon GC. Even after optimizing the reaction temperature, only 16% (105, **Scheme 2.21**) and 12% (106,

**Scheme 2.22)** yields were obtained at 100 °C and 80 °C, respectively. Once again Mes-OAc was observed as a byproduct. An  $^1\text{H}$  NMR experiment analogous to that with 2-thiophene boronic acid was completed for 2-furyl boronic acid. 2-Furyl boronic acid and  $\text{MesI}^{\text{III}}(\text{OAc})_2$  were combined in  $\text{CD}_3\text{CO}_2\text{D}$ , and after 15 min all of the resonances had shifted upfield. This suggested that the oxidant was successfully being formed as in the previous example, and that  $\text{Pd}(\text{OAc})_2$  was not necessary. It also once again suggested that the challenges lie with the C–H activation/heteroarylation, not the *in situ* oxidant generation.

**Scheme 2.21:** *in situ* C–H Arylation with 2-Furylboronic Acid.



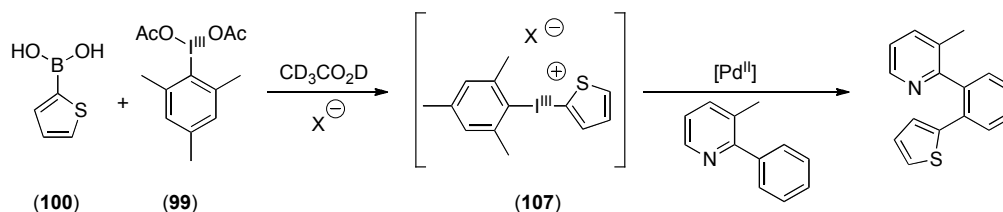
**Scheme 2.22:** *in situ* C–H Arylation with 3-Furylboronic Acid.



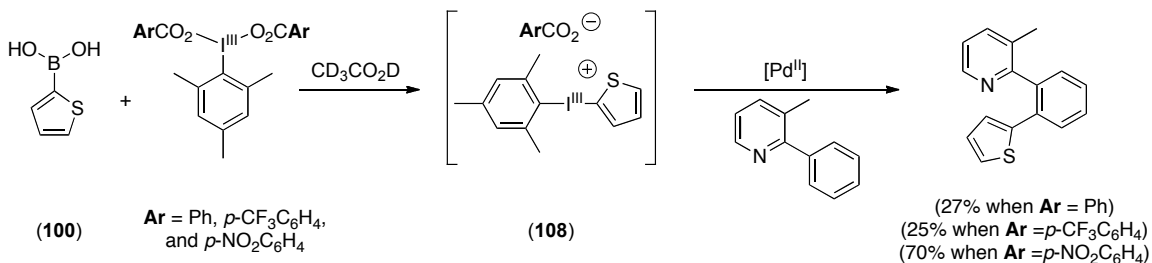
Since Mes-OAc (**102**) was observed repeatedly, we next set out to establish a method to decrease formation of this byproduct. Our method for generating  $[\text{Mes-I}^{\text{III}}-(2\text{-thiophene})]^+$  *in situ* leads to an  $\text{OAc}^-$  counterion that is provided by the initial  $\text{I}^{\text{III}}$  reagent (**99**). It was reasoned that utilizing a less nucleophilic/donating counterion could have two beneficial effects. First, it should render the  $\text{I}^{\text{III}}$  reagent more electrophilic, making it a stronger oxidant and possibly increasing the amount of desired product. Second, this should eliminate any direct nucleophilic attack of the  $\text{AcO}^-$  on the electrophilic  $\text{I}^{\text{III}}$  reagent to generate Mes-OAc. One to install the desired counterion was to exchange the anion *in situ* during the generation of the oxidant to afford **107** (**Scheme 2.23**). This was

first attempted by adding  $\text{Li}^+$ ,  $\text{Na}^+$ , and  $\text{K}^+$  salts that have non-coordinating counterions  $\text{BF}_4^-$ ,  $\text{SO}_3\text{CF}_3^-$ , and  $\text{PF}_6^-$ , and halide salts. Additionally, strong acids such as  $\text{CH}_3\text{SO}_3\text{H}$ ,  $\text{H}_2\text{SO}_4$ ,  $\text{CF}_3\text{CO}_2$  and  $\text{HBF}_4$  were added to the reaction mixture. However, under the conditions described above, none of the additives resulted in increased yields. A second approach for achieving a more non-coordinating counterion was to begin with  $\text{MesI}^{\text{III}}(\text{O}_2\text{CAr})_2$ , ( $\text{Ar} = \text{Ph}$ ,  $p\text{-CF}_3\text{C}_6\text{H}_4$ , and  $p\text{-NO}_2\text{C}_6\text{H}_4$ ), where the counterion  $\text{ArCO}_2^-$  for  $[\text{Mes-I}^{\text{III}}-(2\text{-thiophene})]^+$  (**108**) would originate from the  $\text{I}^{\text{III}}$  starting material (**Scheme 2.24**). It was found that while benzoate and  $p$ -trifluoromethylbenzoate analogs could only be generated in low yields (27% and 25% respectively),  $p$ -nitrobenzoate provided the desired product in an improved 70% yield by GC. Nevertheless, this reaction could not be driven to completion, so we chose to peruse other methods of forming oxidants *in situ*.

**Scheme 2.23:** Control of Oxidant Counterion by the Addition of Additives.



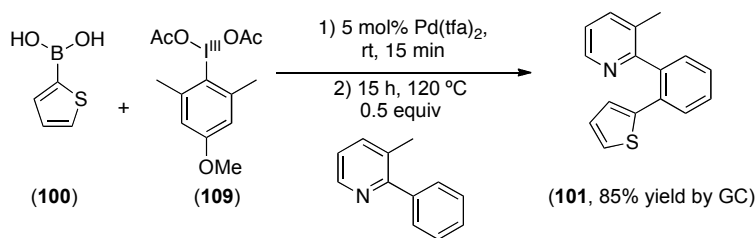
**Scheme 2.24:** Control of Oxidant Counterion by Variation of  $\text{I}^{\text{III}}$  Ligands.



We expected that a more electron rich arene for  $\text{ArI}^{\text{III}}(\text{OAc})_2$  would provide a less electrophilic  $[\text{Mes-I}^{\text{III}}-(2\text{-thiophene})]^+$  oxidant, and was expected to result in a decrease in the direct reduction to  $\text{ArOAc}$ . As shown in **Scheme 2.25** the reaction of  $\text{ArI}^{\text{III}}(\text{OAc})_2$  ( $\text{Ar} = 2,5\text{-dimethyl-3-methoxyphenyl}$ , **109**) with 2-thiophene boronic acid and 3-methyl-

2-phenylpyridine under the conditions described above provided the desired product **101** in 85% yield. The challenge to expanding upon this approach is the difficulty associated with oxidizing electron rich aryl iodides to the corresponding diacetates using common methods. For example, **109** was isolated in only a 1% yield using  $\text{NaBO}_3 \cdot 4\text{H}_2\text{O}$  as an oxidant, while oxidation with  $\text{AcOOH}$  was completely unsuccessful.<sup>20,28</sup> Additionally, 2,4,6-trimethoxy-1-iodobenzene diacetate could not be tested catalytically because we were unable to oxidize the corresponding aryl iodide using  $\text{NaBO}_3 \cdot 4\text{H}_2\text{O}$ ,  $\text{NaIO}_4$ , or  $\text{Na}_2\text{S}_2\text{O}_8$ .<sup>20,29,30</sup> Due to these challenges, no attempts were made to preparatively isolate products from these reactions.

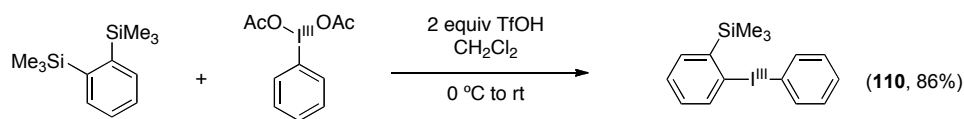
**Scheme 2.25:** Variation of  $\text{Ar}^{\text{III}}(\text{OAc})_2$  for *in situ* Oxidant Generation



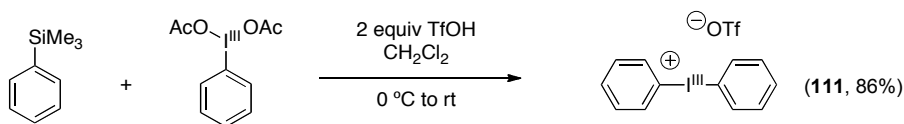
**Silane Reagents**

Arylsilane reagents have also been viable coupling partners for  $\text{Ar}^{\text{III}}(\text{OAc})_2$  to give  $[\text{Ar}'\text{-I}^{\text{III}}\text{-Ar}]^+$  reagents. Fujiwara has previously demonstrated that 1,2-trimethylsilylbenzene can be coupled with  $\text{PhI}^{\text{III}}(\text{OAc})_2$  to generate the diaryl iodonium salt **110** (Scheme 2.26).<sup>31</sup> Prior to attempting sequential oxidant formation and C–H arylation, we first confirmed that the coupling of  $\text{PhI}^{\text{III}}(\text{OAc})_2$  and  $\text{PhSiMe}_3$  could be used to afford **111** in good yields (88%) under the reported conditions (Scheme 2.27).

**Scheme 2.26:** Coupling Aryltrimethylsilanes with  $\text{PhI}^{\text{III}}(\text{OAc})_2$ .<sup>31</sup>

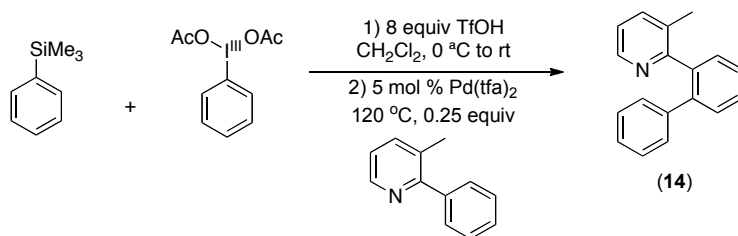


**Scheme 2.27:** Coupling of PhSiMe<sub>3</sub> with PhI<sup>III</sup>(OAc)<sub>2</sub>.



The one pot oxidant generation/arylation reaction was next explored. This was attempted by combining PhSiMe<sub>3</sub>, PhI<sup>III</sup>(OAc)<sub>2</sub> and TfOH in CH<sub>2</sub>Cl<sub>2</sub> at 0 °C for 2h, then allowing the solution to return to room temperature. Next, 5 mol % Pd(tfa)<sub>2</sub> and 0.25 equiv of **11** were added and the reaction was heated to 120 °C for 15 h (**Scheme 2.28**). Initial attempts resulted in no product by GC analysis leading us to probe alternative reaction conditions. We began by studying the effect of added bases under otherwise analogous conditions. Bases that were examined included NaHCO<sub>3</sub>, K<sub>2</sub>CO<sub>3</sub>, NaOAc, pyridine, and KOH. With the addition of 3 equiv of NaHCO<sub>3</sub> it was found that this reaction provided the desired product **14** with an average yield of 80% by gas chromatography, while the other bases resulted in no product or low yield (<20%). Next, a solvent screen was undertaken with 2 equiv of PhSiMe<sub>3</sub> and PhI<sup>III</sup>(OAc)<sub>2</sub> relative to substrate. High yields (>70%) could be achieved in a variety of solvents including CH<sub>2</sub>Cl<sub>2</sub>, CHCl<sub>3</sub>, dichloroethane, trifluorotoluene, benzene, and chlorobenzene, with the best being CHCl<sub>3</sub> (94% yield). However, unfortunately, when this reaction was scaled from 0.06 to 0.4 mmol of substrate, the reaction only proceeded in 33% yield. Low yields on the larger scale may be due to challenges of maintaining a constant 0 °C temperature during the exothermic oxidant generation, resulting in an incomplete oxidant formation and low yields. Further optimization and careful control of conditions will be necessary for this method to prove valuable.

**Scheme 2.28:** *In situ* Oxidant Generation with PhSiMe<sub>3</sub> and PhI<sup>III</sup>(OAc)<sub>2</sub>.



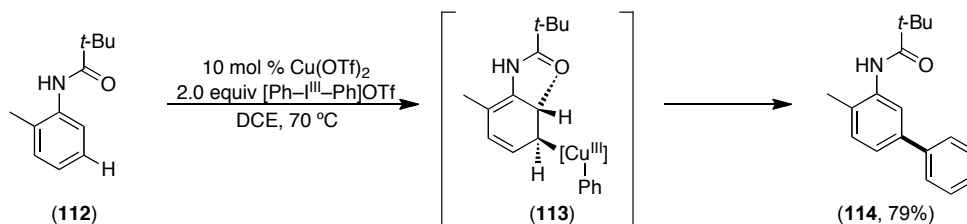
In summary, attempts to generate the requisite  $[\text{Ar-I}^{\text{III}}-\text{Ar}]\text{BF}_4$  *in situ* followed by  $\text{Pd}^{\text{II}}$  catalyzed C–H arylation has proven to be challenging for both boronic acid and silane starting materials. While these methods have successfully been employed to provide the desired products, the results were found to be inconsistent for each case. Even successful cases did not meet the initial aims of utilizing readily available starting materials and being operationally simple. Due to these deficiencies, other projects were pursued.

## 2.6 Subsequent Examples of C–H Arylation Methodology

Following our publication of this methodology, numerous literature reports have appeared exploring palladium-catalyzed C–H arylation, and several of these are particularly notable.<sup>32</sup> These examples of C–H arylation fall into 4 general categories: (1) further utilization of  $[\text{Ar-I}^{\text{III}}-\text{Ar}]^+$  reagents, (2) employment of  $\text{Ag}^+$  salts with Ar–I oxidants, (3) the development of  $\text{Pd}^{\text{II/0}}$  catalyzed methodologies that introduce the arene via a transmetallating reagent, and (4) oxidative coupling.

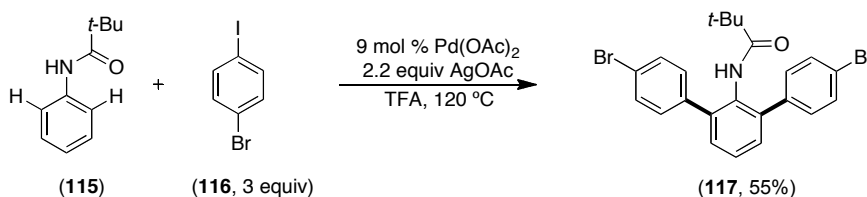
In the first general category, there are two important examples further exploring the utility of  $[\text{Ar-I}^{\text{III}}-\text{Ar}]^+$  oxidants for C–H arylation. First, Daugulis demonstrated an analogous palladium-catalyzed C–H phenylation using  $[\text{Ph-I}^{\text{III}}-\text{Ph}]\text{PF}_6$  oxidants with substrates containing pivalate directing groups.<sup>33</sup> Second, the Gaunt group demonstrated copper-catalyzed meta C–H arylation with  $[\text{Ph-I}^{\text{III}}-\text{Ph}]\text{OTf}$  reagents (**Scheme 2.29**).<sup>34,35</sup> This latter reaction was proposed to proceed through intermediate **113** to provide the product **114**. This is notable because it provides the *meta* arylation which is complimentary to the *ortho* arylation developed in our laboratory.

**Scheme 2.29:** *Meta* C–H Arylation Using a Copper Catalyst.<sup>34</sup>



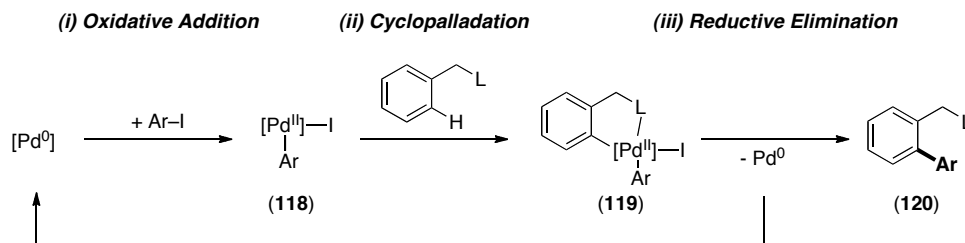
The second general category of reactions developed for C–H arylation utilizes Ar–I with a stoichiometric silver additive. Daugulis initially demonstrated that combining substrates containing a pivalate directing group such as **115** with an Ar–I (**116**) and AgOAc afforded the C–H arylation product **117** (**Scheme 2.30**).<sup>33</sup> This was then extended to a variety of additional directing groups by his lab and others.<sup>36-43</sup> The mechanism of this arylation is proposed to involve an Ar–Pd<sup>IV</sup> intermediate, however experiments to elucidate the details have not been reported.

**Scheme 2.30:** C–H Arylation Employing Ar–I and Stoichiometric AgOAc.<sup>33</sup>



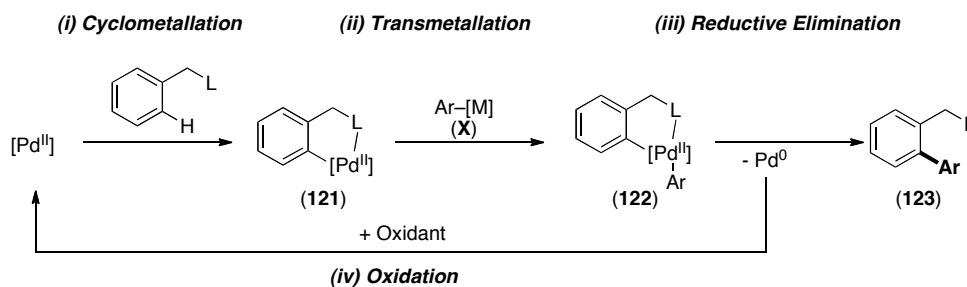
The third general category employs a transmetallating reagent to provide the aryl group for functionalization. This is in contrast to Miura’s pioneering work that introduced the arene from the oxidant (*e.g.* an aryl halide). The general mechanism of previous methodology developed by Miura is shown in **Scheme 2.31** and is believed to proceed through: (i) oxidative addition of an Ar–I to Pd<sup>0</sup> to give **118**, followed by (ii) cyclometallation at Ar–Pd<sup>II</sup> to afford **119**, and final (iii) C–C bond forming reductive elimination to afford the product **120**.<sup>44-52</sup>

**Scheme 2.31:** General Mechanism of Miura’s C–H Arylation.<sup>44-52</sup>



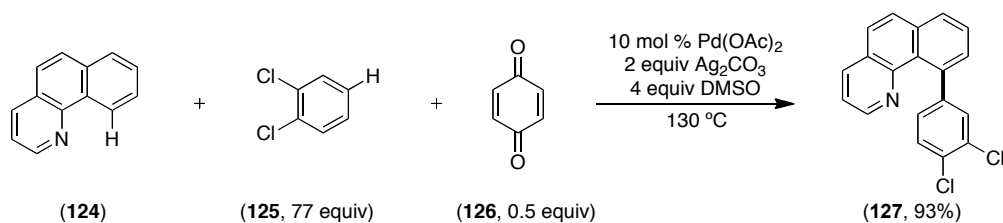
In contrast, the recently developed chemistry employing boron and silane transmetallating reagents is believed to proceed through the general mechanism shown in **Scheme 2.32**.<sup>43,53-57</sup> This involves: (i) cyclometallation of Pd<sup>II</sup>, (ii) transmetalation of the Ar group from Ar-[M] (**121**) to palladium to afford a cyclometallated Ar-[Pd<sup>II</sup>] (**122**), (iii) C-C bond forming reductive elimination to release the product (**123**), and (iv) oxidation of palladium to Pd<sup>II</sup> by oxidants such as benzoquinone, silver, and copper. Importantly in this mechanism, the order of the cyclometallation and transmetalation steps can be reversed.

**Scheme 2.32:** General Mechanism of C-H Arylation using a Transmetalating Reagent.



Finally, our lab and others have demonstrated an oxidative coupling approach to biaryl formation.<sup>58-64</sup> This method results in the direct coupling of two unfunctionalized C-H bonds (**Scheme 2.33**). An example of this from our lab employed substrate **124** containing a nitrogen directing group along with the simple arene **125**, Pd(OAc)<sub>2</sub>, AgOAc, and benzoquinone **126** to provide the oxidative coupling product **127**.<sup>58,59</sup> This example is proposed to proceed through a Pd<sup>0/II</sup> catalytic cycle, and the mechanistic details of this transformation have been investigated.<sup>60</sup>

**Scheme 2.33:** C-H Arylation through Oxidative Coupling.<sup>59</sup>





## 2.7 Conclusions

We have developed a ligand-directed, Pd<sup>II</sup> catalyzed C–H activation/C–C bond forming reaction which employs [Ar–I<sup>III</sup>–Ar]BF<sub>4</sub> reagents as the terminal oxidant. We propose that these reactions proceed through a Pd<sup>II/IV</sup> mechanism analogous to the C–H acetoxylation previously studied in our group. The utility of this reaction has been established by exploring both nitrogen and oxygen based directing groups for the site selective installation of different aryl substituents. Additionally, we have demonstrated installation of a diverse set of arenes with a broad functional group tolerance, which includes complementary reactivity to arylations via Pd<sup>0/II</sup> catalytic cycles. Efforts were then directed toward the development of an *in situ* oxidant generation from more readily available materials, which would eliminate the need for isolation of the oxidant. Although this succeeded conceptually, the conditions and materials required, as well as issues with reproducibility, limited its practical utility.

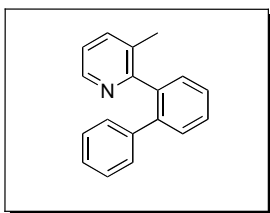
## 2.8 General Procedures and Materials and Methods

**General Procedures:** NMR spectra were obtained on a Varian Inova 500 (499.90 MHz for <sup>1</sup>H; 125.70 MHz for <sup>13</sup>C) or a Varian Inova 400 (399.96 MHz for <sup>1</sup>H; 100.57 MHz for <sup>13</sup>C) spectrometer. <sup>1</sup>H NMR chemical shifts are reported in parts per million (ppm) relative to TMS, with the residual solvent peak used as an internal reference. Multiplicities are reported as follows: singlet (s), doublet (d), doublet of doublets (dd), doublet of triplets (dt), triplet (t), quartet (q), multiplet (m), and broad resonance (br).

**Materials and Methods:** 8-methylquinoline, 2-phenylquinoline, *N*-phenylpyrrolidinone, *N*-phenyloxazolidinone, 1-(indolin-1-yl)ethanone, and *N*-(3-chlorophenyl)acetamide were obtained from commercial sources and used as received. Substrate **11** was prepared by Suzuki cross-coupling of phenyl boronic acid and 2-bromo-3-methylpyridine according to a literature procedure.<sup>65</sup> Pyridine substrates in Table 2.1 (entries 1, 2, 3, and 6) and substrate **71** were prepared by Stille cross-coupling of 2-tributylpyridyltin with the corresponding aryl bromides.<sup>66</sup> Amide substrates in Table 2.1 entries 8, 9, and 10 were prepared by palladium-catalyzed arylation of the corresponding lactam.<sup>67</sup> Pd(OAc)<sub>2</sub> was

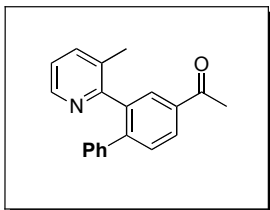
obtained from Pressure Chemical and used as received and  $\text{PhI}(\text{OAc})_2$  was obtained from Acros and used as received. Solvents were obtained from Fisher Chemical and used without further purification. Gas chromatography was carried out using a Shimadzu 17A using a Restek Rtx®-5 (Crossbond 5% diphenyl – 95% dimethyl polysiloxane; 15 m, 0.25 mm ID, 0.25 mm ID, 0.25  $\mu\text{m}$  df) column. Flash chromatography was performed on EM Science silica gel 60 (0.040–0.063 mm particle size, 230–400 mesh) and thin layer chromatography was performed on Merck TLC plates pre-coated with silica gel 60 F254. Control reactions (in the absence of Pd catalyst) were run for each substrate, and generally showed no reaction under our standard conditions. In general, crude reaction mixtures were filtered through glass wool or Celite to remove insoluble materials that form at the end of the reaction before workup. GC yields were calculated from the peak area of the product divided by the total peak area of starting material and products, unless otherwise noted.

## Experimental Procedures



**Product 14:** 3-methyl-2-phenylpyridin (200 mg, 1.18 mmol, 1 equiv),  $[\text{Ph}_2\text{I}]\text{BF}_4$  (500 mg, 1.36 mmol, 1.15 equiv) and  $\text{Pd}(\text{OAc})_2$  (13.2 mg, 0.059 mmol, 5 mol%) were combined in acetic acid (10 mL) in a 20 mL vial. The vial was sealed with a Teflon lined cap, and the reaction was stirred at 100 °C for 12 h. The reaction mixture was filtered through a plug of Celite and then concentrated under vacuum. The resulting crude oil was dissolved in  $\text{CH}_2\text{Cl}_2$  and extracted with saturated aqueous  $\text{NaHCO}_3$  (2 x 30 mL) and brine (1 x 30 mL). The organic layer was dried over  $\text{MgSO}_4$ , filtered, and concentrated to afford an orange oil, which was purified by chromatography on silica gel ( $R_f = 0.2$  in 95%  $\text{CH}_2\text{Cl}_2$ /5% ethyl acetate). The product was obtained as a viscous yellow oil (255 mg, 88% yield);  $^1\text{H}$  NMR ( $d_6$ -acetone):  $\delta$  8.47 (d,  $J = 4.8$  Hz, 1H), 7.55-7.43 (multiple peaks, 3H), 7.40 (d,  $J = 7.5$  Hz, 1H), 7.37-7.35 (m, 1H), 7.21-7.10 (multiple peaks, 6H), 1.75 (s, 3H).  $^{13}\text{C}\{^1\text{H}\}$  NMR ( $d_6$ -acetone):  $\delta$  161.29, 148.19, 142.99, 142.40, 141.62,

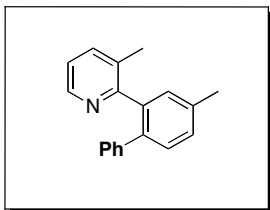
139.03, 133.06, 131.80, 131.32, 130.92, 130.04, 129.58, 128.98, 128.48, 124.00, 19.95. Anal. Calcd for C<sub>18</sub>H<sub>15</sub>N: C, 88.13, H, 6.16, N, 5.71; Found: C, 88.15, H, 6.17, N, 5.43. IR (thin film) 1418 cm<sup>-1</sup>.



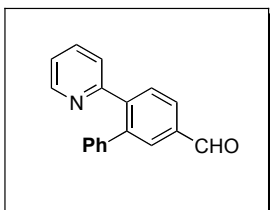
**Product 15:** 1-(3-(3-methylpyridin-2-yl)phenyl)ethanone (150 mg, 0.76 mmol, 1 equiv), [Ph<sub>2</sub>I]BF<sub>4</sub> (420 mg, 1.14 mmol, 1.5 equiv), and Pd(OAc)<sub>2</sub> (8.5 mg, 0.038 mmol, 5 mol%) were combined in acetic acid (6 mL) in a 20 mL vial. The vial was sealed with a Teflon lined cap and the reaction was heated at 100 °C for 2 days. The reaction mixture was filtered through a plug of Celite and then evaporated to dryness. The resulting oil was dissolved in CH<sub>2</sub>Cl<sub>2</sub> and extracted with saturated aqueous NaHCO<sub>3</sub> (2 x 30 mL) and brine (1 x 30 mL). The organic layer was dried over MgSO<sub>4</sub>, filtered, and concentrated to afford an orange oil, which was purified by chromatography on silica gel (R<sub>f</sub> = 0.25 in 88% CH<sub>2</sub>Cl<sub>2</sub>/12% ethyl acetate). The product was obtained as an orange/brown solid (189 mg, 91% yield); mp 77-78 °C. <sup>1</sup>H NMR (acetone-*d*<sub>6</sub>): δ 8.59-8.57 (m, 1H), 8.07 (dd, *J* = 8.0, 1.9 Hz, 1H), 8.24 (d, *J* = 1.8 Hz, 1H), 7.55 (d, *J* = 8.0, 1H), 7.50 (td, *J* = 7.7, 1.8 Hz, 1H), 7.26-7.25 (m, 3H), 7.21-7.18 (m, 1H), 7.16-7.13 (m, 2H), 6.96-6.93 (m, 1H), 2.63 (s, 3H). <sup>13</sup>C{<sup>1</sup>H} NMR (CDCl<sub>3</sub>): δ 197.80, 158.50, 149.81, 145.36, 140.37, 139.93, 136.43, 135.63, 131.12, 129.64, 128.44, 128.18, 127.64, 125.49, 122.99, 26.96. HRMS-electrospray (*m/z*): [M<sup>+</sup> + H] calcd for C<sub>19</sub>H<sub>15</sub>NO, 274.1232; found, 274.1233. Anal. Calcd for C<sub>19</sub>H<sub>15</sub>NO: C, 83.94, H, 5.53, N, 5.12; Found: C, 83.56, H, 5.45, N, 5.04. IR (KBr) 1683, 1586 cm<sup>-1</sup>.

The regioselectivity of this reaction could not be definitively determined from the <sup>1</sup>H NMR spectrum of **15** due to overlapping aromatic resonances. As a result, a deuterated version of this product was prepared by reaction of 1-(3-(3-methylpyridin-2-yl)phenyl)ethanone with [Mes-I-C<sub>6</sub>D<sub>5</sub>]BF<sub>4</sub> under analogous conditions to those described above. The <sup>1</sup>H NMR data for the deuterated product (**15-*d*<sub>5</sub>**) was as follows: <sup>1</sup>H

NMR ( $d_6$ -acetone):  $\delta$  8.69- 8.67 (m, 1H), 8.30 (d,  $J = 2.0$  Hz, 1H), 8.17 (dd,  $J = 8.0, 2.0$  Hz, 1H), 7.68 (d,  $J = 8$  Hz, 1H), 7.63 (dt,  $J = 7.5, 1.5$  Hz, 1H), 7.34-7.32 (m, 1H), 7.15-7.13 (m, 1H).

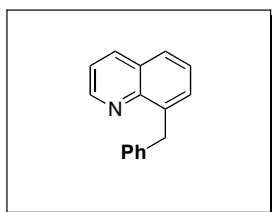


**Product 16:** 3-methyl-2-*m*-tolylpyridine (150 mg, 0.89 mmol, 1 equiv),  $[\text{Ph}_2\text{I}]\text{BF}_4$  (489 mg, 1.33 mmol, 1.5 equiv), and  $\text{Pd}(\text{OAc})_2$  (9.9 mg, 0.044 mmol, 5 mol%) were combined in acetic acid (4 mL) and acetic anhydride (4 mL) in a 20 mL vial. The vial was sealed with a Teflon lined cap and the reaction was heated at 100 °C for 12 h. The reaction mixture was filtered through a plug of Celite and then evaporated to dryness. The resulting oil was dissolved in  $\text{CH}_2\text{Cl}_2$  and extracted with saturated aqueous  $\text{NaHCO}_3$  (2 x 30 mL) and brine (1 x 30 mL). The organic layer was dried over  $\text{MgSO}_4$ , filtered, and concentrated to afford a yellow oil, which was purified by chromatography on silica gel ( $R_f = 0.24$  in 97.5%  $\text{CH}_2\text{Cl}_2/2.5\%$  ethyl acetate). The product was obtained as a brown solid (156 mg, 74% yield); mp 80-84 °C.  $^1\text{H}$  NMR ( $\text{C}_6\text{D}_6$ ):  $\delta$  8.58 (d,  $J = 4.8$  Hz, 1H), 7.79 (s, 1H), 7.27 (d,  $J = 7.8$  Hz, 1H), 7.22-7.20 (m, 2H), 7.04-6.95 (multiple peaks, 4H), 6.83- 6.79 (m, 2H), 6.77-6.75 (m, 1H), 2.17 (s, 3H).  $^{13}\text{C}\{^1\text{H}\}$  NMR ( $\text{CDCl}_3$ ):  $\delta$  158.88, 148.94, 140.85, 138.76, 137.36, 136.92, 134.68, 130.66, 130.03, 129.28, 128.86, 127.59, 126.08, 125.04, 120.84, 20.66. HRMS-electrospray ( $m/z$ ):  $[\text{M}^+ + \text{H}]$  calcd for  $\text{C}_{18}\text{H}_{15}\text{N}$ , 246.1283; found, 246.1290. IR (KBr) 1584  $\text{cm}^{-1}$ .



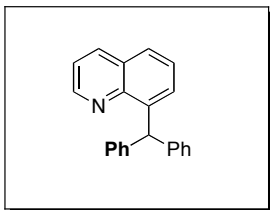
**Product 17:** 4-(pyridin-2-yl)benzaldehyde (200 mg, 1.09 mmol, 1 equiv),  $[\text{Ph}_2\text{I}]\text{BF}_4$  (441 mg, 1.20 mmol, 1.1 equiv), and  $\text{Pd}(\text{OAc})_2$  (12.2 mg, 0.054 mmol, 5 mol%) were combined in AcOH (9 mL) in a 20 mL vial. The vial was sealed with a Teflon lined cap,

and the reaction was heated at 100 °C overnight. GC analysis at the completion of the reaction showed 11% starting material, 67% mono-arylated product and 21% of the analogous diarylated product. The reaction mixture was filtered through a plug of Celite and evaporated to dryness. The resulting oil was dissolved in CH<sub>2</sub>Cl<sub>2</sub> and extracted with saturated aqueous NaHCO<sub>3</sub> (2 x 30 mL) and brine (1 x 30 mL). The organic extracts were dried over MgSO<sub>4</sub> and concentrated under vacuum to afford a yellow oil, which was purified by chromatography on silica gel ( $R_f = 0.25$  in 65% hexanes/35% ethyl acetate). The product was obtained as pale yellow solid (142 mg, 51% yield); mp 90-94 °C. <sup>1</sup>H NMR (C<sub>6</sub>D<sub>6</sub>): δ 9.71 (s, 1H), 8.51-8.49 (m, 1H), 7.87 (d,  $J = 9.7$  Hz, 1H), 7.74 (d,  $J = 1.5$  Hz, 1H), 7.61 (dd,  $J = 7.9, 1.5$ , 1H), 7.04-7.01 (m, 2H), 6.99-6.96 (multiple peaks, 3H), 6.74-6.66 (m, 2H), 6.52-6.28 (m, 1H). <sup>13</sup>C{<sup>1</sup>H} NMR (CDCl<sub>3</sub>): δ 191.60, 157.49, 149.32, 144.64, 141.15, 139.63, 135.77, 135.11, 131.60, 131.08, 129.17, 128.14, 127.97, 127.01, 124.97, 121.78. HRMS-electrospray ( $m/z$ ): [ $M^+ - H$ ] calcd for C<sub>18</sub>H<sub>13</sub>NO, 258.0919; found, 258.0922. IR (KBr): 1696, 1585 cm<sup>-1</sup>.

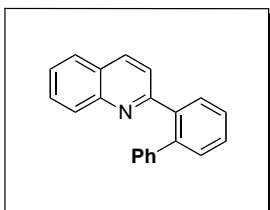


**Product 18:** 8-methylquinoline (619 mg, 4.32 mmol, 2 equiv), [Ph<sub>2</sub>I]BF<sub>4</sub> (794 mg, 2.16 mol, 1 equiv) and Pd(OAc)<sub>2</sub> (24 mg, 0.108 mmol, 5 mol%) were combined in a solution of benzene (9 mL) and acetic anhydride (9 mL) in a sealed container with a Teflon lined cap, and the reaction was stirred at 100 °C for 12 h. The reaction mixture was filtered through a plug of glass wool, and the resulting solution was concentrated under vacuum to afford a yellow oil, which was purified by chromatography on silica gel ( $R_f = 0.22$  in 70% CH<sub>2</sub>Cl<sub>2</sub>/30% hexanes). The product was obtained as a brown-orange solid (337 mg, 72% yield based on [Ph<sub>2</sub>I]BF<sub>4</sub>); mp: 52-53 °C. <sup>1</sup>H NMR (*d*<sub>6</sub>-acetone): δ 8.96 (dd,  $J = 4.2, 1.8$  Hz, 1H), 8.26 (dd,  $J = 8.3, 1.8$  Hz, 1H), 7.78 (dd,  $J = 8.1, 1.4$  Hz, 1H), 7.58-7.55 (m, 1H), 7.50-7.45 (multiple peaks, 2H), 7.38-7.36 (m, 2H), 7.26- 7.22 (m, 2H), 7.17-7.12 (m, 1H), 4.69 (s, 2H). <sup>13</sup>C{<sup>1</sup>H} NMR (*d*<sub>6</sub>-acetone): δ 151.36, 148.41, 143.67, 142.07, 137.91, 131.17, 130.88, 130.29, 129.96, 128.23, 128.12, 127.48, 122.97, 38.18. Anal.

Calcd for C<sub>16</sub>H<sub>13</sub>N: C, 87.64, H, 5.98, N, 6.39; Found: C, 87.63, H, 5.91, N, 6.35. IR (KBr) 1497, 1491 cm<sup>-1</sup>.

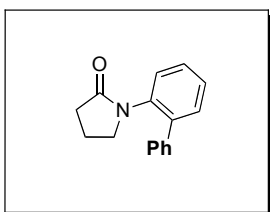


**Product 19: 18** (182 mg, 0.83 mmol, 1 equiv), [Ph<sub>2</sub>I]BF<sub>4</sub> (367 mg, 1.00 mmol, 1.2 equiv), and Pd(OAc)<sub>2</sub> (9.3 mg, 0.042 mmol, 5 mol%) were combined in acetic acid (3.5 mL) and acetic anhydride (3.5 mL) in a 20 mL vial. The vial was sealed with a Teflon lined cap and the reaction was heated at 100 °C for 12 h. The reaction mixture was filtered through a plug of Celite and then evaporated to dryness. The resulting oil was dissolved in CH<sub>2</sub>Cl<sub>2</sub> and extracted with saturated aqueous NaHCO<sub>3</sub> (2 x 30 mL) and brine (1 x 30 mL). The organic layer was dried over MgSO<sub>4</sub>, filtered, and concentrated to afford a pale yellow oil, which was purified by chromatography on silica gel (R<sub>f</sub> = 0.22 in 50% CH<sub>2</sub>Cl<sub>2</sub>/50% hexanes). The product was obtained as a white solid (147 mg, 60% yield); mp 135-137 °C. <sup>1</sup>H NMR (CDCl<sub>3</sub>): δ 8.97 (d, *J* = 3.9 Hz, 1H), 8.17 (d, *J* = 8.2 Hz, 1H), 7.77 (d, *J* = 8.0 Hz, 1H), 7.54 (t, *J* = 7.6 Hz, 2H), 7.46 (d, *J* = 8.2 Hz, 1H), 7.41-7.35 (multiple peaks, 6H) 7.32-7.27 (multiple peaks, 5H). <sup>13</sup>C {<sup>1</sup>H} NMR (CDCl<sub>3</sub>): δ 149.33, 145.98, 144.14, 142.37, 135.79, 130.01, 129.31, 128.01, 127.82, 126.20, 125.73, 125.67, 120.68, 49.67. Anal. Calcd for C<sub>22</sub>H<sub>17</sub>N: C, 89.46, H, 5.80, N, 4.74; Found: C, 89.24, H, 5.96, N, 4.63. IR (KBr) 1492 cm<sup>-1</sup>. Note: Product **19** is formed in 16% yield by GC in the absence of Pd catalyst.

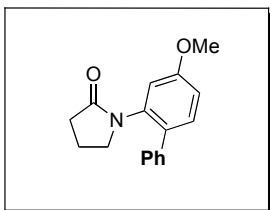


**Product 20:** 2-phenylquinoline (200 mg, 0.97 mmol, 1 equiv), [Ph<sub>2</sub>I]BF<sub>4</sub> (428 mg, 1.16 mmol, 1.2 equiv), and Pd(OAc)<sub>2</sub> (10.9 mg, 0.054 mmol, 5 mol%) were combined in AcOH (8 mL) in a 20 mL vial. The vial was sealed with a Teflon lined cap, and the

reaction was heated at 100 °C overnight. GC analysis at the completion of the reaction showed 19% starting material, 71% mono-arylated product (**20**) and 10% of the analogous diarylated product. The reaction mixture was filtered through a plug of Celite and then evaporated to dryness. The resulting oil was dissolved in CH<sub>2</sub>Cl<sub>2</sub> and extracted with saturated aqueous NaHCO<sub>3</sub> (2 x 30 mL) and brine (1 x 30 mL). The organic extracts were dried over MgSO<sub>4</sub> and concentrated under vacuum to afford a yellow oil, which was purified by chromatography on silica gel (R<sub>f</sub> = 0.22 in 94% hexanes/6% ethyl acetate). The product was obtained as a pale yellow solid (157 mg, 58% yield); mp 134-138 °C. <sup>1</sup>H NMR (C<sub>6</sub>D<sub>6</sub>): δ 8.38 (d, *J* = 8.4 Hz, 1H), 8.14 (dd, *J* = 7.60, 1.45, 1H), 7.39-7.34 (m, 2H), 7.31-7.28 (m, 2H), 7.26-7.16 (multiple peaks, 6H), 6.95-6.90 (m, 2H), 6.88-6.86 (m, 1H). <sup>13</sup>C{<sup>1</sup>H} NMR (CDCl<sub>3</sub>): δ 159.60, 147.94, 140.86, 140.46, 139.45, 134.43, 130.62, 130.21, 129.52, 129.26, 129.06, 128.62, 128.04, 127.88, 127.59, 127.18, 126.60, 126.27, 123.13. HRMS-electrospray (*m/z*): [M<sup>+</sup> – H] calcd for C<sub>21</sub>H<sub>15</sub>N, 280.1126; found, 280.1127. IR (KBr) 1699, 1589 cm<sup>-1</sup>.



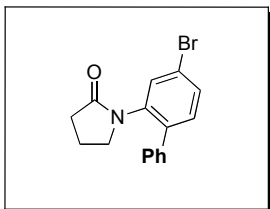
**Product 21:** *N*-phenylpyrrolidinone (152 mg, 0.94 mmol, 1 equiv), [Ph<sub>2</sub>I]BF<sub>4</sub> (521 mg, 1.41 mmol, 1.5 equiv), NaHCO<sub>3</sub> (119 mg, 1.14 mmol, 1.5 equiv) and Pd(OAc)<sub>2</sub> (11.9 mg, 0.053 mmol, 5 mol%) were combined in toluene (8 mL) in a 20 mL vial fitted with a Teflon lined cap, and the reaction was stirred at 100 °C for 24 h. The reaction mixture was filtered through a plug of Celite and concentrated under vacuum to afford a yellow oil, which was purified by chromatography on silica gel (R<sub>f</sub> = 0.1 in 50% ethyl acetate/50% hexanes). The product was obtained as an orange oil (170 mg, 75% yield). <sup>1</sup>H NMR (CDCl<sub>3</sub>): δ 7.44-7.35 (multiple peaks, 6H), 7.34-7.33 (m, 2H), 7.32 (t, *J* = 1.7 Hz, 1H), 3.21 (t, *J* = 7.0 Hz, 2H), 2.43 (t, *J* = 8.1 Hz, 2H), 1.90-1.83 (m, 2H). <sup>13</sup>C{<sup>1</sup>H} NMR (*d*<sub>6</sub>-acetone): δ 174.18, 140.09, 140.03, 137.60, 130.95, 129.13, 128.78, 128.59, 128.44, 127.71, 127.59, 49.65, 31.06, 18.99. Anal. Calcd for C<sub>16</sub>H<sub>15</sub>NO: C, 80.98, H, 6.37, N, 5.90; Found: C, 80.67, H, 6.46, N, 5.67. IR (thin film) 1715, 1377 cm<sup>-1</sup>.



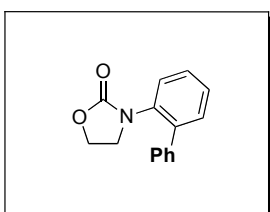
**Product 22:** *N*-(*m*-methoxyphenyl)-pyrrolidinone (180 mg, 0.94 mmol, 1 equiv), [Ph<sub>2</sub>I]BF<sub>4</sub> (692 mg, 1.88 mmol, 2 equiv), Pd(OAc)<sub>2</sub> (10.5 mg, 0.047 mmol, 5 mol%) and NaHCO<sub>3</sub> (158 mg, 1.88 mmol, 2 equiv) were combined in toluene (8 mL) in a 20 mL vial. The vial was sealed with a Teflon lined cap and the reaction was heated at 100 °C for 12 h. The reaction mixture was evaporated to dryness, and the residue was redissolved in CH<sub>2</sub>Cl<sub>2</sub> and filtered through a plug of Celite. The solution was concentrated to afford a yellow oil, which was purified by chromatography on silica gel (*R*<sub>f</sub> = 0.25 in 70% ethyl acetate/30% hexanes). The product was obtained as a yellow solid (211 mg, 84% yield); mp 61-64 °C. <sup>1</sup>H NMR (C<sub>6</sub>D<sub>6</sub>): δ 7.41-7.39 (m, 2H), 7.18-7.16 (m, 1H), 7.14-7.05 (multiple peaks, 4H), 6.73 (dd, *J* = 8.5, 2.6 Hz, 1H), 3.30 (s, 3H), 2.78 (t, *J* = 6.9 Hz, 2H), 2.03 (t, *J* = 8.0 Hz, 2H), 1.19-1.12 (m, 2H). <sup>13</sup>C{<sup>1</sup>H} NMR (CDCl<sub>3</sub>): δ 175.15, 159.10, 138.41, 136.62, 131.46, 131.09, 127.92, 127.89, 126.74, 113.70, 112.89, 54.95, 49.66, 30.74, 18.46. HRMS-electrospray (*m/z*): [M<sup>+</sup> + Na] calcd for C<sub>17</sub>H<sub>17</sub>NO<sub>2</sub>, 290.1157; found, 290.1167. IR (KBr) 1687, 1609 cm<sup>-1</sup>.

The regioselectivity of this reaction could not be definitively determined from the <sup>1</sup>H NMR spectrum of **22** due to overlapping aromatic resonances. As a result, a deuterated version of this product was prepared by reaction of **22** with [Mes-I-C<sub>6</sub>D<sub>5</sub>]BF<sub>4</sub> under analogous conditions to those described above. The <sup>1</sup>H NMR data for the deuterated product (**22-d<sub>5</sub>**) was as follows: <sup>1</sup>H NMR (*d*<sub>6</sub>-acetone): δ 7.31 (d, *J* = 8.5 Hz, 1H), 6.98 (dd, *J* = 8.5, 2.6 Hz, 1H), 6.92 (d, *J* = 2.6 Hz, 1H), 3.84 (s, 3H), 3.26 (t, *J* = 6.9 Hz, 2H), 2.26 (t, *J* = 8.0 Hz, 2H), 1.91-1.84 (m, 2H).



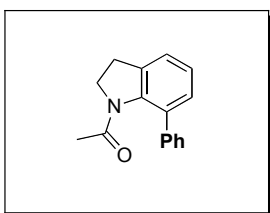


**Product 23:** *N*-(*m*-bromophenyl)-pyrrolidinone (180 mg, 0.75 mmol, 1 equiv),  $[\text{Ph}_2\text{I}]\text{BF}_4$  (689 mg, 1.87 mmol, 2.5 equiv), and  $\text{Pd}(\text{OAc})_2$  (8.4 mg, 0.038 mmol, 5 mol%) were combined in toluene (6.25 mL) in a 20 mL vial. The vial was sealed with a Teflon lined cap and the reaction was heated at 100 °C for 12 h. The reaction mixture was filtered through a plug of Celite and then evaporated to dryness. The resulting oil was dissolved in methylene chloride and extracted with saturated aqueous  $\text{NaHCO}_3$  (2 x 30 mL) and brine (1 x 30 mL). The organic layer was dried over  $\text{MgSO}_4$ , filtered, and concentrated to afford an orange oil, which was purified by chromatography on silica gel ( $R_f = 0.23$  in 96%  $\text{CH}_2\text{Cl}_2$ /4% ethyl acetate). The product was obtained as an orange-brown solid (180 mg, 78% yield); mp 116-118 °C.  $^1\text{H}$  NMR ( $\text{C}_6\text{D}_6$ ):  $\delta$  7.52 (s, 1H), 7.23 (d,  $J = 7.3$  Hz, 2H), 7.13-7.06 (multiple peaks, 4H), 6.79 (d,  $J = 8.1$  Hz, 1H), 2.59 (t,  $J = 6.8$  Hz, 2H), 1.93 (t,  $J = 8.0$  Hz, 2H), 1.13-1.06 (m, 2H).  $^{13}\text{C}\{^1\text{H}\}$  NMR ( $\text{CDCl}_3$ ):  $\delta$  175.39, 138.49, 137.84, 137.38, 131.89, 131.26, 130.90, 128.39, 127.93, 127.75, 121.44, 49.77, 30.85, 18.79. Anal. Calcd for  $\text{C}_{16}\text{H}_{14}\text{BrNO}$ : C, 60.78, H, 4.46, N, 4.43; Found: C, 61.08, H, 4.66, N, 4.19. IR (KBr) 1697, 1413  $\text{cm}^{-1}$ .

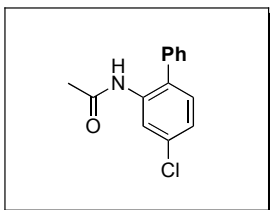


**Product 24:** *N*-phenyloxizolidinone (150 mg, 0.92 mmol, 1 equiv),  $[\text{Ph}_2\text{I}]\text{BF}_4$  (676 mg, 1.84 mmol, 2 equiv),  $\text{Pd}(\text{OAc})_2$  (10.2 mg, 0.046 mmol, 5 mol%) and  $\text{NaHCO}_3$  (155 mg, 1.84 mmol, 2 equiv) were combined in benzene (8 mL) in a 20 mL vial. The vial was sealed with a Teflon lined cap and the reaction was heated at 100 °C for 12 h. The reaction mixture was filtered through a plug of Celite and then evaporated to dryness. The resulting oil was dissolved in  $\text{CH}_2\text{Cl}_2$  and extracted with saturated aqueous  $\text{NaHCO}_3$  (2 x 30 mL) and brine (1 x 30 mL). The organic layer was dried over  $\text{MgSO}_4$ , filtered,

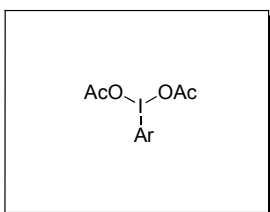
and concentrated to afford an orange oil, which was purified by chromatography on silica gel ( $R_f = 0.23$  in 97.5%  $\text{CH}_2\text{Cl}_2/2.5\%$  ethyl acetate). The product was obtained as a yellow solid (182 mg, 83% yield); mp 107-109 °C.  $^1\text{H}$  NMR ( $\text{C}_6\text{D}_6$ ):  $\delta$  7.38 (dd,  $J = 7.8$ , 1.2 Hz, 1H), 7.32-7.30 (m, 2H), 7.14-7.12 (m, 1H), 7.10-7.06 (multiple peaks, 3H), 7.05-6.99 (m, 2H) 3.24 (dd,  $J = 8.6$ , 7.2 Hz, 2H), 2.55 (dd,  $J = 8.5$ , 7.2 Hz, 2H).  $^{13}\text{C}\{^1\text{H}\}$  NMR ( $\text{CDCl}_3$ ):  $\delta$  157.78, 139.62, 139.00, 135.08, 131.10, 128.89, 128.87, 128.58, 128.41, 128.25, 127.99, 62.43, 47.13. Anal. Calcd for  $\text{C}_{15}\text{H}_{13}\text{NO}_2$ : C, 75.30, H, 5.48, N, 5.85; Found: C, 75.50, H, 5.66, N, 5.68. IR (KBr) 1740, 1483  $\text{cm}^{-1}$ .



**Product 25:** 1-acetyl-5-aminoindoline (150 mg, 0.93 mmol, 1 equiv),  $[\text{Ph}_2\text{I}]\text{BF}_4$  (685 mg, 1.86 mmol, 2 equiv), and  $\text{Pd}(\text{OAc})_2$  (10.4 mg, 0.047 mmol, 5 mol%) were combined in AcOH (5 mL) and  $\text{Ac}_2\text{O}$  (5 mL) in a 20 mL vial. The vial was sealed with a Teflon lined cap, and the reaction was heated at 100 °C overnight. GC analysis at the completion of the reaction showed 29% starting material and 71% of the mono-arylated product (**25**). Notably, attempts to optimize the reaction conditions did not lead to further conversion with this substrate. The reaction mixture was evaporated to dryness, and the remaining solid residue was taken up in MeOH (20 mL) and filtered through a plug of Celite. The methanol was removed under vacuum and the solids were taken up in  $\text{CH}_2\text{Cl}_2$  and extracted with saturated aqueous  $\text{NaHCO}_3$  (3 x 30 mL). The organic extracts were concentrated under vacuum to afford a red oil, which was purified by chromatography on silica gel ( $R_f = 0.2$  in 70% hexanes/30% ethyl acetate). The product was obtained as pale yellow solid (108 mg, 49% yield); mp 117-119 °C.  $^1\text{H}$  NMR ( $d_6$ -acetone):  $\delta$  7.52-7.14 (multiple peaks, 8H), 4.23 (t,  $J = 7.2$  Hz, 2H), 3.02 (t,  $J = 7.2$  Hz, 2H), 1.50 (br s, 3H).  $^{13}\text{C}\{^1\text{H}\}$  NMR ( $d_6$ -acetone):  $\delta$  141.58, 129.77, 128.16, 127.78, 126.02, 124.67, 51.15, 22.89. (The  $^{13}\text{C}$  NMR peaks of **25** are broad and several are missing, presumably as a result of fluxional motion of the amide.) Anal. Calcd for  $\text{C}_{16}\text{H}_{15}\text{NO}$ : C, 80.98, H, 6.37, N, 5.90; Found: C, 80.89, H, 6.52, N, 5.58. IR (KBr) 1648  $\text{cm}^{-1}$ .

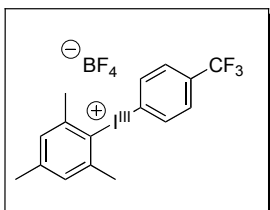


**Product 26:** *N*-(3-chlorophenyl)acetamide (250 mg, 1.47 mmol, 1 equiv),  $[\text{Ph}_2\text{I}]\text{BF}_4$  (1.08 g, 2.95 mmol, 2 equiv), and  $\text{Pd}(\text{OAc})_2$  (16.5 mg, 0.074 mmol, 5 mol%) were combined in benzene (12 mL) in a 20 mL vial. The vial was sealed with a Teflon lined cap and the reaction was heated at 100 °C for 12 h. The reaction mixture was filtered through a plug of Celite and then evaporated to dryness. The resulting oil was dissolved in  $\text{CH}_2\text{Cl}_2$  and extracted with saturated aqueous  $\text{NaHCO}_3$  (2 x 30 mL) and brine (1 x 30 mL). The organic layer was dried over  $\text{MgSO}_4$ , filtered, and concentrated to afford an orange oil, which was purified by chromatography on silica gel ( $R_f = 0.28$  in 55% diethyl ether/45% hexanes). The product was obtained as an orange-brown solid (240 mg, 67% yield); mp 125-126 °C.  $^1\text{H}$  NMR ( $\text{C}_6\text{D}_6$ ):  $\delta$  9.02 (s, 1H), 7.10-7.05 (multiple peaks, 3H), 6.97-6.95 (m, 2H), 6.91 (dd,  $J = 8.2, 2.2$  Hz, 1H), 6.75 (d,  $J = 8.2$  Hz, 1H), 6.64 (s, 1H), 1.25 (s, 3H).  $^{13}\text{C}\{^1\text{H}\}$  NMR ( $\text{CDCl}_3$ ):  $\delta$  167.96, 136.65, 135.27, 133.40, 130.55, 130.19, 128.82, 128.66, 127.88, 123.94, 121.24, 24.04. Anal. Calcd for  $\text{C}_{14}\text{H}_{12}\text{ClNO}$ : C, 68.44, H, 4.92, N, 5.70; Found: C, 68.38, H, 4.99, N, 5.47. IR (KBr) 3224, 3026, 1648, 1532  $\text{cm}^{-1}$ . The regioselectivity of this reaction could not be definitively assigned from the  $^1\text{H}$  NMR spectrum of **26** due to overlapping aromatic resonances. As a result, a deuterated version of this product was prepared by reaction with  $[\text{Mes-I-C}_6\text{D}_5]\text{BF}_4$  under analogous conditions to those described above. The  $^1\text{H}$  NMR data for the deuterated product (**26-*d*<sub>5</sub>**) was as follows:  $^1\text{H}$  NMR ( $\text{C}_6\text{D}_6$ ):  $\delta$  9.02 (br. s, 1H), 6.92 (dd,  $J = 8.2, 2.1$  Hz, 1H), 6.75 (d,  $J = 8.2$  Hz, 1H), 6.64 (br. s, 1H), 1.25 (s, 3H).



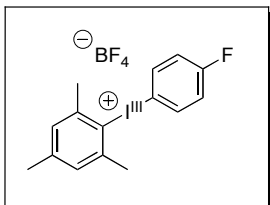
**General Procedure for  $\text{ArI}^{\text{III}}(\text{OAc})_2$  Synthesis:** The published procedure for the synthesis of  $\text{ArI}^{\text{III}}(\text{OAc})_2$  was followed.<sup>20</sup>  $\text{NaBO}_3 \cdot \text{H}_2\text{O}$  (100 mmol, 10 equiv) was slowly added in portions over 20 min to a stirring solution of  $\text{Ar-I}$  (10 mmol, 1 equiv) in  $\text{AcOH}$  (90 mL) at 45 °C. The reactions were allowed to stir at 45 °C for a minimum of 8 hr, at which point the solvent was reduced under vacuum to approximately 30 mL of  $\text{AcOH}$ . To this solution was added  $\text{H}_2\text{O}$  (200 mL) resulting in a white solid to crash out. This solution was filtered, and the solid was further washed with  $\text{H}_2\text{O}$  (350 mL), then hexanes (250 mL). The white solid was collected and dried under vacuum and taken directly on for coupling to make the  $[\text{Ar-I}^{\text{III}}-\text{Ar}]\text{BF}_4$  oxidants.

**General Procedure for  $[\text{Ar-I}^{\text{III}}-\text{Ar}]\text{BF}_4$  Synthesis:** The published procedure for the synthesis of  $[\text{Ar-I}^{\text{III}}-\text{Ar}]\text{BF}_4$  was followed.<sup>19</sup> To a solution of  $\text{ArB}(\text{OH})_2$  (3.05 mmol, 1.05 equiv) and  $\text{BF}_3 \cdot \text{OEt}_2$  (3.35 mmol, 1.05 equiv) in  $\text{CH}_2\text{Cl}_2$  (20 mL) at 0 °C was added to a 0 °C solution of  $\text{ArI}^{\text{III}}(\text{OAc})_2$  (2.75 mmol, 1 equiv) in  $\text{CH}_2\text{Cl}_2$  (20 mL) via cannula transfer. This solution was allowed to stir at 0 °C for 2 hr, then a saturated aqueous solution of  $\text{NaBF}_4$  was added (150 mL) and allowed to stir as a biphasic solution for 30 min at room temperature. The organic layer was separated and the aqueous layer was washed with 3 x 40 mL of  $\text{CH}_2\text{Cl}_2$ , then the combined organic layers were dried with  $\text{MgSO}_4$  and the solvent was reduced to the minimal amount necessary to keep the product in solution. To this concentrated solution was added  $\text{Et}_2\text{O}$  or hexanes and the desired  $[\text{Ar-I}^{\text{III}}-\text{Ar}]\text{BF}_4$  crashed out of solution. In some cases  $^1\text{H}$  NMR revealed remaining boronic acid. This can be removed by dissolving the product in  $\text{CH}_2\text{Cl}_2$  then performing an extraction with aqueous solution of  $\text{HBF}_4$  (20%) to remove the boronic acid.

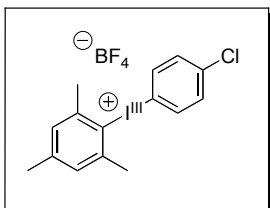


**Oxidant 38:** General Procedure for  $[\text{Ar-I}^{\text{III}}-\text{Ar}]\text{BF}_4$  Synthesis was followed. This reaction combined  $\text{MesI}^{\text{III}}(\text{OAc})_2$  (1.0 g, 2.75 mmol) and  $p\text{-CF}_3\text{C}_6\text{H}_4\text{B}(\text{OH})_2$  (0.579 g, 3.05 mmol) and resulted in the desired oxidant as a white powder (900 mg, 68% yield).

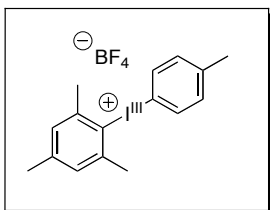
$^1\text{H}$  NMR ( $\text{CDCl}_3$ ):  $\delta$  7.84 (d,  $J = 8.7$  Hz, 2H), 7.65 (d,  $J = 8.4$  Hz, 2H), 7.14 (s, 2H), 2.63 (s, 6H), 2.37 (s, 3H).  $^{13}\text{C}\{^1\text{H}\}$  NMR ( $\text{CDCl}_3$ ):  $\delta$  144.01, 142.01, 133.08 (q,  $^2J_F = 29.7$  Hz), 132.93, 130.26, 128.34 (q,  $^3J_F = 3.9$  Hz), 123.46, 123.10 (q,  $^1J_F = 270.9$  Hz), 119.72, 27.16, 21.08.



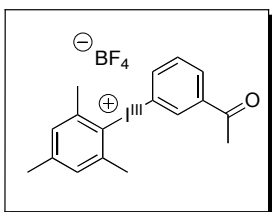
**Oxidant 39:** General Procedure for  $[\text{Ar}-\text{I}^{\text{III}}-\text{Ar}]\text{BF}_4$  Synthesis was followed. This reaction combined  $\text{MesI}^{\text{III}}(\text{OAc})_2$  (1.0 g, 2.75 mmol) and  $p\text{-FC}_6\text{H}_4\text{B}(\text{OH})_2$  (0.639 g, 3.05 mmol) and resulted in the desired oxidant as a white powder (686 mg, 58% yield).  $^1\text{H}$  NMR ( $\text{CDCl}_3$ ):  $\delta$  7.76-7.70 (multiplet, 2H), 7.16-7.10 (multiple peaks, 4H), 2.63 (s, 6H), 2.36 (s, 3H).  $^{13}\text{C}\{^1\text{H}\}$  NMR ( $\text{CD}_3\text{OD}$ ):  $\delta$  166.32 (d,  $^1J_F = 252$  Hz), 146.11, 138.25 (d,  $^3J_F = 8.9$  Hz), 131.51, 122.79, 120.76 (d,  $^2J_F = 23.2$ ), 107.86 (d,  $^2J_F = 3.4$ ), 27.12, 21.15.



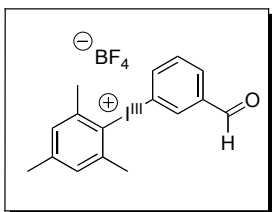
**Oxidant 40:** General Procedure for  $[\text{Ar}-\text{I}^{\text{III}}-\text{Ar}]\text{BF}_4$  Synthesis was followed. This reaction combined  $\text{MesI}^{\text{III}}(\text{OAc})_2$  (1.5 g, 4.1 mmol) and  $p\text{-ClC}_6\text{H}_4\text{B}(\text{OH})_2$  (0.719 g, 4.6 mmol) and resulted in the desired oxidant as a white powder (962 mg, 53% yield).  $^1\text{H}$  NMR ( $\text{CDCl}_3$ ):  $\delta$  7.63 (d,  $J = 9.3$  Hz, 2H), 7.39 (d,  $J = 8.7$  Hz, 2H), 7.13 (s, 2H), 2.63 (s, 6H), 2.37 (s, 3H).



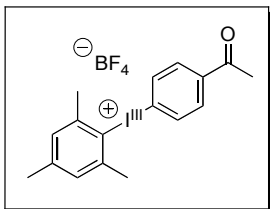
**Oxidant 41:** General Procedure for [Ar-I<sup>III</sup>-Ar]BF<sub>4</sub> Synthesis was followed. This reaction combined MesI<sup>III</sup>(OAc)<sub>2</sub> (1.0 g, 2.75 mmol) and *p*-MeC<sub>6</sub>H<sub>4</sub>B(OH)<sub>2</sub> (0.414g, 4.6 mmol) and resulted in the desired oxidant as a white powder (983 mg, 85% yield). <sup>1</sup>H NMR (CDCl<sub>3</sub>): δ 7.79 (d, *J* = 8.0 Hz, 2H), 7.24 (d, *J* = 8.0 Hz, 2H), 7.12 (s, 2H), 2.63 (s, 6H), 2.38 (s, 3H), 2.36 (s, 3H). <sup>13</sup>C{<sup>1</sup>H} NMR (CDCl<sub>3</sub>): δ 144.75, 143.19, 142.7, 133.33, 133.11, 130.53, 119.06, 106.85, 27.14, 21.25, 21.10.



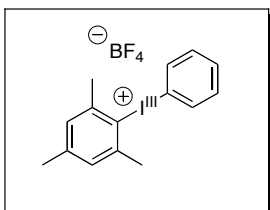
**Oxidant 42:** General Procedure for [Ar-I<sup>III</sup>-Ar]BF<sub>4</sub> Synthesis was followed. This reaction combined MesI<sup>III</sup>(OAc)<sub>2</sub> (1.0 g, 2.75 mmol) and *m*-(COMe)C<sub>6</sub>H<sub>4</sub>B(OH)<sub>2</sub> (0.500 g, 4.6 mmol) and resulted in the desired oxidant as a white powder (yield not determined). <sup>1</sup>H NMR (CDCl<sub>3</sub>): δ 8.34 (s, 1H), 8.10 (d, *J* = 7.5 Hz, 1H), 7.83 (d, *J* = 9.0 Hz, 1H), 7.55 (t, *J* = 8 Hz, 1H), 7.16 (s, 2H), 2.65 (s, 6H), 2.62 (s, 3H), 2.39 (s, 3H). <sup>13</sup>C{<sup>1</sup>H} NMR (CDCl<sub>3</sub>): δ 195.72, 145.11, 142.95, 140.38, 136.42, 132.86, 132.56, 131.31, 130.65, 118.78, 111.05, 27.19, 26.61, 21.15.



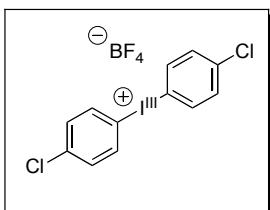
**Oxidant 43:** General Procedure for [Ar-I<sup>III</sup>-Ar]BF<sub>4</sub> Synthesis was followed. This reaction combined MesI<sup>III</sup>(OAc)<sub>2</sub> (1.0 g, 2.75 mmol) and *m*-(CHO)C<sub>6</sub>H<sub>4</sub>B(OH)<sub>2</sub> (0.457 g, 4.6 mmol) and resulted in the desired oxidant as a white powder (861 mg, 72% yield). <sup>1</sup>H NMR (CDCl<sub>3</sub>): δ 9.94 (s, 1H), 8.13 (s, 1H), 8.06-8.00 (multiple peaks, 2H), 7.64 (t, *J* = 10.0 Hz, 1H), 7.15 (s, 2H), 2.64 (s, 6H), 2.38 (s, 3H). <sup>13</sup>C{<sup>1</sup>H} NMR (CDCl<sub>3</sub>): δ 189.46, 145.29, 142.99, 139.41, 138.17, 133.55, 132.99, 132.48, 130.75, 118.79, 111.32, 27.23, 21.18.



**Oxidant 44:** General Procedure for  $[\text{Ar-I}^{\text{III}}-\text{Ar}]\text{BF}_4$  Synthesis was followed. This reaction combined  $\text{MesI}^{\text{III}}(\text{OAc})_2$  (2.0 g, 7.4 mmol) and  $p\text{-(COMe)C}_6\text{H}_4\text{B(OH)}_2$  (1.27 g, 7.8 mmol) and resulted in the desired oxidant as a white powder (840 mg, 25% yield).  $^1\text{H}$  NMR ( $\text{CDCl}_3$ ):  $\delta$  7.97 (d,  $J = 8.8$  Hz, 2H), 7.79 (d,  $J = 8.4$  Hz, 2H), 7.17 (s, 2H), 2.62 (s, 6H), 2.60 (s, 3H), 2.40 (s, 3H).  $^{13}\text{C}\{^1\text{H}\}$  NMR ( $d_6\text{-acetone}$ ):  $\delta$  197.23, 145.83, 143.77, 140.77, 135.40, 132.46, 131.41, 121.36, 117.23, 27.19, 26.92, 21.07.

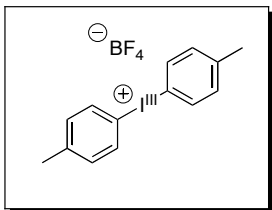


**Oxidant 45:** General Procedure for  $[\text{Ar-I}^{\text{III}}-\text{Ar}]\text{BF}_4$  Synthesis was followed. This reaction combined  $\text{MesI}^{\text{III}}(\text{OAc})_2$  (5.78 g, 15.9 mmol) and  $\text{PhB(OH)}_2$  (2.03 g, 16.7 mmol) and resulted in the desired oxidant as a white powder (6.52 g, 81% yield).  $^1\text{H}$  NMR ( $\text{CDCl}_3$ ):  $\delta$  7.68 (d,  $J = 8.0$  Hz, 2H), 7.58 (t,  $J = 8.0$  Hz, 1H), 7.45 (t,  $J = 8.0$ , 2H), 7.15 (s, 2H), 2.63 (s, 6H), 2.39 (s, 3H).  $^{13}\text{C}\{^1\text{H}\}$  NMR ( $\text{CD}_3\text{OD}$ ):  $\delta$  146.02, 143.65, 135.38, 133.45, 133.43, 131.47, 122.32, 114.56, 27.16, 21.15.

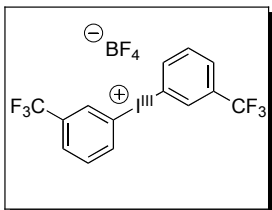


**Oxidant 46:** General Procedure for  $[\text{Ar-I}^{\text{III}}-\text{Ar}]\text{BF}_4$  Synthesis was followed. This reaction combined  $p\text{-ClC}_6\text{H}_4\text{I}^{\text{III}}(\text{OAc})_2$  (3.28 g, 9.2 mmol) and  $p\text{-ClC}_6\text{H}_4\text{B(OH)}_2$  (1.60 g, 10.2 mmol) and resulted in the desired oxidant as a white powder (4.0 g, 93% yield).  $^1\text{H}$

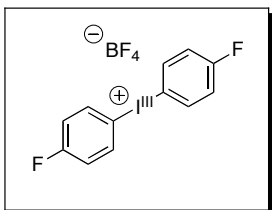
NMR (CDCl<sub>3</sub>): δ 7.96 (d, *J* = 8.5 Hz, 4H), 7.34 (d, *J* = 9.0 Hz, 4H). <sup>13</sup>C NMR (CD<sub>3</sub>OD): δ 139.9, 136.9, 132.4, 109.6. <sup>13</sup>C{<sup>1</sup>H} NMR (CD<sub>3</sub>OD): δ 139.90, 136.92, 132.94, 109.58.



**Oxidant 47:** General Procedure for [Ar-I<sup>III</sup>-Ar]BF<sub>4</sub> Synthesis was followed. This reaction combined *p*-MeC<sub>6</sub>H<sub>4</sub>I<sup>III</sup>(OAc)<sub>2</sub> (2.96 g, 8.8 mmol) and *p*-MeC<sub>6</sub>H<sub>4</sub>B(OH)<sub>2</sub> (1.23 g, 9.7 mmol) and resulted in the desired oxidant as a white powder (2.2 g, 63% yield). <sup>1</sup>H NMR (CDCl<sub>3</sub>): δ 7.89 (d, *J* = 9.5 Hz, 4H), 7.24 (d, *J* = 9.5 Hz, 4H), 2.38 (s, 6H). <sup>13</sup>C{<sup>1</sup>H} NMR (CD<sub>3</sub>OD): δ 143.89, 135.22, 133.22, 108.51, 21.38.



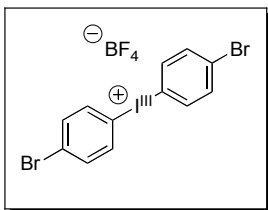
**Oxidant 48:** General Procedure for [Ar-I<sup>III</sup>-Ar]BF<sub>4</sub> Synthesis was followed. This reaction combined *m*-CF<sub>3</sub>C<sub>6</sub>H<sub>4</sub>I<sup>III</sup>(OAc)<sub>2</sub> (1.1 g, 2.9 mmol) and *m*-CF<sub>3</sub>C<sub>6</sub>H<sub>4</sub>B(OH)<sub>2</sub> (0.61 g, 3.23 mmol) and resulted in the desired oxidant as a white powder (0.73 g, 50% yield). <sup>1</sup>H NMR (CD<sub>3</sub>OD): δ 8.72 (s, 2H), 8.54 (d, *J* = 8.0 Hz, 2H), 8.08 (d, *J* = 8.0 Hz, 2H), 7.81 (t, *J* = 8.0 Hz, 2H).



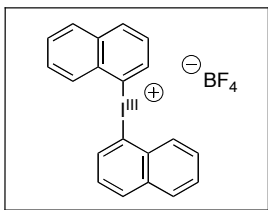
**Oxidant 49:** General Procedure for [Ar-I<sup>III</sup>-Ar]BF<sub>4</sub> Synthesis was followed. This reaction combined *p*-FC<sub>6</sub>H<sub>4</sub>I<sup>III</sup>(OAc)<sub>2</sub> (3.1 g, 9.1 mmol) and *p*-FC<sub>6</sub>H<sub>4</sub>B(OH)<sub>2</sub> (1.42 g, 10.1 mmol) and resulted in the desired oxidant as a white powder (3.0 g, 82% yield). <sup>1</sup>H



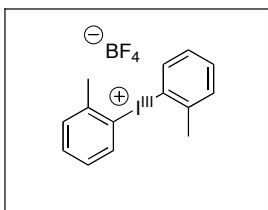
NMR (CD<sub>3</sub>OD):  $\delta$  8.20-8.10 (multiplet, 4H), 7.25-7.15 (multiplet, 4H). <sup>13</sup>C{<sup>1</sup>H} NMR (CD<sub>3</sub>OD):  $\delta$  166.57 (d, <sup>1</sup>J<sub>F</sub> = 252 Hz), 139.48 (d, <sup>3</sup>J<sub>F</sub> = 8.9 Hz) 120.70 (d, <sup>2</sup>J<sub>F</sub> = 23.2), 110.36 (d, <sup>2</sup>J<sub>F</sub> = 3.5).



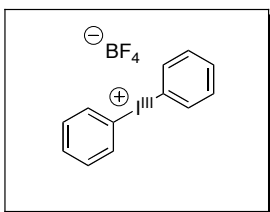
**Oxidant 50:** General Procedure for [Ar-I<sup>III</sup>-Ar]BF<sub>4</sub> Synthesis was followed. This reaction combined *p*-BrC<sub>6</sub>H<sub>4</sub>I<sup>III</sup>(OAc)<sub>2</sub> (3.70 g, 9.23 mmol) and *p*-BrC<sub>6</sub>H<sub>4</sub>B(OH)<sub>2</sub> (2.06 g, 1.03 mmol) and resulted in the desired oxidant as a white powder (3.80 g, 78% yield). <sup>1</sup>H NMR (CD<sub>3</sub>OD):  $\delta$  7.98 (d, *J* = 15.0 Hz, 4H), 7.62 (d, *J* = 15.0 Hz, 4H). <sup>13</sup>C{<sup>1</sup>H} NMR (CD<sub>3</sub>OD):  $\delta$  138.28, 136.47, 128.91, 114.59.



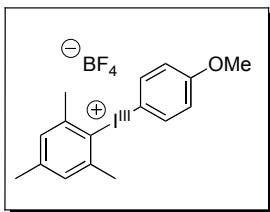
**Oxidant 51:** General Procedure for [Ar-I<sup>III</sup>-Ar]BF<sub>4</sub> Synthesis was followed. This reaction combined 1-naphthyl-I<sup>III</sup>(OAc)<sub>2</sub> (3.63 g, 9.7 mmol) and 1-naphthyl-B(OH)<sub>2</sub> (1.86 g, 10.8 mmol) and resulted in the desired oxidant as a white powder (3.18 g, 70% yield). <sup>1</sup>H NMR (CD<sub>3</sub>OD):  $\delta$  8.71 (d, *J* = 7.6 Hz, 2H), 8.37 (d, *J* = 7.6 Hz, 2H), 8.21 (d, *J* = 7.6 Hz, 2H), 8.00 (d, *J* = 8.0 Hz, 2H), 7.82 (t, *J* = 8.0 Hz, 2H), 7.71 (t, *J* = 8.0 Hz, 2H), 7.55 (t, *J* = 7.6 Hz, 2H). <sup>13</sup>C{<sup>1</sup>H} NMR (CD<sub>3</sub>OD):  $\delta$  138.85, 136.52, 135.35, 132.93, 131.23, 130.95, 129.61, 129.39, 128.59, 118.85.



**Oxidant 52:** General Procedure for  $[\text{Ar-I}^{\text{III}}-\text{Ar}]\text{BF}_4$  Synthesis was followed. This reaction combined *o*-tolyl- $\text{I}^{\text{III}}(\text{OAc})_2$  (1.97 g, 5.86 mmol) and *o*-tolyl- $\text{B}(\text{OH})_2$  (0.884 g, 6.50 mmol) and resulted in the desired oxidant as a white powder (1.96 g, 85% yield).  $^1\text{H}$  NMR ( $\text{CD}_3\text{OD}$ ):  $\delta$  8.12 (d,  $J = 8.0$  Hz, 2H), 7.51-7.46 (multiple peaks, 4H), 7.21 (t,  $J = 8.0$  Hz, 2H), 2.56 (s, 6H).  $^{13}\text{C}\{^1\text{H}\}$  NMR ( $\text{CD}_3\text{OD}$ ):  $\delta$  142.63, 138.57, 134.55, 133.25, 130.82, 120.02, 25.68.

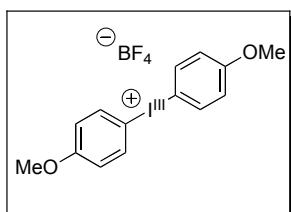


**Oxidant 53:** General Procedure for  $[\text{Ar-I}^{\text{III}}-\text{Ar}]\text{BF}_4$  Synthesis was followed. This reaction combined  $\text{PhI}^{\text{III}}(\text{OAc})_2$  (11.9 g, 37 mmol) and  $\text{PhB}(\text{OH})_2$  (5.0 g, 41 mmol) and resulted in the desired oxidant as a white powder (12.4 g, 82% yield).  $^1\text{H}$  NMR ( $\text{CDCl}_3$ ):  $\delta$  8.02 (d,  $J = 8.0$  Hz, 2H), 7.65 (t,  $J = 8.0$  Hz, 2H), 7.49 (t,  $J = 8.0$  Hz, 2H).  $^{13}\text{C}\{^1\text{H}\}$  NMR ( $\text{CD}_3\text{OD}$ ):  $\delta$  136.61, 133.81, 133.32, 116.12.

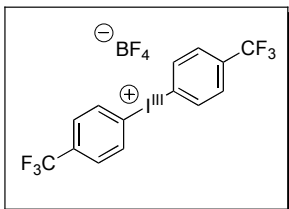


**Oxidant 55:** General procedure for  $\text{ArI}^{\text{III}}(\text{OAc})_2$  synthesis was followed to synthesize  $\text{MesI}^{\text{III}}(\text{OAc})_2$ . This was then used to obtain  $\text{MesI}^{\text{III}}=\text{O}$  according to literature precedent.<sup>21</sup> This intermediate was then taken on to  $[\text{Mes-I}^{\text{III}}-(p\text{-MeOC}_6\text{H}_4)]\text{BF}_4$  using a modified literature procedure.<sup>22</sup> This began by adding  $\text{H}_2\text{SO}_4$  (0.12 mL) dropwise to a stirring solution of  $\text{MesI}^{\text{III}}=\text{O}$  (487 mg, 1.85 mmol, 1 equiv) in  $\text{AcOH}/\text{Ac}_2\text{O}$  (12:1.2mL) and allowing to stir for 1 hr. Then  $\text{H}_2\text{O}$  (100 mL) was added to the solution, and the organic products were extracted in  $\text{CH}_2\text{Cl}_2$  3 x 20 mL. The combined organic extracts were then stirred as a biphasic mixture with 150 mL of aqueous saturated  $\text{NaBF}_4$ . The organic layer was separated and the aqueous layer was washed with 3 x 40 mL of  $\text{CH}_2\text{Cl}_2$ , then the combined organic layers were dried with  $\text{MgSO}_4$  and the solvent was reduced to the

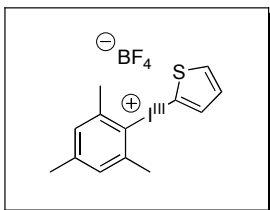
minimal amount necessary to keep the product in solution. To this concentrated solution was added Et<sub>2</sub>O or hexanes and the desired [Ar-I<sup>III</sup>-Ar]BF<sub>4</sub> crashed out of solution. Multiple recrystallizations (≥3) from CH<sub>2</sub>Cl<sub>2</sub> and Et<sub>2</sub>O were completed until the obtained product was an off white crystalline solid (0.638 g, 81% yield). <sup>1</sup>H NMR (CDCl<sub>3</sub>): δ 7.64 (dd, *J* = 7.5, 2.5 Hz, 2H), 7.05 (s, 2H), 6.90 (dd, *J* = 7.5, 2.0 Hz, 2H), 3.78 (s, 3H), 2.64 (s, 6H), 2.32 (s, 3H). <sup>13</sup>C{<sup>1</sup>H} NMR (CDCl<sub>3</sub>): δ 162.68, 144.59, 142.53, 135.62, 130.48, 119.69, 118.27, 98.64, 55.73, 27.06, 21.06.



**Oxidant 56:** General procedure for ArI<sup>III</sup>(OAc)<sub>2</sub> synthesis was followed to synthesize *p*-*p*-MeOC<sub>6</sub>H<sub>4</sub>I<sup>III</sup>(OAc)<sub>2</sub>. This intermediate was then taken on to [(*p*-MeOC<sub>6</sub>H<sub>4</sub>)<sub>2</sub>-I<sup>III</sup>]BF<sub>4</sub> using a modified literature procedure.<sup>23</sup> This began by adding CF<sub>3</sub>COOH (0.4 mL) to a stirring solution of *p*-MeOC<sub>6</sub>H<sub>4</sub>I<sup>III</sup>(OAc)<sub>2</sub> (760 mg, 2.16 mmol) in CH<sub>2</sub>Cl<sub>2</sub> at -30 °C; reaction was and stirred for 20 min, then warmed to 0 °C for 20 min, and then room temperature for 1 hr. The solution was then cooled back to -30 °C and anisole (467 mg, 4.32 mmol) was added dropwise, the solution was then warmed to 0 °C for 30 min, then to room temperature for 30 min. The reaction volume was then increased by adding CH<sub>2</sub>Cl<sub>2</sub> (100mL), then stirred as a biphasic mixture with 150 mL of aqueous saturated NaBF<sub>4</sub>. The organic layer was separated and the aqueous layer was washed with 3 x 40 mL of CH<sub>2</sub>Cl<sub>2</sub>, then the combined organic layers were dried with MgSO<sub>4</sub> and the solvent was reduced to the minimal amount necessary to keep the product in solution. To this concentrated solution was added Et<sub>2</sub>O or hexanes and the desired [Ar-I<sup>III</sup>-Ar]BF<sub>4</sub> crashed out of solution. Multiple recrystallizations (≥3) were completed until the obtained product was an off white crystalline solid (1.9 g, 72% yield). <sup>1</sup>H NMR (CD<sub>3</sub>OD): δ 7.95 (d, *J* = 6.9 Hz, 4H), 6.96 (d, *J* = 6.9 Hz, 4H), 3.75 (s, 6H). <sup>13</sup>C{<sup>1</sup>H} NMR (CD<sub>3</sub>OD): δ 164.53, 138.27, 118.86, 105.28, 56.46.

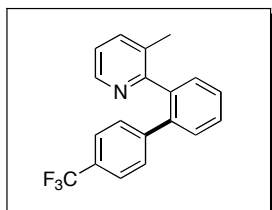


**Oxidant 57:** The literature procedure described by Olofsson was employed.<sup>24</sup> To a solution of *m*-CPBA (1.1 g, 4.5 mmol, 1.1 equiv) in CH<sub>2</sub>Cl<sub>2</sub> (15 mL) at 0 °C was added first *p*-CF<sub>3</sub>C<sub>6</sub>H<sub>4</sub>I (1.18 g, 4.05 mmol, 1.0 equiv), then BF<sub>3</sub>•OEt<sub>2</sub> (1.3 mL) and allowed to stir for 30 min. Then *p*-CF<sub>3</sub>C<sub>6</sub>H<sub>4</sub>B(OH)<sub>2</sub> was added and the reaction was stirred for an additional 15 min at rt. The solution was then run through a plug of silica with CH<sub>2</sub>Cl<sub>2</sub> (10mL) to remove the unreacted starting materials, then CH<sub>2</sub>Cl<sub>2</sub>/MeOH (20:1) to elute the product. The solution containing the product was concentrated (~5 mL) and the product was precipitated out by adding Et<sub>2</sub>O (~200 mL) affording the product as a white powder (0.853 g, 42% yield). <sup>1</sup>H NMR (*d*<sub>6</sub>-DMSO): δ 8.50 (d, *J* = 8 Hz, 4H), 7.93 (d, *J* = 8Hz, 4H). <sup>13</sup>C NMR (*d*<sub>6</sub>-DMSO): δ 136.24, 132.01 (q, <sup>2</sup>*J*<sub>CF3</sub> = 32.1 Hz), 128.52 (q, <sup>3</sup>*J*<sub>CF3</sub> = 3.9 Hz), 123.38 (q, <sup>1</sup>*J*<sub>CF3</sub> = 271.3 Hz), 120.95.

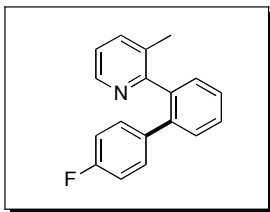


**Oxidant 81:** The Ir<sup>III</sup> reagent [Mes-Ir<sup>III</sup>-(2-thiophene)]OTs (**80**) was first synthesized according to a literature example.<sup>25</sup> Thiophene (0.543 g, 6.46 mmol, 2 equiv) and MesIr<sup>III</sup>(OH)(OTs) (1.40 g, 3.23 mmol, 1 equiv) were refluxed in CHCl<sub>3</sub> (15 mL) for 2 hr. The solution was cooled to room temperature, and Et<sub>2</sub>O was added to the solution until it became cloudy and was allowed to further stir for 25 min. Then Et<sub>2</sub>O (200 mL) was added and white precipitate was collected (1.27 g, 2.5 mmol). <sup>1</sup>H NMR (CD<sub>3</sub>OD): δ 7.80-7.70 (multiple peaks, 2H), 7.58 (d, *J* = 7.6 Hz, 2H), 7.13-7.10 (multiple peaks, 4H), 7.05 (dd, *J* = 5.5, 3.5 Hz, 1H), 2.62 (s, 6H), 2.26 (s, 3H), 2.34 (s, 3H). To obtain the product with a BF<sub>4</sub><sup>-</sup> counterion the same procedure was followed, with a saturated solution of NaBF<sub>4</sub> added after the reaction was cooled, then and stirred for 45 min. The organic layer was collected and the aqueous layer was washed with CHCl<sub>3</sub> (3 x 45 mL). The organic

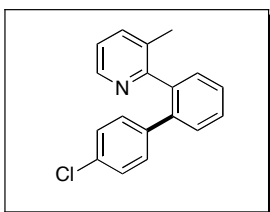
layer was dried with MgSO<sub>4</sub> and the solvent was reduced so it was saturated (~10 mL) in product and Et<sub>2</sub>O (300 mL) was added and the product crashed out. The <sup>1</sup>H NMR revealed that complete anion exchange was not achieved with ca. 20% OTs remaining. <sup>1</sup>H NMR (CDCl<sub>3</sub>): δ 7.80 (dd, *J* = 4.0, 1.0 Hz, 1H), 7.63 (dd, *J* = 5.0, 1.5 Hz, 1H), 7.27 (d, *J* = 35 Hz, 0.4H), 7.10 (dd, *J* = 5.0, 4.0 Hz, 1H), 7.06 (s, 2H), 6.98 (d, *J* = 13 Hz, 0.4H). 3.73 (s, 6H), 2.32 (s, 3H), 2.30 (s, 0.6H).



**Product 63:** 3-methyl-2-phenylpyridine (150 mg, 0.89 mmol, 1 equiv), [Mes-I-*p*-CF<sub>3</sub>C<sub>6</sub>H<sub>5</sub>]BF<sub>4</sub> (466 mg, 0.98 mmol, 1.1 equiv) and Pd(OAc)<sub>2</sub> (10 mg, 0.044 mmol, 5 mol %) were combined in acetic acid (8 mL) in a 20 mL vial. The vial was sealed with a Teflon lined cap, and the reaction was stirred at 100 °C for 12 h. The reaction mixture was filtered through a plug of glass wool and concentrated under vacuum. The resulting oil was dissolved in CH<sub>2</sub>Cl<sub>2</sub> and extracted with saturated aqueous NaHCO<sub>3</sub> (1 x 30 mL). The organic layer was dried over MgSO<sub>4</sub>, filtered, and concentrated to afford an orange oil, which was purified by chromatography on silica gel (*R*<sub>f</sub> = 0.25 in 75% hexanes/25% ethyl acetate). The product was obtained as a yellow oil (242 mg, 87% yield). <sup>1</sup>H NMR (*d*<sub>6</sub>-acetone): δ 8.42 (d, *J* = 4.2 Hz, 1H), 7.57-7.53 (multiple peaks, 5H), 7.46-7.40 (multiple peaks, 2H), 7.35 (d, *J* = 8.4 Hz, 2H), 7.18 (dd, *J* = 8.0 Hz, 7.6 Hz, 1H). <sup>13</sup>C{<sup>1</sup>H} NMR (*d*<sub>6</sub>-acetone): δ 159.83, 147.84, 146.27, 140.87, 140.13, 138.42, 132.21, 131.06, 130.76, 130.59, 129.34, 129.08 (d, <sup>2</sup>*J*<sub>CF3</sub> = 32 Hz), 128.99, 125.59 (q, <sup>3</sup>*J*<sub>CF3</sub> = 4 Hz), 124.43 (q, <sup>1</sup>*J*<sub>CF3</sub> = 270 Hz), 123.39, 19.08. Anal. Calcd for C<sub>19</sub>H<sub>14</sub>F<sub>3</sub>N: C, 72.83, H, 4.50, N, 4.47; Found: C, 72.53, H, 4.60, N, 4.36.

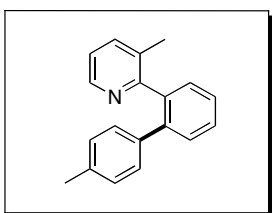


**Product 64:** 3-methyl-2-phenylpyridine (153 mg, 0.91 mmol, 1 equiv), [Mes-I-*p*-FC<sub>6</sub>H<sub>5</sub>]BF<sub>4</sub> (446 mg, 1.04 mmol, 1.15 equiv) and Pd(OAc)<sub>2</sub> (10.1 mg, 0.043 mmol, 5 mol%) were combined in acetic acid (8 mL) in a 20 mL vial. The vial was sealed with a Teflon lined cap, and the reaction was stirred at 100 °C for 12 h. The reaction mixture was filtered through a plug of glass wool and concentrated under vacuum. The resulting oil was dissolved in CH<sub>2</sub>Cl<sub>2</sub> and extracted with saturated aqueous NaHCO<sub>3</sub> (1 x 30 mL). The organic layer was dried over MgSO<sub>4</sub>, filtered, and concentrated to afford an orange oil, which was purified by chromatography on silica gel (R<sub>f</sub> = 0.3 in 75% hexanes/25% ethyl acetate). The product was obtained as a yellow solid (210 mg, 88% yield); mp 135-137 °C. <sup>1</sup>H NMR (*d*<sub>6</sub>-acetone): δ 8.43 (d, *J* = 4.0 Hz, 1H), 7.57-7.32 (multiple peaks, 5H), 7.22-7.12 (multiple peaks, 3H), 6.97-6.93 (m, 2H), 1.77 (s, 3H). <sup>13</sup>C{<sup>1</sup>H} NMR (*d*<sub>6</sub>-acetone): δ 162.60 (d, <sup>1</sup>*J*<sub>CF</sub> = 243 Hz), 160.15, 147.34, 140.76, 140.35, 138.29 (d, <sup>4</sup>*J*<sub>CF</sub> = 3.0 Hz), 138.12, 131.99, 131.82 (d, <sup>3</sup>*J*<sub>CF</sub> = 7.6 Hz), 130.79, 130.30, 129.07, 128.16, 123.10, 115.35 (d, <sup>2</sup>*J*<sub>CF</sub> = 21 Hz), 18.91. Anal. Calcd for C<sub>18</sub>H<sub>14</sub>FN: C, 82.11, H, 5.36, N, 5.32; Found: C, 81.86, H, 5.52, N, 5.15. IR (KBr) 1482 cm<sup>-1</sup>.

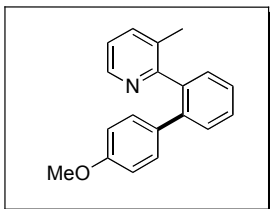


**Product 65:** 3-methyl-2-phenylpyridine (150 mg, 0.89 mmol, 1 equiv), [Mes-I-*p*-ClC<sub>6</sub>H<sub>5</sub>]BF<sub>4</sub> (453 mg, 1.02 mmol, 1.15 equiv) and Pd(OAc)<sub>2</sub> (10 mg, 0.044 mmol, 5 mol%) were combined in acetic acid (8 mL) in a 20 mL vial. The vial was sealed with a Teflon lined cap, and the reaction was stirred at 100 °C for 12 h. The reaction mixture was filtered through a plug of glass wool and concentrated under vacuum. The resulting oil was dissolved in CH<sub>2</sub>Cl<sub>2</sub> and extracted with saturated aqueous NaHCO<sub>3</sub> (1 x 30 mL). The organic layer was dried over MgSO<sub>4</sub>, filtered, and concentrated to afford an orange

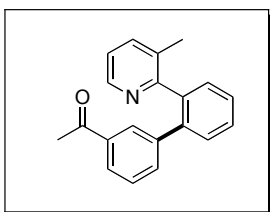
oil, which was purified by chromatography on silica gel ( $R_f = 0.25$  in 75% hexanes/25% ethyl acetate). The product was obtained as a yellow solid (205 mg, 83% yield); mp 106-107 °C.  $^1\text{H}$  NMR ( $d_6$ -acetone):  $\delta$  8.42 (dd,  $J = 4.8, 1.2$  Hz, 1H), 7.55-7.46 (multiple peaks, 3H), 7.43 (dt,  $J = 7.5, 0.8$  Hz, 1H), 7.38-7.36 (m, 1H), 7.21-7.12 (multiple peaks, 5H), 1.79 (s, 3H).  $^{13}\text{C}\{^1\text{H}\}$  NMR ( $d_6$ -acetone):  $\delta$  160.11, 147.48, 140.84, 140.82, 140.25, 138.31, 133.25, 132.12, 131.71, 130.95, 130.39, 129.25, 128.81, 128.53, 123.27, 19.07. Anal. Calcd for  $\text{C}_{18}\text{H}_{14}\text{ClN}$ : C, 77.28, H, 5.04, N, 5.01; Found: C, 77.59, H, 4.91, N, 4.63. IR (KBr) 1477, 1449  $\text{cm}^{-1}$ .



**Product 66:** 3-methyl-2-phenylpyridine (150 mg, 0.89 mmol, 1 equiv), [Mes-I-*p*- $\text{CH}_3\text{C}_6\text{H}_5$ ]BF<sub>4</sub> (432 mg, 1.02 mmol, 1.15 equiv) and Pd(OAc)<sub>2</sub> (10 mg, 0.044 mmol, 5 mol%) were combined in acetic acid (8 mL) in a 20 mL vial. The vial was sealed with a Teflon lined cap, and the reaction was stirred at 100 °C for 12 h. The reaction mixture was filtered through a plug of glass wool and concentrated under vacuum. The resulting oil was dissolved in  $\text{CH}_2\text{Cl}_2$  and extracted with saturated aqueous  $\text{NaHCO}_3$  (1 x 30 mL). The organic layer was dried over  $\text{MgSO}_4$ , filtered, and concentrated to afford an orange oil, which was purified by chromatography on silica gel ( $R_f = 0.25$  in 80% hexanes/20% ethyl acetate). The product was obtained as a yellow solid (193 mg, 84% yield); mp 59-62 °C.  $^1\text{H}$  NMR ( $d_6$ -acetone):  $\delta$  8.45 (d,  $J = 4.4$  Hz, 1H), 7.50-7.43 (multiple peaks, 3H), 7.39-7.33 (multiple peaks, 2H), 7.15 (t,  $J = 7.6$  Hz, 1H), 7.04-6.98 (multiple peaks, 4H), 2.23 (s, 3H), 1.74 (s, 3H).  $^{13}\text{C}\{^1\text{H}\}$  NMR ( $d_6$ -acetone):  $\delta$  159.68, 146.39, 140.49, 139.81, 138.29, 137.15, 136.14, 131.16, 129.95, 129.43, 128.98, 128.46, 128.13, 126.91, 122.12. Anal. Calcd for  $\text{C}_{19}\text{H}_{17}\text{N}$ : C, 87.99, H, 6.61, N, 5.40; Found: C, 87.73, H, 6.45, N, 5.11. IR (KBr) 1449  $\text{cm}^{-1}$ .



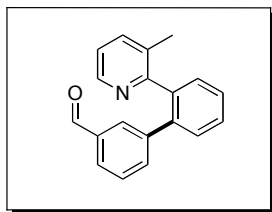
**Product 67:** 3-methyl-2-phenylpyridine (150 mg, 0.89 mmol, 1 equiv), [Mes-I-*p*-MeOC<sub>6</sub>H<sub>5</sub>]<sub>2</sub>BF<sub>4</sub> (449 mg, 1.02 mmol, 1.1 equiv) and Pd(OAc)<sub>2</sub> (10 mg, 0.044 mmol, 5 mol%) were combined in acetic acid (8 mL) in a 20 mL vial. The vial was sealed with a Teflon lined cap, and the reaction was stirred at 120 °C for 12 h. The reaction mixture was filtered through a plug of glass wool and concentrated under vacuum. The resulting oil was dissolved in CH<sub>2</sub>Cl<sub>2</sub> and extracted with saturated aqueous NaHCO<sub>3</sub> (1 x 30 mL). The organic layer was dried over MgSO<sub>4</sub>, filtered, and concentrated to afford an orange oil, which was purified by chromatography on silica gel (R<sub>f</sub> = 0.20 in 80% hexanes/20% ethyl acetate). The product was obtained as a clear oil (197 mg, 81% yield); <sup>1</sup>H NMR (*d*<sub>6</sub>-acetone): δ 8.42 (d, *J* = 4.4 Hz, 1H), 7.46-7.28 (multiple peaks, 5H), 7.14-7.11 (m, 1H), 7.02 (d, *J* = 8.4 Hz, 2H), 6.70 (d, *J* = 8.4 Hz, 2H), 3.68 (s, 3H), 1.70 (s, 3H). <sup>13</sup>C{<sup>1</sup>H} NMR (*d*<sub>6</sub>-acetone): δ 159.73, 158.68, 146.42, 140.22, 139.73, 137.18, 133.40, 131.17, 130.17, 129.94, 129.33, 128.13, 126.68, 122.12, 113.22, 54.49, 18.09. HRMS (electrospray) [M<sup>+</sup>] calcd for C<sub>19</sub>H<sub>17</sub>NO, 275.1310; found, 275.1303. IR (KBr) 1609, 1516 cm<sup>-1</sup>.



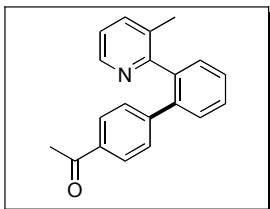
**Product 68:** 3-methyl-2-phenylpyridine (169.2 mg, 1.0 mmol, 1.0 equiv), [Mes-I-(*m*-MeC(O)C<sub>6</sub>H<sub>4</sub>)]<sub>2</sub>BF<sub>4</sub> (497.2 mg, 1.1 mmol, 1.1 equiv) and Pd(OAc)<sub>2</sub> (11.2 mg, 0.05 mmol, 0.05 equiv) were combined in AcOH (10 mL) in a 20 mL scintillation vial, and the vial was sealed with a Teflon-lined cap. The reaction was stirred at 100 °C for 12 h, then cooled to room temperature. The reaction mixture was filtered through a plug of Celite and rinsed with CH<sub>2</sub>Cl<sub>2</sub>, and the solvent was then removed under vacuum. The residue was taken up in CH<sub>2</sub>Cl<sub>2</sub> and extracted with saturated aqueous NaHCO<sub>3</sub> (3 × 30 mL). The



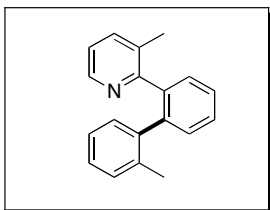
organic layer was then dried over  $\text{MgSO}_4$ , filtered, and concentrated onto silica gel for purification by column chromatography. The product was obtained as a yellow solid (232 mg, 81% yield,  $R_f = 0.15$  in 70% hexanes/30% EtOAc, mp = 95-99 °C).  $^1\text{H}$  NMR ( $\text{CDCl}_3$ ):  $\delta$  8.50 (d,  $J = 4.7$  Hz, 1H), 7.77 (dt,  $J = 7.8, 1.6$  Hz, 1H), 7.69 (t,  $J = 1.6$  Hz, 1H), 7.50-7.37 (multiple peaks, 5H), 7.33-7.25 (multiple peaks, 2H), 7.10 (dd,  $J = 7.6, 4.8$  Hz, 1H), 2.37 (s, 3H), 1.75 (s, 3H).  $^{13}\text{C}\{^1\text{H}\}$  NMR ( $\text{CDCl}_3$ ):  $\delta$  197.58, 158.87, 146.33, 141.00, 139.21, 139.13, 137.46, 136.22, 133.39, 131.33, 129.63, 129.47, 129.27, 128.32, 128.03, 127.71, 126.00, 122.08, 26.27, 18.52. IR (NaCl):  $1685\text{ cm}^{-1}$ . HRMS electrospray (m/z):  $[\text{M}+\text{H}]^+$  calcd for  $\text{C}_{20}\text{H}_{18}\text{NO}$ , 288.1388; found, 288.1385.



**Product 69:** 3-methyl-2-phenylpyridine (169.2 mg, 1.0 mmol, 1.0 equiv),  $[\text{Mes-I}(m\text{-CHOC}_6\text{H}_4)]\text{BF}_4$  (481.8 mg, 1.1 mmol, 1.1 equiv) and  $\text{Pd}(\text{OAc})_2$  (11.2 mg, 0.05 mmol, 0.05 equiv) were combined in AcOH (10 mL) in a 20 mL scintillation vial, and the vial was sealed with a Teflon-lined cap. The reaction was stirred at 100 °C for 12 h, then cooled to room temperature. The reaction mixture was filtered through a plug of Celite and rinsed with  $\text{CH}_2\text{Cl}_2$ , and the solvent was then removed under vacuum. The residue was taken up in  $\text{CH}_2\text{Cl}_2$  and extracted with saturated aqueous  $\text{NaHCO}_3$  ( $3 \times 30$  mL). The organic layer was then dried over  $\text{MgSO}_4$ , filtered, and concentrated onto silica gel for purification by column chromatography. The product was obtained as a viscous pale yellow oil (240 mg, 88% yield,  $R_f = 0.32$  in 65% hexanes/35% EtOAc).  $^1\text{H}$  NMR ( $\text{CDCl}_3$ ):  $\delta$  9.89 (s, 1H), 8.54 (d,  $J = 4.7$  Hz, 1H), 7.78-7.70 (multiple peaks, 2H), 7.60-7.30 (multiple peaks, 7H), 7.14 (dd,  $J = 7.8, 4.7$  Hz, 1H), 1.83, (s, 3H).  $^{13}\text{C}\{^1\text{H}\}$  NMR ( $\text{CDCl}_3$ ):  $\delta$  191.55, 158.37, 146.19, 141.57, 138.99, 138.72, 137.33, 135.78, 134.74, 131.08, 130.40, 129.54, 129.16, 128.19, 128.09, 127.71, 127.14, 122.01, 18.43. IR (NaCl):  $1699\text{ cm}^{-1}$ . HRMS electrospray (m/z):  $[\text{M}+\text{H}]^+$  calcd for  $\text{C}_{19}\text{H}_{16}\text{NO}$ , 274.1232; found, 274.1225.

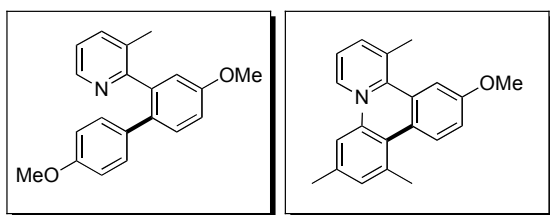


**Product 70:** 3-methyl-2-phenylpyridine (130.3 mg, 0.70 mmol, 1.0 equiv), [Mes-I-(*p*-MeC(O)C<sub>6</sub>H<sub>4</sub>)]BF<sub>4</sub> (348.0 mg, 0.77 mmol, 1.1 equiv) and Pd(OAc)<sub>2</sub> (7.84 mg, 0.035 mmol, 0.05 equiv) were combined in AcOH (7 mL) in a 20 mL scintillation vial, and the vial was sealed with a Teflon-lined cap. The reaction was stirred at 100 °C for 12 h, then cooled to room temperature. The reaction mixture was filtered through a plug of Celite and rinsed with CH<sub>2</sub>Cl<sub>2</sub>, and the solvent was then removed under vacuum. The residue was taken up in CH<sub>2</sub>Cl<sub>2</sub> and extracted with saturated aqueous NaHCO<sub>3</sub> (3 × 30 mL). The organic layer was then dried over MgSO<sub>4</sub>, filtered, and concentrated onto silica gel for purification by column chromatography. The product was obtained as a pale yellow crystalline solid (163 mg, 81% yield, R<sub>f</sub> = 0.09 in 70% hexanes/30% EtOAc, mp = 98-101 °C). <sup>1</sup>H NMR (CDCl<sub>3</sub>): δ 8.47 (d, *J* = 4.8 Hz, 1H), 7.77-7.73 (m, 2H), 7.52-7.38 (multiple peaks, 4H), 7.33-7.29 (m, 1H), 7.23-7.18 (multiple peaks, 2H), 7.10 (dd, *J* = 7.7, 4.8 Hz, 1H), 2.53 (s, 3H), 1.77 (s, 3H). <sup>13</sup>C{<sup>1</sup>H} NMR (CDCl<sub>3</sub>): δ 197.80, 158.87, 146.63, 146.00, 139.44, 139.42, 137.61, 135.15, 131.44, 129.98, 129.52, 129.33, 128.41, 128.15, 127.85, 122.27, 26.51, 18.79. IR (NaCl): 1682 cm<sup>-1</sup>. HRMS electrospray (*m/z*): [M+H]<sup>+</sup> calcd for C<sub>20</sub>H<sub>18</sub>NO, 288.1388; found, 288.1384.



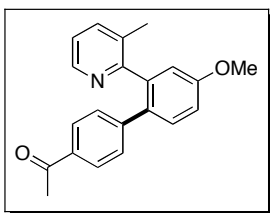
**Product 71:** 3-methyl-2-phenylpyridine (150 mg, 0.89 mmol, 1 equiv), [Mes-I-*p*-CH<sub>3</sub>C<sub>6</sub>H<sub>5</sub>]]BF<sub>4</sub> (489 mg, 1.15 mmol, 1.3 equiv) and Pd(OAc)<sub>2</sub> (10 mg, 0.044 mmol, 5 mol%) were combined in acetic acid (8 mL) in a 20 mL vial. The vial was sealed with a Teflon lined cap, and the reaction was stirred at 100 °C for 12 h. The reaction mixture was filtered through a plug of glass wool and concentrated under vacuum. The resulting oil was dissolved in CH<sub>2</sub>Cl<sub>2</sub> and extracted with saturated aqueous NaHCO<sub>3</sub> (1 x 30 mL).

The organic layer was dried over MgSO<sub>4</sub>, filtered, and concentrated to afford an orange oil, which was purified by chromatography on silica gel ( $R_f = 0.25$  in 80% hexanes/20% ethyl acetate). The product was obtained as a white solid (165 mg, 72% yield); mp 73-77 °C. <sup>1</sup>H NMR (*d*<sub>6</sub>-acetone): δ 8.30 (d, *J* = 3.6 Hz, 1H), 7.48-7.44 (multiple peaks, 2H), 7.39-7.36 (multiple peaks, 2H), 7.32-7.30 (m, 1H), 7.10-7.03 (multiple peaks, 3H), 6.96-6.92 (multiple peaks, 2H), 2.16 (s, 3H), 1.95 (s, 3H). <sup>13</sup>C{<sup>1</sup>H} NMR (*d*<sub>6</sub>-acetone): δ 160.12, 147.01, 141.58 (br), 141.42, 137.95, 136.67 (br), 131.97, 131.13, 130.67, 130.63, 128.35, 127.81, 125.53, 122.81, 20.74, 19.34. (Several of the <sup>13</sup>C NMR peaks are broad and three are missing – this is believed to be the result of fluxional motion about the aryl-aryl bonds.) Anal. Calcd for C<sub>19</sub>H<sub>17</sub>N: C, 87.99, H, 6.61, N, 5.40; Found: C, 88.09, H, 6.51, N, 5.24. IR (KBr) 1418 cm<sup>-1</sup>.



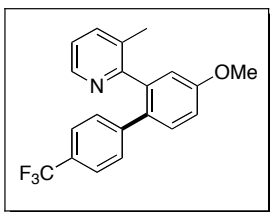
**Products 74 and 73:** 2-(3-methoxyphenyl)-3-methylpyridine (118.4 mg, 0.594 mmol, 1.0 equiv), [Mes-I-(*p*-MeOC<sub>6</sub>H<sub>4</sub>)]BF<sub>4</sub> (522.7 mg, 1.188 mmol, 2.0 equiv) and Pd(OAc)<sub>2</sub> (6.7 mg, 0.0297 mmol, 0.05 equiv) were combined in AcOH (6 mL) in a 20 mL scintillation vial, and the vial was sealed with a Teflon-lined cap. The reaction was stirred at 100 °C for 12 h, then cooled to room temperature. The reaction mixture was filtered through a plug of Celite and rinsed with CH<sub>2</sub>Cl<sub>2</sub>, and the solvent was then removed under vacuum. The residue was taken up in CH<sub>2</sub>Cl<sub>2</sub> and extracted with saturated aqueous NaHCO<sub>3</sub> (3 × 30 mL). The organic layer was then dried over MgSO<sub>4</sub>, filtered, and concentrated onto silica gel for purification by column chromatography. The product of *p*-MeOC<sub>6</sub>H<sub>4</sub> addition was obtained as a pale yellow solid (101 mg, 56% yield,  $R_f = 0.32$  in 70% hexanes/30% EtOAc, mp = 88-92 °C) and the product of Mes addition was obtained as a white crystalline solid (17 mg, 9% yield,  $R_f = 0.50$  in 70% hexanes/30% EtOAc, mp = 95-99 °C). GC of the crude reaction mixture showed that the ratio of *p*-MeOC<sub>6</sub>H<sub>4</sub> : Mes transfer was 6 : 1 (uncorrected ratio based on the areas of the respective peaks). **Mes Addition Product 73.** <sup>1</sup>H NMR (CDCl<sub>3</sub>): δ 8.30 (d, *J* = 4.7 Hz, 1H), 7.36-

7.32 (m, 1H), 7.10 (m, 1H), 7.02-6.97 (multiple peaks, 2H), 6.93 (d,  $J = 2.7$  Hz, 1H), 6.71 (s, 2H), 3.87 (s, 3H), 2.20 (s, 3H), 2.08 (s, 3H), 2.00 (s, 6H).  $^{13}\text{C}\{^1\text{H}\}$  NMR ( $\text{CDCl}_3$ ):  $\delta$  158.61, 158.11, 146.04, 141.21, 137.50, 136.97, 136.71, 135.88, 132.26, 131.92, 131.07, 127.59, 121.76, 114.98, 113.89, 55.31, 20.97, 20.93, 19.27. HRMS electrospray ( $m/z$ ):  $[\text{M}+\text{H}]^+$  calcd for  $\text{C}_{22}\text{H}_{24}\text{NO}_2$ , 318.1858; found, 318.1848. ***p*-MeOC<sub>6</sub>H<sub>4</sub> Addition Product 74.**  $^1\text{H}$  NMR ( $\text{CDCl}_3$ ):  $\delta$  8.50 (d,  $J = 4.7$  Hz, 1H), 7.35-7.27 (multiple peaks, 2H), 7.10 (dd,  $J = 7.4, 4.7$  Hz, 1H), 7.02-6.95 (multiple peaks, 3H), 6.91 (d,  $J = 2.7$  Hz, 1H), 6.70-6.65 (multiple peaks, 2H), 3.85 (s, 3H), 3.72 (s, 3H), 1.74 (s, 3H).  $^{13}\text{C}\{^1\text{H}\}$  NMR ( $\text{CDCl}_3$ ):  $\delta$  159.46, 158.54, 158.04, 146.48, 140.26, 137.51, 133.23, 133.01, 131.56, 130.66, 130.14, 122.09, 114.62, 114.71, 113.18, 55.34, 50.05, 16.71. HRMS electrospray ( $m/z$ ):  $[\text{M}+\text{H}]^+$  calcd for  $\text{C}_{20}\text{H}_{20}\text{NO}_2$ , 306.1494; 306.1496.

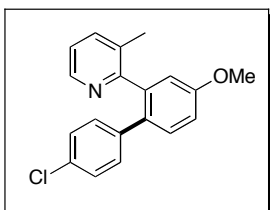


**Product 75:** 2-(3-methoxyphenyl)-3-methylpyridine (133.8 mg, 0.67 mmol, 1.0 equiv),  $[\text{Mes-I-(}p\text{-C(O)MeC}_6\text{H}_4\text{)]BF}_4$  (632.8 mg, 1.4 mmol, 2.0 equiv) and  $\text{Pd}(\text{OAc})_2$  (7.8 mg, 0.035 mmol, 0.05 equiv) were combined in AcOH (7 mL) in a 20 mL scintillation vial, and the vial was sealed with a Teflon-lined cap. The reaction was stirred at 100 °C for 12 h, then cooled to room temperature. The reaction mixture was filtered through a plug of Celite and rinsed with  $\text{CH}_2\text{Cl}_2$ , and the solvent was then removed under vacuum. The residue was taken up in  $\text{CH}_2\text{Cl}_2$  and extracted with saturated aqueous  $\text{NaHCO}_3$  ( $3 \times 30$  mL). The organic layer was then dried over  $\text{MgSO}_4$ , filtered, and concentrated onto silica gel for purification by column chromatography (193.0 mg, 91% yield,  $R_f = 0.2$  in 70% hexanes/30% EtOAc). GC of the crude reaction mixture showed that the ratio of ***p*-MeOC<sub>6</sub>H<sub>4</sub>** : **Mes** transfer was 58 : 1 (uncorrected ratio based on the areas of the respective peaks).  $^1\text{H}$  NMR ( $\text{CDCl}_3$ ):  $\delta$  8.49 (d,  $J = 4.0$  Hz, 1H), 7.72 (dd,  $J = 6.6, 1.8$  Hz, 2H), 7.34 (d,  $J = 8.4$ , 1H), 7.30 (d,  $J = 6.8$ , 1H), 7.16-7.05 (multiple peaks, 3H), 7.03 (dd,  $J = 8.4, 2.8$ , 1H), 6.94 (d,  $J = 2.8$ , 1H), 3.85 (s, 3H), 2.51, (s, 3H), 1.75, (s, 3H).  $^{13}\text{C}\{^1\text{H}\}$

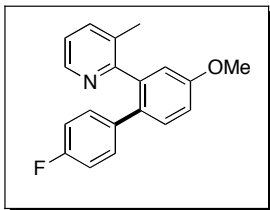
NMR (CDCl<sub>3</sub>):  $\delta$  197.78, 159.40, 158.73, 146.59, 145.75, 140.58, 137.69, 134.74, 132.06, 131.43, 130.81, 129.16, 127.84, 122.34, 114.32, 114.67, 55.36, 26.47, 18.69.



**Product 76:** 2-(3-methoxyphenyl)-3-methylpyridine (75.8 mg, 0.38 mmol, 1.0 equiv), [Mes-I-(*p*-CF<sub>3</sub>C<sub>6</sub>H<sub>4</sub>)]BF<sub>4</sub> (200.0 mg, 0.418 mmol, 1.1 equiv) and Pd(OAc)<sub>2</sub> (4.3 mg, 0.019 mmol, 0.05 equiv) were combined in AcOH (4 mL) in a 20 mL scintillation vial, and the vial was sealed with a Teflon-lined cap. The reaction was stirred at 100 °C for 12 h, then cooled to room temperature. The reaction mixture was filtered through a plug of Celite and rinsed with CH<sub>2</sub>Cl<sub>2</sub>, and the solvent was then removed under vacuum. The residue was taken up in CH<sub>2</sub>Cl<sub>2</sub> and extracted with saturated aqueous NaHCO<sub>3</sub> (3 × 30 mL). The organic layer was then dried over MgSO<sub>4</sub>, filtered, and concentrated onto silica gel for purification by column chromatography. The product was obtained as a pale yellow crystalline solid (106 mg, 81% yield, R<sub>f</sub> = 0.2 in 70% hexanes/30% EtOAc, mp = 89-93 °C). GC of the crude reaction mixture showed that the ratio of *p*-CF<sub>3</sub>C<sub>6</sub>H<sub>4</sub> : Mes transfer was 108 : 1 (uncorrected ratio based on the areas of the respective peaks). <sup>1</sup>H NMR (CDCl<sub>3</sub>):  $\delta$  8.49 (d, *J* = 4.7 Hz, 1H), 7.41-7.30 (multiple peaks, 4H), 7.18 (d, *J* = 8.6 Hz, 2H), 7.12 (dd, *J* = 7.8, 4.7 Hz, 1H), 7.04 (dd, *J* = 8.5, 2.3 Hz, 1H), 6.94 (d, *J* = 2.3 Hz, 1H), 3.86 (s, 3H), 1.77 (s, 3H). <sup>13</sup>C{<sup>1</sup>H} NMR (CDCl<sub>3</sub>):  $\delta$  159.41, 158.67, 146.62, 144.43 (q, <sup>4</sup>*J*<sub>CF3</sub> = 1 Hz), 140.58, 137.75, 131.83, 131.41, 130.89, 129.29, 128.19 (q, <sup>2</sup>*J*<sub>CF3</sub> = 32 Hz), 124.20 (q, <sup>1</sup>*J*<sub>CF3</sub> = 272 Hz), 124.64 (q, <sup>3</sup>*J*<sub>CF3</sub> = 4 Hz), 122.44, 114.77, 114.71, 55.37, 18.67. HRMS electrospray (*m/z*): [M+H]<sup>+</sup> calcd for C<sub>20</sub>H<sub>17</sub>F<sub>3</sub>NO, 344.1262; found, 344.1263.

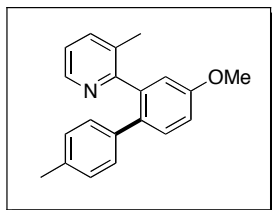


**Product 77:** 2-(3-methoxyphenyl)-3-methylpyridine (81.5 mg, 0.41 mmol, 1.0 equiv), [Mes-I-(*p*-ClC<sub>6</sub>H<sub>4</sub>)]BF<sub>4</sub> (200.0 mg, 0.45 mmol, 1.1 equiv) and Pd(OAc)<sub>2</sub> (4.6 mg, 0.0205 mmol, 0.05 equiv) were combined in AcOH (4 mL) in a 20 mL scintillation vial, and the vial was sealed with a Teflon-lined cap. The reaction was stirred at 100 °C for 12 h, then cooled to room temperature. The reaction mixture was filtered through a plug of Celite and rinsed with CH<sub>2</sub>Cl<sub>2</sub>, and the solvent was then removed under vacuum. The residue was taken up in CH<sub>2</sub>Cl<sub>2</sub> and extracted with saturated aqueous NaHCO<sub>3</sub> (3 × 30 mL). The organic layer was then dried over MgSO<sub>4</sub>, filtered, and concentrated onto silica gel for purification by column chromatography. The product was obtained as a pale yellow solid (100 mg, 79% yield, R<sub>f</sub> = 0.24 in 70% hexanes/30% EtOAc, mp = 88.0-93 °C). GC of the crude reaction mixture showed that the ratio of *p*-ClC<sub>6</sub>H<sub>4</sub> : Mes transfer was 29 : 1 (uncorrected ratio based on the areas of the respective peaks). <sup>1</sup>H NMR (CDCl<sub>3</sub>): δ 8.49 (d, *J* = 4.6 Hz, 1H), 7.50-7.30 (multiple peaks, 2H), 7.14-7.07 (multiple peaks, 3H), 7.04-6.96 (multiple peaks, 3H), 6.92 (d, *J* = 8.5, 2.7 Hz, 1H), 3.85 (s, 3H), 1.76 (s, 3H). <sup>13</sup>C{<sup>1</sup>H} NMR (CDCl<sub>3</sub>): δ 159.06, 158.92, 146.57, 140.40, 139.22, 137.69, 132.24, 132.05, 131.44, 130.71, 130.36, 127.91, 122.32, 114.69, 114.58, 55.37, 18.72. HRMS electrospray (*m/z*): [M+H]<sup>+</sup> calcd for C<sub>19</sub>H<sub>17</sub>ClNO, 310.0999; found, 310.1009.



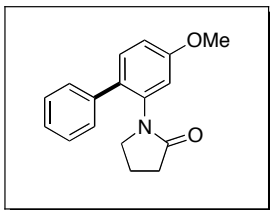
**Product 78:** 2-(3-methoxyphenyl)-3-methylpyridine (118.4 mg, 0.594 mmol, 1.0 equiv), [Mes-I-(*p*-FC<sub>6</sub>H<sub>4</sub>)]BF<sub>4</sub> (279.9 mg, 0.654 mmol, 1.1 equiv) and Pd(OAc)<sub>2</sub> (6.7 mg, 0.0297 mmol, 0.05 equiv) were combined in AcOH (6 mL) in a 20 mL scintillation vial, and the vial was sealed with a Teflon-lined cap. The reaction was stirred at 100 °C for 12 h, then cooled to room temperature. The reaction mixture was filtered through a plug of Celite and rinsed with CH<sub>2</sub>Cl<sub>2</sub>, and the solvent was then removed under vacuum. The residue was taken up in CH<sub>2</sub>Cl<sub>2</sub> and extracted with saturated aqueous NaHCO<sub>3</sub> (3 × 30 mL). The organic layer was then dried over MgSO<sub>4</sub>, filtered, and concentrated onto silica gel for purification by column chromatography. The product was obtained as a viscous

pale yellow oil (138 mg, 79% yield,  $R_f = 0.17$  in 70% hexanes/30% EtOAc). GC of the crude reaction mixture showed that the ratio of ***p*-FC<sub>6</sub>H<sub>4</sub>** : **Mes** transfer was 12 : 1 (uncorrected ratio based on the areas of the respective peaks). <sup>1</sup>H NMR (CDCl<sub>3</sub>): δ 8.49 (d,  $J = 5.1$  Hz, 1H), 7.38-7.28 (multiple peaks, 2H), 7.11 (dd,  $J = 7.8, 4.7$  Hz, 1H), 7.06-6.98 (multiple peaks, 3H), 6.95 (d,  $J = 2.7$  Hz, 1H), 6.86-6.78 (multiple peaks, 2H), 3.85 (s, 3H), 1.76 (s, 3H). <sup>13</sup>C{<sup>1</sup>H} NMR (CDCl<sub>3</sub>): δ 161.48 (d,  $^1J_F = 246$  Hz), 159.05, 158.90, 146.50, 140.40, 137.59, 136.73 (d,  $^4J_F = 3$  Hz), 132.26, 131.44, 130.72, 130.61 (d,  $^3J_F = 8$  Hz), 122.25, 114.59, 114.59 (d,  $^2J_F = 21$  Hz), 114.55, 55.30, 18.64. HRMS electrospray (m/z): [M+H]<sup>+</sup> calcd for C<sub>19</sub>H<sub>17</sub>FNO, 294.1294; found, 294.1288.

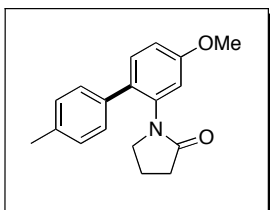


**Product 79:** 2-(3-methoxyphenyl)-3-methylpyridine (118.4 mg, 0.594 mmol, 1.0 equiv), [Mes-I-(*p*-MeC<sub>6</sub>H<sub>4</sub>)]BF<sub>4</sub> (279.9 mg, 0.654 mmol, 1.1 equiv) and Pd(OAc)<sub>2</sub> (6.7 mg, 0.0297 mmol, 0.05 equiv) were combined in AcOH (6 mL) in a 20 mL scintillation vial, and the vial was sealed with a Teflon-lined cap. The reaction was stirred at 100 °C for 12 h, then cooled to room temperature. The reaction mixture was filtered through a plug of Celite and rinsed with CH<sub>2</sub>Cl<sub>2</sub>, and the solvent was then removed under vacuum. The residue was taken up in CH<sub>2</sub>Cl<sub>2</sub> and extracted with saturated aqueous NaHCO<sub>3</sub> (3 × 30 mL). The organic layer was then dried over MgSO<sub>4</sub>, filtered, and concentrated onto silica gel for purification by column chromatography. The product was obtained as a viscous pale yellow oil (134 mg, 80% yield,  $R_f = 0.10$  in 85% hexanes/15% EtOAc). GC of the crude reaction mixture showed that the ratio of ***p*-MeC<sub>6</sub>H<sub>4</sub>** : **Mes** transfer was 20 : 1 (uncorrected ratio based on the areas of the respective peaks). <sup>1</sup>H NMR (CDCl<sub>3</sub>): δ 8.51 (d,  $J = 4.7$  Hz, 1H), 7.36 (d,  $J = 8.6$  Hz, 1H), 7.29 (d,  $J = 7.4$  Hz, 1H), 7.10 (dd,  $J = 7.6, 4.8$  Hz, 1H), 7.01 (dd,  $J = 8.6, 2.7$  Hz, 1H), 6.99-6.91 (multiple peaks, 5H), 3.85 (s, 3H), 2.25 (s, 3H), 1.75 (s, 3H). <sup>13</sup>C{<sup>1</sup>H} NMR (CDCl<sub>3</sub>): δ 159.29, 158.51, 146.27, 140.16, 137.66, 137.32, 135.54, 133.16, 131.38, 130.66, 128.79, 128.31, 121.94, 114.41, 114.35,

55.14, 20.82, 18.58. HRMS electrospray (m/z):  $[M+H]^+$  calcd for  $C_{20}H_{20}NO$ , 290.1545; found, 290.1548.



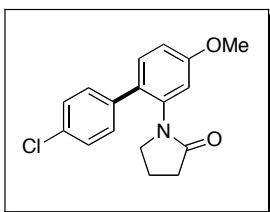
**Product 84:** *N*-(*m*-methoxyphenyl)pyrrolidinone (133.8 mg, 0.7 mmol, 1.0 equiv),  $[Ph_2I]BF_4$  (367.9 mg, 1.4 mmol, 2.0 equiv),  $NaHCO_3$  (88.2 mg, 1.05 mmol, 1.5 equiv), and  $Pd(OAc)_2$  (7.8 mg, 0.035 mmol, 0.05 equiv) were combined in toluene (7 mL) in a 20 mL scintillation vial, and the vial was sealed with a Teflon-lined cap. The reaction was stirred at 100 °C for 17 h and then cooled to room temperature. The reaction mixture was filtered through a plug of Celite and rinsed with  $CH_2Cl_2$ , and concentrated onto silica gel for purification by column chromatography (136.9 mg, 73% yield,  $R_f = 0.1$  in 50% hexanes/50% EtOAc).  $^1H$  NMR ( $CDCl_3$ ):  $\delta$  7.42-7.26 (multiple peaks, 7H), 6.93 (dd,  $J = 8.4, 2.6$ , 1H), 6.86 (d,  $J = 2.4$ , 1H), 3.83 (s, 3H), 3.20 (t,  $J = 7.0$  Hz, 2H), 2.42 (t,  $J = 8.2$  Hz, 2H), 1.86 (m, 2H).  $^{13}C\{^1H\}$  NMR ( $CDCl_3$ ):  $\delta$  175.55, 159.53, 138.85, 137.04, 131.92, 131.54, 128.34, 128.33, 127.14, 114.15, 113.27, 55.40, 50.05, 31.16, 18.91.



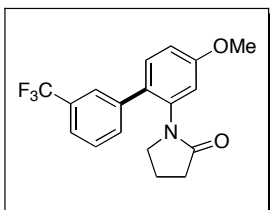
**Product 85:** *N*-(*p*-methoxyphenyl)pyrrolidinone (100 mg, 0.523 mmol, 1.0 equiv),  $[(p-MeC_6H_4)_2I]BF_4$  (414.2 mg, 1.05 mmol, 2.0 equiv),  $NaHCO_3$  (65.9 mg, 0.785 mmol, 1.5 equiv), and  $Pd(OAc)_2$  (5.9 mg, 0.0262 mmol, 0.05 equiv) were combined in toluene (10 mL) in a 20 mL scintillation vial, and the vial was sealed with a Teflon-lined cap. The reaction was stirred at 100 °C for 17 h and then cooled to room temperature. The reaction mixture was filtered through a plug of Celite and rinsed with  $CH_2Cl_2$ , and concentrated onto silica gel for purification by column chromatography. The product was obtained as a yellow solid (122 mg, 83% yield,  $R_f = 0.17$  in 50% hexanes/50% EtOAc, mp = 115-119



°C).  $^1\text{H}$  NMR ( $d_6$ -acetone):  $\delta$  7.29 (d,  $J = 8.6$  Hz, 1H), 7.25-7.18 (multiple peaks, 4H), 6.96 (dd,  $J = 8.2, 2.7$  Hz, 1H), 6.90 (d,  $J = 2.7$  Hz, 1H), 3.83 (s, 3H), 3.26 (t,  $J = 7.0$  Hz, 2H), 2.35 (s, 3H), 2.26 (t,  $J = 8.0$  Hz, 2H), 1.89 (m, 2H).  $^{13}\text{C}\{^1\text{H}\}$  NMR ( $\text{CDCl}_3$ ):  $\delta$  175.48, 159.28, 136.92, 136.72, 135.82, 131.77, 131.47, 128.98, 128.09, 114.07, 113.16, 55.31, 49.92, 31.13, 21.05, 18.85. IR (NaCl):  $1695\text{ cm}^{-1}$ . HRMS electrospray ( $m/z$ ):  $[\text{M}+\text{H}]^+$  calcd for  $\text{C}_{18}\text{H}_{20}\text{NO}_2$ , 282.1494; found, 282.1484.

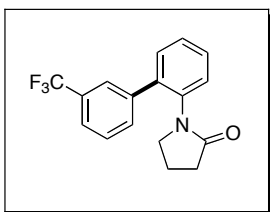


**Product 86:** *N*-(*m*-methoxyphenyl)pyrrolidinone (133.8 mg, 0.7 mmol, 1.0 equiv), [ $(p\text{-MeC}_6\text{H}_4)_2\text{I}]\text{BF}_4$  (554.4 mg, 1.4 mmol, 2.0 equiv),  $\text{NaHCO}_3$  (88.2 mg, 1.05 mmol, 1.5 equiv), and  $\text{Pd}(\text{OAc})_2$  (7.8 mg, 0.035 mmol, 0.05 equiv) were combined in toluene (7 mL) in a 20 mL scintillation vial, and the vial was sealed with a Teflon-lined cap. The reaction was stirred at  $100\text{ }^\circ\text{C}$  for 17 h and then cooled to room temperature. The reaction mixture was filtered through a plug of Celite and rinsed with  $\text{CH}_2\text{Cl}_2$ , and concentrated onto silica gel for purification by column chromatography (167.2 mg, 85% yield,  $R_f = 0.17$  in 50% hexanes/50% EtOAc).  $^1\text{H}$  NMR ( $\text{CDCl}_3$ ):  $\delta$  7.38-7.32 (multiple peaks, 2H), 7.30-7.24 (multiple peaks, 3H) 6.93 (dd,  $J = 8.6, 2.6$ , 1H), 6.85 (d,  $J = 2.6$ , 1H), 3.83 (s, 3H), 3.25 (t,  $J = 7.0$  Hz, 2H), 2.43 (t,  $J = 8.0$  Hz, 2H), 1.92 (m, 2H).  $^{13}\text{C}\{^1\text{H}\}$  NMR ( $\text{CDCl}_3$ ):  $\delta$  175.56, 159.84, 137.37, 137.01, 133.21, 131.45, 130.79, 129.71, 128.55, 114.23, 113.39, 55.46, 50.22, 31.13, 18.90.

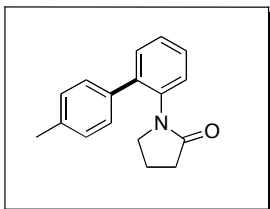


**Product 87:** *N*-(*m*-methoxyphenyl)pyrrolidinone (94.8 mg, 0.496 mmol, 1.0 equiv), [ $(m\text{-CF}_3\text{C}_6\text{H}_4)_2\text{I}]\text{BF}_4$  (500 mg, 0.99 mmol, 2.0 equiv),  $\text{NaHCO}_3$  (62.5 mg, 0.744 mmol, 1.5 equiv), and  $\text{Pd}(\text{OAc})_2$  (5.6 mg, 0.0250 mmol, 0.05 equiv) were combined in toluene (5

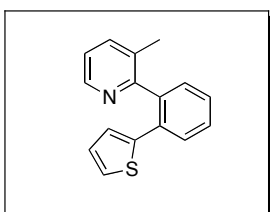
mL) in a 20 mL scintillation vial, and the vial was sealed with a Teflon-lined cap. The reaction was stirred at 100 °C for 17 h and then cooled to room temperature. The reaction mixture was filtered through a plug of Celite and rinsed with CH<sub>2</sub>Cl<sub>2</sub>, and concentrated onto silica gel for purification by column chromatography. The product was obtained as a viscous yellow oil (139 mg, 84% yield, R<sub>f</sub> = 0.15 in 50% hexanes/50% EtOAc). <sup>1</sup>H NMR (*d*<sub>6</sub>-acetone): δ 7.62-7.45 (multiple peaks, 4H), 7.31, (d, *J* = 8.6 Hz, 1H), 6.95 (dd, *J* = 5.9, 2.6 Hz, 1H), 6.86 (d, *J* = 2.6 Hz, 1H), 3.83 (s, 3H), 3.27 (t, *J* = 7.0 Hz, 2H), 2.40 (t, *J* = 8.0 Hz, 2H), 1.90 (m, 2H). <sup>13</sup>C{<sup>1</sup>H} NMR (CDCl<sub>3</sub>): δ 175.35, 160.12, 139.71, 137.24, 131.81 (q, <sup>4</sup>*J*<sub>CF3</sub> = 1 Hz), 131.42, 130.68 (q, <sup>2</sup>*J*<sub>CF3</sub> = 32 Hz), 130.45, 128.89, 125.0 (q, <sup>3</sup>*J*<sub>CF3</sub> = 4 Hz), 128.04 (q, <sup>1</sup>*J*<sub>CF3</sub> = 272 Hz), 123.79 (q, <sup>3</sup>*J*<sub>CF3</sub> = 4 Hz), 114.26, 113.44, 55.43, 50.23, 30.97, 18.83. IR (NaCl): 1696 cm<sup>-1</sup>. HRMS electrospray (*m/z*): [M+H]<sup>+</sup> calcd for C<sub>18</sub>H<sub>17</sub>F<sub>3</sub>NO<sub>2</sub>, 336.1211; found, 335.1205.



**Product 88:** *N*-phenylpyrrolidinone (118.4 mg, 0.734 mmol, 1.0 equiv), [(*m*-CF<sub>3</sub>C<sub>6</sub>H<sub>4</sub>)<sub>2</sub>I]BF<sub>4</sub> (503.9 mg, 1.4 mmol, 2.0 equiv), NaHCO<sub>3</sub> (88.2 mg, 1.05 mmol, 1.5 equiv), and Pd(OAc)<sub>2</sub> (7.8 mg, 0.035 mmol, 0.05 equiv) were combined in toluene (7 mL) in a 20 mL scintillation vial, and the vial was sealed with a Teflon-lined cap. The reaction was stirred at 100 °C for 17 h and then cooled to room temperature. The reaction mixture was filtered through a plug of Celite and rinsed with CH<sub>2</sub>Cl<sub>2</sub>, and concentrated onto silica gel for purification by column chromatography (171.2 mg, 73% yield, R<sub>f</sub> = 0.2 in 50% hexanes/50% EtOAc). <sup>1</sup>H NMR (CDCl<sub>3</sub>): δ 7.65-7.30 (multiple peaks, 8H), 3.29 (t, *J* = 7.0 Hz, 2H), 2.41 (t, *J* = 8.2 Hz, 2H), 1.91 (m, 2H). <sup>13</sup>C{<sup>1</sup>H} NMR (CDCl<sub>3</sub>): δ 174.84, 141.38, 139.26, 138.21, 133.08 (q, <sup>4</sup>*J*<sub>CF3</sub> = 1 Hz), 131.22, 130.88 (q, <sup>2</sup>*J*<sub>CF3</sub> = 32 Hz), 130.21, 129.86, 129.24, 128.69, 125.74 (q, <sup>3</sup>*J*<sub>CF3</sub> = 4 Hz), 125.27 (q, <sup>1</sup>*J*<sub>CF3</sub> = 272 Hz), 124.80 (q, <sup>3</sup>*J*<sub>CF3</sub> = 4 Hz), 50.80, 31.32, 19.62.

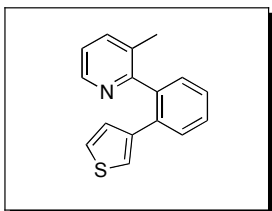


**Product 89:** *N*-phenylpyrrolidinone (118.4 mg, 0.734 mmol, 1.0 equiv), [(*p*-MeC<sub>6</sub>H<sub>4</sub>)<sub>2</sub>I]BF<sub>4</sub> (554.4 mg, 0.14 mmol, 2.0 equiv), NaHCO<sub>3</sub> (88.2 mg, 1.05 mmol, 1.5 equiv), and Pd(OAc)<sub>2</sub> (7.8 mg, 0.0350 mmol, 0.05 equiv) were combined in toluene (7 mL) in a 20 mL scintillation vial, and the vial was sealed with a Teflon-lined cap. The reaction was stirred at 100 °C for 17 h and then cooled to room temperature. The reaction mixture was filtered through a plug of Celite and rinsed with CH<sub>2</sub>Cl<sub>2</sub>, and concentrated onto silica gel for purification by column chromatography. The product was obtained as a viscous yellow oil (149 mg, 81% yield, R<sub>f</sub> = 0.16 in 50% hexanes/50% EtOAc). <sup>1</sup>H NMR (*d*<sub>6</sub>-acetone): δ 7.42-7.21 (multiple peaks, 8H), 3.45, (t, *J* = 7.3 Hz, 2H), 2.37, (s, 3H), 2.26 (t, *J* = 8.1 Hz, 2H), 2.85 (m, 2H). <sup>13</sup>C{<sup>1</sup>H} NMR (*d*<sub>6</sub>-acetone): δ 175.96, 141.51, 139.09, 138.82, 138.39, 132.28, 130.85, 130.58, 129.96, 129.74, 129.38, 51.48, 32.47, 22.19, 20.65. IR (NaCl): 1697 cm<sup>-1</sup>. HRMS electrospray (*m/z*): [M+H]<sup>+</sup> calcd for C<sub>17</sub>H<sub>18</sub>NO<sub>2</sub>, 252.1388; found, 252.1378.



**Product 101:** Iodomesitylene diacetate (728.4 mg, 2.0 mmol, 2.0 equiv), and 2-thiophene boronic acid (256.0 mg, 2.0 mmol, 2.0 equiv) were combined in AcOH (10 mL) and stirred for 15 minutes in a 20 mL scintillation vial. Then 3-methyl-2-phenylpyridine (169.2 mg, 1.0 mmol, 1.0 equiv) and Pd(tfa)<sub>2</sub> (16.6 mg, 0.05 mmol, 0.05 equiv) were added to the reaction mixture. The vial was then sealed with a Teflon-lined cap, and heated to 120 °C for 12 h. The reaction mixture was filtered through a plug of Celite and rinsed with CH<sub>2</sub>Cl<sub>2</sub>, and the solvent was then removed under vacuum. The residue was taken up in CH<sub>2</sub>Cl<sub>2</sub> and extracted with saturated aqueous NaHCO<sub>3</sub> (3 × 30 mL). The organic layer was then dried over MgSO<sub>4</sub>, filtered, and concentrated onto silica gel for

purification by column chromatography (67.9 mg, 23% yield,  $R_f = 0.10$  in 90% hexanes/10% EtOAc).  $^1\text{H NMR}$  ( $\text{CDCl}_3$ ):  $\delta$  8.53 (d,  $J = 3.2$ , 1H), 7.61 (dd,  $J = 6.4$ , 1.0 Hz, 1H), 7.47-7.37 (multiple peaks, 3H), 7.36-7.32 (multiplet, 1H), 7.19 (dd,  $J = 6.0$ , 4.0 Hz, 1H), 7.14 (dd,  $J = 4.0$ , 0.8 Hz, 1H), 6.82 (dd,  $J = 4.0$ , 2.8 Hz, 1H), 6.59 (dd,  $J = 2.8$ , 0.8 Hz, 1H) 1.88 (s, 3H).



**Product 104:** Iodomesitylene diacetate (579.4 mg, 1.6 mmol, 2.0 equiv), and 3-thiophene boronic acid (204.8 mg, 1.6 mmol, 2.0 equiv) were combined in AcOH (8 mL) and stirred for 15 minutes in a 20 mL scintillation vial. Then 3-methyl-2-phenylpyridine (135.4 mg, 0.80 mmol, 1.0 equiv) and  $\text{Pd}(\text{tfa})_2$  (13.3 mg, 0.04 mmol, 0.05 equiv) were added to the reaction mixture. The vial was then sealed with a Teflon-lined cap, and heated to 120 °C for 12 h. The reaction mixture was filtered through a plug of Celite and rinsed with  $\text{CH}_2\text{Cl}_2$ , and the solvent was then removed under vacuum. The residue was taken up in  $\text{CH}_2\text{Cl}_2$  and extracted with saturated aqueous  $\text{NaHCO}_3$  ( $3 \times 30$  mL). The organic layer was then dried over  $\text{MgSO}_4$ , filtered, and concentrated onto silica gel for purification by column chromatography (120.9 mg, 60% yield,  $R_f = 0.14$  in 90% hexanes/10% EtOAc).  $^1\text{H NMR}$  ( $\text{CDCl}_3$ ):  $\delta$  8.52 (d,  $J = 7$ , 1H), 7.55-7.50 (multiplet, 1H), 7.48-7.34 (multiple peaks, 4H), 7.15 (dd,  $J = 9.5$ , 6.0Hz, 1H), 7.10 (dd,  $J = 6.8$ , 4.0Hz, 1H), 6.85 (dd,  $J = 4.0$ , 1.5Hz, 1H) 6.77 (dd,  $J = 6.0$ , 1.5Hz, 1H), 1.79 (s, 3H).

## 2.9 References

1. Dick, A. R.; Hull, K. L.; Sanford, M. S. *J. Am. Chem. Soc.* **2004**, *126*, 2300-2301.
2. Desai, L. V.; Hull, K. L.; Sanford, M. S. *J. Am. Chem. Soc.* **2004**, *126*, 9542-9543.
3. Kalyani, D.; Deprez, N. R.; Desai, L. V.; Sanford, M. S. *J. Am. Chem. Soc.* **2005**, *127*, 7330-7331.
4. Desai, L. V.; Malik, H. A.; Sanford, M. S. *Org. Lett.* **2006**, *8*, 1141-1144.
5. Kalberer, E. W.; Whitfield, S. R.; Sanford, M. S. *J. Mol. Catal. A: Chem.* **2006**, *251*, 108-113.
6. Canty, A. J.; Patel, J.; Rodemann, T.; Ryan, J. H.; Skelton, B. W.; White, A. H. *Organometallics* **2004**, *23*, 3466-3473.
7. Bayler, A.; Canty, A. J.; Ryan, J. H.; Skelton, B. W.; White, A. H. *Inorg. Chem. Commun.* **2000**, *3*, 575-578.
8. Canty, A. J.; Rodemann, T. *Inorg. Chem. Commun.* **2003**, *6*, 1382-1384.
9. Canty, A. J.; Rodemann, T.; Skelton, B. W.; White, A. H. *Inorg. Chem. Commun.* **2005**, *8*, 55-57.
10. Canty, A. J.; Rodemann, T.; Skelton, B. W.; White, A. H. *Organometallics* **2006**, *25*, 3996-4001.
11. Chaudhuri, P. D.; Guo, R.; Malinakova, H. C. *J. Organomet. Chem.* **2008**, *693*, 567-573.
12. Canty, A. J.; Gardiner, M. G.; Jones, R. C.; Rodemann, T.; Sharma, M. *J. Am. Chem. Soc.* **2009**, *131*, 7236-7237.
13. Lagunas, M.-C.; Gossage, R. A.; Spek, A. L.; van Koten, G. *Organometallics* **1998**, *17*, 731-741.
14. Dick, A. R.; Kampf, J. W.; Sanford, M. S. *J. Am. Chem. Soc.* **2005**, *127*, 12790-12791.
15. Whitfield, S. R.; Sanford, M. S. *J. Am. Chem. Soc.* **2007**, *129*, 15142-15143.
16. Racowski, J. M.; Dick, A. R.; Sanford, M. S. *J. Am. Chem. Soc.* **2009**, *131*, 10974-10983.
17. Kalyani, D.; Sanford, M. S. *Org. Lett.* **2005**, *7*, 4149-4152.

18. Desai, L. V.; Stowers, K. J.; Sanford, M. S. *J. Am. Chem. Soc.* **2008**, *130*, 13285-13293.
19. Chen, D.-W.; Ochiai, M. *J. Org. Chem.* **1999**, *64*, 6804-6814.
20. McKillop, A.; Kemp, D. *Tetrahedron* **1989**, *45*, 3299-3306.
21. Dauban, P.; Saniere, L.; Tarrade, A.; Dodd, R. H. *J. Am. Chem. Soc.* **2001**, *123*, 7707-7708.
22. Beringer, F. M.; Drexler, M.; Gindler, E. M.; Lumpkin, C. C. *J. Am. Chem. Soc.* **1953**, *75*, 2705-2708.
23. Shah, A.; Pike, V. W.; Widdowson, D. A. *J. Chem. Soc., Perkin Trans. 1* **1997**, 2463-2465.
24. Bielawski, M.; Aili, D.; Olofsson, B. *J. Org. Chem.* **2008**, *73*, 4602-4607.
25. Margida, A. J.; Koser, G. F. *J. Org. Chem.* **1984**, *49*, 3643-3646.
26. Okuyama, T. *Acc. Chem. Res.* **2002**, *35*, 12-18.
27. Schank, K.; Lick, C. *Synthesis* **1983**, 392-395.
28. Kitamura, T.; Abe, T.; Fujiwara, Y.; Yamaji, T. *Synthesis* **2003**, 213-216.
29. Hossain, D.; Kitamura, T. *Synthesis* **2005**, 1932-1934.
30. Kazmierczak, P.; Skulski, L.; Kraszkiewicz, L. *Molecules* **2001**, *6*, 881-891.
31. Kitamura, T.; Yamane, M.; Inoue, K.; Todaka, M.; Fukatsu, N.; Meng, Z.; Fujiwara, Y. *J. Am. Chem. Soc.* **1999**, *121*, 11674-11679.
32. Lyons, T. W.; Sanford, M. S. *Chem. Rev.* **in press**.
33. Daugulis, O.; Zaitsev, V. G. *Angew. Chem., Int. Ed.* **2005**, *44*, 4046-4048.
34. Phipps, R. J.; Gaunt, M. J. *Science* **2009**, *323*, 1593-1597.
35. Phipps, R. J.; Grimster, N. P.; Gaunt, M. J. *J. Am. Chem. Soc.* **2008**, *130*, 8172-8174.
36. Yang, F.; Wu, Y.; Li, Y.; Wang, B.; Zhang, J. *Tetrahedron* **2009**, *65*, 914-919.
37. Shabashov, D.; Daugulis, O. *Org. Lett.* **2005**, *7*, 3657-3659.
38. Zaitsev, V. G.; Daugulis, O. *J. Am. Chem. Soc.* **2005**, *127*, 4156-4157.
39. Yang, F.; Wu, Y.; Zhu, Z.; Zhang, J.; Li, Y. *Tetrahedron* **2008**, *64*, 6782-6787.
40. Chiong, H. A.; Pham, Q.-N.; Daugulis, O. *J. Am. Chem. Soc.* **2007**, *129*, 9879-9884.

41. Shabashov, D.; Molina Maldonado, J. R.; Daugulis, O. *J. Org. Chem.* **2008**, *73*, 7818-7821.
42. Thirunavukkarasu, V. S.; Parthasarathy, K.; Cheng, C.-H. *Angew. Chem., Int. Ed.* **2008**, *47*, 9462-9465.
43. Giri, R.; Mangel, N.; Li, J.-J.; Wang, D.-H.; Breazzano, S. P.; Saunders, L. B.; Yu, J.-Q. *J. Am. Chem. Soc.* **2007**, *129*, 3510-3511.
44. Satoh, T.; Kawamura, Y.; Miura, M.; Nomura, M. *Angew. Chem., Int. Ed. Engl.* **1997**, *36*, 1740-1742.
45. Kametani, Y.; Satoh, T.; Miura, M.; Nomura, M. *Tetrahedron Lett.* **2000**, *41*, 2655-2658.
46. Kawamura, Y.; Satoh, T.; Miura, M.; Nomura, M. *Chem. Lett.* **1999**, 961-962.
47. Satoh, T.; Inoh, J.-i.; Kawamura, Y.; Kawamura, Y.; Miura, M.; Nomura, M. *Bull. Chem. Soc. Jpn.* **1998**, *71*, 2239-2246.
48. Terao, Y.; Kametani, Y.; Wakui, H.; Satoh, T.; Miura, M.; Nomura, M. *Tetrahedron* **2001**, *57*, 5967-5974.
49. Wakui, H.; Kawasaki, S.; Satoh, T.; Miura, M.; Nomura, M. *J. Am. Chem. Soc.* **2004**, *126*, 8658-8659.
50. Terao, Y.; Wakui, H.; Satoh, T.; Miura, M.; Nomura, M. *J. Am. Chem. Soc.* **2001**, *123*, 10407-10408.
51. Terao, Y.; Wakui, H.; Nomoto, M.; Satoh, T.; Miura, M.; Nomura, M. *J. Org. Chem.* **2003**, *68*, 5236-5243.
52. Hennings, D. D.; Iwasa, S.; Rawal, V. H. *J. Org. Chem.* **1997**, *62*, 2-3.
53. Dogan, O.; Gurbuz, N.; Ozdemir, I.; Cetinkaya, B. *Heteroatom Chem.* **2008**, *19*, 569-574.
54. Shi, Z.; Li, B.; Wan, X.; Cheng, J.; Fang, Z.; Cao, B.; Qin, C.; Wang, Y. *Angew. Chem., Int. Ed.* **2007**, *46*, 5554-5558.
55. Kirchberg, S.; Vogler, T.; Studer, A. *Synlett* **2008**, 2841-2845.
56. Yang, S.; Li, B.; Wan, X.; Shi, Z. *J. Am. Chem. Soc.* **2007**, *129*, 6066-6067.
57. Zhou, H.; Xu, Y.-H.; Chung, W.-J.; Loh, T.-P. *Angew. Chem., Int. Ed.* **2009**, *48*, 5355-5357.

58. Hull, K. L.; Lanni, E. L.; Sanford, M. S. *J. Am. Chem. Soc.* **2006**, *128*, 14047-14049.
59. Hull, K. L.; Sanford, M. S. *J. Am. Chem. Soc.* **2007**, *129*, 11904-11905.
60. Hull, K. L.; Sanford, M. S. *J. Am. Chem. Soc.* **2009**, *131*, 9651-9653.
61. Xia, J.-B.; You, S.-L. *Organometallics* **2007**, *26*, 4869-4871.
62. Li, B.-J.; Tian, S.-L.; Fang, Z.; Shi, Z.-J. *Angew. Chem., Int. Ed.* **2008**, *47*, 1115-1118.
63. Li, B.-J.; Yang, S.-D.; Shi, Z.-J. *Synlett* **2008**, 949-957.
64. Brasche, G.; Garcia-Fortanet, J.; Buchwald, S. L. *Org. Lett.* **2008**, *10*, 2207-2210.
65. Littke, A. F.; Dai, C.; Fu, G. C. *J. Am. Chem. Soc.* **2000**, *122*, 4020-4028.
66. Littke, A. F.; Schwarz, L.; Fu, G. C. *J. Am. Chem. Soc.* **2002**, *124*, 6343-6348.
67. Shakespeare, W. C. *Tetrahedron Lett.* **1999**, *40*, 2035-2038.



## Chapter 3

# Mechanistic Investigations of Ligand Directed C–H Activation/Arylation Reactions

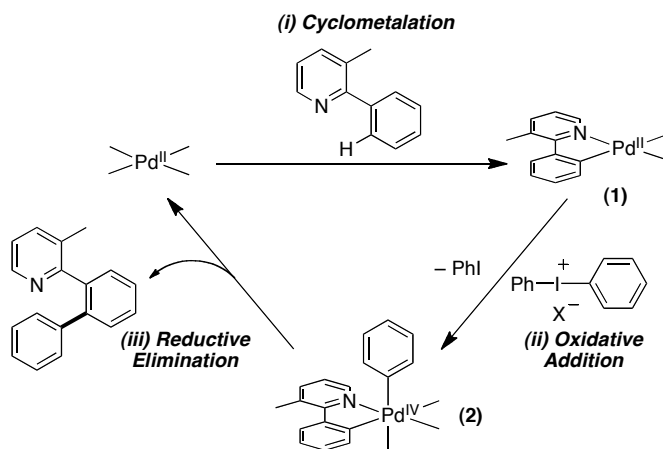
### 3.1 Background and Significance

We next investigated the details of the mechanism of ligand directed C–H arylation. A comprehensive understanding of the mechanism would help address remaining challenges for this methodology. These include: (1) decreasing the catalyst loadings, (2) employing a broader set of effective directing groups, (3) generalizing the reaction conditions for all substrates, (4) expanding to other I<sup>III</sup> reagents, and (5) understanding how to improve the *in situ* oxidant generation. These studies could also provide insights into a mechanistically unique C–H arylation reaction including a high oxidation state Ar–Pd intermediate, and this would be the first example of a detailed investigation of any C–H activation/arylation mechanism.

To accomplish these goals, the proposed catalytic cycle outlined in the development of this transformation (*Chapter 2*) was investigated. This mechanism is proposed to proceed through: (i) coordination of Pd<sup>II</sup> and directed C–H activation of a proximal C–H bond to give intermediate **1**, (ii) oxidation with [Ph–I<sup>III</sup>–Ph]<sup>+</sup> to the key Ar–Pd<sup>IV</sup> intermediate **2**, and (iii) C–C bond forming reductive elimination affording the desired product and regenerating Pd<sup>II</sup> (**Scheme 3.1**). Although each of these individual steps have precedent in stoichiometric reactions presented in the literature, it is important to provide evidence for each of them in the context of this catalytic cycle. To accomplish this several key items involving this reaction mechanism must be addressed including: (1) exploring other possible mechanistic pathways, (2) obtaining evidence for key intermediates, (3) examining specific details about the role of each reaction component in

the catalytic cycle, and (4) characterizing of the ligand environment around the palladium.

**Scheme 3.1:** Initially Proposed Catalytic Cycle for C–H Arylation.



Initial experiments began with item (1), addressing the possibility of alternative mechanistic pathways that could be envisaged. These studies aimed to probe the possibilities of both  $\text{Pd}^{0/\text{II}}$  reaction pathway, and reactions involving free radical intermediates.

The next series of investigations focused on item (2), and they sought to provide evidence for, and gain information about, the key intermediates **1** and **2**. Intermediates such as the cyclometallated complex **1** were studied to demonstrate their catalytic viability, stoichiometric reactivity, and their interaction with various reaction components.<sup>1</sup> Analogue of the second key intermediate,  $\text{Ar-Pd}^{\text{IV}}$  intermediate **2**, have been shown in previous model studies to be accessible by oxidation  $\text{Pd}^{\text{II}}$  with  $[\text{Ar-I}^{\text{III}}-\text{Ar}]^+$  reagents. We sought to provide evidence for oxidation to this intermediate in the catalytic cycle by performing Hammett investigations.<sup>2-7</sup>

Finally, the combination of several studies aim to address item (3), which is elucidation of the role of each reaction component in the catalytic cycle, and (4) understanding the ligand environment around the palladium center. First, the kinetic order in the substrate, oxidant, and catalyst were investigated. Second, we explored kinetic isotope experiments to examine the effects of isotopic labeling on the rate of the

reaction. Finally, the resting states of catalytic intermediates were identified to understand the important interactions occurring at both palladium and oxidant in the reaction. The combination of studies involving aim 3 and 4 allowed for the determination of a rate law and identification of the rate-limiting step of the catalytic cycle. These investigations provided insight into the ancillary ligands present on palladium throughout the catalytic cycle, which to this point have been depicted only as sticks (**Scheme 3.1**).

Investigations of these key aspects of the reaction, amongst others, are discussed individually in detail below. The culmination of all of the above-described experiments can then be analyzed as a whole, to provide a detailed mechanistic picture of this transformation. These experiments establish oxidation as the rate-limiting step of the catalytic cycle, and additionally, provide evidence for the intermediacy of a dimeric high oxidation state palladium species. The implications of these mechanistic investigations will then be discussed.

### 3.2 Preliminary Mechanistic Experiments

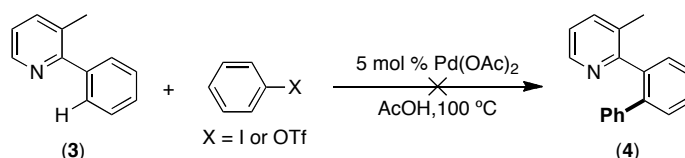
My colleague, Dr. Dipannita Kalyani, began efforts to examine the mechanism of this transformation by completing a series of mechanistic investigations outlined here. These experiments probed a number of potential reaction pathways that could lead to the observed products. Although a Pd<sup>II/IV</sup> mechanism was proposed, it is equally important to explore the possibility of alternative mechanisms such as a Pd<sup>0/II</sup> catalytic cycle and free radical pathways.

For all of the kinetic rate studies, choice of the model substrate is very important and the substrate 3-methyl-2-phenylpyridine (**3**) was chosen for two important reasons. First, the arylation of this substrate has been demonstrated to proceed efficiently with several I<sup>III</sup> oxidants containing a range of diverse aryl groups. Second, excellent control of both mono-arylation and selective addition of the desired aryl groups from the I<sup>III</sup> reagent has been achieved. Each of these is important for kinetic studies where low reaction efficiency and the formation of multiple products can complicate the analysis.

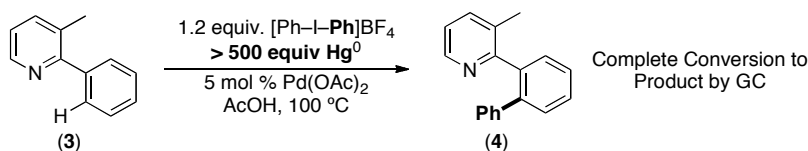
Efforts began by conducting experiments to probe a possible Pd<sup>0/II</sup> mechanism. First, the oxidant [Ph-I<sup>III</sup>-Ph]BF<sub>4</sub> was replaced with Ph-I and Ph-OTf, electrophiles commonly used for Pd<sup>0/II</sup> chemistry (**Scheme 3.2**). In each case <1% of the desired

phenylation product was observed by gas chromatography. Next, the involvement of Pd<sup>0</sup> nanoparticles was explored by addition of >500 equiv of Hg, which is known to be a poison for heterogeneous catalysis (**Scheme 3.3**). Under the standard reaction conditions with the addition of Hg, complete conversion to product **4** was observed by gas chromatography.<sup>8,9</sup> Finally, it has been observed that aryl halides, which are known to be reactive with low valent palladium, remain unaffected under the reaction conditions.<sup>10,11</sup> Each of these experiments suggest against a Pd<sup>0/II</sup> catalytic cycle in this system.

**Scheme 3.2:** Replacement of [Ph-I<sup>III</sup>-Ph]BF<sub>4</sub> with Ph-I and Ph-OTf.



**Scheme 3.3:** Addition of Hg<sup>0</sup> to the Standard C–H Arylation Reaction.

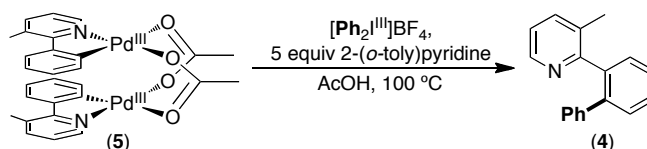


Next, an alternative reaction pathway involving the intermediacy of free radicals could be envisaged.<sup>12</sup> To probe for such intermediates, the free radical inhibitors MEHQ (O-methylhydroquinone) and galvinoxyl were included in the catalytic reaction mixture under otherwise standard conditions. The reaction proceeded unaffected by the additives, suggesting against a free radical chain process playing a role in the reaction.

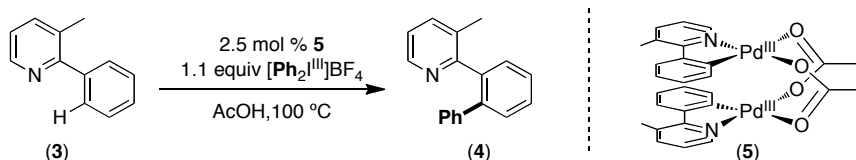
Finally, we investigated whether palladacycle **1** was a catalytic intermediate. This can be demonstrated if **1** will undergo a stoichiometric reaction with a diaryl iodonium oxidant to provide product **4**, and also by demonstrating that **1** is a kinetically viable catalyst itself for this transformation. To accomplish this, the acetate bridged palladacycle **5** was easily synthesized according to literature precedent.<sup>13</sup> First, the stoichiometric reaction of palladacycle **5** with the oxidant [Ph-I<sup>III</sup>-Ph]BF<sub>4</sub>, was successful and led to the desired product **4** in 90% yield (**Scheme 3.4**). Second, **5** was employed as a catalyst (2.5

mol %) in the reaction with 1 equiv of **3**, and 1.1 equiv  $[\text{Ph-I}^{\text{III}}\text{-Ph}]\text{BF}_4$  in AcOH at 100 °C for 12 h (**Scheme 3.6**). This efficiently provided product **5** as determined by gas chromatography, and furthermore displayed a nearly identical reaction profile as compared with  $\text{Pd}(\text{OAc})_2$  as the catalyst. Each of these experiments suggests the competency of palladacycle **5** as a catalytic intermediate.

**Scheme 3.4:** Stoichiometric Reaction of **5** with  $[\text{Ph}_2\text{I}^{\text{III}}]\text{BF}_4$ .



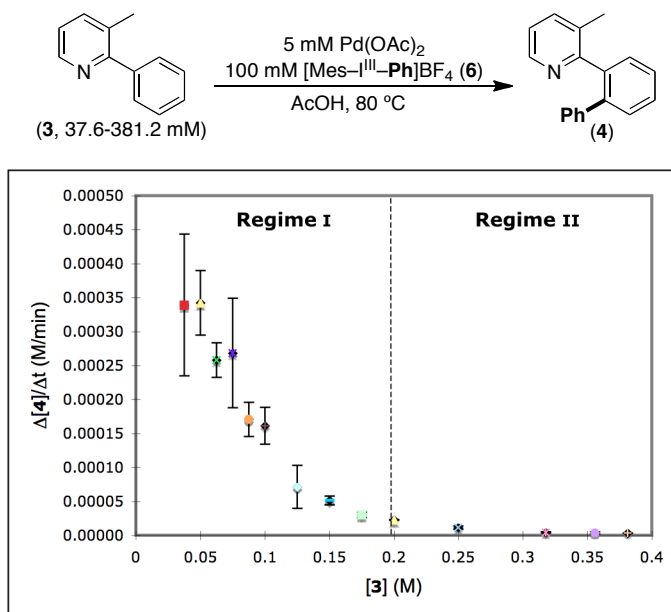
**Scheme 3.5:** Replacement of  $\text{Pd}(\text{OAc})_2$  with **5**.



### 3.3 Kinetic Orders

We next sought to establish the kinetic order in each component of the reaction to ascertain information about the rate-determining step, as well as probe the role of each reaction component. These studies focused specifically on the ligand-directed, palladium-catalyzed C–H phenylation of the model substrate 3-methyl-2-phenylpyridine (**3**) utilizing the oxidant  $[\text{Mes-I}^{\text{III}}\text{-Ph}]\text{BF}_4$  (**6**). Initial experiments involved varying the concentration of **3** (18.8 to 190.6 mM) in the presence of  $[\text{Mes-I}^{\text{III}}\text{-Ph}]\text{BF}_4$  (**6**) (100 mM) and  $\text{Pd}(\text{OAc})_2$  (2.5 mM) in AcOH at 80 °C. The reaction progress was monitored by gas chromatography and the method of initial rates was utilized to determine the reaction rate at each **[3]**. A plot of initial rate ( $\Delta[\mathbf{4}]/\Delta t$ ) versus **[3]** was non-linear, and intriguingly the reaction demonstrated an inverse dependence on **[3]** (**Figure 3.1**). Next, initial rate ( $\Delta[\mathbf{4}]/\Delta t$ ) was plotted versus  $[\mathbf{3}]^{-1}$ ,  $[\mathbf{3}]^{-2}$ , and  $[\mathbf{3}]^{-3}$ . None of these afforded straight lines, suggesting that this data is not inverse 1<sup>st</sup>, 2<sup>nd</sup>, or 3<sup>rd</sup> order over this range.

**Figure 3.1:** Kinetic Order in Substrate at 80 °C.



Further examination of this data allows it to be broken into two regimes, Regime 1 where  $[6] > [3]$ , and Regime 2 where  $[6] < [3]$ . After careful analysis, it was determined that in Regime II a plot of initial rate ( $\Delta[4]/\Delta t$ ) versus  $[3]^{-3}$  afforded a straight line suggestive of an inverse third order dependence on  $[3]$  (**Figure 3.2**). Additional evidence for an inverse third order dependence was provided by performing a non-linear least squares fit to the equation  $f(x) = a[3]^n$  where the order ( $n$ ) in  $[3]$  was found to be  $3.4 \pm 0.5$  ( $a = 1.0 \pm 0.5 \times 10^{-7}$  M/min, **Figure 3.3**). Importantly, this result indicates that to obtain an integer kinetic order in substrate, the reaction must be conducted in the presence of excess **3** relative to I<sup>III</sup>.

**Figure 3.2:** Plot of Initial Rate ( $\Delta[4]/\Delta t$ ) versus  $[3]^{-3}$  in Regime II.

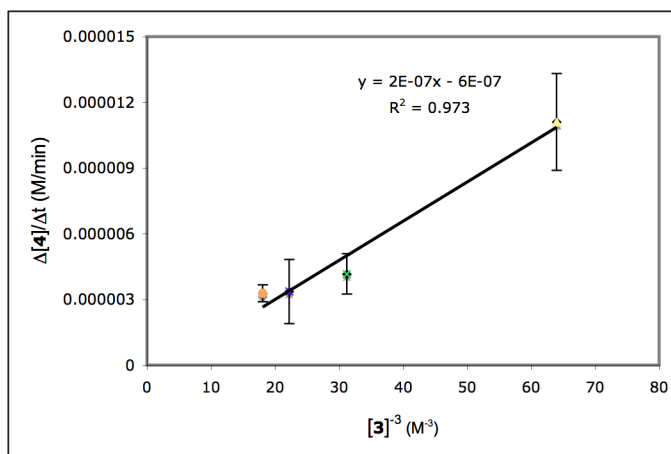
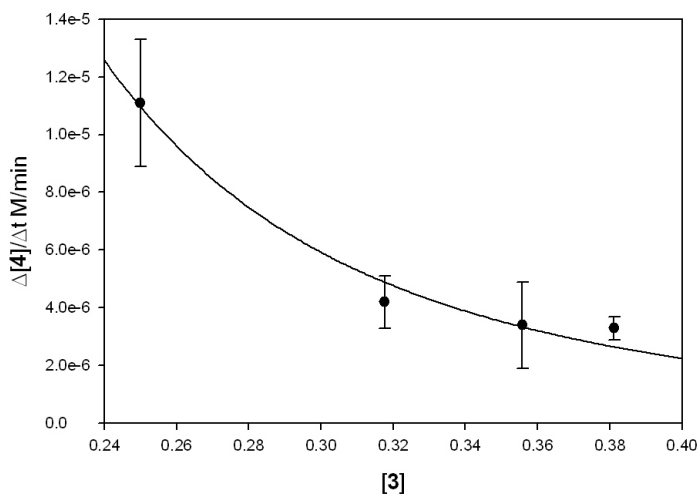


**Figure 3.3:** Data Fit of Initial Rate ( $\Delta[4]/\Delta t$ ) versus  $[4]$  in Regime II.



At the temperature described (80 °C), the reaction rates were exceedingly slow and a suitable yield (<3%) could not be obtained in a reasonable time frame leading to large errors in the rates. It was reasoned that more representative data could be achieved if the reactions were followed to higher yield (~10%). Thus for further confirmation, the experiments described above were repeated at 110 °C. Additionally the determination of the reaction order focused on conditions employing excess substrate to obtain an integer order in **3**. These experiments were accomplished by combining varying concentrations

of 3-methyl-2-phenylpyridine (**3**, 202 to 304 mM) with [Mes-I<sup>III</sup>-Ph]BF<sub>4</sub> (**6**, 100 mM) and Pd(OAc)<sub>2</sub> (5 mM) in AcOH at 110 °C. These experiments again showed an inverse dependence on [**3**] (**Figure 3.4**). A plot of the initial rate ( $\Delta[\mathbf{4}]/\Delta t$ ) versus [**3**]<sup>-3</sup> showed a linear relationship, confirming an inverse third order dependence (**Figure 3.5**). This was further corroborated when this data was treated with a non-linear least squares fit to the equation  $f(x) = a[\mathbf{3}]^n$  and the order (n) was determined to be  $-3.1 \pm 0.2$  ( $a = 6.3 \pm 1.5 \times 10^{-7}$ , **Figure 3.6**). The data obtained suggests that three equiv of **3** must be lost to progress from the resting state to the transition state of the rate-limiting step of the catalytic cycle.

**Figure 3.4:** Plot of Initial Rate ( $\Delta[\mathbf{4}]/\Delta t$ ) versus [**3**].

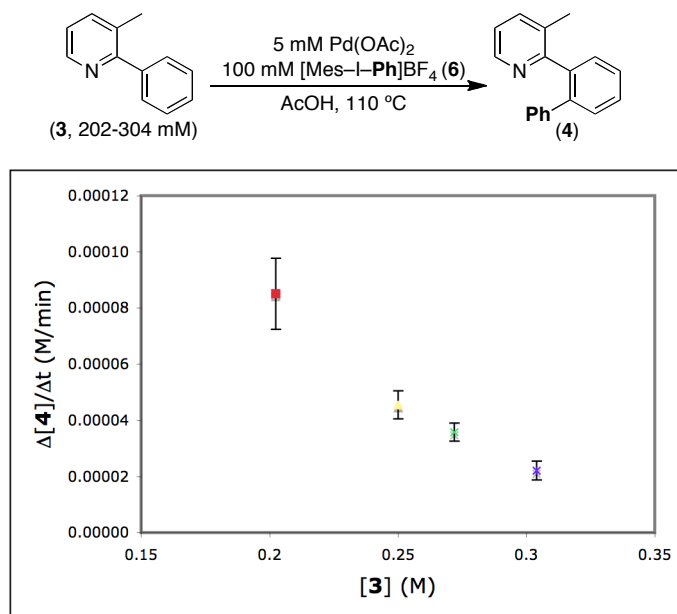




**Figure 3.5:** Plot of Initial Rate ( $\Delta[4]/\Delta t$ ) versus  $[3]^{-3}$ .

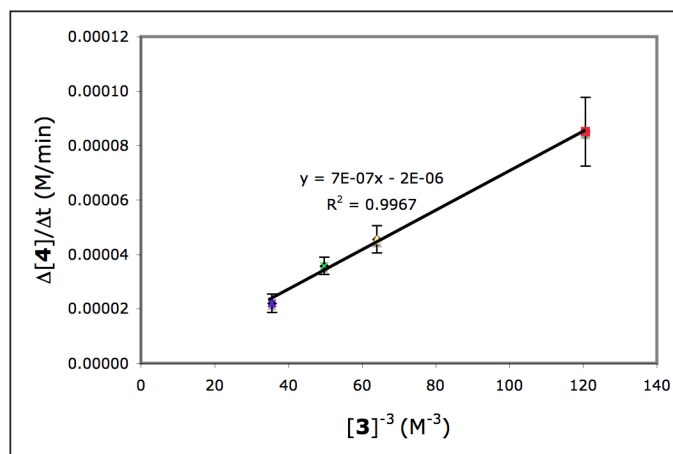
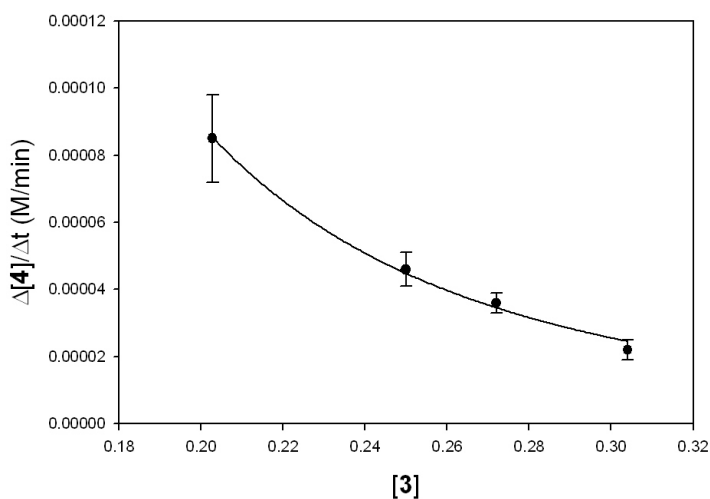


**Figure 3.6:** Data Fit of Initial Rate ( $\Delta[4]/\Delta t$ ) versus  $[3]$ .



Next the kinetic order in  $I^{III}$  reagent was determined by conducting experiments under similar conditions ( $[3] > I^{III}$ ). This was carried out utilizing the above protocol by combining 3-methyl-2-phenylpyridine (**3**, 250 mM) with varying concentrations of [Mes- $I^{III}$ -Ph] $BF_4$  (**6**, 75.2 to 175.2 mM) and  $Pd(OAc)_2$  (5 mM) in AcOH at 110 °C. A plot of initial rate ( $\Delta[4]/\Delta t$ ) versus  $[I^{III}]$  was linear, thereby demonstrating a first order dependence on  $[I^{III}]$  (**Figure 3.7**). This was further confirmed by performing a non-linear least squares fit of the data to the equation  $f(x) = a[I^{III}]^n$  where the order ( $n$ ) in  $I^{III}$  was

found to be  $1.12 \pm 0.08$  (Figure 3.8). This result suggests that the oxidant is involved at the rate-determining step of the reaction.

**Figure 3.7:** Initial Rate ( $\Delta[4]/\Delta t$ ) versus  $[I^{III}]$ .

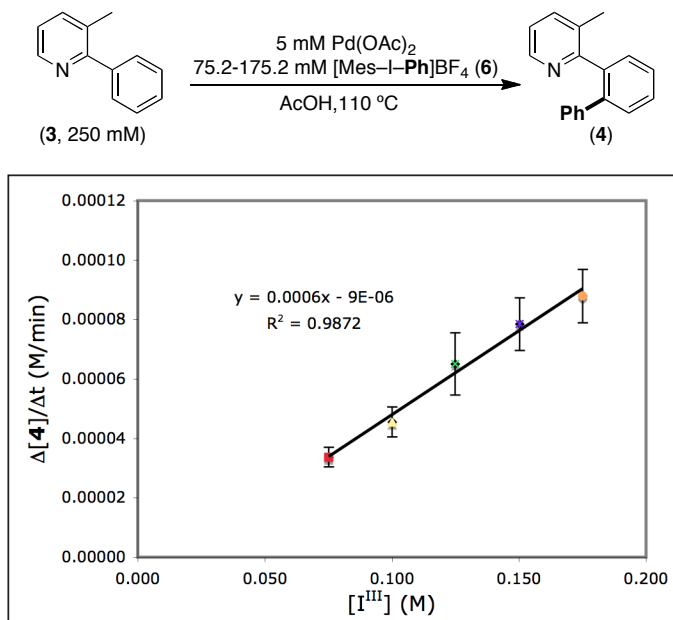
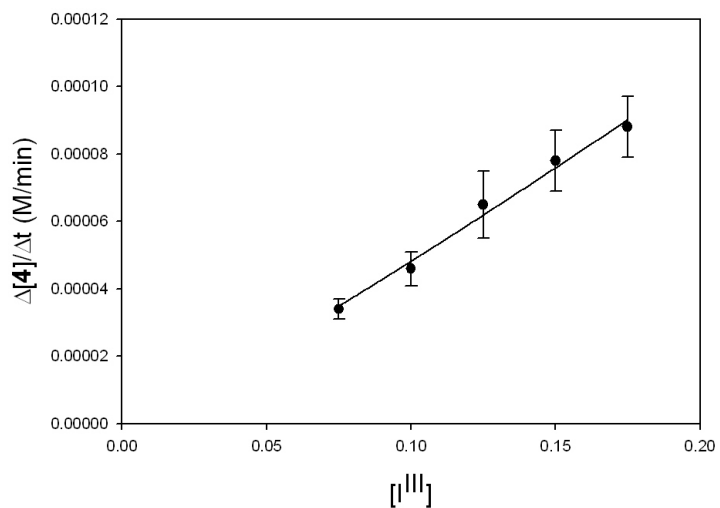


**Figure 3.8:** Data Fit of Initial Rate ( $\Delta[4]/\Delta t$ ) versus  $[I^{III}]$ .



We next determined the order in [Pd] using the analogous method above, while again employing conditions of excess substrate. In these experiments 3-methyl-2-phenylpyridine (**3**, 250 mM) was combined with [Mes-I<sup>III</sup>-Ph]BF<sub>4</sub> (**6**, 100 mM) and varying amounts of Pd(OAc)<sub>2</sub> (3.8 to 10 mM) in AcOH at 110 °C. A plot of the initial rate ( $\Delta[4]/\Delta t$ ) versus [Pd] displayed a non-linear relationship (**Figure 3.9**). However a plot of the initial rate versus [Pd]<sup>2</sup> afforded a straight line, suggesting a second order dependence on [Pd] (**Figure 3.10**). For further confirmation, the kinetic order (n) in [Pd] was determined to be  $2.09 \pm 0.08$  ( $a = 6 \pm 1$  M/min) by performing a non-linear least squares fit to  $f(x) = a[\text{Pd}]^n$  (**Figure 3.11**). A second order dependence on catalyst suggests that the ratio of stoichiometry of the resting state to the transition state of the catalytic cycle is 1:2, implicating a monomeric palladium resting state and a dimeric palladium transition state (*vide infra*).

In summary of the kinetic order data obtained, it was found that this reaction must be carried out under conditions of excess substrate to obtain interger order values. Under these conditions, an inverse third order dependence was observed in substrate. Order studies in the oxidant revealed a first order dependence. Finally it was determined that this reaction has a second order dependence on catalyst.

**Figure 3.9:** Plot of Initial Rate ( $\Delta[4]/\Delta t$ ) versus [Pd].

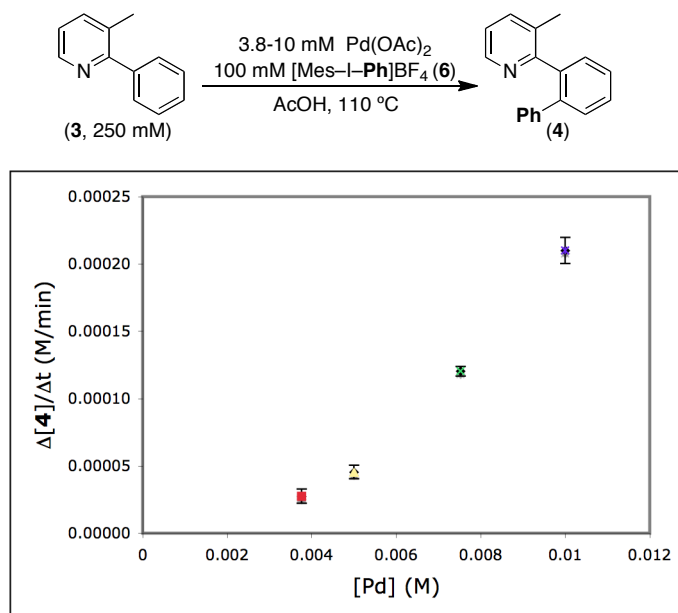


**Figure 3.10:** Plot of Initial Rate ( $\Delta[4]/\Delta t$ ) versus  $[Pd]^2$ .

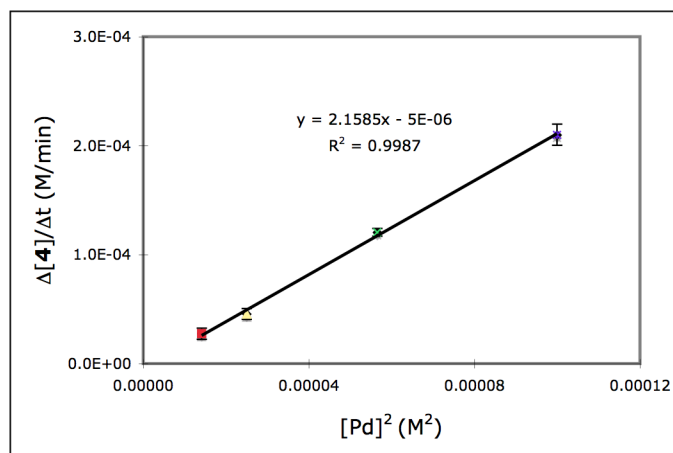
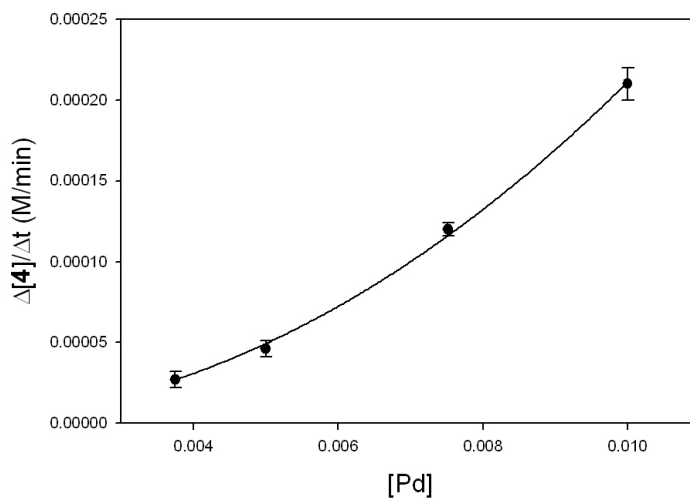


**Figure 3.11:** Data Fit of Initial Rate ( $\Delta[4]/\Delta t$ ) versus  $[Pd]$ .

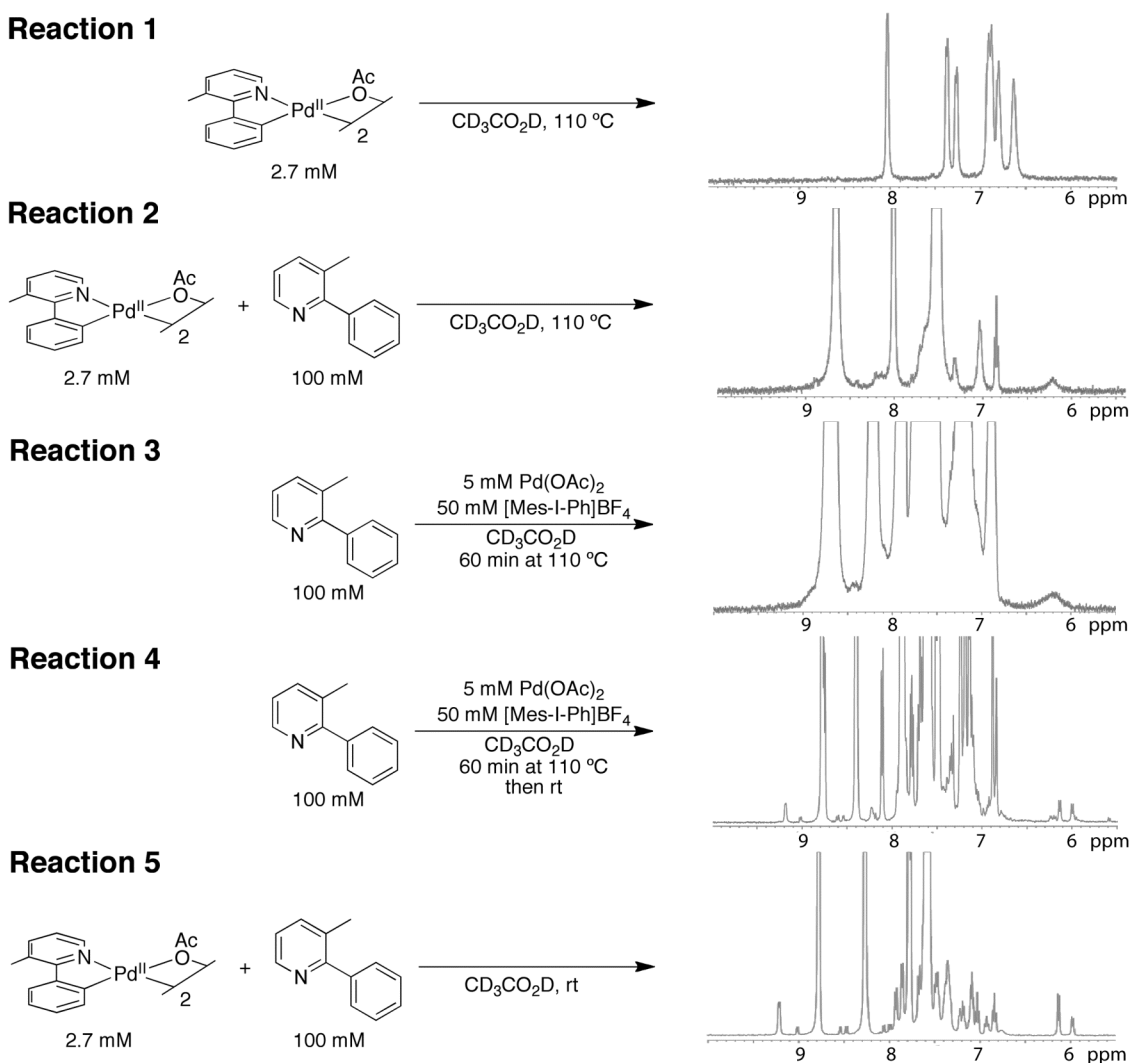


### 3.4 Catalyst Resting State

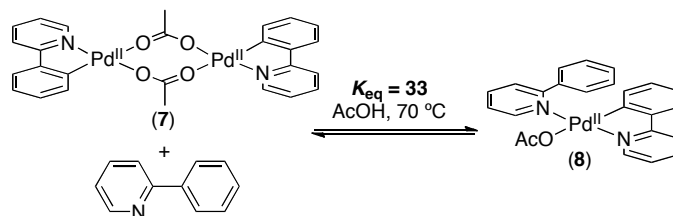
Since our kinetic order studies implicated a monomeric catalyst resting state, we sought further evidence of the exact nature of the catalyst resting state. Previously, the dimeric palladacycle **5** was demonstrated to be a viable catalyst for the arylation reactions, and furthermore provided the phenylation product by the stoichiometric reaction with diaryliodonium reagents (**Scheme 3.4** and **3.5**). To investigate this further,

the potential catalytic intermediate **5** and substrate **3** were examined by  $^1\text{H}$  NMR spectroscopy under conditions mimicking the catalytic reaction conditions (20 equiv **3**,  $110\text{ }^\circ\text{C}$ ,  $\text{CD}_3\text{CO}_2\text{D}$ ). This revealed a new resonance at  $\sim 6.2$  ppm (**Figure 3.12**, Reaction 2), which is diagnostic of a monomeric palladium species<sup>1</sup>, and does not appear in the  $^1\text{H}$  NMR spectra of **5** (**Figure 3.12** Reaction 1). This observation is consistent with Ryabov's investigation demonstrating the closely related complex **7** favors the monomeric species **8** in the presence of excess 2-phenylpyridine under very similar conditions ( $K_{\text{eq}} = 33 \pm 2 \text{ M}^{-1}$ , AcOH,  $70\text{ }^\circ\text{C}$ , **Scheme 3.6**).<sup>1</sup>

**Figure 3.13:**  $^1\text{H}$  NMR Experiments to Observe the Catalyst Resting State.

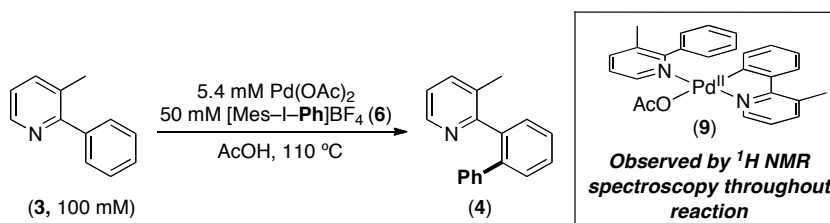


**Scheme 3.6:** Rybov's Example of the Monomer Dimer Equilibrium.<sup>1</sup>



To compare of this observed resonance with the kinetic order data obtained, spectroscopic evidence for any observable palladium species in the catalytic reaction species was next investigated. When the catalytic reaction of **3** (0.05 mmol) with [Mes-<sup>I</sup>Ph]BF<sub>4</sub> (**6**, 0.025 mmol) and Pd(OAc)<sub>2</sub> (0.0027 mmol) in CD<sub>3</sub>CO<sub>2</sub>D at 110 °C was monitored by <sup>1</sup>H NMR spectroscopy, an analogous diagnostic peak at 6.2 ppm was observed to persist at a constant concentration throughout the duration of the reaction. This is displayed in **Figure 3.12**, Reaction 3, which shows the reaction after 60 min (30 % conversion). This suggests the presence of the monomeric palladium species **9** throughout the reaction, implicating it as the catalyst resting state (**Scheme 3.7**). Finally, **Figure 3.12**, Reaction 4 shows the reaction mixture from **Figure 3.12**, Reaction 3 cooled to room temperature. In this spectrum, a pair of doublets is observed at 6.00 and 6.14 ppm, which directly correlate with those of the addition of **3** to **5** in CD<sub>3</sub>CO<sub>2</sub>D at room temperature (**Figure 3.12**, Reaction 5). It is believed that these two peaks represent two isomers of the monomeric palladacycle. Notably, heating of both samples leads to coalescence of these peaks into a single broad resonance at 6.2 ppm. Based on these experiments we propose that the catalyst resting state is monomer **9** (**Scheme 3.7**)

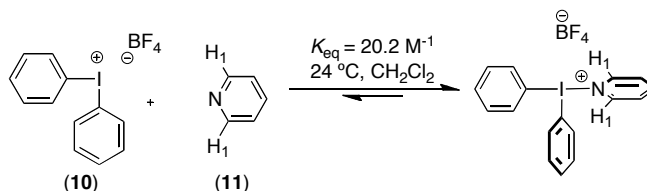
**Scheme 3.7:** Observation of the **9** Under the Reaction Conditions.



### 3.5 Oxidant Resting State

With an understanding of the catalyst resting state, interactions between the I<sup>III</sup> reagent and other reaction components was next investigated. Previous literature reports have demonstrated that pyridine derivatives coordinate to cationic diaryliodonium I<sup>III</sup> reagents.<sup>14-17</sup> A notable example was reported by Ochiai, who demonstrated that pyridine coordinates to [Ph-I<sup>III</sup>-Ph]BF<sub>4</sub> (**10**).<sup>16</sup> This interaction was examined by <sup>1</sup>H NMR spectroscopy to determine that the coordination stoichiometry was 1:1, and that *K*<sub>eq</sub> favored the bound state (*K*<sub>eq</sub> = 20.2 M<sup>-1</sup> at 24 °C in CH<sub>2</sub>Cl<sub>2</sub>). Notably, the discrete bound and free states in this system cannot be observed due to fast exchange on the NMR time scale. Thus to examine this interaction, a Job plot and titration experiments were employed. These analyses are completed by following the change in chemical shift of H<sub>1</sub> of pyridine (**Scheme 3.8**). An upfield shift of this proton was observed in the presence of **10**. This effect was hypothesized to be the result of shielding effects due to ring currents associated with the phenyl groups of [Ph-I<sup>III</sup>-Ph]BF<sub>4</sub> (**10**). Additionally, this interaction was further confirmed by an X-Ray crystal structure of pyridine (**11**) bound to **10**.

**Scheme 3.8:** Equilibrium Between the I<sup>III</sup> Reagent and Pyridine.<sup>16</sup>



We conducted an analogous set of studies to examine the interaction between **1** and [Mes-I-Ph]BF<sub>4</sub> (**6**) under our catalytic conditions. First, we used a Job plot to establish the stoichiometry of complexation. A series of solutions with a constant total concentration ([**3**] + [**6**] = 23.6 mM in CD<sub>3</sub>CO<sub>2</sub>D, **Scheme 3.9**), but varying mole fractions of the two components was examined by <sup>1</sup>H NMR spectroscopy at 110 and 80 °C. At each temperature, the chemical shift of H<sub>1</sub> and H<sub>4</sub> of **3** moved downfield as the mole fraction of **6** increased. This is in contrast to Ochiai's observation in which H<sub>1</sub> moved upfield. This is likely due to the increased role of the resonance structure with a

positive charge localized on the carbon bearing H<sub>1</sub> in more polar AcOH relative to CH<sub>2</sub>Cl<sub>2</sub>. The change in chemical shift of H<sub>4</sub> relative to free **3** ( $\Delta\delta_{H(4)}$ ) was used to construct a Job plot (**Figure 3.14** and **3.15**). H<sub>4</sub> was chosen over H<sub>1</sub> due to the larger change relative to free **3**, but similar effects were observed for each resonance. The plots at 110 °C and 80 °C each showed a maximum at  $\chi = 0.5$ , indicating that complexation between **3** and **6** occurs with a 1:1 stoichiometry at each temperature.<sup>18</sup> This data implicates the formation of I<sup>III</sup> adduct **12** under the catalytic reaction conditions.

**Scheme 3.9:** Equilibrium Between [Mes-I<sup>III</sup>-Ph]BF<sub>4</sub> **6** and **3**.

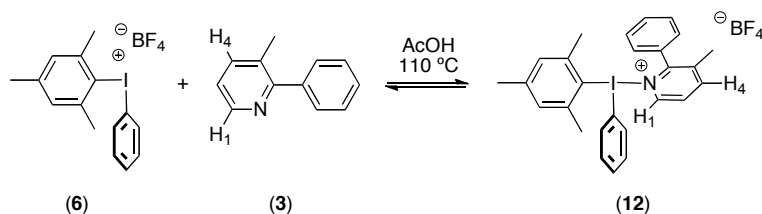


**Figure 3.14:** Job Plot of  $\Delta\delta \cdot \chi$  versus  $\chi$  at 110 °C.

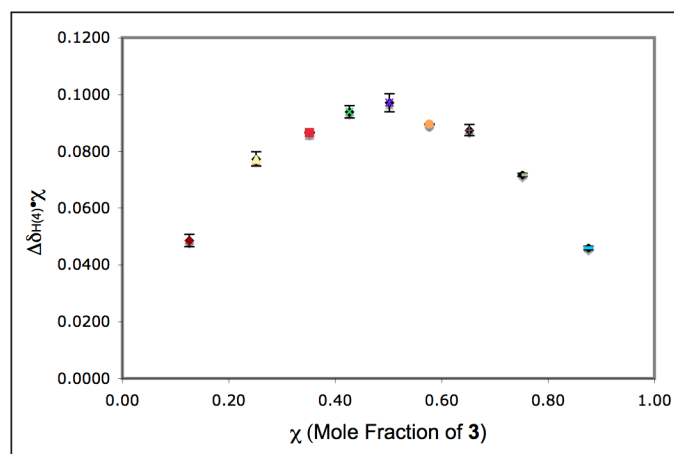
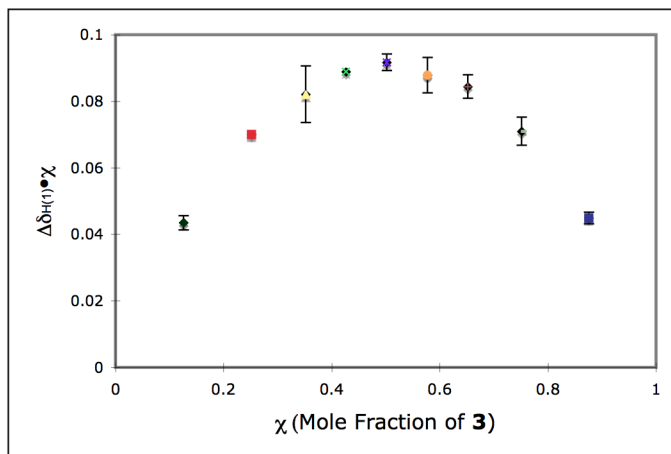




**Figure 3.15:** Job Plot of  $\Delta\delta \cdot \chi$  versus  $\chi$  at 80 °C.



With the stoichiometry of the complex determined, the equilibrium constant between bound and free substrate was next probed by examining the chemical shift of H<sub>4</sub>. These experiments measured the chemical shift in solutions containing constant [3] with an increasing concentration of [Mes-I-Ph]BF<sub>4</sub> (6) in CD<sub>3</sub>CO<sub>2</sub>D at both 110 °C and 80 °C (Figure 3.16 and 3.17). This data was then analyzed using a non-linear least squares fit to a series of equations described by Funasak (eq. 3.1, 3.2, 3.3) for a 1:1 binding model, and the curves representing those fits are shown.<sup>19-21</sup> The equilibrium constant was found to be  $111 \pm 18 \text{ M}^{-1}$  at 110 °C ( $\delta_{\text{max}} = 8.52 \pm 0.03$ ) and  $154 \pm 24 \text{ M}^{-1}$  at 80 °C ( $\delta_{\text{max}} = 8.51 \pm 0.02$ ). This analysis clearly demonstrates that under conditions relevant to the catalytic cycle the bound complex 12 is favored.

**Figure 3.16:**  $\delta_{H(4)}$  as a Function of  $[I^{III}]$  at 110 °C.

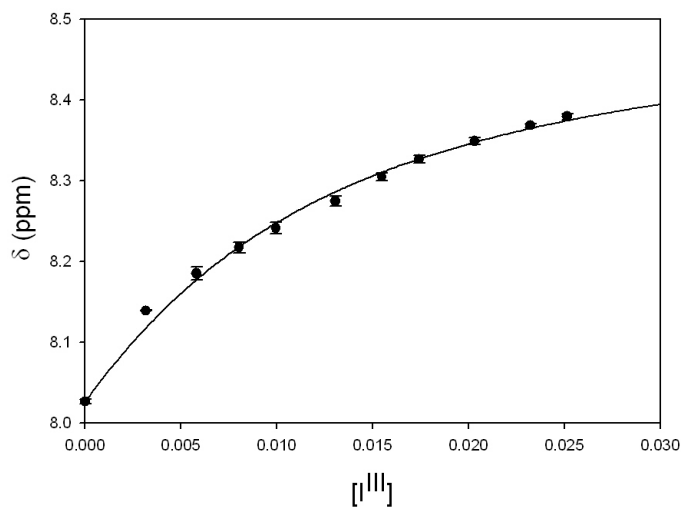
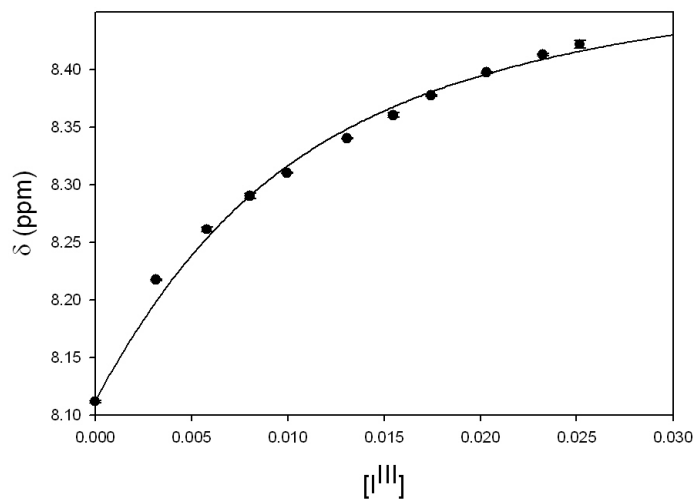


**Figure 3.17:**  $\delta_{H(4)}$  as a Function of  $[I^{III}]$  at 80 °C.



$$\delta = \frac{[3]\delta_{free} + K_{eq}[3][6]\delta_{bound}}{[3]_{Total}} \quad (3.1)$$

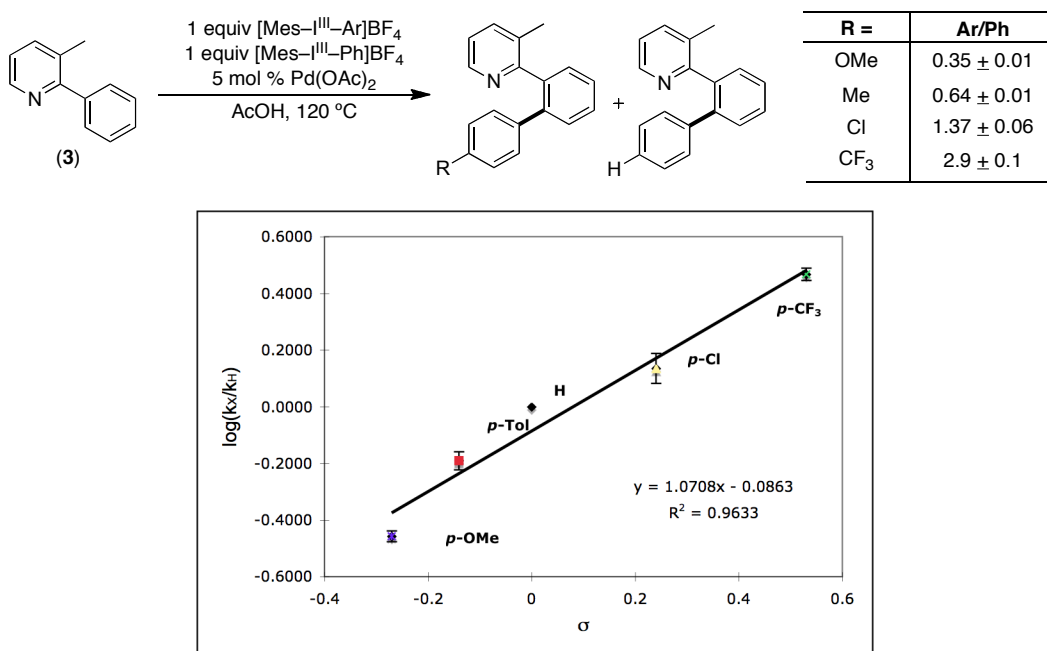
$$[6] = \frac{K_{eq}[6]_{Total} - K_{eq}[3]_{Total} - 1 + \sqrt{(K_{eq}[3]_{Total} - K_{eq}[6]_{Total} - 1)^2 + 4K_{eq}[6]_{Total}}}{2K_{eq}} \quad (3.2)$$

$$[\mathbf{3}] = \frac{K_{eq}[\mathbf{3}]_{Total} - K_{eq}[\mathbf{6}]_{Total} - 1 + \sqrt{(K_{eq}[\mathbf{6}]_{Total} - K_{eq}[\mathbf{3}]_{Total} - 1)^2 + 4K_{eq}[\mathbf{3}]_{Total}}}{2K_{eq}} \quad (3.3)$$

### 3.6 Hammett Studies

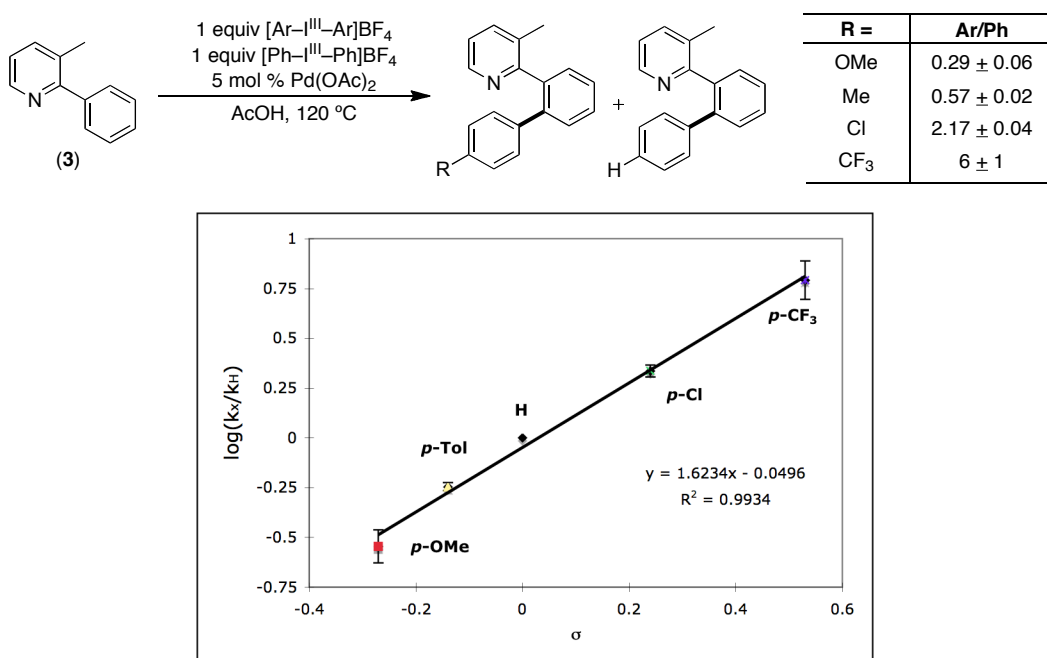
Next, investigations focused on the effect of oxidant electronics on the rate of the reaction. The first approach to probe these effects was to use competition studies between electronically diverse oxidants. The product distributions of these reactions were analyzed and correlated to the relative reaction rates of each oxidant. This method was employed because it enabled us to obtain information about the oxidation step, regardless of its position in the catalytic cycle (*i.e.* at or after the rate-limiting step). In these experiments 1 equiv of 3-methyl-2-phenylpyridine (**3**) was combined with 1 equiv [Mes-I<sup>III</sup>-Ph]BF<sub>4</sub>, 1 equiv of [Mes-I<sup>III</sup>-Ar]BF<sub>4</sub> and 5 mol % of Pd(OAc)<sub>2</sub> in AcOH and the reaction was heated at 120 °C for 12 h (**Figure 3.18**). The value for  $k_{Ar}/k_{Ph}$  was determined from the ratio of Ar to Ph products based on calibrated GC yields. A Hammett plot was constructed by plotting  $\log(k_{Ar}/k_{Ph})$  versus  $\sigma$  and provided a straight line with  $\rho = +1.1 \pm 0.1$ , indicating that electron poor oxidants react at a faster rate.

**Figure 3.18:** Competition Study with [Mes-I<sup>III</sup>-Ph]BF<sub>4</sub> and [Mes-I<sup>III</sup>-Ar]BF<sub>4</sub>.



Next, the same experiments were completed with the symmetric oxidants  $[\text{Ar-I}^{\text{III}}-\text{Ar}]\text{BF}_4$  and  $[\text{Ph-I}^{\text{III}}-\text{Ph}]\text{BF}_4$ . In these experiments 1 equiv of 3-methyl-2-phenylpyridine was combined with 1 equiv  $[\text{Ph-I}^{\text{III}}-\text{Ph}]\text{BF}_4$ , 1 equiv of  $[\text{Ar-I}^{\text{III}}-\text{Ar}]\text{BF}_4$  and 5 mol % of  $\text{Pd}(\text{OAc})_2$  in  $\text{AcOH}$  the resulting mixture was then heated at  $120\text{ }^\circ\text{C}$  for 12 h (**Figure 3.19**). The analysis of the data was completed by the analogous method and the Hammett plot was constructed by plotting  $\log(k_{\text{Ar}}/k_{\text{Ph}})$  versus  $\sigma$  and provided a linear relationship with  $\rho = +1.62 \pm 0.08$ , again indicating that electron poor oxidants react at a faster rate.

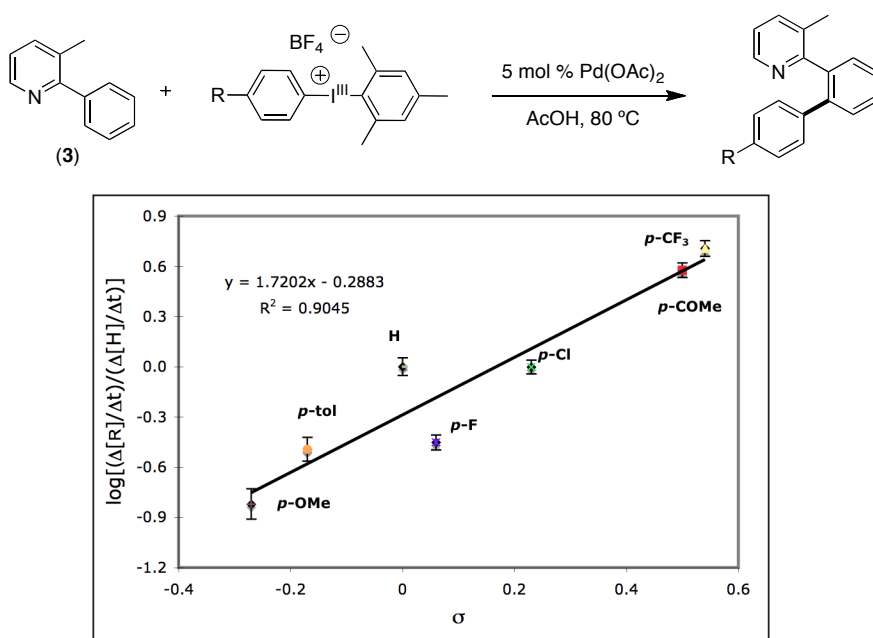
**Figure 3.19:** Competition Study with  $[\text{Ph-I}^{\text{III}}-\text{Ph}]\text{BF}_4$  and  $[\text{Ar-I}^{\text{III}}-\text{Ar}]\text{BF}_4$ .



To confirm the electronic trend obtained from the competition studies, a Hammett plot based upon initial rate data with a series of oxidants was also sought. These experiments were completed by combining 1 equiv of 3-methyl-2-phenylpyridine (**3**) with 2 equiv of  $[\text{Mes-I}^{\text{III}}-\text{Ar}]\text{BF}_4$  (**6**) and 5 mol % of  $\text{Pd}(\text{OAc})_2$  in  $\text{AcOH}$  at  $80\text{ }^\circ\text{C}$ . The reactions were followed to 6–10% conversion as determined by GC by comparison to an internal standard. A Hammett plot was constructed based on this data with a variety of Ar groups, and it displayed a linear relationship between  $\log(k_{\text{Ar}}/k_{\text{Ph}})$  vs.  $\sigma$ , with a  $\rho$  value of

+1.7 ± 0.3 (**Figure 3.20**). This data agrees with each of the competition studies and suggest the C–H arylation is strongly accelerated by electron deficient oxidants. However, the  $\rho$  value determined using the method of initial rates is however different than the competition Hammett plot ( $\rho = +1.1 \pm 0.1$ ). This may be a result of the difference in conversions the reactions were followed to and may be resolved if the competition Hammett studies were stopped at lower conversion (~10%), Utilizing this method it was observed that oxidant electronics impacted the initial reaction rate, suggesting that the oxidation is involved in the rate-determining step of the reaction.

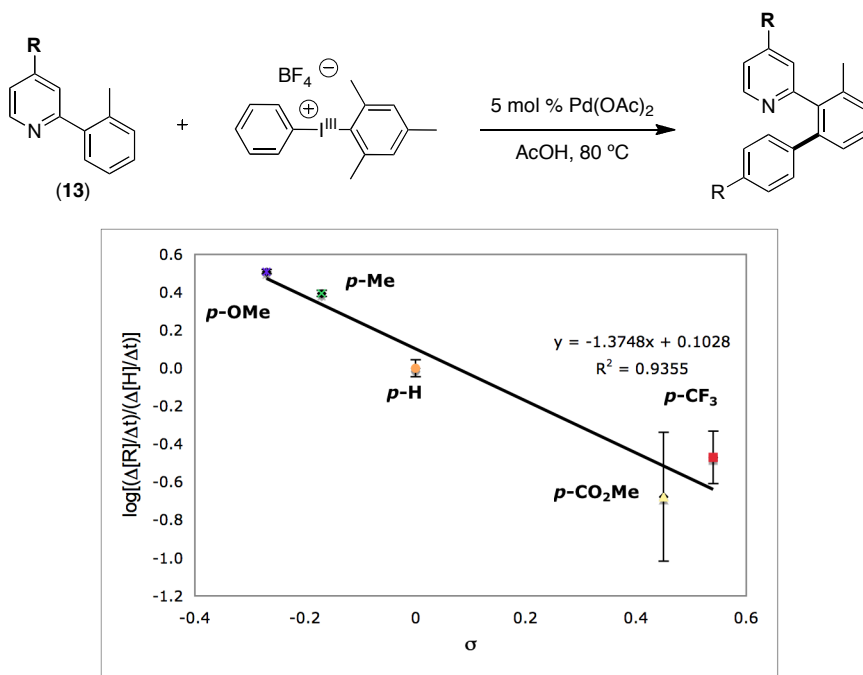
**Figure 3.20:** Initial Rate Hammett Plot with [Mes–I<sup>III</sup>–Ar]BF<sub>4</sub> Oxidants.



Hammett studies probing the effect of directing group electronics were also undertaken. These experiments also utilized the method of initial rates and were completed by combining 2 equiv of [Mes–I<sup>III</sup>–Ph]BF<sub>4</sub> and 5 mol % of Pd(OAc)<sub>2</sub> in AcOH at 80 °C with 2-(o-tolyl)-4-(X)-pyridine (**13**) (X = OMe, Me, C(O)Me, CF<sub>3</sub>) (**Figure 3.21**). The reactions were followed by gas chromatography by comparison to an internal standard to provide the initial reaction rate (based on the calibration for R = H). A Hammett plot was constructed based upon this data and displayed a linear relationship

between  $\log(k_{Ar}/k_{Ph})$  and  $\sigma$  resulting in a  $\rho$  value of  $-1.4 \pm 0.2$ . This result suggests that electron-donating groups on the directing group accelerate the reaction rate (**Figure 3.21**).

**Figure 3.21:** Initial Rate Directing Group Hammett Study with  $[\text{Mes-I}^{\text{III}}\text{-Ph}]\text{BF}_4$ .



### 3.7 Oxidant Counterion Effect

Next, we sought to explore the effect of the oxidant counterions on the rate of the reaction by varying the counterion coordinating ability. To accomplish this, several  $[\text{Ph-I}^{\text{III}}\text{-Ph}]\text{X}$  reagents were synthesized with a variety of different counterions (**Table 3.1**). Installation of these counterions was accomplished by synthesizing  $[\text{Ph-I}^{\text{III}}\text{-Ph}]\text{Cl}$  (**14**) through the coupling of  $\text{PhI}^{\text{III}}(\text{OAc})_2$  with  $\text{PhB}(\text{OH})_2$  followed by quenching with a saturated solution of  $\text{NaCl}$  (**Scheme 3.10**).<sup>22,23</sup> The product is sparingly soluble in  $\text{CH}_2\text{Cl}_2$  and  $\text{H}_2\text{O}$ . To attain the desired counterion from this common intermediate, another anion exchange was completed by combining  $[\text{Ph-I}^{\text{III}}\text{-Ph}]\text{Cl}$  in a stirring solution of  $\text{CH}_2\text{Cl}_2$  and  $\text{H}_2\text{O}$  with the appropriate  $\text{NaX}$  salt (20 equiv). The resulting products were all soluble in  $\text{CH}_2\text{Cl}_2$ . To confirm the validity of this method the  $^1\text{H}$  NMR spectra of the

isolated [Ph-I<sup>III</sup>-Ph]OTf was compared to a sample synthesized through an independent method and found to be the same.<sup>24</sup>

**Scheme 3.10:** Synthesis of [Ph-I<sup>III</sup>-Ph]X Oxidants.

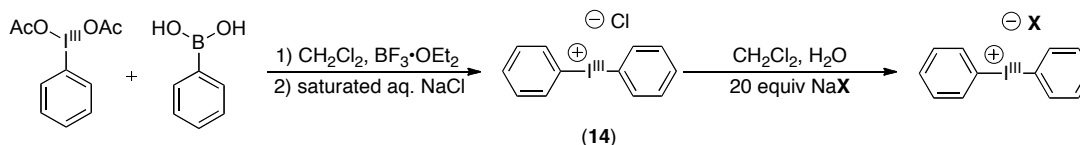


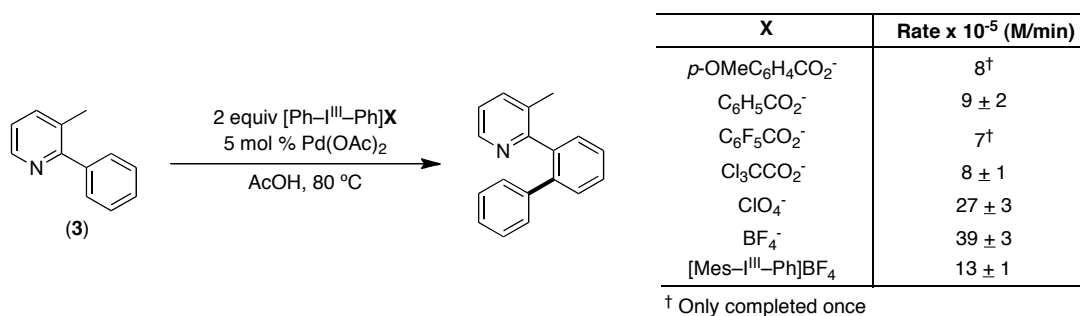
**Table 3.1:** [Ph-I<sup>III</sup>-Ph]X Oxidants.

Counterion	Yield
Cl <sup>-</sup>	93% ( <b>14</b> )
C <sub>6</sub> H <sub>5</sub> CO <sub>2</sub> <sup>-</sup>	68% ( <b>15</b> )
C <sub>6</sub> F <sub>5</sub> CO <sub>2</sub> <sup>-</sup>	75% ( <b>16</b> )
Cl <sub>3</sub> CCO <sub>2</sub> <sup>-</sup>	79% ( <b>17</b> )
ClO <sub>4</sub> <sup>-</sup>	63% ( <b>18</b> )
<sup>-</sup> OTs	43% ( <b>19</b> )
<sup>-</sup> OTf	58% ( <b>20</b> )

These studies again focused on examining the initial rates of ligand-directed palladium-catalyzed C–H phenylation. Experiments were completed by combining 1 equiv of 3-methyl-2-phenylpyridine (**3**) with 2 equiv of [Ph-I<sup>III</sup>-Ph]X and 5 mol % of Pd(OAc)<sub>2</sub> in AcOH at 80 °C, and the reaction progress was monitored by GC (**Scheme 3.11**). A series of counterions were examined, revealing a clear distinction between counterions characterized as less coordinating (BF<sub>4</sub> and ClO<sub>4</sub>), versus those that are more coordinating (carboxylates). Reactions with oxidants containing carboxylate counterions displayed very similar rates, which was approximately four times slower than that of the most commonly used BF<sub>4</sub><sup>-</sup> counterion. The perchlorate anion (ClO<sub>4</sub><sup>-</sup>), which is also non-coordinating, was only slightly slower than the BF<sub>4</sub><sup>-</sup> counterion. Studies with additional counterions were attempted, but the oxidants were either insoluble in AcOH at elevated temperature (Cl<sup>-</sup>), or presented reproducibility problems (<sup>-</sup>OTs, <sup>-</sup>OTf). Finally this investigation also provided insight into the difference in reactivity between the oxidants [Ph-I<sup>III</sup>-Ph]BF<sub>4</sub> and [Mes-I<sup>III</sup>-Ph]BF<sub>4</sub>. It was determined that the relative reaction rate of

[Ph-I<sup>III</sup>-Ph]BF<sub>4</sub> is approximately four times faster than with [Mes-I<sup>III</sup>-Ph]BF<sub>4</sub> (39 ± 3 vs 13 ± 1 M/min). This decrease in reactivity with the mesityl oxidant may be attributed to a combination of steric effects and the electron donating ability of the methyl groups. These results have demonstrated the important role that counterions play as well as the difference in reaction rates between the oxidants [Ph-I<sup>III</sup>-Ph]BF<sub>4</sub> and [Mes-I<sup>III</sup>-Ph]BF<sub>4</sub>.

**Scheme 3.11:** Study of Counterion Effects on the Reaction Rate.

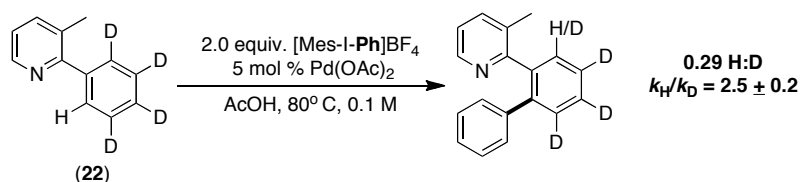


### 3.8 Kinetic Isotope Effect Studies

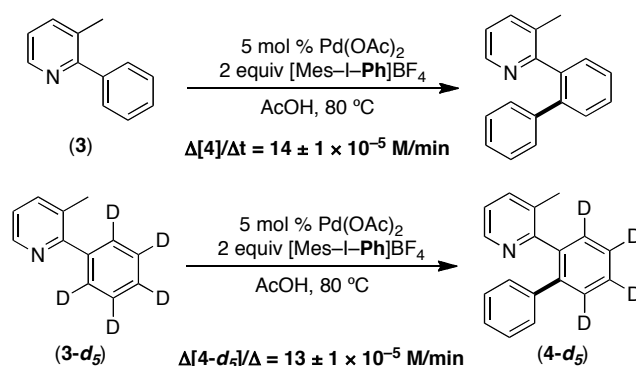
Finally, investigating the kinetic isotope effect was of interest for comparison to other C–H bond functionalization reactions. Initial experiments explored the intramolecular kinetic isotope effect using substrate **22**. This was accomplished by product analysis of the reaction employing substrate **22** for phenylation using <sup>1</sup>H NMR spectroscopy to compare H:D, ratios and it was determined that the  $k_H/k_D$  was 2.5 ± 0.2 (**Scheme 3.12**). This is in agreement with other ligand-directed palladium-catalyzed C–H functionalization reactions, which have 1° intramolecular kinetic isotope effects ranging from 2.2–6.7.<sup>25-32</sup> Next, the intermolecular kinetic isotope effect was determined by comparing initial reaction rates of 3-methyl-2-phenylpyridine (**3**) with 3-methyl-2-(*d*<sub>5</sub>)-phenylpyridine (**3-*d*<sub>5</sub>**) (**Scheme 3.13**). Interestingly the  $k_H/k_D$  was determined to be 1 (initial rate for **3** = 14 ± 1 × 10<sup>-5</sup> M/min; initial rate for **3-*d*<sub>5</sub>** = 13 ± 1 × 10<sup>-5</sup> M/min). This was further confirmed with substrate **23**, where the  $k_H/k_D$  was also determined to be 1 (initial rate for **23** = 27 ± 3 × 10<sup>-5</sup> M/min; initial rate for **23-*d*** = 24 ± 2 × 10<sup>-5</sup> M/min, **Scheme 3.14**). A kinetic isotope effect of 1 suggests the C–H activation is occurring subsequent to the rate-determining step of the catalytic cycle.



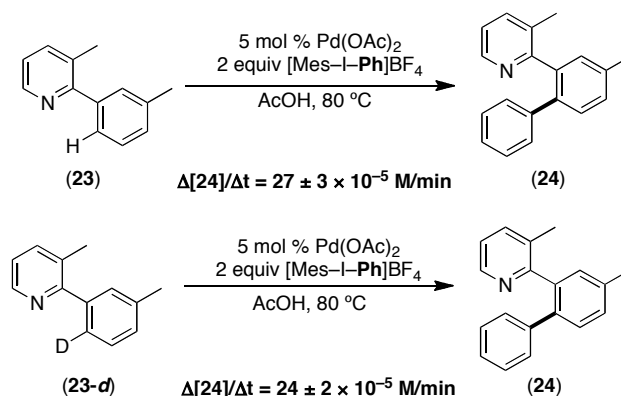
**Scheme 3.12:** Intramolecular Kinetic Isotope Effect Study of **22**.



**Scheme 3.13:** Intermolecular Kinetic Isotope Effect Study of **3**.



**Scheme 3.14:** Intermolecular Kinetic Isotope Effect Study of **23**.

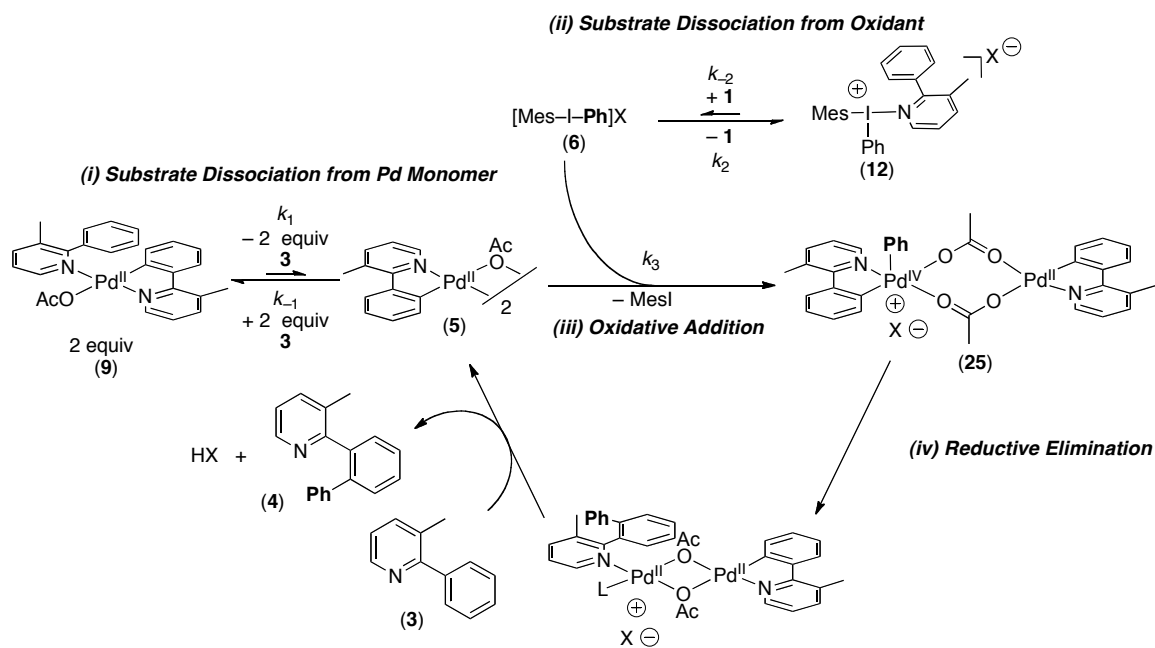


### 3.9 Summary of the Mechanistic Data

The mechanistic data above allowed the proposal of a complete catalytic cycle for this reaction (**Scheme 3.15**). We propose that the resting state of the catalyst is the monomeric Pd<sup>II</sup> species **9**, while the resting state of the oxidant is the pyridine bound I<sup>III</sup> reagent **12**. Free oxidant **6** enters the catalytic cycle through loss of 1 equiv of **3**, while Pd

enters the catalytic cycle with loss of 2 equiv **3** from 2 equiv of the cyclometallated Pd<sup>II</sup> monomer **9** resulting in palladium dimer **5**. The cyclometallated Pd<sup>II</sup> dimer **5** undergoes rate-limiting oxidation with **6** resulting in the high oxidation palladium dimer **25**. Subsequent C–C bond forming reductive elimination provides the desired product **4** upon ligand exchange for free substrate. Finally, ligand exchange of product for substrate of Pd<sup>II</sup> followed by fast C–H activation returns the Pd<sup>II</sup> to the resting state of the catalytic cycle. Based on this proposed catalytic cycle, the rate law eq. 3.4 can be derived, and application of the pre-equilibrium approximation for **6** and **5** provides the final rate expression eq. 3.5.

**Scheme 3.15:** The Final Proposed Mechanism of C–H Activation/Arylation.



$$\text{rate} = k_3[\mathbf{6}][\mathbf{5}] \quad (3.4)$$

$$\text{rate} = \frac{k_1 k_2 k_3 [\mathbf{12}][\mathbf{9}]^2}{k_{-1} k_{-2} [\mathbf{3}]^3} \quad (3.5)$$

This mechanistic proposal, including the catalyst and oxidant resting state, kinetic reaction orders, rate limiting step, and kinetic isotope effect all agree with the

mechanistic studies completed. First, under these reaction conditions the resting state of the catalyst has been determined to be the monomeric species **9** based on its observation during the catalytic reaction. The resting state of the oxidant has been determined to be the pyridine bound  $I^{III}$  species. This was accomplished through examination of the equilibrium between bound and free oxidant, which demonstrated that under the reaction conditions the bound species **12** is greatly favored.

Additionally, the rate equation derived based upon the proposed mechanism predicts a first order dependence on  $[I^{III}]$ , a second order dependence on  $[Pd]$ , and an inverse third order dependence on  $[3]$  (eq. 3.5). Each of these agrees with the experimentally determined kinetic orders. More support for the proposed catalytic cycle is provided by the observation that the substrate order deviates from inverse third when  $[6] > [3]$  (**Figure 3.1**, Regime 1). This result becomes clear upon considering that under these conditions the resting state is no longer **9**, but is instead be a mixture of **9** and **5**, leading to a non-integer reaction order. Thus, it was important to determine all of the reaction orders under conditions where  $[3] > [Pd] + [6]$  to provide integer orders to allow for deconvolution of the mechanism (**Figure 3.1**, Regime 1).

Next, rate-limiting oxidation is supported by several of the experiments performed. Hammett studies of oxidants ( $\rho = +1.7$ ) demonstrated that electron poor oxidants provide faster reaction rates, consistent with oxidation of  $Pd^{II}$  being involved in the rate-limiting step of the catalytic cycle. Notably, this is similar to the  $\rho$  values observed in  $Pd^{0/II}$  reactions with rate limiting oxidation to  $Ar-I$ .<sup>33</sup> Directing group Hammett studies provided evidence of rate limiting oxidation with a  $\rho$  value determined to be  $-1.3$ . This result suggests that more electron donating groups *para* to the pyridine-directing group lead to an increased reaction rate. This is expected, because electron-donating groups provide a more electron rich cyclometallated  $Pd^{II}$  species that will undergo faster oxidation than its electron poor analogues. Further, the observation that equiv or electronics of the oxidant (Hammett Studies and oxidant order) effect the initial rate of the reaction implies that oxidation is at or before the rate-limiting step of the reaction.

Finally, an experimentally determined intermolecular kinetic isotope effect of 1 implies that C–H activation is after the rate-limiting step. This agrees with the proposed

mechanism, where the C–H activation lies after rate limiting oxidation and before the resting state of the reaction. Thus C–H activation should have no impact on the reaction rate. This is particularly interesting given that in most C–H activation/functionalization processes, C–H activation has been determined to be the rate determining step of the reaction.<sup>25,30-32,34-37</sup>

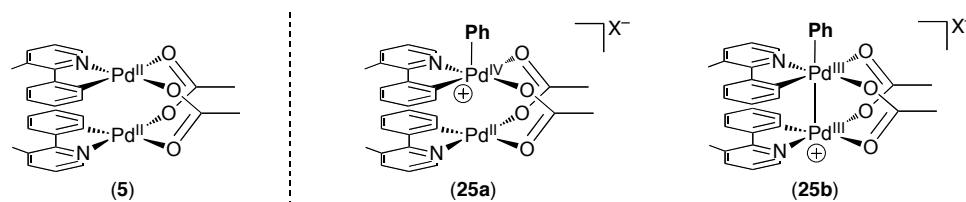
### 3.10 Mechanistic Implications

An interesting comparison can now be made between the mechanism of the methodology described and that of the palladium catalyzed C–H activation/acetoxylation utilizing  $\text{PhI}^{\text{III}}(\text{OAc})_2$  as the terminal oxidant. In the aforementioned methodology it has been determined that C–H activation is the rate limiting step of the catalytic cycle under similar conditions (100 °C,  $\text{Pd}(\text{OAc})_2$ ). Evidence of this was provided by a zero order dependence on  $\text{PhI}^{\text{III}}(\text{OAc})_2$ , and the observation of a large primary kinetic isotope effect, each suggestive of rate limiting C–H activation.<sup>37,38</sup> This is in contrast to the first order dependence on  $\text{I}^{\text{III}}$  and absence of kinetic isotope effect found for C–H activation/arylation. This highlights the difference in reactivity between the two  $\text{I}^{\text{III}}$  oxidants despite the similar reaction pathways. This also suggests that the  $[\text{Ar}-\text{I}^{\text{III}}-\text{Ar}]^+$  reacts with the palladium intermediate at a slower relative rate than  $\text{PhI}^{\text{III}}(\text{OAc})_2$ . This in particular has implications for extending the use of  $[\text{Ar}-\text{I}^{\text{III}}-\text{Ar}]\text{BF}_4$  to other systems that employ  $\text{PhI}^{\text{III}}(\text{OAc})_2$  as the oxidant. Several recently developed transformations have relied on intercepting an alkyl– $\text{Pd}^{\text{II}}$  intermediate via oxidation with  $\text{PhI}^{\text{III}}(\text{OAc})_2$ , which happens at a faster rate than  $\beta$ –hydride elimination.<sup>39-51</sup> Implementation of the  $[\text{Ar}-\text{I}^{\text{III}}-\text{Ar}]\text{BF}_4$  oxidants for these transformations may prove challenging and suffer from competing  $\beta$ –hydride elimination.

While these differences in reactivity may limit extension of the  $[\text{Ar}-\text{I}^{\text{III}}-\text{Ar}]\text{BF}_4$  in other transformations, the slow relative rate of oxidation provides an opportunity to gain insight into this step of these catalytic reactions. Specifically, these studies have implicated a high oxidation, state bimetallic palladium species **25**. This intermediate can be depicted as two limiting structures. The first, (**25a**) contains a  $\text{Pd}^{\text{IV}}$  tethered to a  $\text{Pd}^{\text{II}}$  by bridging acetates, and results from one palladium center being oxidized by two electrons. The second (**25b**) contains a  $\text{Pd}^{\text{III}}-\text{Pd}^{\text{III}}$  bond and results from the net oxidation

of each palladium center by 1 electron. The latter limiting structure is particularly intriguing due to the close proximity of the palladium centers of the dimer **5** based upon reported X-Ray crystallographic.<sup>52,53</sup> The orientation of this complex based on these analysis is depicted in **Figure 3.22**.

**Figure 3.22:** Structure of **5**, and the Two Limiting Structures of **25**.



Several rare examples of M<sup>III</sup>-M<sup>III</sup> have recently been reported involving both palladium and platinum, which is often used as a model for palladium. Our lab has described the oxidation of a monomeric platinum complex with PhI<sup>III</sup>(OAc)<sub>2</sub> to afford the dimeric complex **26** containing a Pt<sup>III</sup>-Pt<sup>III</sup> bond (**Figure 3.23**).<sup>54</sup> Similarly, Cotton and Ritter have recently demonstrated the oxidation of acetate bridged palladium complexes by PhI<sup>III</sup>Cl<sub>2</sub> resulting in the corresponding complexes **27** and **28** each containing Pd<sup>III</sup>-Pd<sup>III</sup> bonds.<sup>55-57</sup> The latter of these examples was then implicated in a palladium catalyzed C-H activation/chlorination reaction. Ritter also isolated product **29** from oxidation of the dimeric palladium species with PhI<sup>III</sup>(OAc)<sub>2</sub> and proposed that it was a catalytic intermediate in C-H acetoxylation.<sup>58</sup> A particularly pertinent example was recently reported by Canty (**Figure 3.24**). He demonstrated that the platinum complex **30** was oxidized to the Pt<sup>III</sup>-Pt<sup>III</sup> dimer **31** upon subjection to the I<sup>III</sup> oxidant **32**, providing a C-Pt<sup>IV</sup> similarly to what has been proposed in this methodology.

**Figure 3.23:** Examples of Palladium and Platinum  $M^{III}-M^{III}$  Bonds.

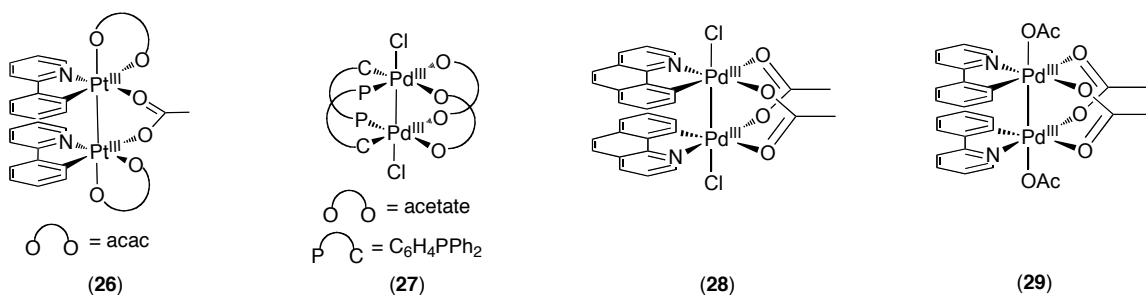
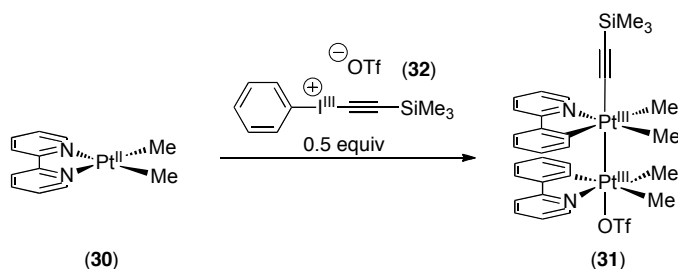


**Figure 3.24:** Oxidation of the Pt Complex **X** to the  $\text{Pt}^{III}-\text{Pt}^{III}$  Dimer **31**.



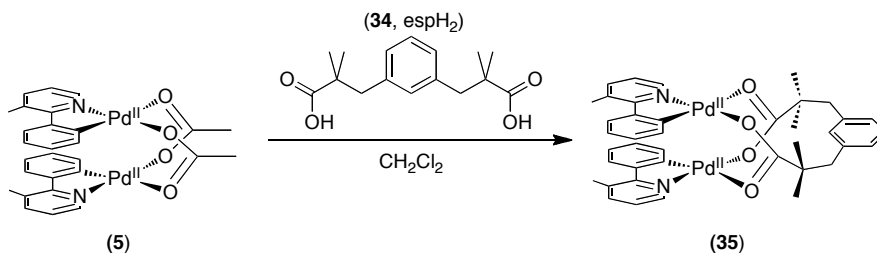
Each of the above examples supports the possible intermediacy of complex **25b**, but the exact nature of the bonding structure remains unknown. However, it is clear that the cyclometallated dimer **5** is necessary for the oxidation of  $\text{Pd}^{II}$  to occur. Several possible explanations can be proposed for this. First, the additional palladium center may be serving as an ancillary ligand to facilitate the oxidation. Second, steric factors associated with the monomer **9** may prevent oxidation by the  $\text{I}^{III}$  reagent. This is a distinct possibility given the observed impact oxidant sterics had on arylation selectivities, and the nearly four-fold difference in rate between  $[\text{Ph}-\text{I}^{III}-\text{Ph}]\text{BF}_4$  and  $[\text{Mes}-\text{I}^{III}-\text{Ph}]\text{BF}_4$ . This may be the result of the acetate and substrate ligands on monomer **9** blocking the  $d_z^2$  orbital of the palladium, where it is required to approach the  $\text{I}^{III}$  reagent as oxidation occurs. Although these details are yet to be understood, the results give insight toward the development to the next generation of catalysts that may help explain these observations.

### 3.11 Investigations Towards New Catalysts

Initial investigations toward the development of a second-generation catalyst focused on exploiting the dimeric palladium intermediate **5**. To accomplish this we sought to shift the equilibrium between monomer **9** and dimer **5** toward **5**. This would prevent the catalyst resting state from lying outside of the catalytic cycle. It was reasoned this could be accomplished by constraining the palladium centers together, which prevents substrate **3** from breaking up the dimer **5**, and ultimately resulting in an increased the reaction rate. Thus, a palladium complex that remains tethered as a dimer is expected to display 1<sup>st</sup> order kinetics in [Pd].

The approach taken toward this experiment was to employ the dicarboxylate ligand esp ( $\alpha,\alpha',\alpha',\alpha'$ -tetramethyl-1,3-benzenedipropionate, **33**) to maintain the dimeric Pd species.<sup>57</sup> This complex was synthesized as reported for a similar complex, by combining complex **5** with commercially available espH<sub>2</sub> (**34**). After stirring in CH<sub>2</sub>Cl<sub>2</sub> for 30 min the solvent was removed to afford complex **35** (86%, **Scheme 3.16**).

**Scheme 3.16:** Synthesis of the esp Tethered Complex **35**.



Complex **35** was then used as a catalyst in the identical order studies originally completed with Pd(OAc)<sub>2</sub>. In these experiments 3-methyl-2-phenylpyridine (**3**, 250 mM) was combined with [Mes-I<sup>III</sup>-Ph]BF<sub>4</sub> (**6**, 100 mM) and varying amounts of **35** (1.9 to 5.0 mM) in AcOH at 110 °C. A plot of the initial rate ( $\Delta[\mathbf{4}]/\Delta t$ ) versus [Pd] displayed a nearly identical relationship when both Pd(OAc)<sub>2</sub> and complex **35** were used as the catalyst (**Figure 3.25**). To confirm a second order dependence on [Pd] using this complex as a catalyst, the initial rate ( $\Delta[\mathbf{4}]/\Delta t$ ) versus [Pd]<sup>2</sup> was plotted and revealed a linear relationship (**Figure 3.26**). A second order dependence was further confirmed by

performing a non-linear least squares fit to the data using the equation  $f(x) = a[\text{Pd}]^n$ , where the order (n) in [Pd] was determined to be  $1.9 \pm 0.4$  ((**Figure 3.27**)).

These results confirm that this approach did not achieve the initial goal and there are two possible explanations for this result. First, this may suggest the esp ligand is not preventing excess substrate from breaking the complex into a monomeric form. Second, the esp ligands could be exchanging for bridging acetates, which is a likely possibility given that the reaction is in AcOH. Based on these results, a more tightly coordinating ligand is required.

**Figure 3.25:** Initial Rate ( $\Delta[4]/\Delta t$ ) versus [Pd] for  $\text{Pd}(\text{OAc})_2$  and Complex **35**.

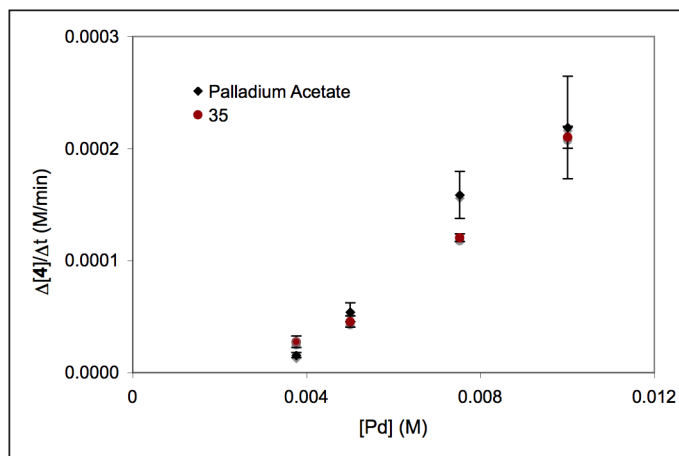
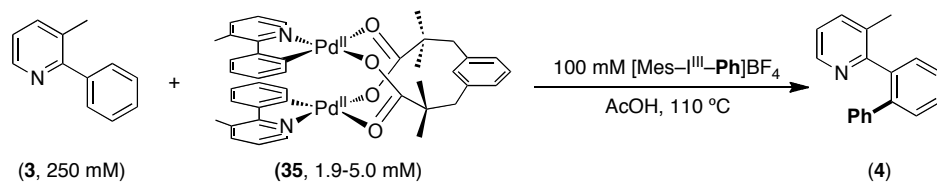




**Figure 3.26:** Plot of initial rate ( $\Delta[4]/\Delta t$ ) versus  $[Pd]^2$  using complex **35** as the catalyst.

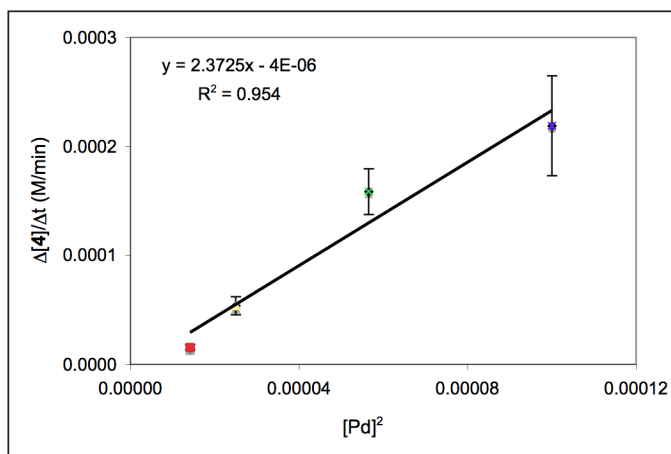
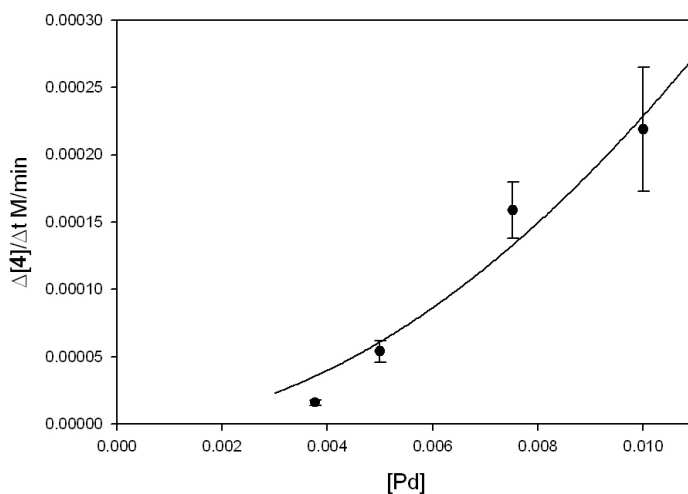


**Figure 3.27:** Data Fit of Initial Rate ( $\Delta[4]/\Delta t$ ) versus  $[Pd]$  for Complex **35**.



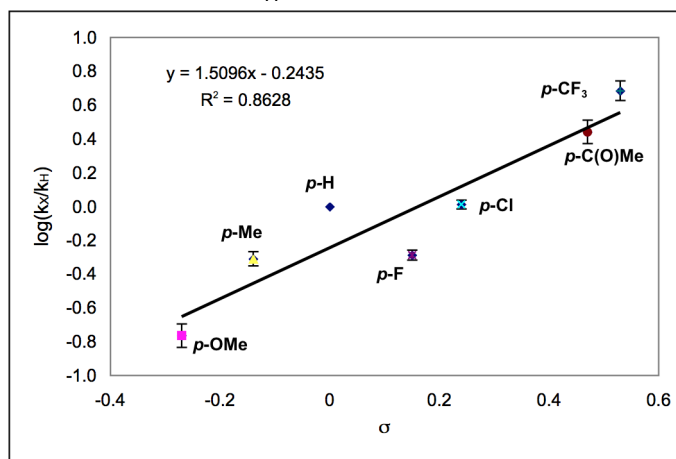
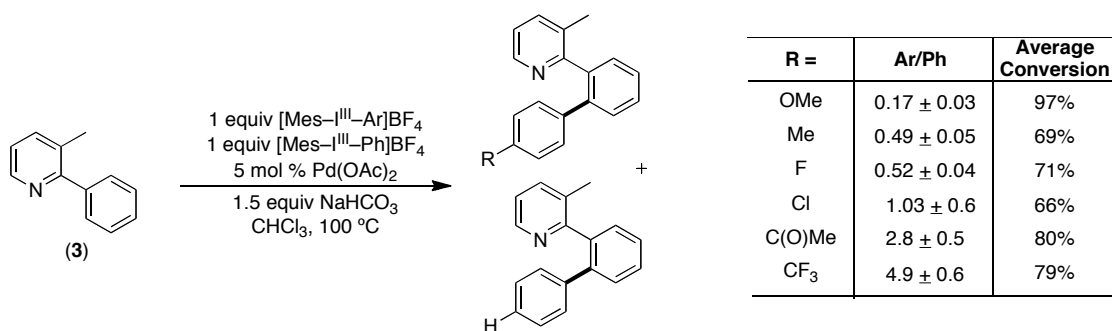
### 3.12 Preliminary Investigations of the Generality of the Mechanism

It was next of interest to obtain preliminary information about the generality of the now established mechanism, with respect to substrate. This was examined by comparing competition Hammett studies between several substrates containing nitrogen as well as oxygen directing groups with the oxidants  $[Mes-I^{III}-Ar]BF_4$  and  $[Ar-I^{III}-Ar]BF_4$ . Importantly, direct comparison of several substrates necessitated that all of the experiments be completed under identical conditions.

The substrates chosen for comparison were 3-methyl-2-phenylpyridine (**3**), 2-(*o*-methoxyphenyl)-3-methyl-pyridine (**36**) with nitrogen directing groups and *N*-phenylpyrrolidinone (**37**) and *N*-(*m*-methoxyphenyl)pyrrolidinone (**38**) containing oxygen-directing groups. The conditions chosen to complete these studies included CHCl<sub>3</sub> as the solvent with added NaHCO<sub>3</sub> because it proved to be most general amongst the substrates chosen. These Hammett studies were conducted as previously described by combining **3**, **36**, **37** or **38** with 1 equiv of [Mes-I<sup>III</sup>-Ph]BF<sub>4</sub> (**6**), 1 equiv of [Mes-I<sup>III</sup>-Ar]BF<sub>4</sub>, 1.5 equiv of NaHCO<sub>3</sub> and 5 mol % of Pd(OAc)<sub>2</sub> in CHCl<sub>3</sub>, then heated at 100 °C for 12 h. The Hammett plots were then constructed by plotting log(k<sub>Ar</sub>/k<sub>Ph</sub>) versus  $\sigma$  (**Figures 3.28–3.31**). The value of k<sub>X</sub>/k<sub>H</sub> was determined from the ratio of Ar to Ph products based on their respective uncorrected peak areas as determined by GC. Importantly, in most of the reactions used to construct these Hammett plots across all substrates and oxidants, the starting material was not completely consumed. For each substrate the average conversion is noted in the respective tables. Thus although the data is interpreted it is important to consider that further mechanistic investigations would be necessary to confirm this data.

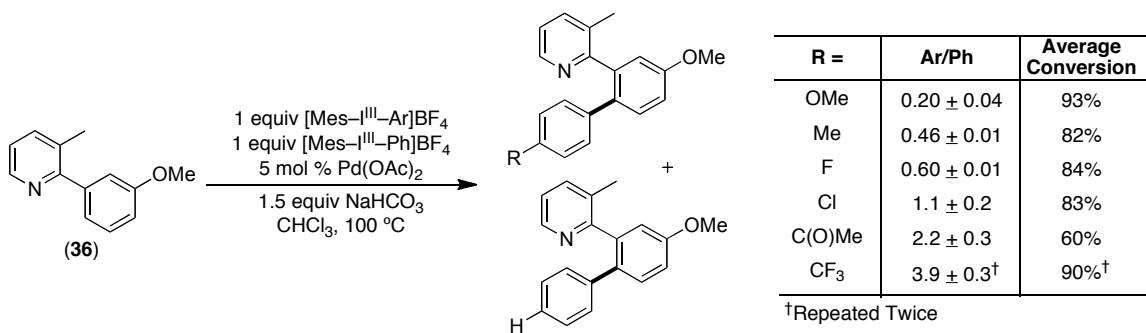
The first important analysis made from these results is the comparison of the results with 3-methyl-2-phenylpyridine (**3**) in CHCl<sub>3</sub>, to the data previously obtained in AcOH to provide preliminary evidence that the mechanisms are similar in each solvent. The Hammett plot employing **3** in CHCl<sub>3</sub> displayed  $\rho = +1.5 \pm 0.2$  (**Figure 3.28**), which is the same electronic trend and a similar magnitude of  $\rho$  as the results completed in AcOH where  $\rho = +1.1 \pm 0.1$  (**Figure 3.18**). Each of these values imply that C–H arylation is strongly facilitated by electron deficient oxidants in each solvent. This result provides evidence that the mechanism is generally the same as determined in AcOH. Specifically, this data suggests that the reaction proceeds through oxidation of Pd<sup>II</sup> to an Ar–Pd<sup>IV</sup> intermediate under both sets of conditions. Based on this analysis it was reasoned that valid comparisons could be made between substrates.

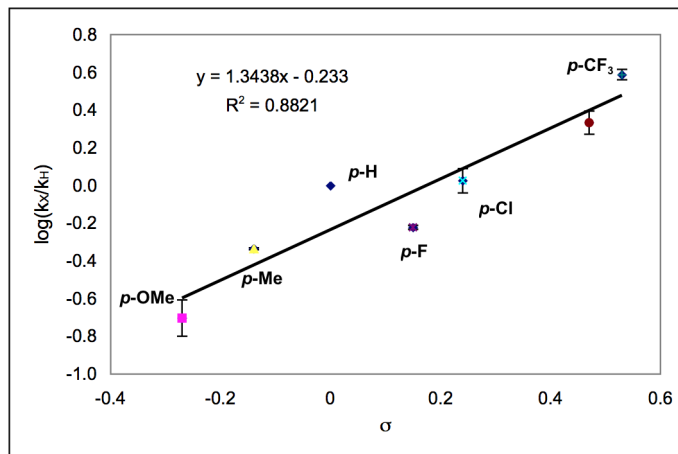
**Figure 3.28:** Competition Study of **3** with Mesityl Oxidants in  $\text{CHCl}_3$ .



First the comparison was made to the substrate 2-(*o*-methoxyphenyl)-3-methylpyridine (**36**). With this substrate,  $\rho = +1.3 \pm 0.2$  (**Figure 3.29**), implying that electron deficient oxidants facilitate the reaction, very similarly to **3**. This result is not surprising given the similarities between the substrates.

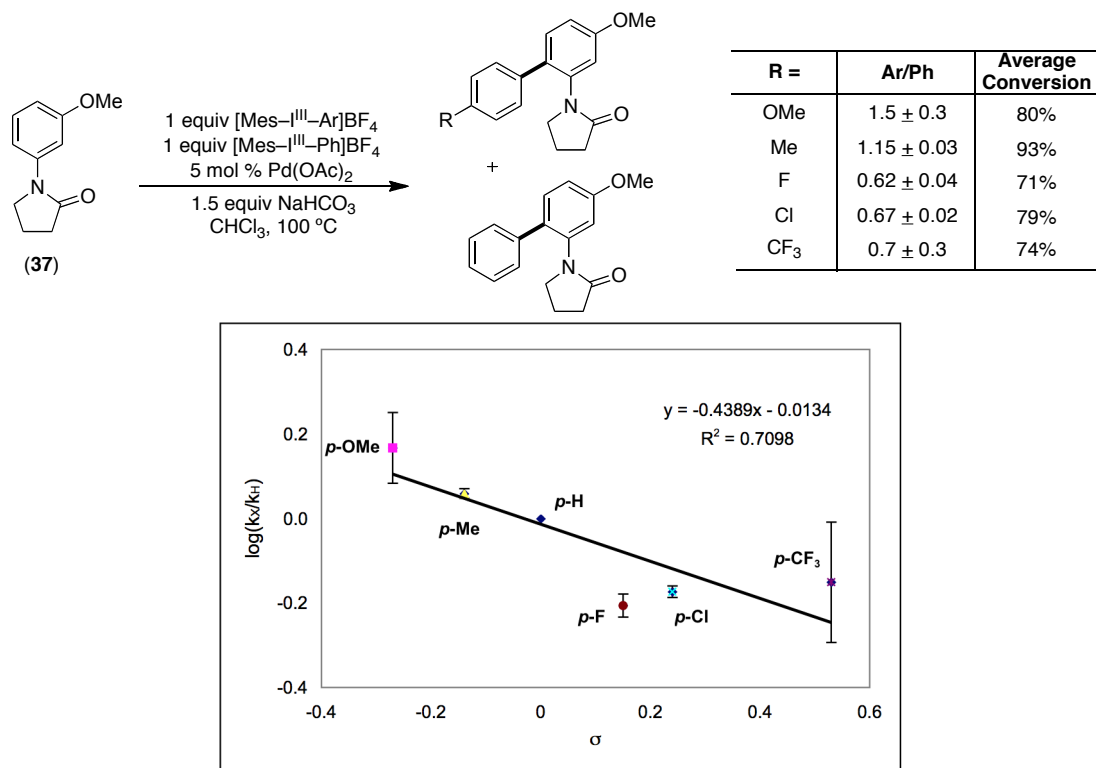
**Figure 3.29:** Competition Study of **36** with Mesityl Oxidants in  $\text{CHCl}_3$ .



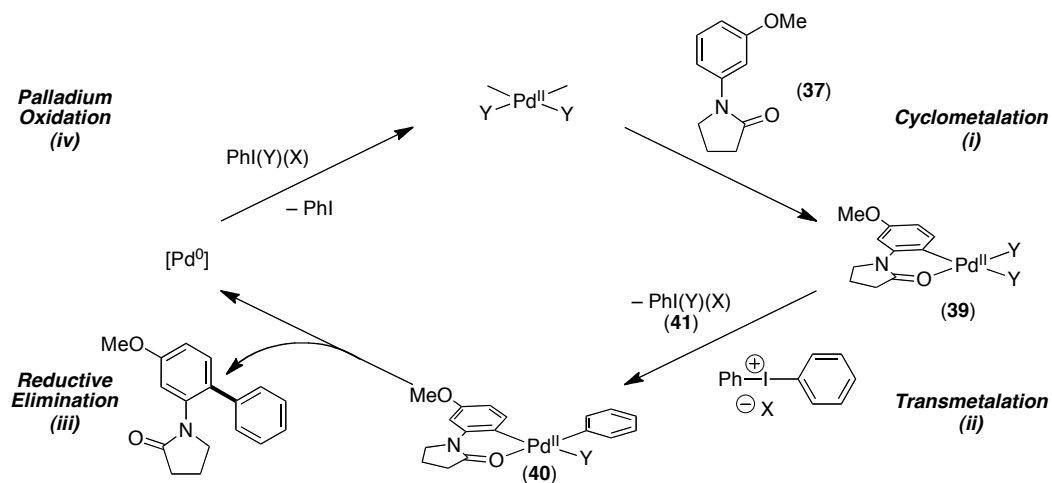


Next, comparisons were made between substrates containing nitrogen directing groups and oxygen directing groups. Analysis of the Hammett plot constructed using substrate **37** (*N*-(*m*-methoxyphenyl)pyrrolidinone) demonstrated a linear relationship in a plot of  $\log(k_X/k_H)$  versus  $\sigma$  where  $\rho$  was determined to be  $-0.4 \pm 0.1$  (**Figure 3.30**). Interestingly both the magnitude and sign of  $\rho$  have changed versus that with 3-methyl-2-phenylpyridine. A negative  $\rho$  suggests that electron-donating groups facilitate this reaction, and the smaller magnitude suggests that the oxidant electronics do not as greatly affect the reaction rates. This result is intriguing because the observed electronic effects are the opposite of what is expected if the  $I^{III}$  reagent were oxidizing  $Pd^{II}$  to  $Ar-Pd^{IV}$ . This result may imply an alternative mechanistic possibility.<sup>59</sup> This pathway would involve an aryl-transfer from the  $I^{III}$  reagent to a  $Pd^{II}$  species rather than oxidation to  $Pd^{IV}$  (**Scheme 3.18**). This mechanistic pathway would proceed through (i) cyclometallation at  $Pd^{II}$  to give **39**, (ii) aryl-transfer from  $[Mes-I^{III}-Ar]^+$  to the  $Pd^{II}$  species resulting in **40**, and (X)(Y) $I^{III}-Ar$  (**41**), (iii) C–C bond forming reductive elimination from  $Pd^{II}$  afford the product and generate  $Pd^0$ , and (iv) oxidation of  $Pd^0$  back to  $Pd^{II}$  by (X)(Y) $I^{III}-Ar$ . Importantly, further detailed mechanistic investigations will be necessary to provide more evidence for this mechanism.

**Figure 3.30:** Competition Study of **37** with Mesityl Oxidants in  $\text{CHCl}_3$ .



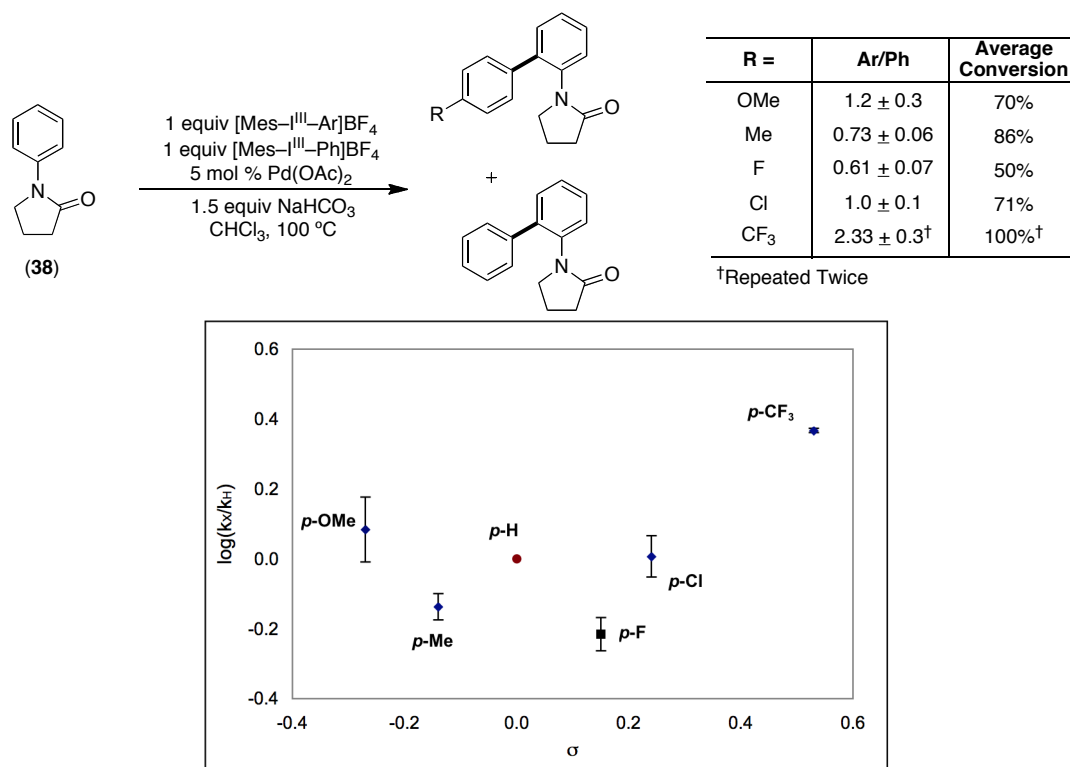
**Scheme 3.17:** Alternative C–H Activation/Arylation Mechanism.



Finally, in light of the interesting result obtained with **37**, the Hammett plot constructed using substrate **38** (*N*-phenylpyrrolidinone) was also examined for comparison. Unfortunately, this plot of  $\log(k_{\text{Ar}}/k_{\text{Ph}})$  versus  $\sigma$  demonstrated no linear

correlation, thus making it challenging to interpret this data and providing no further insight (**Figure 3.31**).

**Figure 3.31:** Competition Study of **38** with Mesityl Oxidants in  $\text{CHCl}_3$ .

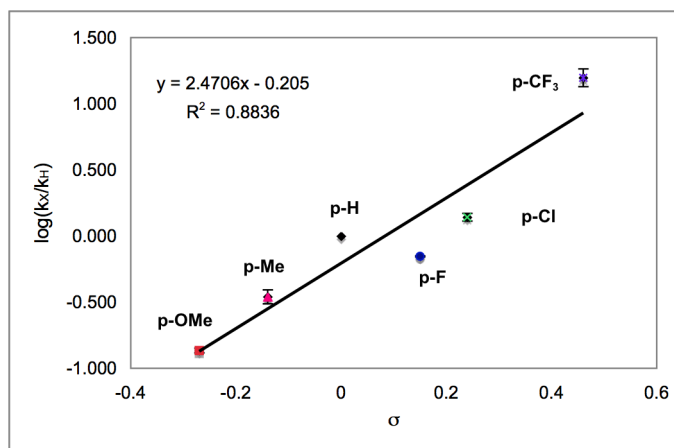
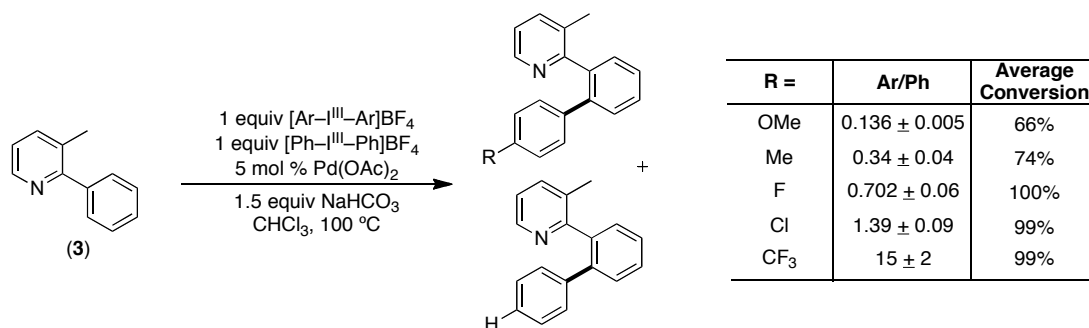


Next, the analogous competition Hammett studies were completed employing the symmetric oxidants [Ar-I<sup>III</sup>-Ar]BF<sub>4</sub>, thus allowing for direct comparison to the [Mes-I<sup>III</sup>-Ar]BF<sub>4</sub> oxidants. These Hammett studies were completed as previously described by combining **3**, **36**, **37** or **38** with 1 equiv of [Ph-I<sup>III</sup>-Ph]BF<sub>4</sub>, 1 equiv of [Ar-I<sup>III</sup>-Ar]BF<sub>4</sub>, 1.5 equiv of NaHCO<sub>3</sub> and 5 mol % of Pd(OAc)<sub>2</sub> in CHCl<sub>3</sub>, and then heating the reactions to 100 °C for 12 h. The value of  $k_X/k_H$  was determined from the ratio of Ar to Ph products based on their respective uncorrected peak areas determined by GC, and Hammett plots were constructed by plotting  $\log(k_X/k_H)$  versus  $\sigma$  (**Figures 3.32–3.35**).

The Hammett plot constructed for **3** revealed a linear relationship in a plot of  $\log(k_X/k_H)$  versus  $\sigma$  resulting in  $\rho = +2.5 \pm 0.5$  (**Figure 3.32**). The positive slope is similar to that obtained with the [Mes-I<sup>III</sup>-Ar]BF<sub>4</sub> oxidants in both AcOH ( $\rho = +1.1 \pm 0.1$ ) and

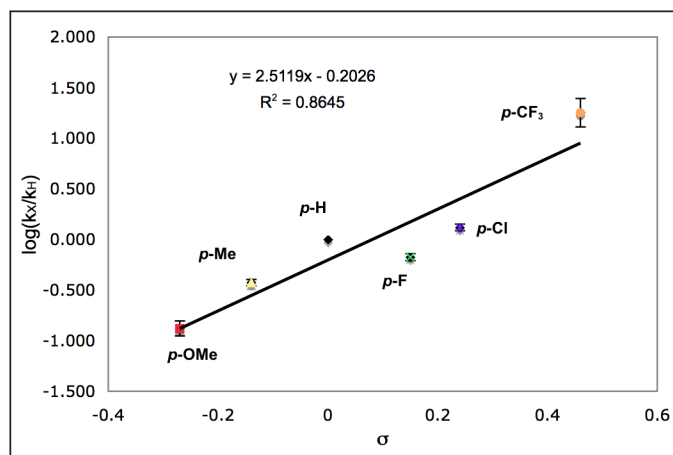
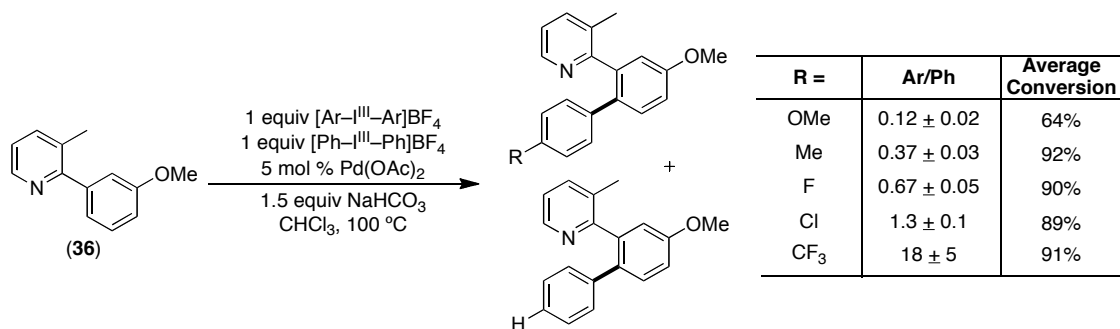
$\text{CHCl}_3$  ( $\rho = +1.5 \pm 0.2$ ). However, the magnitude of the  $\rho$  value is much larger for these oxidants. This may be due to the additive effects of varying the electronics on two aryl groups for the  $[\text{Ar}-\text{I}^{\text{III}}-\text{Ar}]\text{BF}_4$  oxidants, versus varying only one aryl group for the  $[\text{Mes}-\text{I}^{\text{III}}-\text{Ar}]\text{BF}_4$  oxidants.

**Figure 3.32:** Competition Study of **3** with Symmetric Oxidants in  $\text{CHCl}_3$ .



The Hammett plot constructed for **36** also shows a linear relationship between  $\log(k_X/k_H)$  versus  $\sigma$  leading to  $\rho = +2.5 \pm 0.5$  (**Figure 3.33**). Again, the sign of the  $\rho$  agrees with the  $[\text{Mes}-\text{I}^{\text{III}}-\text{Ar}]\text{BF}_4$  results obtained with this substrate in  $\text{CHCl}_3$  ( $\rho = +1.3 \pm 0.2$ ). This once again shows an additive effect of electronic variation of both of the aryl groups on the oxidant.

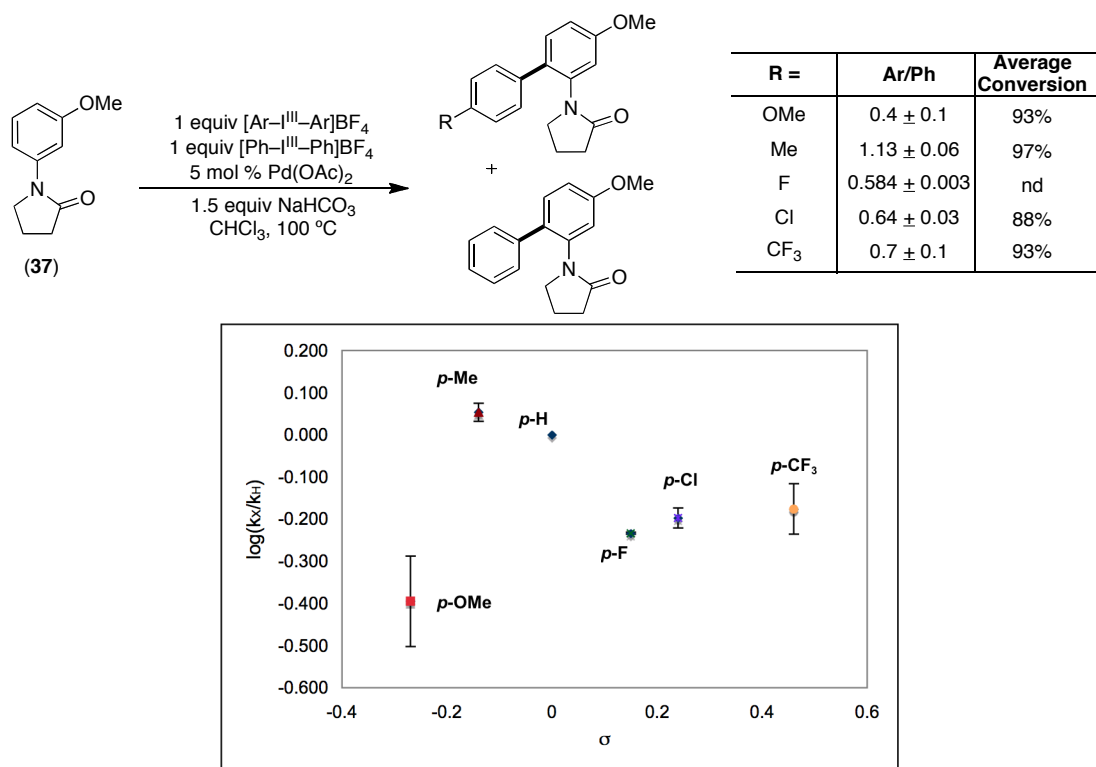
**Figure 3.33:** Competition Study of **36** with Symmetric Oxidants in  $\text{CHCl}_3$ .



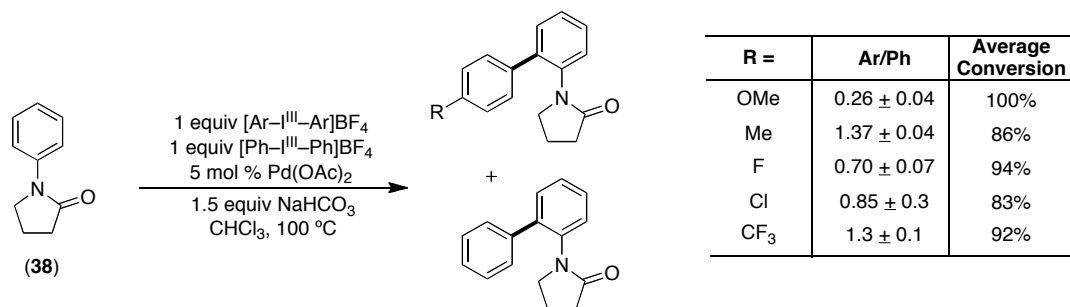
Finally, the competition Hammett studies using the pyrrolidinone substrates **37** and **38** were analyzed (**Figures 3.34** and **3.35** respectively). For each substrate a linear correlation was observed with the exception of the data point corresponding to *p*-MeOC<sub>6</sub>H<sub>4</sub>. In the absence of this data point  $\rho$  values of  $-0.43 \pm 0.2$  and  $-0.08 \pm 0.3$  would be obtained respectively. A potential explanation for this phenomenon is the difficulty associated with purifying the  $[(p\text{-MeOC}_6\text{H}_4)_2\text{-I}^{\text{III}}]\text{BF}_4$  oxidant which led to inconsistent reactivities. However, this was not the case when considering either of the substrates **3** and **36** with the  $[\text{Ar-I}^{\text{III}}\text{-Ar}]\text{BF}_4$ , in which case the data point for this oxidant correlated well. Thus, it is challenging to interpret this data to provide any further insight.

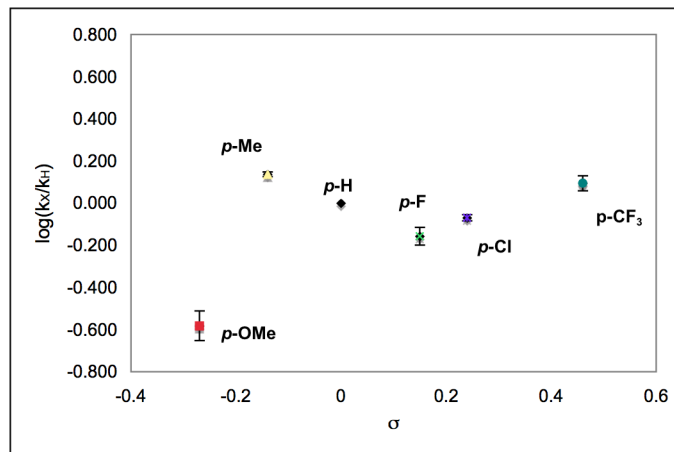


**Figure 3.34:** Competition Study of **37** with Symmetric Oxidants in  $\text{CHCl}_3$ .



**Figure 3.35:** Competition Study of **38** with Symmetric Oxidants in  $\text{CHCl}_3$ .





### 3.13 Conclusions

In summary we have reported the first thorough mechanistic investigation of a palladium catalyzed C–H activation/C–C bond formation. These studies implicate a mechanism proceeding through a high oxidation palladium dimer, while suggesting against alternative Pd<sup>0/II</sup> pathways and free radical intermediates. The role of each reaction component has been examined by the completion of kinetic order studies, kinetic isotope effect studies, and investigations of the resting state of the catalyst and oxidant. These studies allowed for the determination of the rate law, and establish oxidation as the rate-limiting step of this reaction. The combination of all of the experiments provided a detailed mechanistic picture of this transformation.

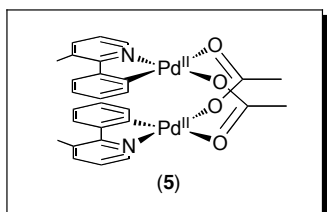
### 3.14 General Procedures and Materials and Methods

**General Procedures:** NMR spectra were obtained on a Varian Inova 500 (499.90 MHz for <sup>1</sup>H; 125.70 MHz for <sup>13</sup>C) or a Varian Inova 400 (399.96 MHz for <sup>1</sup>H; 100.57 MHz for <sup>13</sup>C) spectrometer. <sup>1</sup>H NMR chemical shifts are reported in parts per million (ppm) relative to TMS, with the residual solvent peak used as an internal reference. Multiplicities are reported as follows: singlet (s), doublet (d), doublet of doublets (dd), doublet of triplets (dt), triplet (t), quartet (q), multiplet (m), and broad resonance (br).

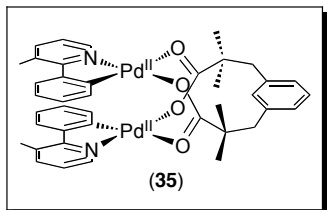
**Materials and Methods:** *N*-phenylpyrrolidinone, was obtained from commercial sources and used as received. Substrates 4-(*R*)-2-(*o*-tolyl)pyridine were prepared by Suzuki cross-coupling of phenyl boronic acid and 2-bromo-3-methylpyridine according to a literature

procedure.<sup>60</sup> *N*-(*m*-methoxyphenyl)pyrrolidinone (**37**) was prepared by palladium-catalyzed arylation of the corresponding lactam.<sup>61</sup> Pd(OAc)<sub>2</sub> was obtained from Pressure Chemical and used as received and PhI(OAc)<sub>2</sub> was obtained from Acros and used as received. Solvents were obtained from Fisher Chemical and used without further purification. Gas chromatography was carried out using a Shimadzu 17A using a Restek Rtx®-5 (Crossbond 5% diphenyl – 95% dimethyl polysiloxane; 15 m, 0.25 mm ID, 0.25 mm ID, 0.25 μm df) column. Flash chromatography was performed on EM Science silica gel 60 (0.040–0.063 mm particle size, 230–400 mesh) and thin layer chromatography was performed on Merck TLC plates pre-coated with silica gel 60 F254. The curve fittings were carried out using the program SigmaPlot for Window's v. 10.0 (Systat Software, Inc, San Jose, CA).

## Experimental Procedures



**Product 5:** 3-methyl-2-phenylpyridine (385 mg, 2.34 mmol, 1.05 equiv) and Pd(OAc)<sub>2</sub> was combined in MeOH. A yellow precipitate began to form and after 12 h the solution was filtered and the solid was rinsed with Et<sub>2</sub>O. <sup>13</sup>C NMR (95% CDCl<sub>3</sub>/5% *d*<sub>5</sub>-pyridine): δ 8.55 (d, *J* = 5.4 Hz, 1H), 7.66 (d, *J* = 7.8 Hz, 1H), 7.58 (d, *J* = 7.8 Hz, 1H), 7.07-7.00 (multiple peaks, 2H), 6.85 (t, *J* = 7.4 Hz, 1H), 6.25 (d, *J* = 7.8 Hz, 1H), 2.70 (s, 3H), 1.92 (s, 3H).



**Product 35:** Palladium complex **5** (479.6 mg, 718.5  $\mu\text{mol}$ , 1.0 equiv) was combined with  $\alpha,\alpha,\alpha',\alpha'$ -tetramethyl-1,3-benzenedipropionic acid (**34**) (200 mg, 718.5  $\mu\text{mol}$ , 1 equiv) in  $\text{CH}_2\text{Cl}_2$  and stirred at room temperature. After 30 min the solvent was removed in vacuo and the product was filtered followed by washing with  $\text{Et}_2\text{O}$ . The product was obtained as an orange solid (512 mg, 86% yield) **Major Regioisomer**  $^1\text{H NMR}$  ( $\text{CDCl}_3$ ):  $\delta$  7.91 (d,  $J = 5.6$  Hz, 2H), 7.47 (s, 1H), 7.38 (d,  $J = 7.6$  Hz, 2H), 7.27 (d,  $J = 7.2$  Hz, 2H), 7.10 (t,  $J = 3.6$  Hz) 6.99-6.92 (multiple peaks, 4H), 6.86-6.75 (multiple peaks, 5H), 6.38 (dd,  $J = 7.6, 5.6$  Hz, 2H), 2.84-2.78 (multiple peaks, 8H), 2.45 (s, 6H), 1.34 (s, 6H), 1.27 (s, 6H). **Minor regioisomer** is present in a 1:8 mixture as determined by  $^1\text{H NMR}$ . Not all resonances could be clearly observed due to overlap.  $^1\text{H NMR}$  ( $\text{CDCl}_3$ ):  $\delta$  8.01 (d,  $J = 5$  Hz, 2H), 7.23 (d,  $J = 8$  Hz, 2H), 6.71 (t,  $J = 8$  Hz, 2H), 6.63 (t,  $J = 8$  Hz, 2H), 6.57 (t,  $J = 6.8$  Hz, 2H) HRMS electrospray ( $m/z$ ):  $[\text{M}+\text{Na}]^+$  calcd for  $\text{C}_{40}\text{H}_{40}\text{N}_2\text{O}_4\text{Pd}_2\text{Na}$ , 847.0955; found, 847.0967.

**Reaction of 5 with Ph-I.** Substrate **3** (15.0 mg, 0.09  $\mu\text{mol}$ , 1 equiv), Ph-I (21.7 mg, 0.11  $\mu\text{mol}$ , 1.20 equiv), and  $\text{Pd}(\text{OAc})_2$  (1.00 mg, 0.004  $\mu\text{mol}$ , 5 mol%) were combined in AcOH (1.04 mL) in a 2 mL vial equipped with a small magnetic stir bar. The vial was sealed with a Teflon-lined cap and heated at 100  $^\circ\text{C}$  for 12 h. The reaction was cooled to room temperature and analyzed by gas chromatography, which showed only starting material and Ph-I with <1% of product **4**.

**Reaction of 5 with Ph-OTf.** Substrate **3** (15.0 mg, 0.09  $\mu\text{mol}$ , 1 equiv), Ph-OTf (24.1 mg, 0.11  $\mu\text{mol}$ , 1.20 equiv), and  $\text{Pd}(\text{OAc})_2$  (1.00 mg, 0.0044  $\mu\text{mol}$ , 5 mol%) were combined in AcOH (1.04 mL) in a 2 mL vial equipped with a small magnetic stir bar. The vial was sealed with a Teflon-lined cap and heated at 100  $^\circ\text{C}$  for 12 h. The reaction was cooled to room temperature and analyzed by gas chromatography, which showed only starting material **3** and Ph-OTf with <1% of product **4**.

**Reaction of 3 with  $[\text{Ph}_2\text{I}]\text{BF}_4$  in the Presence of Hg.** Substrate **3** (10.0 mg, 0.059  $\mu\text{mol}$ , 1 equiv),  $[\text{Ph}_2\text{I}]\text{BF}_4$  (26.1 mg, 0.071  $\mu\text{mol}$ , 1.20 equiv), and  $\text{Pd}(\text{OAc})_2$  (0.700 mg, 0.0031  $\mu\text{mol}$ , 5 mol %) were combined in AcOH (0.50 mL) in a 2 mL vial equipped with a

small magnetic stir bar. Metallic Hg (>500 equiv) was added to the reaction mixture, and the vial was sealed with a Teflon-lined cap and heated at 100 °C for 12 h. The reaction was cooled to room temperature and analyzed by gas chromatography, which revealed quantitative conversion to product **4**. **SAFETY NOTE: These reactions should be handled with extreme caution, as the reaction of excess [Ph<sub>2</sub>I<sup>III</sup>]BF<sub>4</sub> is known to generate highly toxic phenyl mercury compounds!**

**Reaction of 3 with [Ph<sub>2</sub>I]BF<sub>4</sub> in the Presence of MEHQ.** Substrate **3** (10.0 mg, 0.059 mmol, 1 equiv), [Ph<sub>2</sub>I]BF<sub>4</sub> (26.1 mg, 0.071 mmol, 1.20 equiv), and Pd(OAc)<sub>2</sub> (0.700 mg, 0.0031 mmol, 5 mol%) were combined in AcOH (0.50 mL) in a 2 mL vial equipped with a small magnetic stir bar. MEHQ (1.83 mg, 0.015 mmol, 25 mol%) was added to the reaction mixture, and the vial was sealed with a Teflon-lined cap and heated at 100 °C for 12 h. The reaction was cooled to room temperature and analyzed by gas chromatography, which revealed quantitative conversion to product **4**.

**Reaction of 3 with [Ph<sub>2</sub>I]BF<sub>4</sub> in the Presence of Galvinoxyl.** Substrate **3** (10.0mg, 0.059 mmol, 1 equiv), [Ph<sub>2</sub>I]BF<sub>4</sub> (26.1 mg, 0.071 mmol, 1.20 equiv), and Pd(OAc)<sub>2</sub> (0.700 mg, 0.0031 mmol, 5 mol%) were combined in AcOH (0.50 mL) in a 2 mL vial equipped with a small magnetic stir bar. Galvinoxyl (6.23 mg, 0.015 mmol, 25 mol%) was added to the reaction mixture, and the vial was sealed with a Teflon-lined cap and heated at 100 °C for 12 h. The reaction was cooled to room temperature and analyzed by gas chromatography, which revealed quantitative conversion to product **4**.

**Stoichiometric Reaction of 5 with [Ph<sub>2</sub>I]BF<sub>4</sub>.** Complex **5** (15.0 mg, 0.02 mmol, 1 equiv), [Ph<sub>2</sub>I]BF<sub>4</sub> (61.1 mg, 0.17 mmol, 3.2 equiv per Pd), and 2-(*o*-tolyl)pyridine (19.0 mg, 0.11 mmol, 2.5 equiv per Pd) were combined in AcOH (0.37 mL) in a 2 mL vial equipped with a small magnetic stir bar. The vial was sealed with a Teflon-lined cap and heated at 100 °C for 12 h. The reaction was cooled to room temperature and analyzed by gas chromatography, which showed 90 % yield of **4** (determined relative to an internal standard). Significant quantities of phenylated 2-(*o*-tolyl)pyridine were also observed by GC (as expected since an excess of oxidant was utilized). Importantly, when [Ph<sub>2</sub>I]BF<sub>4</sub>

was replaced with Ph-I or Ph-OTf under otherwise identical conditions <1% of product **4** was observed by GC.

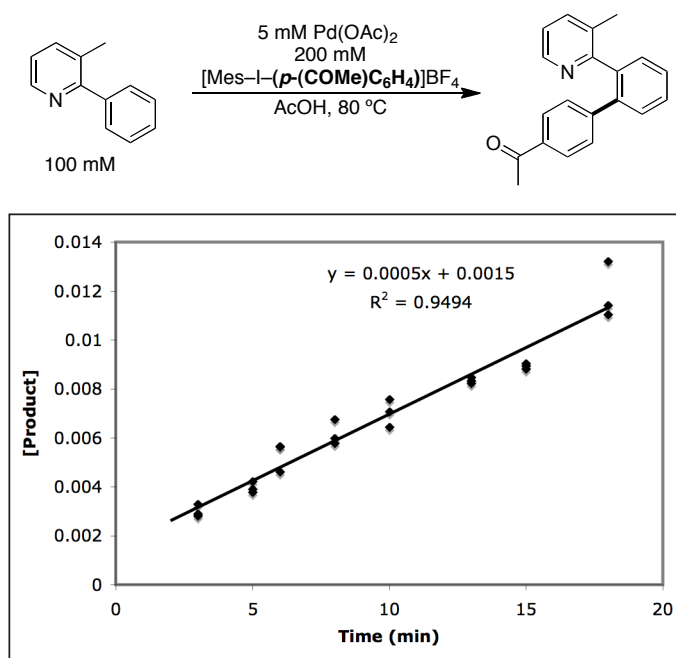
When the stoichiometric reaction between **5** and [Ph<sub>2</sub>I]BF<sub>4</sub> reaction was conducted in the absence of added 2-(*o*-tolyl)pyridine (under the following conditions: complex **5** (1 equiv, 0.02 mmol), [Ph<sub>2</sub>I]BF<sub>4</sub> (1.2 equiv per Pd, 0.05 mmol), AcOH (0.37 mL), 12 h, 100 °C) product **4** was obtained in 20% yield (determined relative to an internal standard) as the major product detectable by GC analysis. <sup>1</sup>H NMR spectroscopy and electrospray mass spectrometry revealed a complex mixture of additional high molecular weight organic products, and the MS data is consistent with the formation of a mixture of polyphenylated monomers and dimers of **3**. While the origin of these products and the details of this reactivity remains under investigation, we hypothesize that added 2-(*o*-tolyl)pyridine may act to trap reactive cationic palladium species (generated after initial C-C bond forming reductive elimination) that may be responsible for producing these polyphenylated products. Notably, under catalytic conditions, a large excess of substrate is present relative to catalyst, so such reactive species are expected to be trapped rapidly in a productive manner.

**General Procedure for Kinetic Experiments.** Kinetics experiments were run in 2 dram vials sealed with Teflon-lined caps. Each data point within a kinetics run represents a reaction in an individual vial, with each vial containing a constant concentration of oxidant, catalyst, and substrate. Reactions were run to between 6-10% conversion, and the data ([product] versus time) was analyzed using the initial rates method. The reported value of initial rate is the average of the three kinetic experiments, and the reported error in the initial rate is the standard deviation of those three kinetic experiments. A representative example is shown in **Figure 3.36**.

**Procedure:** For each experiment, the arylating reagent [Ar-I<sup>III</sup>-Ar']BF<sub>4</sub> was weighed into a vial, then 0.5 mL of a standard solution of Pd(OAc)<sub>2</sub> and phenanthrene (internal standard) (0.05 M) in AcOH was added. Finally, the substrate was added neat via a 10 or 25 µL syringe. The reactions were heated to 80 °C or 110 °C for the appropriate amount

of time using an aluminum-heating block with stirring set at the highest rpm (IKA stirplate setting of 11). The reactions were quenched by freezing in a dry ice/acetone bath followed by addition of a saturated aqueous solution of  $K_2CO_3$  (2 mL). The resulting mixture was warmed slowly to room temperature, then EtOAc (0.3 mL) was added, and the vial was shaken vigorously. The organic layer was collected, diluted with additional EtOAc (0.5 mL) and pyridine (0.1 mL), and the reaction was analyzed by gas chromatography. The yield of product for each time point was determined versus phenanthrene as the internal standard on the basis of the average of 3 successive GC analyses of the same sample.

**Figure 3.36:** A Representative Kinetic Plot.

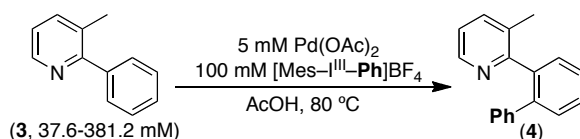


**Order in 3-methyl-2-phenylpyridine (3) under conditions where  $[3] < [6]$ .** Under conditions where  $[3] < [6]$ , the order in substrate deviated from inverse 3<sup>rd</sup> order. This is expected based on the overall mechanism, since, under these conditions, the resting state of the oxidant is no longer **9**, but instead is a mixture of **9** and **5**.

Notably, these experiments were conducted at  $80\text{ }^\circ C$ . The general procedure was used with  $[Mes-I^{III}-Ph]BF_4$  (41.0 mg, 0.1 mmol), 3-methyl-2- phenylpyridine (3.2-32.3 mg, 3-

30.5  $\mu\text{L}$ , 0.0188-0.1906 mmol), and 0.5 mL of a standard solution containing (per aliquot)  $\text{Pd}(\text{OAc})_2$  (0.56 mg, 0.0025 mmol), and phenanthrene (internal standard) (4.46 mg, 0.025 mmol). Reactions were conducted at 80  $^\circ\text{C}$ , and each initial rate represents an average of three unique kinetic experiments. A plot of initial rate ( $\Delta[4]/\Delta t$ ) versus [3-methyl-2-phenylpyridine] did not afford a straight line, nor did a plot of initial rate ( $\Delta[4]/\Delta t$ ) versus  $[3]^{-3}$ , suggesting against inverse third order dependence on substrate over all concentrations. A plot of initial rate versus  $[3]^{-3}$  under conditions where  $[3] > [6]$  (Regime 2) did afford a straight line ( $R^2 = 0.973$ ), suggesting an inverse third order dependence on substrate in this Regime (**Figure 3.1**). This was confirmed by a non-linear least squares fit of this data to the equation:  $f(x) = a[3]^n$  (**Figure 3.2**,  $n = -3.4 \pm 0.4$ ). However, rates were extremely slow in Regime 2 at 80  $^\circ\text{C}$ , thus all of the proceeding kinetic studies were completed under conditions where  $[3] > [6]$  and at 110  $^\circ\text{C}$ .

**Table 3.2:** Initial Reaction Rates for Each [3] Conducted at 80  $^\circ\text{C}$ .



[Substrate] (M)	Rate (M/min)
0.0376	$3 \pm 1 \times 10^{-4}$
0.05	$34 \pm 5 \times 10^{-5}$
0.0625	$26 \pm 83 \times 10^{-5}$
0.075	$27 \pm 8 \times 10^{-5}$
0.0875	$17 \pm 3 \times 10^{-5}$
0.1	$16 \pm 3 \times 10^{-5}$
0.125	$7 \pm 3 \times 10^{-5}$
0.15	$51 \pm 7 \times 10^{-6}$
0.175	$30 \pm 4 \times 10^{-6}$
0.2	$227 \pm 5 \times 10^{-7}$
0.25	$111 \pm 22 \times 10^{-7}$
0.312	$42 \pm 9 \times 10^{-7}$
0.355	$34 \pm 15 \times 10^{-7}$
0.381	$33 \pm 4 \times 10^{-7}$

**Order in Substrate (3).** The order in 3-methyl-2-phenylpyridine (3) was determined by studying the initial rate of reactions with different [3]. The general procedure was used with  $[\text{Mes-I}^{\text{III}}\text{-Ph]BF}_4$  (20.5 mg, 0.05 mmol), 3-methyl-2-phenylpyridine (17.1-25.7 mg,



16-24  $\mu\text{L}$ , 0.101-0.152 mmol), and 0.5 mL of a standard solution containing (per aliquot)  $\text{Pd}(\text{OAc})_2$  (0.56 mg, 0.0025 mmol) and phenanthrene (internal standard) (4.46 mg, 0.025 mmol). Reactions were conducted at 110  $^\circ\text{C}$ , and each initial rate represents an average of three unique kinetic experiments. A plot of initial rate ( $\Delta[4]/\Delta t$ ) versus [3-methyl-2-phenylpyridine] (**Figure 3.4**) did not afford a straight line, while a plot of initial rate ( $\Delta[4]/\Delta t$ ) versus [3-methyl-2-phenylpyridine] $^{-3}$  (**Figure 3.5**) gave a straight line ( $R^2 = 0.9967$ ), suggesting an inverse 3<sup>rd</sup> order dependence on substrate. This was confirmed by a non-linear least squares fit of the data to the equation:  $f(x) = a[1]^n$ . As shown in **Figure 3.6**, this afforded  $n = -3.1 \pm 0.2$  ( $a = 6.3 \pm 1.5 \times 10^{-7}$ ).

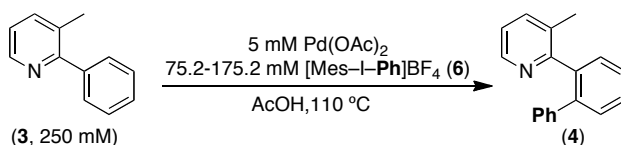
**Table 3.3:** Initial Reaction Rates for Each [3] Conducted at 110  $^\circ\text{C}$ .

(3, 202-304 mM)  $\xrightarrow[\text{AcOH, 110 }^\circ\text{C}]{\text{5 mM Pd(OAc)}_2, \text{100 mM [Mes-I-Ph]BF}_4}$  (4)

[Substrate] (M)	Rate (M/min)
0.2024	$9 \pm 1 \times 10^{-5}$
0.25	$46 \pm 5 \times 10^{-6}$
0.272	$36 \pm 3 \times 10^{-6}$
0.304	$22 \pm 3 \times 10^{-5}$

**Order in I<sup>III</sup> (6).** The order in  $[\text{Mes-I}^{\text{III}}\text{-Ph}]\text{BF}_4$  was determined by studying the initial rate of reactions with different [oxidant]. The general procedure was used with  $[\text{Mes-I}^{\text{III}}\text{-Ph}]\text{BF}_4$  (15.4-35.9 mg, 0.0376-0.0876 mmol), 3-methyl-2-phenylpyridine (21.2 mg, 20  $\mu\text{L}$ , 0.125 mmol), and 0.5 mL of a standard solution containing (per aliquot)  $\text{Pd}(\text{OAc})_2$  (0.56 mg, 0.0025 mmol) and phenanthrene (internal standard) (4.46 mg, 0.025 mmol) in AcOH. Reactions were conducted at 110  $^\circ\text{C}$ , and each reported initial rate represents an average of three unique kinetics experiments. A plot of initial rate ( $\Delta[4]/\Delta t$ ) versus  $[\text{I}^{\text{III}}]$  (**Figure 3.7**) gave a straight line ( $R^2 = 0.9861$ ), indicative of a 1st order dependence on  $[\text{I}^{\text{III}}]$ . This was confirmed by a non-linear least squares fit of the data to the equation:  $f(x) = a[\text{I}^{\text{III}}]^n$ . As shown in **Figure 3.8**, this afforded  $n = 1.12 \pm 0.08$  ( $a = 6 \pm 1 \times 10^{-4}$ ).

**Table 3.4:** Initial Reaction Rates for Each [6] Conducted at 110 °C.



[ <sup>III</sup> ] (M)	Rate (M/min)
0.075	34 ± 6 × 10 <sup>-6</sup>
0.100	46 ± 5 × 10 <sup>-6</sup>
0.125	6.5 ± 1 × 10 <sup>-5</sup>
0.150	78 ± 9 × 10 <sup>-6</sup>
0.175	88 ± 3 × 10 <sup>-6</sup>

**Order in [Pd].** The order in Pd(OAc)<sub>2</sub> was determined by studying the initial rate of reactions with different [Pd]. The general procedure was used with [Mes-I<sup>III</sup>-Ph]BF<sub>4</sub> (20.5 mg, 0.05 mmol), 3-methyl-2-phenylpyridine (21.2 mg, 20 μL, 0.125 mmol), and 0.5 mL of a standard solution containing (per aliquot) Pd(OAc)<sub>2</sub> (0.425-1.125 mg, 0.00189-0.005 mmol) and phenanthrene (internal standard) (4.46 mg, 0.025 mmol) in AcOH. Reactions were conducted at 110 °C, and each initial rate represents an average of three unique kinetic experiments. A plot of initial rate (Δ[4]/Δt) versus [Pd] (**Figure 3.9**) did not afford a straight line, while a plot of initial rate (Δ[4]/Δt) versus [Pd]<sup>2</sup> (**Figure 3.10**) gave a straight line (R<sup>2</sup> = 0.9987), suggesting a 2nd order dependence on catalyst. This was confirmed by a non-linear least squares fit of the data to the equation:  $f(x) = a[\text{Pd}]^n$ . As shown in **Figure 3.11**, this afforded  $n = 2.09 \pm 0.08$  ( $a = 3 \pm 1$  M/min).

For **35** the same procedure as used above was employed, except the standard solutions of [Pd] contained (per aliquot) **35** (0.77-2.06 mg, 0.00189-0.005 mmol). A plot of initial rate (Δ[4]/Δt) versus [Pd] (**Figure 3.26**) did not afford a straight line, while a plot of initial rate (Δ[4]/Δt) versus [Pd]<sup>2</sup> (**Figure 3.27**) gave a straight line (R<sup>2</sup> = 0.954), suggesting a 2nd order dependence on catalyst. This was confirmed by a non-linear least squares fit of the data to the equation:  $f(x) = a[\text{Pd}]^n$ . As shown in **Figure 3.28**, this afforded  $n = 1.9 \pm 0.08$  ( $a = 1 \pm 3$  M/min).

**Table 3.5:** Initial Reaction Rates for each [Pd] with Pd(OAc)<sub>2</sub> and **35** at 100 °C.

(3, 250 mM)  $\xrightarrow[\text{AcOH, 110 } ^\circ\text{C}]{\text{3.8-10 mM [Pd], 100 mM [Mes-I-Ph]BF}_4}$  Ph (4)

[Pd] (M)	Rate (M/min) with Pd(OAc) <sub>2</sub>	Rate (M/min) with <b>35</b>
0.00376	$27 \pm 5 \times 10^{-5}$	$16 \pm 2 \times 10^{-5}$
0.005	$46 \pm 5 \times 10^{-6}$	$54 \pm 8 \times 10^{-6}$
0.00752	$120 \pm 4 \times 10^{-6}$	$16 \pm 2 \times 10^{-7}$
0.01	$21 \pm 1 \times 10^{-7}$	$22 \pm 5 \times 10^{-7}$

**Competition Hammett Plots in AcOH:** [Mes-I<sup>III</sup>-Ar]<sup>+</sup> Oxidants: Substrate **3** (8.46mg, 0.05 mmol, 1 equiv), [Mes-I<sup>III</sup>-Ph]BF<sub>4</sub> (20.5 mg, 0.05 mmol, 1.0 equiv), [Mes-I<sup>III</sup>-Ar]BF<sub>4</sub> (0.05 mmol, 1.0 equiv), phenanthrene (4.46 mg, 0.025 mmol, 0.5 equiv) as an internal standard and Pd(OAc)<sub>2</sub> (0.56 mg, 0.0025 mmol, 5 mol %) were combined in AcOH (0.10 mL) in a 4 mL vial equipped with a small magnetic stir bar. The vial was sealed with a Teflon-lined cap and heated at 100 °C for 12 h. The reaction was cooled to room temperature and analyzed by gas chromatography to give a calibrated yield of each product. The value for  $k_{\text{Ar}}/k_{\text{H}}$  was determined by % yield Ar divided by % yield Ph and plotted against  $\sigma$ .

[Ar-I<sup>III</sup>-Ar]<sup>+</sup> Oxidants: The analogous procedure was followed with substrate **3** (8.46mg, 0.05 mmol, 1 equiv), [Ph-I<sup>III</sup>-Ph]BF<sub>4</sub> (20.5 mg, 0.05 mmol, 1.0 equiv), [Ar-I<sup>III</sup>-Ar]BF<sub>4</sub> (0.05 mmol, 1.0 equiv), phenanthrene (4.46 mg, 0.025 mmol, 0.5 equiv) as an internal standard and Pd(OAc)<sub>2</sub> (0.56 mg, 0.0025 mmol, 5 mol%) were combined in AcOH (0.10 mL) in a 4 mL vial equipped with a small magnetic stir bar. The vial was sealed with a Teflon-lined cap and heated at 100 °C for 12 h.

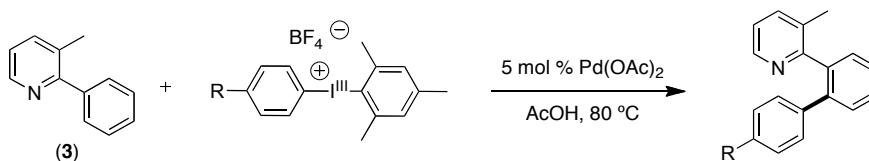
**Competition Hammett Plots in CHCl<sub>3</sub>:** [Mes-I<sup>III</sup>-Ar]<sup>+</sup> Oxidants: The respective substrate (0.05 mmol, 1 equiv), [Mes-I<sup>III</sup>-Ph]BF<sub>4</sub> (20.5 mg, 0.05 mmol, 1.0 equiv), [Mes-I<sup>III</sup>-Ar]BF<sub>4</sub> (0.05 mmol, 1.0 equiv), and Pd(OAc)<sub>2</sub> (0.56 mg, 0.0025 mmol, 5 mol%) were combined in AcOH (0.10 mL) in a 4 mL vial equipped with a small

magnetic stir bar. The vial was sealed with a Teflon-lined cap and heated at 120 °C for 17 h. The reaction was cooled to room temperature and analyzed by gas chromatography. The ratios of products and starting material uncorrected and based on the areas of the respective peaks. The value for  $k_{Ar}/k_H$  was determined by Ar peak area divided by Ph peak area and plotted against  $\sigma$ . The average percent conversions are based upon the total area of the products and starting material divided by the products.

[Ar-I<sup>III</sup>-Ar]<sup>+</sup> Oxidants: The respective substrate (0.05 mmol, 1 equiv), [Ph-I<sup>III</sup>-Ph]BF<sub>4</sub> (20.5 mg, 0.05 mmol, 1.0 equiv), [Ar-I<sup>III</sup>-Ar]BF<sub>4</sub> (0.05 mmol, 1.0 equiv), and Pd(OAc)<sub>2</sub> (0.56 mg, 0.0025 mmol, 5 mol%) were combined in AcOH (0.10 mL) in a 4 mL vial.

**Oxidant Hammett Studies Determined by Initial Rate:** Rate data for each oxidant [Mes-I-Ar]BF<sub>4</sub> was obtained using the initial rates method. The general procedure was used with [Mes-I-Ar]BF<sub>4</sub> (0.1 mmol), 3-methyl-2-phenylpyridine (8.46 mg, 8.0 mL, 0.05 mmol), and 0.5 mL of a standard solution containing (per aliquot) Pd(OAc)<sub>2</sub> (0.56 mg, 0.0025 mmol) and phenanthrene (internal standard) (4.46 mg, 0.025 mmol) in AcOH. Reactions were conducted at 80 °C, and each initial rate represents an average of three unique kinetics experiments. The initial rate for each oxidant is listed in **Table 3.6** and a Hammett plot of the data is shown in **Figure 3.20**.

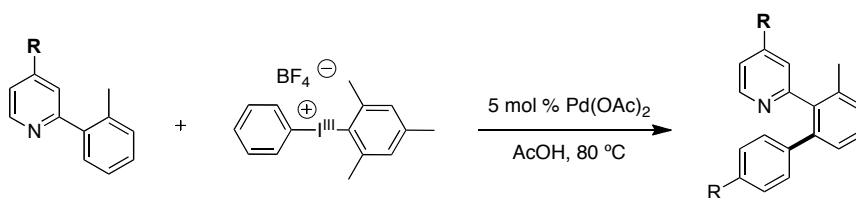
**Table 3.6:** Reaction Rate for Oxidants used in the Hammett Studies.



<i>p</i> -X-Ph	Rate (M/min)
H	13 ± 1 × 10 <sup>-5</sup>
CF <sub>3</sub>	73 ± 5 × 10 <sup>-5</sup>
C(O)Me	54 ± 3 × 10 <sup>-5</sup>
Cl	14.3 ± 0.5 × 10 <sup>-5</sup>
F	5.1 ± 3 × 10 <sup>-5</sup>
Me	4.6 ± 6 × 10 <sup>-5</sup>
OMe	2.2 ± 0.4 × 10 <sup>-5</sup>

**Directing Group Hammett Studies Determined by Initial Rate:** Rate data for each substrate was obtained using the initial rates method. The general procedure was used with [Mes-I-Pa]BF<sub>4</sub> (41.0 mg, 0.1 mmol, 2 equiv), 2-(*o*-tolyl)-4-X-pyridine (0.05 mmol, 1 equiv), and 0.5 mL of a standard solution containing (per aliquot) Pd(OAc)<sub>2</sub> (0.56 mg, 0.0025 mmol) and phenanthrene (internal standard) (4.46 mg, 0.025 mmol) in AcOH. Reactions were conducted at 80 °C, and each initial rate represents an average of three unique kinetics experiments. Rates determined relative to the calibration for 3-methyl-2-phenylpyridine, individual calibrations were not made for each substrate. The initial rate for each oxidant is listed in **Table 3.7** and a Hammett plot of the data is shown in **Figure 3.21**

**Table 3.7:** Reaction Rate for Substrates Used in the Hammett Studies.

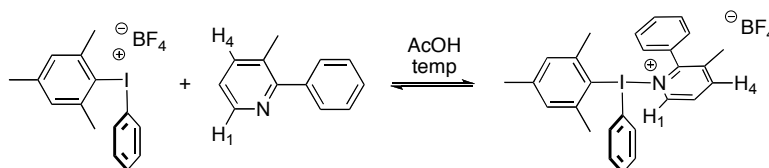


<i>p</i> -X-Ph	Rate (M/min)
H	$9.4 \pm 0.7 \times 10^{-5}$
CF <sub>3</sub>	$3.1 \pm 0.3 \times 10^{-5}$
CO <sub>2</sub> Me	$2.0 \pm 0.3 \times 10^{-5}$
Me	$23 \pm 1 \times 10^{-5}$
OMe	$30 \pm 2 \times 10^{-5}$

**Job Plots:** A Job plot for the complexation of 3-methyl-2-phenylpyridine (**3**) with [Mes-I<sup>III</sup>-Ph]BF<sub>4</sub> (**6**) was constructed using the method described by Newcomb and co-workers.<sup>16,18</sup> A series of <sup>1</sup>H NMR spectra were collected with different relative ratios of **3**:**6**, while maintaining a constant total concentration ([**3**] + [**6**]) of 23.6 mM in CD<sub>3</sub>CO<sub>2</sub>D. At each ratio, the chemical shift (δ) of the proton *para* to the pyridine nitrogen, H(4), was determined, and Δδ values represent the difference between δH(4) in the presence of **6** versus in free **3**. Samples were prepared from standard solutions of

[Mes-I<sup>III</sup>-Ph]BF<sub>4</sub> (0.0235 M in CD<sub>3</sub>CO<sub>2</sub>D) and 3-methyl-2-phenylpyridine (0.0473 M in CD<sub>3</sub>CO<sub>2</sub>D), and additional CD<sub>3</sub>CO<sub>2</sub>D was added such that each sample had a total volume of 0.4 mL. The samples were allowed to equilibrate in the NMR probe at 80 °C or 110 °C for a minimum of 10 min with the VT air flow set to 15 L/min prior to data acquisition, and spectra were referenced to the residual solvent peak ( $\delta = 2.03$  ppm). Each data point is reported as the average of two experiments, and the error represents the standard deviation of the  $\Delta\delta$  values (**Table 3.8** and **3.9**). At both temperatures, the maximum was observed when the mole fraction of 3-methyl-2-phenylpyridine was ca. 0.5, indicative of 1: 1 binding (**Figure 3.14** and **3.15**).

**Table 3.8:** <sup>1</sup>H NMR chemical shift data for Job plot at 110 °C.



3-methyl-2-phenylpyridine (mmol)	[(Mes-I-Ph)BF <sub>4</sub> ] (mmol)	Trial 1 ( $\delta$ ppm)	Trial 2 ( $\delta$ ppm)
0.00118	0.00821	8.389	8.414
0.00236	0.00704	8.316	8.330
0.00331	0.00610	8.262	8.261
0.00402	0.00540	8.232	8.239
0.00473	0.00469	8.213	8.204
0.00544	0.00399	8.171	8.170
0.00615	0.00329	8.147	8.151
0.00709	0.00235	8.110	8.111
0.00827	0.00117	8.068	8.067
0.00946	0.00000	8.015	8.015

**Table 3.9:**  $^1\text{H}$  NMR chemical shift data for Job plot at 80 °C.

3-methyl-2-phenylpyridine (mmol)	[(Mes-I-Ph)BF <sub>4</sub> ] (mmol)	Trial 1 ( $\delta$ ppm)	Trial 2 ( $\delta$ ppm)
0.00118	0.00821	8.452	8.452
0.00236	0.00704	8.386	8.384
0.00331	0.00610	8.335	8.344
0.00402	0.00540	8.315	8.314
0.00473	0.00469	8.289	8.289
0.00544	0.00399	8.256	8.261
0.00615	0.00329	8.235	8.237
0.00709	0.00235	8.199	8.202
0.00827	0.00117	8.158	8.157
0.00946	0.00000	8.108	8.105

**Equilibrium Constant for Binding between 3 and 6.** The equilibrium constant was determined by collecting a series of  $^1\text{H}$  NMR spectra at constant [3] and increasing concentration of [Mes-I<sup>III</sup>-Ph]BF<sub>4</sub>. At each ratio, the chemical shift ( $\delta$ ) of the proton *para* to the pyridine nitrogen (H<sub>4</sub>) was determined. The NMR samples for this experiment contained 3 (0.00632 M) along with varying amounts of [Mes-I<sup>III</sup>-Ph]BF<sub>4</sub> (0-0.0251 M) in CD<sub>3</sub>CO<sub>2</sub>D (0.5-1.8 mL). 10 The samples were allowed to equilibrate in the NMR probe at 80 °C or 110 °C for a minimum of 10 min with the VT airflow set to 15 L/min prior to data acquisition, and spectra were referenced to the residual solvent peak ( $\delta$  = 2.03 ppm). The chemical shift data (Table 3.10 and 3.11) was fit to the eq. 3.1, 3.2 and 3.3 described by Funasak using the Sigma Plot program,<sup>16,19</sup> and the curves representing those fits are shown in Figure 3.16 (110 °C) and Figure 3.17 (80 °C). At 110 °C,  $K_{\text{eq}} = 111 \pm 18$  ( $\delta_{\text{max}} = 8.52 \pm 0.03$ ), while at 80 °C,  $K_{\text{eq}} = 154 \pm 24$  ( $\delta_{\text{max}} = 8.51 \pm 0.02$ ). These values were confirmed using the program described in the literature and provided by the author an available for download on his website.<sup>21</sup>

**Table 3.10:**  $^1\text{H}$  NMR Chemical Shift Data for Equilibrium Determination at 110 °C.

[(Mes-I-Ph)BF <sub>4</sub> ] (M)	Trial 1 (ppm)	Trial 2 (ppm)	Trial 3 (ppm)	Average (ppm)
0.00000	8.027	8.029	8.024	8.0263
0.00317	8.139	8.139	8.140	8.1390
0.00581	8.188	8.192	8.176	8.1850
0.00804	8.217	8.224	8.211	8.2173
0.00996	8.240	8.249	8.235	8.2412
0.01307	8.274	8.281	8.269	8.2755
0.01549	8.305	8.310	8.300	8.3055
0.01742	8.328	8.331	8.322	8.3275
0.02033	8.350	8.353	8.345	8.3492
0.02323	8.369	8.371	8.366	8.3683
0.02516	8.380	8.383	8.376	8.3793

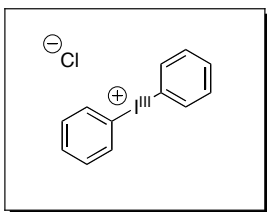
**Table 3.11:**  $^1\text{H}$  NMR Chemical Shift Data for Equilibrium Determination at 110 °C.

[(Mes-I-Ph)BF <sub>4</sub> ] (M)	Trial 1 (ppm)	Trial 2 (ppm)	Average (ppm)
0.00000	8.111	8.113	8.1118
0.00317	8.217	8.218	8.2175
0.00581	8.260	8.263	8.2613
0.00804	8.289	8.292	8.2903
0.00996	8.310	8.311	8.3103
0.01307	8.340	8.340	8.3401
0.01549	8.362	8.359	8.3605
0.01742	8.377	8.378	8.3775
0.02033	8.397	8.398	8.3975
0.02323	8.414	8.412	8.4128
0.02516	8.420	8.425	8.4220

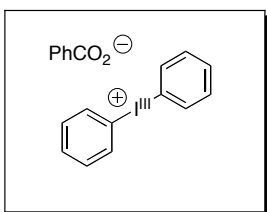
**General Procedure for [Ph-I<sup>III</sup>-Ph]X Synthesis:** A modification of the published procedure for the synthesis of [Ar-I<sup>III</sup>-Ar]BF<sub>4</sub> was followed.<sup>22</sup> To a solution of PhB(OH)<sub>2</sub> (5.45g, 42.6 mmol, 1.05 equiv) and BF<sub>3</sub>•OEt<sub>2</sub> (44.7 mmol, 1.05 equiv) in CH<sub>2</sub>Cl<sub>2</sub> (200 mL) at 0 °C was cannula transferred solution of PhI<sup>III</sup>(OAc)<sub>2</sub> (15 g, 42.6



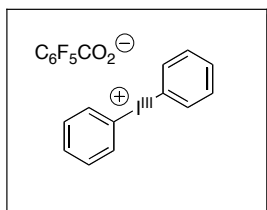
mmol, 1 equiv) in  $\text{CH}_2\text{Cl}_2$  (202 mL) that had also been cooled to  $0\text{ }^\circ\text{C}$ . This solution was allowed to stir at  $0\text{ }^\circ\text{C}$  for 2 h, then a saturated aqueous solution of NaCl was added (300 mL), and the mixture was allowed to stir as a biphasic solution for 30 min at room temperature. The product formed as a solid that is soluble in neither water nor  $\text{CH}_2\text{Cl}_2$ . Isolation consisted of filtering the biphasic mixture to collect the solid. The organic layer was then collected and the aqueous layer was washed with 3 x 40 mL of  $\text{CH}_2\text{Cl}_2$  to remove any soluble products. The combined organic extracts were dried with  $\text{MgSO}_4$  and the solvent was reduced to the minimal amount necessary to keep the product in solution. To conduct the counterion exchange  $[\text{Ph}-\text{I}^{\text{III}}-\text{Ph}]\text{Cl}$  (2.0g, 6.32 mmol, 1 equiv) was added to a solution of 200 mL : 200 mL  $\text{CH}_2\text{Cl}_2$  to  $\text{H}_2\text{O}$  with NaX (126.4 mmol, 20 equiv). This solution was stirred for 45 min. The organic layer was separated, and the aqueous layer was washed 3x with additional  $\text{CH}_2\text{Cl}_2$ . The organic layers were dried with  $\text{MgSO}_4$ , the solvent was reduced until the solution was saturated with  $[\text{Ph}-\text{I}^{\text{III}}-\text{Ph}]\text{X}$ , and the product was precipitated by addition of  $\text{Et}_2\text{O}$ .



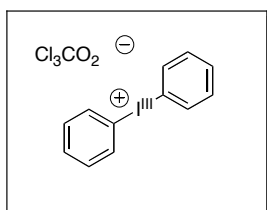
**Oxidant 14:** General procedure for  $[\text{Ph}-\text{I}^{\text{III}}-\text{Ph}]\text{Cl}$  synthesis was followed. This reaction combined  $\text{PhI}^{\text{III}}(\text{OAc})_2$  (15.0 g, 42.6 mmol) and  $\text{PhB}(\text{OH})_2$  (5.45 g, 44.7 mmol) and resulted in the desired oxidant as a white powder (12.53 g, 93% yield).  $^1\text{H}$  NMR ( $d_6$ -acetone):  $\delta$  8.22 (d,  $J = 6.4$  Hz, 4H), 7.66 (t,  $J = 5.6$  Hz, 2H), 7.53 (t,  $J = 6.4$  Hz, 4H).



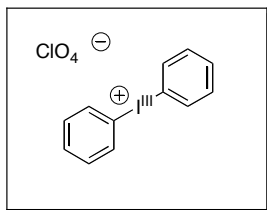
**Oxidant 15:** General procedure for  $[\text{Ph}-\text{I}^{\text{III}}-\text{Ph}]\text{Cl}$  synthesis was followed. This reaction combined  $[\text{Ph}-\text{I}^{\text{III}}-\text{Ph}]\text{Cl}$  (0.74 g, 2.36 mmol) and  $\text{C}_6\text{H}_5\text{CO}_2\text{Na}$  (6.83 g, 47.4 mmol) and resulted in the desired oxidant as a white powder (0.567 g, 60% yield).  $^1\text{H}$  NMR ( $\text{CDCl}_3$ ):  $\delta$  7.98-7.89 (multiple peaks, 6H), 7.50 (t,  $J = 7.2$  Hz, 2H), 7.40-7.26 (multiple peaks, 7H).



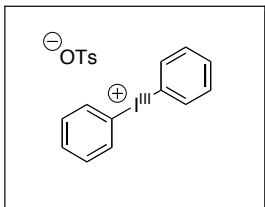
**Oxidant 16:** General procedure for [Ph-I<sup>III</sup>-Ph]Cl synthesis was followed. This reaction combined [Ph-I<sup>III</sup>-Ph]Cl (0.94 g, 2.99 mmol) and C<sub>6</sub>F<sub>5</sub>CO<sub>2</sub>Na (14.0 g, 59.8 mmol) and resulted in the desired oxidant as a white powder (0.898 g, 75% yield). <sup>1</sup>H NMR (d<sub>6</sub>-acetone): δ 8.22 (d, *J* = 6.4 Hz, 4H), 7.66 (t, *J* = 5.6 Hz, 2H), 7.53 (t, *J* = 6.4 Hz, 4H).



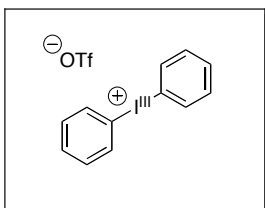
**Oxidant 17:** General procedure for [Ph-I<sup>III</sup>-Ph]Cl synthesis was followed. This reaction combined [Ph-I<sup>III</sup>-Ph]Cl (1.0 g, 3.15 mmol) and Cl<sub>3</sub>CCO<sub>2</sub>Na (11.7 g, 63 mmol) and resulted in the desired oxidant as a white powder (1.10 g, 79% yield). <sup>1</sup>H NMR (CDCl<sub>3</sub>): δ 7.95 (d, *J* = 8.0 Hz, 4H), 7.57 (t, *J* = 7.6 Hz, 2H), 7.43 (t, *J* = 7.6 Hz, 4H). This oxidant appears to have decomposed turning black within a week of its synthesis.



**Oxidant 18:** General procedure for [Ph-I<sup>III</sup>-Ph]Cl synthesis was followed. This reaction combined [Ph-I<sup>III</sup>-Ph]Cl (1.0 g, 3.15 mmol) and NaClO<sub>4</sub> (7.71 g, 63 mmol) and resulted in the desired oxidant as a white powder (1.20 g, 63% yield). <sup>1</sup>H NMR (d<sub>6</sub>-acetone): δ 8.37 (d, *J* = 6.0 Hz, 4H), 7.79 (t, *J* = 4.8 Hz, 2H), 7.64 (t, *J* = 7.2 Hz, 4H).



**Oxidant 19:** General procedure for [Ph-I<sup>III</sup>-Ph]Cl synthesis was followed. This reaction combined [Ph-I<sup>III</sup>-Ph]Cl (2.0 g, 6.3 mmol) and NaOTs (26.7 g, 126 mmol) and resulted in the desired oxidant as a white powder (1.23 mg, 43% yield). <sup>1</sup>H NMR (CDCl<sub>3</sub>): δ 7.94 (d, *J* = 8.0 Hz, 4H), 7.59-7.51 (multiple peaks, 4H), 7.38 (t, *J* = 7.5 Hz, 4H), 7.05 (d, *J* = 8.0 Hz, 2H), 2.31 (s, 3H).



**Oxidant 20:** General procedure for [Ph-I<sup>III</sup>-Ph]Cl synthesis was followed. This reaction combined [Ph-I<sup>III</sup>-Ph]Cl (2.0 g, 6.3 mmol) and NaOTf (26.7 g, 126 mmol) and resulted in the desired oxidant as a white powder (806 mg, 79% yield). <sup>1</sup>H NMR (CDCl<sub>3</sub>): δ 7.97 (d, *J* = 8.4 Hz, 4H), 7.64 (t, *J* = 7.2 Hz, 2H), 7.48 (t, *J* = 8.0 Hz, 4H). Employing the alternative literature synthesis: <sup>1</sup>H NMR (CDCl<sub>3</sub>): δ 7.98 (d, *J* = 8.5 Hz, 4H), 7.64 (t, *J* = 7.5 Hz, 2H), 7.49 (t, *J* = 8.0 Hz, 4H).<sup>24</sup>

**Counterion Effect Studies determined by Initial Rate:** Rate data for each oxidant [Mes-I-Ph]X was obtained using the initial rates method. The general procedure was used with [Mes-I-Ar]X (0.1 mmol), 3-methyl-2-phenylpyridine (8.46 mg, 8.0 mL, 0.05 mmol), and 0.5 mL of a standard solution containing (per aliquot) Pd(OAc)<sub>2</sub> (0.56 mg, 0.0025 mmol) and phenanthrene (internal standard) (4.46 mg, 0.025 mmol) in AcOH. Reactions were conducted at 80 °C, and each initial rate represents an average of three unique kinetics experiments. The initial rate for each oxidant is listed in **Scheme 3.11**.

**Intramolecular Kinetic Isotope Effect.** The intramolecular kinetic isotope effect was obtained using substrate **22**, which was synthesized via a three step sequence involving:

(i) Suzuki-Miyaura coupling of 2-bromo-3-methylpyridine with  $C_6D_5B(OH)_2$ ,<sup>60</sup> (ii) palladium-catalyzed ligand directed iodination<sup>62</sup>, and (iii) lithium/halogen exchange with n-BuLi, followed by a quench with deionized  $H_2O$ . Substrate **22** (50 mg, 0.289 mmol), [Mes-I<sup>III</sup>-Ph]BF<sub>4</sub> (236.7 mg, 0.577 mmol) and Pd(OAc)<sub>2</sub> (3.2 mg, 0.0143 mmol) were combined in acetic acid (3 mL) in a 20 mL vial. The vial was sealed with a Teflon lined cap, and the reaction was stirred at 80 °C for 18 h. The reaction mixture was filtered through a plug of Celite and then concentrated under vacuum. The resulting crude oil was dissolved in CH<sub>2</sub>Cl<sub>2</sub> and extracted with saturated aqueous NaHCO<sub>3</sub> (2 x 30 mL) and brine (1 x 30 mL). The organic layer was dried over MgSO<sub>4</sub>, filtered, and concentrated to afford an orange oil, which was purified by chromatography on silica gel ( $R_f = 0.2$  in 95% CH<sub>2</sub>Cl<sub>2</sub>/5% EtOAc). The product was obtained as a viscous yellow oil (60 mg, 83% yield). <sup>1</sup>H NMR (*d*<sub>6</sub>-benzene): δ 8.49 (d, *J* = 4.7 Hz, 1H), 7.48 (s, 0.29 H), 7.23 (d, *J* = 7.8 Hz, 2H), 7.00-6.87 (multiple peaks, 3H), 6.76 (d, *J* = 7.8 Hz, 2H), 6.63 (dd, *J* = 7.8, 4.7 Hz, 1H), 1.61 (s, 3H). The isotope effect was determined by comparison of the integration of the singlet at 7.48 ppm relative to the doublet of doublets at 6.63 ppm. The average ratio (over 2 runs) was  $0.29 \pm 0.1 : 1$ , resulting in a  $k_H/k_D = 2.5 \pm 0.2$  (0.71/0.29).

**Intermolecular Kinetic Isotope Effect with 3.** The intermolecular kinetic isotope effect was determined by studying the initial rate of reactions with 3-methyl-2-(*d*<sub>5</sub>-phenyl)pyridine and 3-methyl-2-(*H*<sub>5</sub>-phenyl)pyridine (**Scheme 3.12**). The general procedure was used with [Mes-I<sup>III</sup>-Ph]BF<sub>4</sub> (41.0 mg, 0.1 mmol), 3-methyl-2-(*d*<sub>5</sub>-phenyl)pyridine (8.71 mg, 8.0 μL, 0.05 mmol) or 3-methyl-2-(*H*<sub>5</sub>-phenyl)pyridine (8.46 mg, 8.0 μL, 0.05 mmol), and 0.5 mL of a standard solution containing (per aliquot) Pd(OAc)<sub>2</sub> (0.56 mg, 0.0025 mmol) and phenanthrene (internal standard) (4.46 mg, 0.025 mmol) in AcOH. Reactions were conducted at 80 °C, and each reported value of initial rate ( $\Delta[4]/\Delta t$ ) represents an average of three unique kinetics experiments. ( $\Delta[4]/\Delta t$ ) for **3** was determined to be  $14 \pm 1 \times 10^{-5}$  M/min and ( $\Delta[4-d_5]/\Delta t$ ) for **3** was determined to be  $13 \pm 1 \times 10^{-5}$  M/min.

**Intermolecular Kinetic Isotope Effect with 23.**

The intermolecular kinetic isotope effect was determined by studying the initial rate of reactions with **23** and **23-*d*** (Scheme 3.14). The general procedure was used with [Mes-<sup>III</sup>I-Ph]BF<sub>4</sub> (41.0 mg, 0.1 mmol), **23-*d*** (9.21 mg, 8.9 μL, 0.05 mmol) or **23** (9.17 mg, 0.05 mmol), and 0.5 mL of a standard solution containing (per aliquot) Pd(OAc)<sub>2</sub> (0.56 mg, 0.0025 mmol) and phenanthrene (internal standard) (4.46 mg, 0.025 mmol) in AcOH. Reactions were conducted at 80 °C, and each reported value of initial rate (Δ[**4**]/Δt) represents an average of three unique kinetics experiments. (Δ[**24**]/Δt) for **23** was determined to be  $27 \pm 3 \times 10^{-5}$  M/min and (Δ[**24**]/Δt) for **23-*d*** was determined to be  $24 \pm 2 \times 10^{-5}$ .

### 3.15 References

1. Ryabov, A. D. *Inorg. Chem.* **1987**, *26*, 1252-1260.
2. Bayler, A.; Canty, A. J.; Ryan, J. H.; Skelton, B. W.; White, A. H. *Inorg. Chem. Commun.* **2000**, *3*, 575-578.
3. Canty, A. J.; Rodemann, T. *Inorg. Chem. Commun.* **2003**, *6*, 1382-1384.
4. Canty, A. J.; Patel, J.; Rodemann, T.; Ryan, J. H.; Skelton, B. W.; White, A. H. *Organometallics* **2004**, *23*, 3466-3473.
5. Canty, A. J.; Rodemann, T.; Skelton, B. W.; White, A. H. *Inorg. Chem. Commun.* **2005**, *8*, 55-57.
6. Canty, A. J.; Rodemann, T.; Skelton, B. W.; White, A. H. *Organometallics* **2006**, *25*, 3996-4001.
7. Chaudhuri, P. D.; Guo, R.; Malinakova, H. C. *J. Organomet. Chem.* **2008**, *693*, 567-573.
8. Eberhard, M. R. *Org. Lett.* **2004**, *6*, 2125-2128.
9. Weck, M.; Jones, C. W. *Inorg. Chem.* **2007**, *46*, 1865-1875.
10. Kalyani, D.; Deprez, N. R.; Desai, L. V.; Sanford, M. S. *J. Am. Chem. Soc.* **2005**, *127*, 7330-7331.
11. Deprez, N. R.; Sanford, M. S. *J. Am. Chem. Soc.* **2009**, *131*, 11234-11241.
12. Kraatz, H.-B.; Van der Boom, M. E.; Ben-David, Y.; Milstein, D. *Isr. J. Chem.* **2001**, *41*, 163-171.
13. Hartwell, G. E.; Lawrence, R. V.; Smas, M. J. *J. Chem. Soc. D* **1970**, 912.
14. Ochiai, M.; Suefuji, T.; Miyamoto, K.; Shiro, M. *Chem. Commun.* **2003**, 1438-1439.
15. Zhdankin, V. V.; Kuposov, A. Y.; Yashin, N. V. *Tetrahedron Lett.* **2002**, *43*, 5735-5737.
16. Suefuji, T.; Shiro, M.; Yamaguchi, K.; Ochiai, M. *Heterocycles* **2006**, *67*, 391-397.
17. Weiss, R.; Seubert, J. *Angew. Chem., Int. Ed. Engl.* **1994**, *33*, 891-893.
18. Blanda, M. T.; Horner, J. H.; Newcomb, M. J. *Org. Chem.* **1989**, *54*, 4626-36.
19. Funasaki, N.; Ishikawa, S.; Neya, S. *Bull. Chem. Soc. Jpn.* **2002**, *75*, 719-723.

20. Fielding, L. *Tetrahedron* **2000**, *56*, 6151-6170.
21. Bisson, A. P.; Hunter, C. A.; Morales, J. C.; Young, K. *Chem.--Eur. J.* **1998**, *4*, 845-851.
22. Chen, D.-W.; Ochiai, M. *J. Org. Chem.* **1999**, *64*, 6804-6814.
23. McKillop, A.; Kemp, D. *Tetrahedron* **1989**, *45*, 3299-3306.
24. Kitamura, T.; Yamane, M.; Inoue, K.; Todaka, M.; Fukatsu, N.; Meng, Z.; Fujiwara, Y. *J. Am. Chem. Soc.* **1999**, *121*, 11674-11679.
25. Wang, D.-H.; Hao, X.-S.; Wu, D.-F.; Yu, J.-Q. *Org. Lett.* **2006**, *8*, 3387-3390.
26. Cai, G.; Fu, Y.; Li, Y.; Wan, X.; Shi, Z. *J. Am. Chem. Soc.* **2007**, *129*, 7666-7673.
27. Shi, Z.; Li, B.; Wan, X.; Cheng, J.; Fang, Z.; Cao, B.; Qin, C.; Wang, Y. *Angew. Chem., Int. Ed.* **2007**, *46*, 5554-5558.
28. Li, J.-J.; Giri, R.; Yu, J.-Q. *Tetrahedron* **2008**, *64*, 6979-6987.
29. Kirchberg, S.; Vogler, T.; Studer, A. *Synlett* **2008**, 2841-2845.
30. Zaitsev, V. G.; Daugulis, O. *J. Am. Chem. Soc.* **2005**, *127*, 4156-4157.
31. Chen, X.; Goodhue, C. E.; Yu, J.-Q. *J. Am. Chem. Soc.* **2006**, *128*, 12634-12635.
32. Chiong, H. A.; Pham, Q.-N.; Daugulis, O. *J. Am. Chem. Soc.* **2007**, *129*, 9879-9884.
33. Stille, J. K.; Lau, K. S. Y. *Acc. Chem. Res.* **1977**, *10*, 434-442.
34. Boele, M. D. K.; van Strijdonck, G. P. F.; de Vries, A. H. M.; Kamer, P. C. J.; de Vries, J. G.; van Leeuwen, P. W. N. M. *J. Am. Chem. Soc.* **2002**, *124*, 1586-1587.
35. Giri, R.; Chen, X.; Yu, J.-Q. *Angew. Chem., Int. Ed.* **2005**, *44*, 2112-2115.
36. Xia, J.-B.; You, S.-L. *Organometallics* **2007**, *26*, 4869-4871.
37. Desai, L. V.; Stowers, K. J.; Sanford, M. S. *J. Am. Chem. Soc.* **2008**, *130*, 13285-13293.
38. Stowers, K. J.; Sanford, M. S. *Org. Lett.* **2009**, *11*, 4584-4587.
39. Tong, X.; Beller, M.; Tse, M. K. *J. Am. Chem. Soc.* **2007**, *129*, 4906-4907.
40. Alexanian, E. J.; Lee, C.; Sorensen, E. J. *J. Am. Chem. Soc.* **2005**, *127*, 7690-7691.
41. Streuff, J.; Hoevelmann, C. H.; Nieger, M.; Muniz, K. *J. Am. Chem. Soc.* **2005**, *127*, 14586-14587.
42. Liu, G.; Stahl, S. S. *J. Am. Chem. Soc.* **2006**, *128*, 7179-7181.

43. Desai, L. V.; Sanford, M. S. *Angew. Chem., Int. Ed.* **2007**, *46*, 5737-5740.
44. Muniz, K.; Hoevelmann, C. H.; Streuff, J. *J. Am. Chem. Soc.* **2008**, *130*, 763-773.
45. Muniz, K. *J. Am. Chem. Soc.* **2007**, *129*, 14542-14543.
46. Li, Y.; Song, D.; Dong, V. M. *J. Am. Chem. Soc.* **2008**, *130*, 2962-2964.
47. Welbes, L. L.; Lyons, T. W.; Cychosz, K. A.; Sanford, M. S. *J. Am. Chem. Soc.* **2007**, *129*, 5836-5837.
48. Liu, H.; Yu, J.; Wang, L.; Tong, X. *Tetrahedron Lett.* **2008**, *49*, 6924-6928.
49. Yin, G.; Liu, G. *Angew. Chem., Int. Ed.* **2008**, *47*, 5442-5445.
50. Lyons, T. W.; Sanford, M. S. *Tetrahedron* **2009**, *65*, 3211-3221.
51. Tsujihara, T.; Takenaka, K.; Onitsuka, K.; Hatanaka, M.; Sasai, H. *J. Am. Chem. Soc.* **2009**, *131*, 3452-3453.
52. Thu, H.-Y.; Yu, W.-Y.; Che, C.-M. *J. Am. Chem. Soc.* **2006**, *128*, 9048-9049.
53. Kim, M.; Taylor, T. J.; Gabbai, F. P. *J. Am. Chem. Soc.* **2008**, *130*, 6332-6333.
54. Dick, A. R.; Kampf, J. W.; Sanford, M. S. *Organometallics* **2005**, *24*, 482-485.
55. Cotton, F. A.; Gu, J.; Murillo, C. A.; Timmons, D. J. *J. Am. Chem. Soc.* **1998**, *120*, 13280-13281.
56. Cotton, F. A.; Koshevoy, I. O.; Lahuerta, P.; Murillo, C. A.; Sanau, M.; Ubeda, M. A.; Zhao, Q. *J. Am. Chem. Soc.* **2006**, *128*, 13674-13675.
57. Powers, D. C.; Ritter, T. *Nat. Chem.* **2009**, *1*, 302-309.
58. Powers, D. C.; Geibel, M. A. L.; Klein, J. E. M. N.; Ritter, T. *J. Am. Chem. Soc.*, ACS ASAP.
59. Deprez, N. R.; Sanford, M. S. *Inorg. Chem.* **2007**, *46*, 1924-1935.
60. Littke, A. F.; Dai, C.; Fu, G. C. *J. Am. Chem. Soc.* **2000**, *122*, 4020-4028.
61. Shakespeare, W. C. *Tetrahedron Lett.* **1999**, *40*, 2035-2038.
62. Kalyani, D.; Dick, A. R.; Anani, W. Q.; Sanford, M. S. *Tetrahedron* **2006**, *62*, 11483-11498.



## Chapter 4

# Development of Direct C–H Arylation Reactions of Heterocycles and Simple Arenes

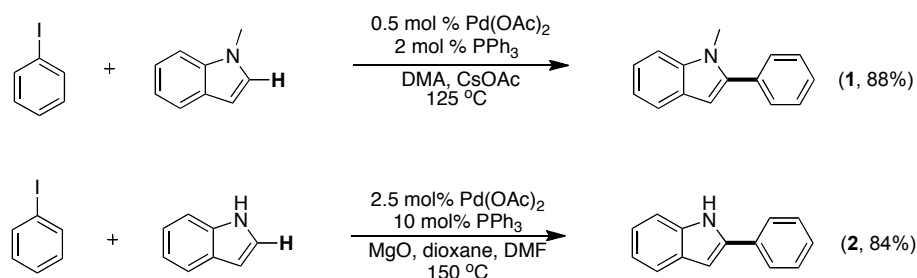
### 4.1 Background and Significance

This chapter describes the development of palladium catalyzed C–H arylation methodology for the functionalization of substrates lacking a ligand directing group. To render this approach synthetically useful, it is necessary to attain site selective functionalization in complex organic molecules containing ubiquitous C–H bonds. Our initial approach to overcoming this challenge was to take advantage of C–H bonds that have inherently different reactivities within a molecule. Thus, the focus of this work was to examine the C–H functionalization of  $sp^2$  bonds of heterocycles and simple arenes.

Indoles are a class of heterocycles that have different reactivity at specific sites on the indole ring. Due to the prevalence of the indole scaffold in many natural products, methods for functionalizing the 1, 2, and 3 positions selectively have been of interest.<sup>1</sup> In particular, the reactivity of indole toward electrophilic aromatic substitution make it an attractive substrate for arylation in the presence of an electrophilic  $Pd^{II}$  catalyst.<sup>2</sup> This concept was used by the Sames lab to develop methodology for the direct C–H arylation of indoles utilizing a palladium catalyst and aryl iodides (**Scheme 4.1**).<sup>3-5</sup> This chemistry allowed the installation of a variety of functionalized aryl groups with high selectivity for the C2 position of indoles (**1**, **2**) and a broad substrate scope. However, this methodology suffered from several key disadvantages. First, these reactions required elevated temperatures to efficiently provide the product ( $>120$  °C). Second, the C2 arylation of free N–H indoles required the addition of a strong base. Third, utilizing sterically hindered aryl iodides remains challenging due to competing arylation at the C3 position

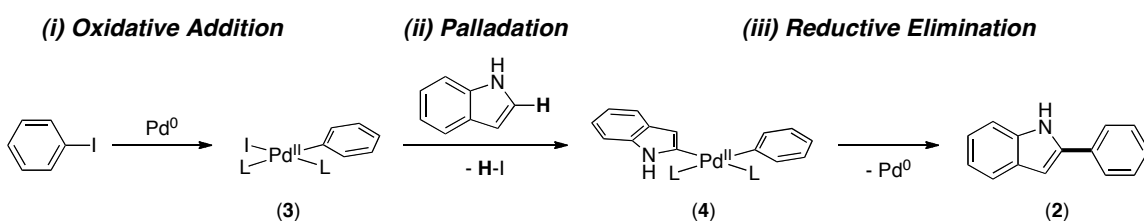
of the indoles. Finally, functional group compatibility is a concern with indole containing aryl halides and/or acidic protons, which can be reactive with low valent Pd and base.

**Scheme 4.1:** Sames' Precedent for C–H Arylation of Indole.<sup>3-5</sup>



Despite these disadvantages, the Sames reaction exploits the inherent nucleophilic reactivity of the nitrogen-containing ring of the indole and the electrophilic nature of Pd<sup>II</sup> to afford selective arylation (**Scheme 4.2**). The proposed mechanism is believed to involve: (i) oxidative addition of Ar–I to Pd<sup>0</sup> forming the Ar–Pd<sup>II</sup> intermediate **3**, (ii) electrophilic palladation of the indole resulting in the Pd<sup>II</sup> species **4**, (iii) C–C bond forming reductive elimination to provide the desired C2 arylation product and regenerate the Pd<sup>0</sup> catalyst.

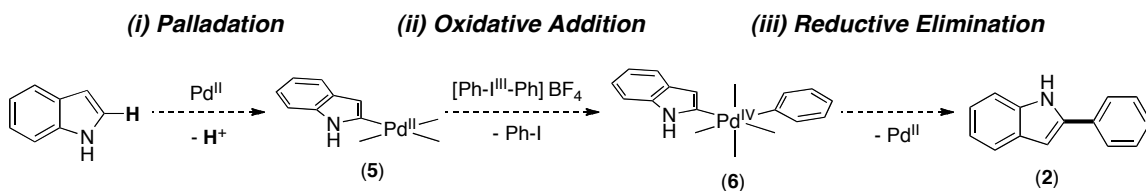
**Scheme 4.2:** Proposed Mechanism of Sames' Indole Arylation.



Analysis of this mechanism led us to propose an alternative indole C–H arylation pathway taking advantage of strategies used for the directed C–H arylation methodology in *Chapters 2 and 3*. In contrast to Sames' methodology, this reaction would employ [Ph–I<sup>III</sup>–Ph]<sup>+</sup> oxidants rather than aryl iodides and proceed through a Pd<sup>II/IV</sup> pathway (**Scheme 4.3**). The proposed mechanism would involve: (i) initial palladation of the indole at Pd<sup>II</sup> resulting in intermediate **5**, (ii) oxidation of the electron rich  $\sigma$ -indole-Pd<sup>II</sup> species **5** by

$[\text{Ph-I}^{\text{III}}\text{-Ph}]\text{BF}_4$  to afford  $\text{Pd}^{\text{IV}}$  intermediate **6**, and (iii) C–C bond forming reductive elimination to generate the C2 phenylated product **2** and release  $\text{Pd}^{\text{II}}$ .

**Scheme 4.3:** Proposed Mechanism of Indole Arylation with  $[\text{Ph-I}^{\text{III}}\text{-Ph}]\text{BF}_4$ .



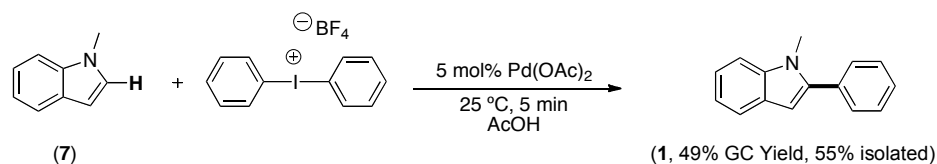
Several important distinctions can be made between the two mechanistic pathways that highlight the potential advantages of the proposed  $\text{Pd}^{\text{II/IV}}$  methodology. The first key difference is the ligand environment at the  $\text{Pd}^{\text{II}}$  species undergoing indole palladation. In the Sames methodology, palladation is rate determining and occurs at an electron rich  $\text{Pd}^{\text{II}}$  species containing a donating  $\sigma\text{-Ar}$  ligand. In contrast, the indole palladation for the proposed  $\text{Pd}^{\text{II/IV}}$  mechanism involves palladation at a more electron deficient  $\text{Pd}^{\text{II}}$  center, which should increase the relative rate of this step. This should allow for the proposed transformation to proceed under milder reaction conditions (<120 °C). Second, the new reaction would proceed via a  $\text{Pd}^{\text{II/IV}}$  catalytic cycle, which would address some of the challenges of the previously described methodology. For example, high oxidation state palladium species are known to be compatible with ambient moisture and atmosphere, eliminating the precautions necessary in  $\text{Pd}^{0/\text{II}}$  chemistry (i.e. special glassware, purification of solvents).<sup>6-15</sup> This pathway should also allow the tolerance of halogen functional groups as demonstrated in the chemistry of *Chapters 2 and 3*.<sup>16,17</sup>

## 4.2 Our Development of Indole Phenylation

Investigations began with the substrate *N*-methylindole (**7**), which was chosen for two reasons. First, **7** circumvents the possibility of *N*-arylation, which may occur with a free *N*-H indole. Second, the methyl group is electron donating, which increases the nucleophilicity of the indole and should facilitate its reaction with the electrophilic  $\text{Pd}^{\text{II}}$ . Initial reactions were conducted under conditions similar to those developed for the directed chemistry, and included a  $\text{Pd}(\text{OAc})_2$  catalyst and the  $[\text{Ph-I}^{\text{III}}\text{-Ph}]\text{BF}_4$  oxidant.

Gratifyingly, the reaction of 1 equiv of **7** with 2 equiv of  $[\text{Ph-I}^{\text{III}}\text{-Ph}]\text{BF}_4$  (2 equiv) and 5 mol % of  $\text{Pd}(\text{OAc})_2$  provided exclusively the C2 phenylation product **1** in 49% yield based on GC by comparison to an internal standard (**Scheme 4.4**). Notably, this reaction took place at room temperature, a substantial improvement on literature examples that require much higher temperature ( $>120\text{ }^\circ\text{C}$ ). This result supports the hypothesis that a  $\text{Pd}^{\text{II/IV}}$  mechanistic pathway should occur under more mild reaction conditions due to the increased rate of palladation. Completing this reaction on a larger scale (1.0 mmol) confirmed the results from the GC analysis and afforded the desired product in 55% isolated yield.

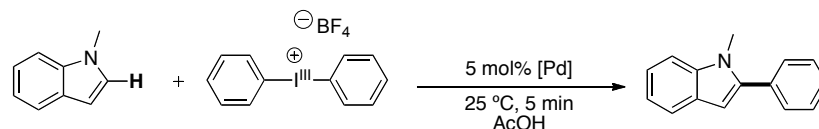
**Scheme 4.4:**  $\text{Pd}(\text{OAc})_2$ -Catalyzed Phenylation of *N*-Methylindole.



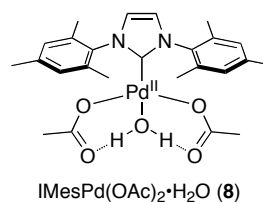
Several observations were made during these initial experiments that aided in further development of this methodology. First, the reaction proceeded to approximately 50% yield, but the remainder of material could not be accounted for. Second, the reaction progressed to maximum conversion in ca. 5 min. It was reasoned that attenuating the reactivity of the palladium by changing the ancillary ligands might lead to higher yields and provide improved mass balance. Thus, a catalyst screen was conducted with 1 equiv of *N*-methyl indole (**7**), 2 equiv of  $[\text{Ph-I}^{\text{III}}\text{-Ph}]\text{BF}_4$  and 5 mol % of a variety of palladium catalysts (**Table 4.1**). This experiment revealed that the catalyst  $\text{IMesPd}(\text{OAc})_2\cdot\text{H}_2\text{O}$  (**8**) bearing the IMes (1,3-Bis(2,4,6-trimethylphenyl)imidazole) N-heterocyclic carbene (NHC) ligand provided the product in an improved yield (80%) relative to catalysts containing traditional halide and carboxylate ligands. The synthesis of this catalyst will be further discussed (*vide infra*). Empirically, a large difference in reaction rate was apparent between  $\text{Pd}(\text{OAc})_2$  and the NHC complex **8**. It was observed that the reaction with **7** required 18 h for complete conversion (80% yield), while the analogous reaction with  $\text{Pd}(\text{OAc})_2$  went to complete conversion (49% yield) in approximately 5 min. The

increased yield is likely due to stabilization of the palladium by the NHC ligand, which limits decomposition of the catalyst. The NHC ligand is also electron donating, providing a more electron rich palladium center. This is expected to decrease the relative rate of electrophilic indole palladation relative to the use of more electron deficient Pd(OAc)<sub>2</sub>.

**Table 4.1:** Catalyst Screening for Pd-Catalyzed Phenylation of Indole.



Catalyst	GC Yield*
PdI <sub>2</sub>	20%
Pd(OAc) <sub>2</sub>	49%
PdBr <sub>2</sub>	58%
Pd(tfa) <sub>2</sub>	59%
PdCl <sub>2</sub>	59%
PdCl <sub>2</sub> (BnCN) <sub>2</sub>	64%
Na <sub>2</sub> PdCl <sub>4</sub>	66%
IMesPd(OAc) <sub>2</sub> ·H <sub>2</sub> O	80%



Conditions: 1 equiv *N*-methylindole, 2 equiv [Ph-I<sup>III</sup>-Ph]BF<sub>4</sub>, 5 mol % [Pd], AcOH (0.1M) rt, \*Based on comparison to an internal standard

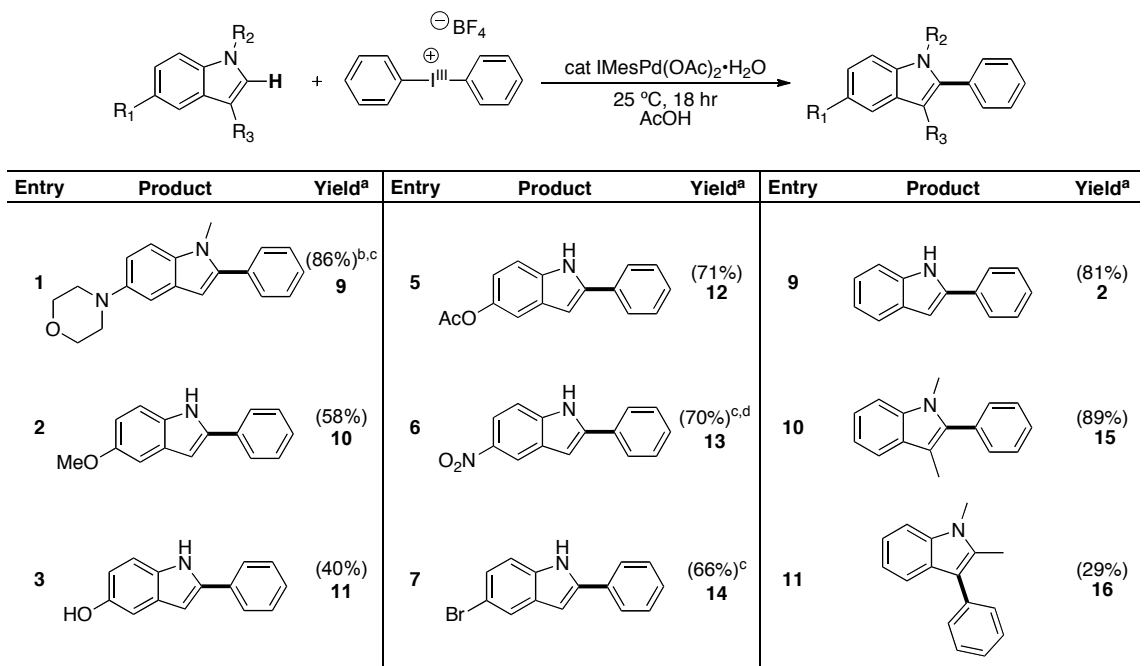
The reaction with catalyst **8** was examined on a larger scale to compare the isolated yield and the GC yield. This was completed by combining 1 equiv of *N*-methylindole (**7**) with 3 equiv of [Ph-I<sup>III</sup>-Ph]BF<sub>4</sub> and 5 mol % catalyst **8** in AcOH at room temperature for 18 h. This afforded the desired product **1** in 86% isolated yield, confirming the results obtained by GC.

### 4.3 Scope of Indole Phenylation

Efforts next turned to exploring the scope of this methodology by employing indoles that contain differing electronic properties and functional groups. A variety of indoles successfully yielded C2 arylation products with catalyst **8** (**Table 4.2**). This transformation proceeded efficiently with indoles containing both electron donating (**9-11**) and electron withdrawing substituents (**12-14**) at the 5 position. The electron

deficient indole **14** required a slightly higher temperature (60 °C) to attain acceptable yields. The even more electron deficient 5-nitro-*N*-methyl indole **13** suffered from the same challenges and required a higher catalyst loading (10 mol %) and more oxidant (6 equiv), in addition to the higher temperature to achieve a more reasonable yield (78%). Due to challenges separating the product from small amounts of starting material, elevated temperature and catalyst loadings were also employed to access product **9**.

**Table 4.2:** Scope of Pd-Catalyzed Phenylation of Indoles.



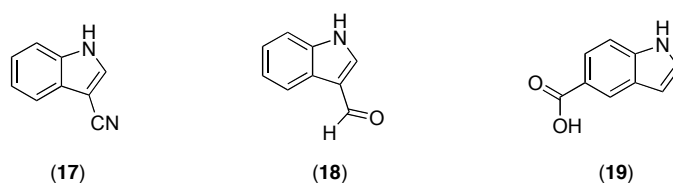
<sup>a</sup> Conditions: 1.0 equiv substrate, 2.0 equiv [Ph-I<sup>III</sup>-Ph]BF<sub>4</sub>, 5 mol % **8** in AcOH (0.1M) for 18 hr, <sup>b</sup> 10 mol % catalyst used, <sup>c</sup> Reactions carried out at 60 °C, <sup>d</sup> 6 equiv of [Ph-I<sup>III</sup>-Ph]BF<sub>4</sub> used

In addition to *N*-methyl indoles, free *N*-H indoles were selectively phenylated at the C2 position in good isolated yields without detectable *N*-arylation (**2**, **10–14**). The phenylation product **11** was obtained in modest yield in the presence of an unprotected alcohol without *O*-arylation or alcohol oxidation. Phenylation of an indole containing an aryl-bromide was achieved in good yield (66%), without affecting the aryl-bromide functionality (**14**). Substitution of a CH<sub>3</sub> group at the 3 position of indole with a methyl group did not adversely affect the reaction and resulted in the desired C2 arylation product in excellent yield (**15**, 89%). Finally, we probed how phenylation would be affected by blocking the C2 position of indole. With 2-methylindole, functionalization

occurred at the C3 position to give **16** in a 29% yield. The remaining material was an inseparable mixture of unreacted starting material and a high molecular weight byproduct.

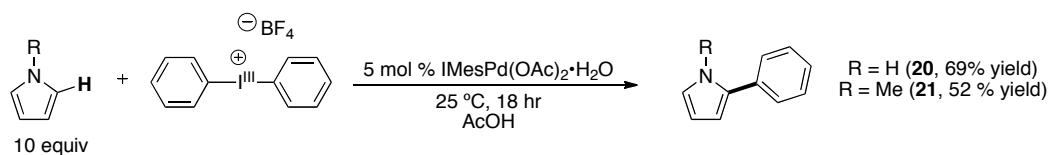
A number of substrates did not provide the desired C–H phenylation products (**Figure 4.1**). Substrates **17** and **18** did not react to afford observable phenylation products by GCMS under the conditions described above, or at elevated temperature (60 °C). This is likely due to the electron withdrawing ability of the CN and CHO, which is that are expected to deactivate the indole. Substrate **19** also did not provide phenylation products under the optimized conditions even at elevated temperatures (25–100 °C). However the starting material was completely consumed, suggesting that decomposition of the indole is likely occurring under the reaction conditions.

**Figure 4.1:** Indoles Unsuccessful for C–H Phenylation.



This strategy was also found to be applicable to the C–H arylation of pyrroles. The largest difference between pyrrole and indole is the possibility of diphenylation. Pyrrole and *N*-methyl-pyrrole were each successfully phenylated at the 2-position by combining 10 equiv of each substrate with 1 equiv of [Ph–I<sup>III</sup>–Ph]BF<sub>4</sub> and 5 mol % of the catalyst **8** to afford the desired products **20** and **21** in 69% and 52%, yields respectively. Selective mono-phenylation required the use of the oxidant as the limiting reagent.

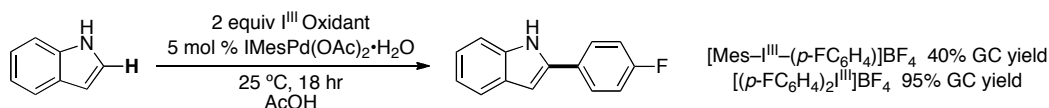
**Scheme 4.5:** Pd-Catalyzed Phenylation of Pyrroles.



## 4.4 Scope of Indole Arylation

Expanding the general applicability of this transformation required conditions that allowed the installation of a diverse set of aryl groups. We have already demonstrated that a variety of  $[\text{Ar-I}^{\text{III}}-\text{Ar}]\text{X}$  species are synthetically accessible and versatile arylating reagents.<sup>17,18</sup> Indole C–H arylations were first attempted using  $[\text{Mes-I}^{\text{III}}-\text{Ar}]\text{BF}_4$  oxidants that were effective for directed C–H arylation in *Chapters 2* and *3*. These arylations were conducted by combining 1 equiv of indole with 2 equiv  $[\text{Mes-I}^{\text{III}}-(p\text{-FC}_6\text{H}_4)]\text{BF}_4$  and 5 mol % **8** in AcOH. This resulted in the C2 arylation product in only a 40% yield by GC based on uncorrected peak areas of starting materials and products (**Scheme 4.6**). However, employing the symmetric oxidant  $[(p\text{-FC}_6\text{H}_4)_2\text{I}^{\text{III}}]\text{BF}_4$  under the same conditions and this led to a much-improved 95% yield based on uncorrected peak areas of starting materials and products. The addition of an uncalibrated internal standard indicated decreased mass balance using the  $[\text{Mes-I}^{\text{III}}-(p\text{-FC}_6\text{H}_4)]\text{BF}_4$  oxidant. This likely suggests the formation of products that cannot be observed by GC.

**Scheme 4.6:** Comparison of  $\text{I}^{\text{III}}$  Oxidants for Pd-Catalyzed Indole Phenylation.

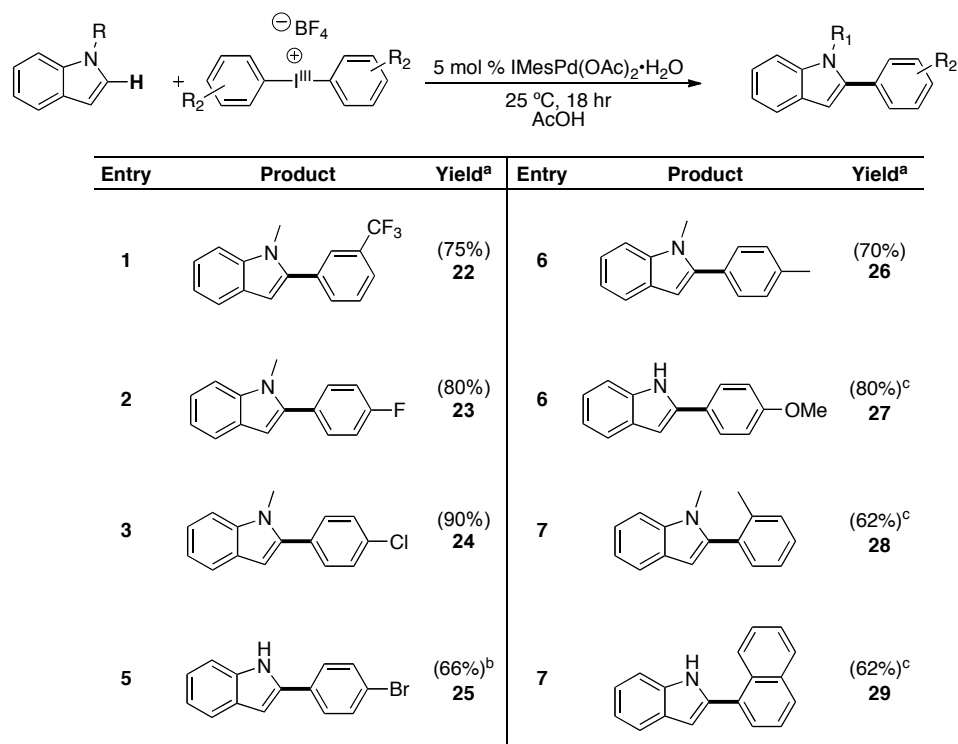


This protocol for the C–H arylation of indoles was next expanded to a variety of substituted  $\text{I}^{\text{III}}$  reagents (**Table 4.3**). This included the selective C2 installation of arenes containing both electron-withdrawing groups (**22–25**) and electron donating groups (**26–28**). Installation of the aryl-bromide in product **25** required an elevated reaction temperature (60 °C) due to the insolubility of the oxidant at room temperature in AcOH. Similarly the reaction of indole with the electron rich  $[(p\text{-OMeC}_6\text{H}_4)_2\text{I}^{\text{III}}]\text{BF}_4$  reagent to afford product **27** also required more forcing conditions (80 °C) due to the attenuated reactivity of this oxidant. In general these reactions showed similar functional group tolerance to the analogous phenylations. This included the selective C2 arylation of free N–H indoles without competing N-arylation. The installation of several aryl halides was



also demonstrated, and these groups were unaffected by the reaction conditions. Once again, this demonstrates the complementarity of this methodology to Pd<sup>0/II</sup> chemistry.

**Table 4.3:** Scope of Pd–Catalyzed Indole Arylation.

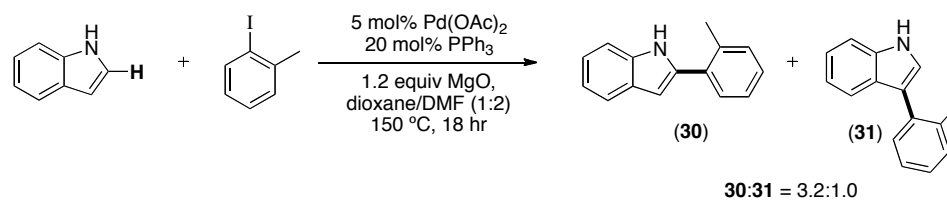


<sup>a</sup> Conditions: 1.0 equiv substrate, 2.0 equiv [Ph–I<sup>III</sup>–Ph]BF<sub>4</sub>, 5 mol % **8** in AcOH (0.1M) for 18 hr,

<sup>b</sup> Reaction carried out at 80 °C, <sup>c</sup> Reactions carried out at 60 °C

Installation of sterically hindered aryl groups also proceeded with high selectivity for the C2 position, which is in contrast to Sames' Pd<sup>0/II</sup> catalyzed reactions. For example, installation of an *o*-tolyl group proved challenging in the Pd<sup>0/II</sup> chemistry and provided mixtures of the C2 and C3 functionalized products in a ratio of 3.2 : 1.0 (**30** : **32**, **Scheme 4.7**).<sup>4</sup> In contrast, the reaction of *N*-methylindole with [(*o*-tol)<sub>2</sub>I<sup>III</sup>]BF<sub>4</sub> afforded the arylated product in >20:1 selectivity (**28**). Similar selectivity was also demonstrated with the sterically hindered [(1-naphthyl)<sub>2</sub>I<sup>III</sup>]BF<sub>4</sub> oxidant, providing **29** as the only detectable regioisomer. The nature of these differences in selectivity compared to the Pd<sup>0/II</sup> chemistry will be further discussed in the context of mechanistic investigations.

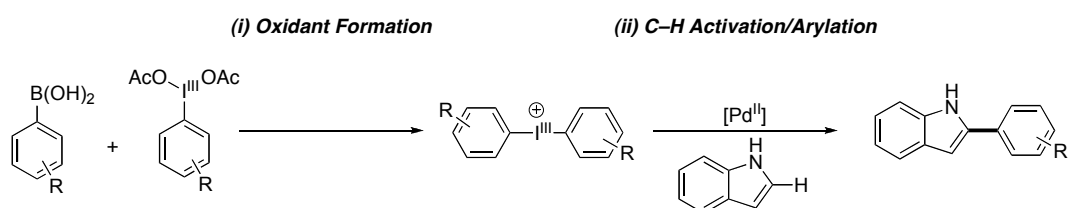
**Scheme 4.7:** C2/C3 Selectivity for Installation of *o*-Tolyl Group Using Pd<sup>0/II</sup> Catalysis.<sup>4</sup>



#### 4.5 *In Situ* Oxidant Generation for Pd-Catalyzed Indole Arylation

To increase the utility of this methodology, *in situ* formation of the arylating reagent prior to C–H functionalization is appealing. This concept was previously discussed in the context of the directed C–H arylation (*Chapter 2*). To accomplish this, a reaction sequence would require first coupling of a boronic acid (step (i), **Scheme 4.8**) and I<sup>III</sup> reagent, followed by C–H arylation (step (ii), **Scheme 4.8**).

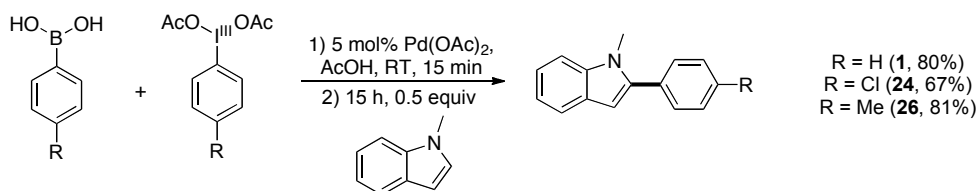
**Scheme 4.8:** Strategy for *in situ* Oxidant Generation/C–H Arylation.



These experiments were completed analogously to those previously described in the directed chemistry, with the exception of substrate and temperature. Thus, 2 equiv of ArI<sup>III</sup>(OAc)<sub>2</sub> and 2 equiv of ArB(OH)<sub>2</sub> were combined with 5 mol % of Pd(OAc)<sub>2</sub> in AcOH and allowed to stir at room temperature for 15 min. Next, *N*-methylindole (**7**) was added and the reaction continued for 17 h at room temperature. My colleague Dr. Dipannita Kalyani demonstrated that this method was effective for installing several aryl groups at the C2 position of indole, including Ph (**1**, 80%), *p*-ClC<sub>6</sub>H<sub>4</sub> (**24**, 67%), and *p*-MeC<sub>6</sub>H<sub>4</sub> (**26**, 81%) (**Scheme 4.9**).

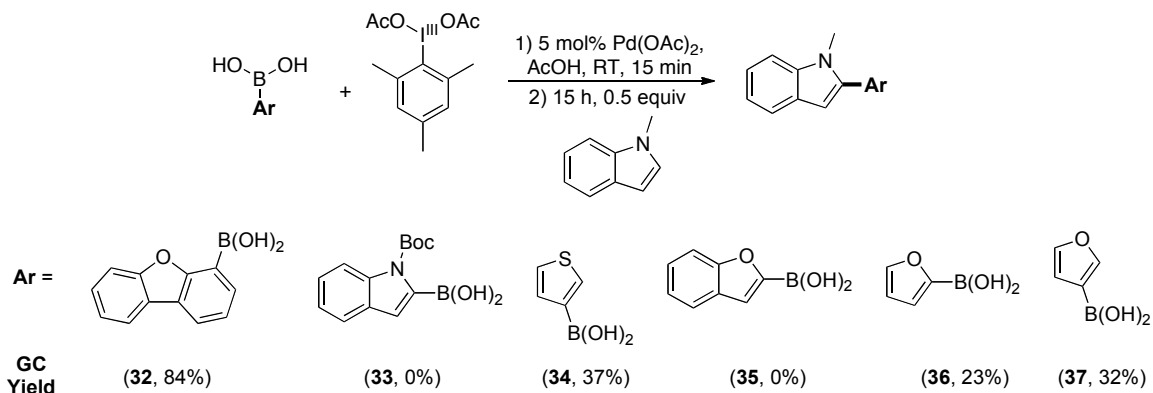
Importantly, the yields were comparable to those obtained with the pre-isolated oxidants (86%, 90%, and 70% respectively). The use of  $\text{MeI}^{\text{III}}(\text{OAc})_2$  also resulted in the C2 arylation products in useful GC yields of 44%, 39%, and 62% respectively.

**Scheme 4.9:** *In situ* Oxidant Generation/C–H Arylation with Substituted Arenes.



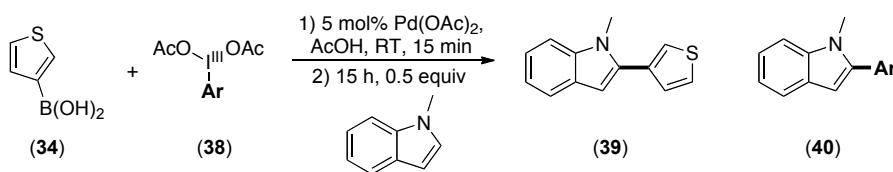
We next sought to develop this strategy for the installation of a variety of heteroaryl groups at the C2 position of indoles. This was accomplished by employing several commercially available boronic acids with the protocol for *in situ* oxidant generation. This led to the formation of heteroarylated products as detected by GCMS (**Scheme 4.10**). Both thiophene (**34**) and furan (**32**, **35**, **36**, **37**) analogs were successfully incorporated, but in modest yields based on uncorrected GC ratios. Notably **32** appears have gone to a higher conversion based on GC yield. However, since GC peak areas correlate with the number of carbons in a molecule, and a very a large arene has been added to the indole, this analysis becomes less representative of an actual yield for this product.

**Scheme 4.10:** *In situ* Oxidant Employing Heteroarenes.



These poor yields were not surprising given that employing the isolated [Mes-I<sup>III</sup>-Ar]BF<sub>4</sub> oxidants in indole arylation led to lower conversions relative to [Ar-I<sup>III</sup>-Ar]BF<sub>4</sub>. However in this case, the symmetric oxidants are not as practical because they would require 1 equiv of sacrificial heteroaryl iodide (which are more valuable molecules). Thus, we next set out to identify an alternative ‘dummy’ I<sup>III</sup> coupling partner that would offer increased reactivity versus the mesityl group. To probe this, the standard reaction conditions were used with ArI<sup>III</sup>(OAc)<sub>2</sub> (**38**) where Ar is Ph, 1-naphthyl, *p*-MeOC<sub>6</sub>H<sub>4</sub>, and *p*-ClC<sub>6</sub>H<sub>4</sub> (**Table 4.4**). As expected, when Ar was Ph or *p*-ClC<sub>6</sub>H<sub>4</sub>, products resulting from competitive addition of the desired 3-thiophene (**39**) and the Ar group (**40**) were observed. It was reasoned however, that 1-naphthyl would allow for steric selectivity, while *p*-MeOC<sub>6</sub>H<sub>4</sub> would allow for electronic control based on the observed selectivity in related reactions.<sup>17,18</sup> However, unfortunately these latter two oxidants also gave a mixture of arene addition products.

**Table 4.4:** Screen of I<sup>III</sup> Regents for *in situ* Oxidant Generation Employing Heteroarenes.



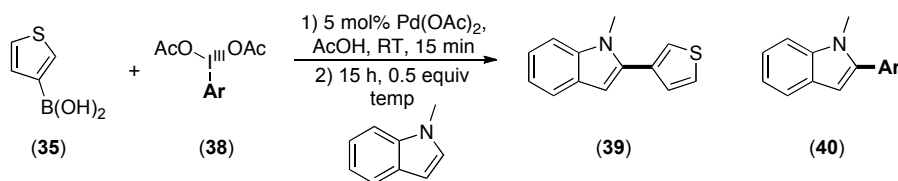
Ar =	Thiophene GC Yield (X)*	Arene GC Yield (X)*
Ph	30%	14%
1-naphthyl	40%	32%
<i>p</i> -OMePh	30%	58%
<i>p</i> -ClPh	25%	9%

Conditions: 2 equiv 3-thiophene boronic acid, 2 equiv ArI<sup>III</sup>(OAc)<sub>2</sub>, 5 mol % Pd(OAc)<sub>2</sub>, were stirred at rt for 15 min in AcOH (0.1M), then 1 equiv *N*-methylindole was added and remainted at rt \*Based on uncorrected GC peak areas

Despite the limited success employing alternative ‘dummy’ ligands on the I<sup>III</sup> reagent, we chose to further investigate (1-naphthyl)I<sup>III</sup>(OAc)<sub>2</sub> along with MesI<sup>III</sup>(OAc)<sub>2</sub> at various temperatures (**Table 4.5**). When these reactions were completed with (1-

naphthyl)I<sup>III</sup>(OAc)<sub>2</sub> no improvement in yield was attained; however an increased yield of C–H arylation with the naphthyl ‘dummy ligand’ was observed. An increase in temperature using MesI<sup>III</sup>(OAc)<sub>2</sub> resulted in higher yield based on GC, without the installation of mesityl. However, it is believed these yields are misrepresentative, due to decomposition of the starting material at this temperature to afford products that cannot be observed by GC. Nevertheless this reaction was completed on a larger scale, and resulted in the isolation of the desired product **39** in a 20% yield (**Scheme 4.11**).

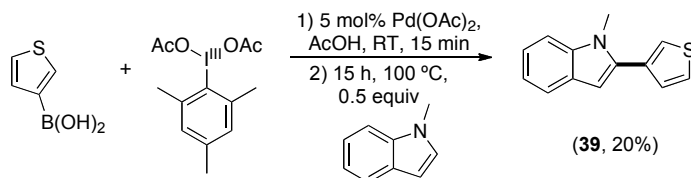
**Table 4.5:** Screen of Temperature for *in situ* Oxidant Employing Heteroarenes.



Ar	Temperature	Thiophene GC Yield (X)*	Arene GC Yield (X)*
1-naphthyl	13 °C	20%	34%
1-naphthyl	25 °C	17%	31%
1-naphthyl	45 °C	26%	50%
1-naphthyl	75 °C	30%	56%
Mes	13 °C	22%	0%
Mes	25 °C	32%	0%
Mes	45 °C	48%	0%
Mes	75 °C	51%	0%
Mes	100 °C	73%	0%

Conditions: 2 equiv 3-thiophene boronic acid, 2 equiv Ar<sup>III</sup>(OAc)<sub>2</sub>, 5 mol % Pd(OAc)<sub>2</sub>, were stirred at rt for 15 min in AcOH (0.1M), then 1 equiv *N*-methylindole was added at heated, \*Based on uncorrected GC peak areas

**Scheme 4.11:** *In situ* Arylation with 3-Thiophene Boronic Acid.

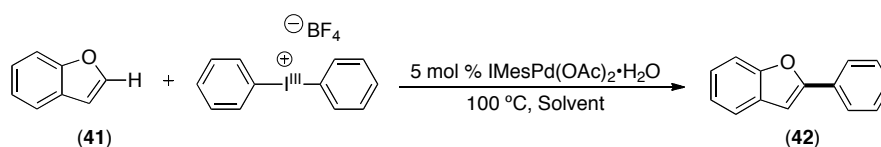


Investigations toward the development of an *in situ* oxidant generation followed by sequential C–H arylation have proved promising. This method has been established for the selective C2 arylation of indoles using substituted I<sup>III</sup> reagents and their complementary boronic acid. Expansion to the installation of heteroarenes has led to encouraging preliminary results, but further optimizations are required to improve yields.

#### 4.6 Expansion to Other Heterocycles

A variety of heterocycles similar to indole and pyrrole were attempted for palladium catalyzed C–H arylation. First, the phenylation of benzofuran (**41**) catalyzed by **8** was examined as a function of solvent. This reaction provided a single phenylation product **42** at 100 °C (as determined by GCMS). A solvent study revealed that several solvents were viable for this substrate, with the most successful being AcOH, trifluorotoluene, CHCl<sub>3</sub>, and ClCH<sub>2</sub>CH<sub>2</sub>Cl (**Table 4.6**).

**Table 4.6:** Solvent Effects on the Arylation of Benzofuran.



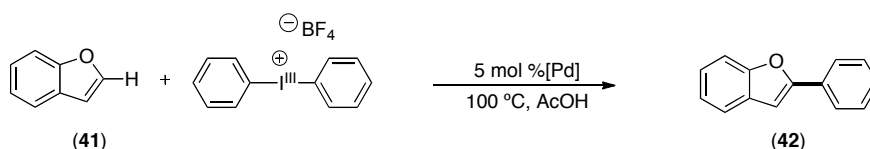
Solvent	GC Yield*
AcOH	60%
NO <sub>2</sub> Ph	39%
CF <sub>3</sub> Ph	57%
THF	17%
CHCl <sub>3</sub>	53%
CH <sub>3</sub> CN	0%
Acetone	24%
MeOH	0%
ClCH <sub>2</sub> CH <sub>2</sub> Cl	50%

Conditions: 1 equiv benzofuran, 2 equiv [Ph–I<sup>III</sup>–Ph]BF<sub>4</sub>, Pd(OAc)<sub>2</sub>, Solvent (0.1M) at 100 °C for 12 hr, \*Based on uncorrected GC peak areas

We next examined benzofuran phenylation as a function of palladium catalyst, since large catalyst effects were observed for indole arylation. A number of palladium complexes were viable catalysts for this transformation, with the most promising being

PdBr<sub>2</sub> and Pd(tfa)<sub>2</sub> (**Table 4.7**). This reaction was conducted on a large scale (1.0 mmol) to isolate the desired product. To do this, 1 equiv of benzofuran **41** was combined with 2 equiv of [Ph-I<sup>III</sup>-Ph]BF<sub>4</sub>, and 5 mol % of Pd(tfa)<sub>2</sub> in AcOH at 100 °C to afford the desired product (**42**) in 65% isolated yield (**Scheme 4.12**). Comparisons of <sup>1</sup>H NMR spectrum of the isolated product with reported literature values demonstrated that the phenylation occurred selectively at the C2 position.<sup>19,20</sup>

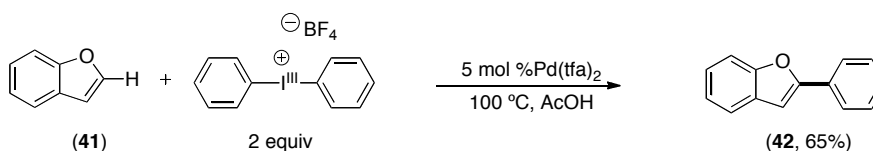
**Table 4.7:** Catalyst Effects on the Arylation of Benzofuran.



Catalyst	GC Yield
Pd(OAc) <sub>2</sub>	60%
PdCl <sub>2</sub>	64%
PdBr <sub>2</sub>	80%
PdI <sub>2</sub>	50%
Pd(tfa) <sub>2</sub>	78%
(PhCN) <sub>2</sub> PdCl <sub>2</sub>	0%
(SEt <sub>2</sub> ) <sub>2</sub> PdCl <sub>2</sub>	7%
(PPh <sub>3</sub> ) <sub>2</sub> PdCl <sub>2</sub>	60%
NaPdCl <sub>4</sub>	56%
IMesPd(OAc) <sub>2</sub> ·H <sub>2</sub> O	69%

Conditions: 1 equiv benzofuran, 2 equiv [Ph-I<sup>III</sup>-Ph]BF<sub>4</sub>, 5 mol % [Pd], AcOH (0.1M) at 100 °C for 12 hr, \*Based on uncorrected GC peak areas

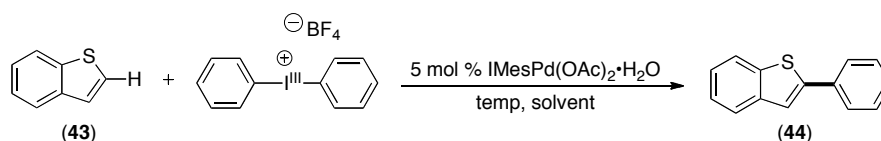
**Scheme 4.12:** Pd-Catalyzed Arylation of Benzofuran.



In addition to substituting the heteroatom for oxygen, sulfur was also employed. Less extensive screening was completed for benzothiophene (**43**), but began with a brief temperature study (**Table 4.8**). Benzothiophene was employed at several different

temperatures under the conditions identified for indole arylation. It was observed that increasing the temperature led to improved yields of a single arylation product (as determined by GCMS) (81% yield at 120 °C). A solvent screen demonstrated that nitrobenzene worked well for the desired phenylation. This reaction was completed on a larger scale (1 mmol) with 1 equiv of benzothiophene (**43**), 2 equiv of [Ph-I<sup>III</sup>-Ph]BF<sub>4</sub> and 5 mol % of I MesPd(OAc)<sub>2</sub>•H<sub>2</sub>O in NO<sub>2</sub>Ph at 120 °C to afford the desired product **44** in a 61% isolated yield (95% purity by GC, **Scheme 4.13**). The regioselectivity of phenylation could not be confirmed by <sup>1</sup>H NMR based on comparisons to reported values, due to similarities in spectra of 2- and 3-phenyl-benzothiophenes.<sup>20,21</sup>

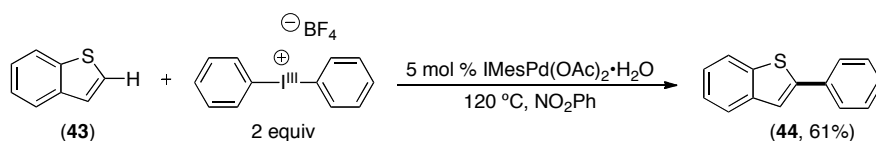
**Table 4.8:** Solvent Effects for the Pd-Catalyzed Arylation of Benzothiophene.



Temp	Solvent	GC Yield*
25 °C	AcOH	0%
80 °C	AcOH	38%
100 °C	AcOH	50%
120 °C	AcOH	81%
120 °C	NO <sub>2</sub> Ph	91%
120 °C	CF <sub>3</sub> Ph	6%

Conditions: 1 equiv benzothiophene, 2 equiv [Ph-I<sup>III</sup>-Ph]BF<sub>4</sub>, Pd(OAc)<sub>2</sub>, Solvent (0.1M) at respective temp for 12 hr, \*Based on uncorrected GC peak areas

**Scheme 4.13:** Pd-Catalyzed Arylation of Benzothiophene.

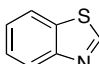
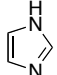
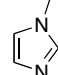
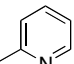
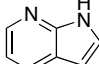
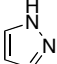
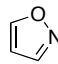
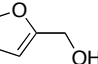


In contrast to the examples above, **Table 4.9** highlights a group of substrates for which phenylation was unsuccessful. These phenylations were attempted under a variety of reaction conditions including variation of temperature ( $\geq 60$  °C) and solvent, but did not result in the addition of a phenyl group. A common feature of most of these substrates



is that they contain a Lewis basic nitrogen functionality that is likely affecting this reaction in two ways (**Table 4.9** entries 1–7). First, Lewis bases are problematic since the mechanism of this reaction relies on nucleophilic attack by an electron rich arene on a Lewis acidic Pd<sup>II</sup>. The Lewis basic functional groups can coordinate to the palladium, making it less electrophilic and thereby preventing nucleophilic attack by the heterocycles. Furthermore, the favorability for Lewis basic nitrogen heterocycles to coordinate to [Ph-I<sup>III</sup>-Ph]BF<sub>4</sub> resulting in an N-I<sup>III</sup> adduct has previously been demonstrated.<sup>17,22-25</sup> This interaction will decrease the electrophilicity of the oxidant and therefore its reactivity towards oxidation of Pd<sup>II</sup> to Pd<sup>IV</sup>. The last substrate that did not prove successful was furfuryl alcohol (**Table 4.9**, entry 8). This is likely due to oxidation and polymerization under the reaction conditions. Thus, this group of substrates has demonstrated the limitations of this methodology and presents a challenge to be overcome with future investigations.

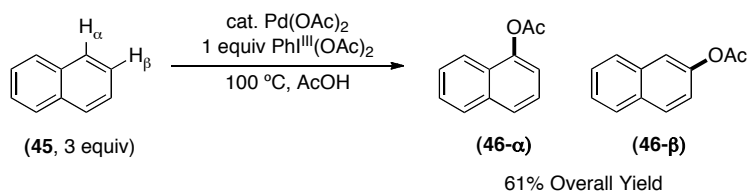
**Table 4.9:** Substrates Unsuccessful in Pd-Catalyzed C–H Phenylation.

Entry	Substrate	Entry	Substrate	Entry	Substrate	Entry	Substrate
1		3		5		7	
2		4		6		8	

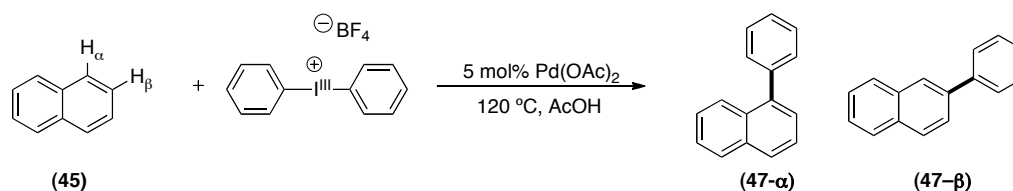
#### 4.7 Expansion to Non-Heterocyclic Substrates

Due to the success achieved with heterocycles, the reactivity of simple unactivated arenes was next probed. Previously, Crabtree had demonstrated C–H acetoxylation of a number of simple arenes with PhI<sup>III</sup>(OAc)<sub>2</sub> as the oxidant.<sup>26</sup> For example, it was reported that 3 equiv of naphthalene (**45**) combined with 0.5 mol % of Pd(OAc)<sub>2</sub> and 1 equiv of PhI<sup>III</sup>(OAc)<sub>2</sub> in AcOH at 100 °C resulted in **46-α** and **46-β** in a 61% overall yield based on oxidant, and in a ratio of 57:43. All of Crabtree's acetoxylation experiments were completed with excess substrate, and oxidant as the limiting reagent of the reaction.

**Scheme 4.14:** Crabtree's Acetoxylation of Naphthalene.<sup>26</sup>



By analogy, our initial experiments focused on naphthalene C–H phenylation and began by probing the effect of excess substrate relative to oxidant. This was completed by combining 2, 5, 10, and 20 equiv of naphthalene (**45**) with 1 equiv of [Ph–I<sup>III</sup>–Ph]BF<sub>4</sub> and 5 mol % of Pd(OAc)<sub>2</sub> in AcOH (0.1 M in naphthalene) and heated to 120 °C. Analysis of these reactions by GCMS provided several interesting results (**Table 4.10**). First, this study demonstrated that higher conversion is achievable with large excesses of substrate relative to limiting oxidant. Second, two peaks were observed in each reaction, with a mass corresponding to the two regioisomers **47-α** and **47-β**. Each reaction favored phenylation at the α position in >5:1 ratio as determined by comparison to an authentic sample. This is particularly interesting given that Crabtree had observed a statistical mixture of the α and β products for the acetoxylation using PhI<sup>III</sup>(OAc)<sub>2</sub>. The nature of the observed selectivity for naphthalene phenylation is not understood, and mechanistic investigations will be required to provide more insight.

**Table 4.10:** Naphthalene Phenylation Equivalents Study.

Equivalents	GC Yield*	$\alpha : \beta$
2	11%	10 : 1
5	23%	9 : 1
10	50%	6 : 1
20	55%	5 : 1

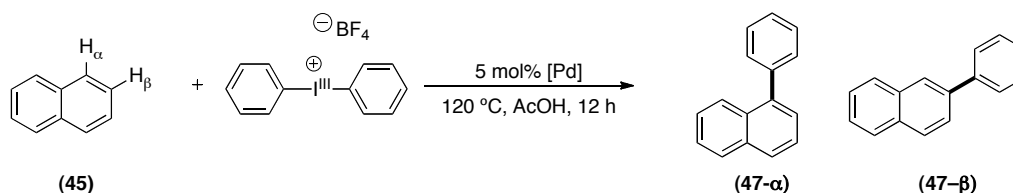
Conditions: X equiv naphthalene, 1 equiv  $[\text{Ph-I}^{\text{III}}\text{-Ph}]\text{BF}_4$ , 5 mol %  $\text{Pd(OAc)}_2$  AcOH (0.1M) at 120 °C for 12 hr, \*Based on uncorrected GC peak areas

The yield was determined from the experimental ratio of uncorrected peak areas of the phenylation products to the remaining starting material versus the theoretical maximum possible ratio. For example, with 5 equiv of naphthalene the experimental ratio of product to starting material was 1:90, and comparison of this to the maximum theoretical ratio of 1:9 results in an 11% conversion. However, this method is inaccurate because it falsely assumes that 1 equiv of starting material and product will have the same peak area. For our purposes, this is only useful to provide an estimate and demonstrate the relative trends.

With the observation that phenylation of naphthalene favors the  $\alpha$  regioisomer over the  $\beta$ , experiments moved forward with three general goals. First, we wanted to identify conditions to give the maximum conversion with the least excess substrate. Second, we hoped to optimize the reaction to achieve the maximum selectivity for the  $\alpha$  regioisomer. Finally, we desired to modify the conditions such that the  $\beta$  regioisomer would be favored. This exploration began with a catalyst screen. We chose employed 10 equiv of naphthalene because it provided the maximum efficiency in the study in **Table 4.10**. These experiments were accomplished by combining 1 equiv of  $[\text{Ph-I}^{\text{III}}\text{-Ph}]\text{BF}_4$  with 10 equiv of naphthalene and 5 mol % of several catalysts in AcOH at 120 °C for 12h (**Table 4.11**). This study showed that the best catalyst for this reaction was  $\text{PdI}_2$ . Furthermore, none of the catalysts screened significantly changed the relative ratio of  $\alpha$

to  $\beta$  products. In instances where the ratio was not determined (ND), the  $\alpha$  regioisomer was still favored, but an accurate GC integration of the  $\beta$  regioisomer could not be obtained due to low yields.

**Table 4.11:** Catalyst Screen for Naphthalene Phenylation.

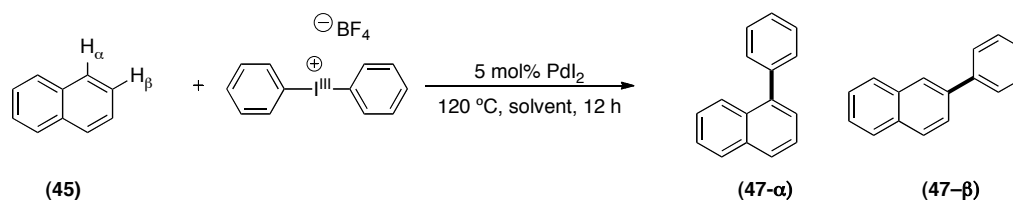


Catalyst	GC Yield*	$\alpha : \beta$
Pd(OAc) <sub>2</sub>	20%	ND
PdCl <sub>2</sub>	38%	8 : 1
PdBr <sub>2</sub>	22%	ND
PdI <sub>2</sub>	63%	6 : 1
Pd(tfa) <sub>2</sub>	33%	8 : 1
(PhCN) <sub>2</sub> PdCl <sub>2</sub>	15%	ND
(SEt <sub>2</sub> ) <sub>2</sub> PdCl <sub>2</sub>	0%	-
(PPh <sub>3</sub> ) <sub>2</sub> PdCl <sub>2</sub>	25%	ND
NaPdCl <sub>4</sub>	36%	8 : 1
IMesPd(OAc) <sub>2</sub> ·H <sub>2</sub> O	36%	8 : 1

Conditions: 10 equiv naphthalene, 1 equiv [Ph-I<sup>III</sup>-Ph]BF<sub>4</sub>, 5 mol % [Pd], AcOH (0.1M) at 120 °C for 12 h, \*Based on uncorrected GC peak areas

Next, a solvent screen was completed with PdI<sub>2</sub> as the catalyst to identify the optimal solvent for this reaction. These experiments involved the combination of 10 equiv naphthalene with 1 equiv of [Ph-I<sup>III</sup>-Ph]BF<sub>4</sub> and 5 mol % of PdI<sub>2</sub> in several solvents at 120 °C for 12 h (**Table 4.12**). This study revealed that phenylation was viable in a number of solvents, with AcOH providing this highest yield, while CH<sub>2</sub>Cl<sub>2</sub> and ClCH<sub>2</sub>CH<sub>2</sub>Cl also proving to be sufficient.

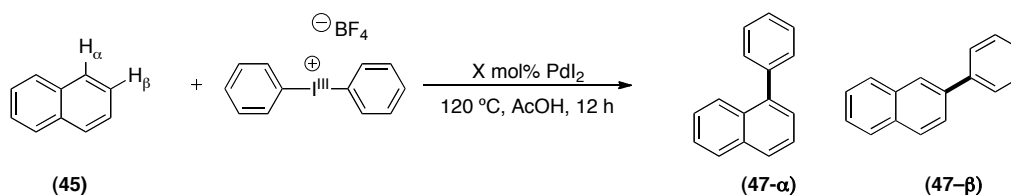
**Table 4.12:** Solvent Screen for Naphthalene Phenylation.



Solvent	GC Yield	$\alpha : \beta$
AcOH	59%	6 : 1
CH <sub>2</sub> Cl <sub>2</sub>	50%	5 : 1
CF <sub>3</sub> Ph	25%	6 : 1
CH <sub>3</sub> CN	2%	ND
THF	10%	6 : 1
ClCH <sub>2</sub> CH <sub>2</sub> Cl	48%	11 : 1

Conditions: 10 equiv naphthalene, 1 equiv [Ph-I<sup>III</sup>-Ph]BF<sub>4</sub>, 5 mol % PdI<sub>2</sub>, solvent (0.1M) at 120 °C for 12 h, \*Based on uncorrected GC peak areas

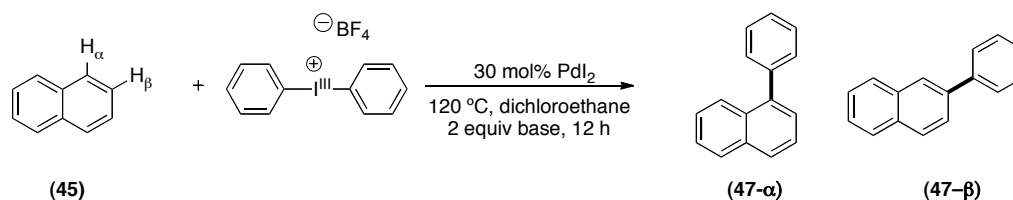
Catalyst loading was next investigated by combining 10 equiv of naphthalene and 1 equiv of [Ph-I<sup>III</sup>-Ph]BF<sub>4</sub> with varying equivalents of PdI<sub>2</sub> in AcOH at 120 °C for 12 h (Table 4.13). Predictably, an increase in yield was observed with an increase in the amount of catalyst. For example, a 30 mol % catalyst loading resulted in near complete conversion. As in previous experiments, no substantial change was seen in the ratio of product regioisomers.

**Table 4.13:** Catalyst Loading Study for Naphthalene Phenylation.

mol % PdI <sub>2</sub>	GC Yield*	$\alpha : \beta$
5	28%	7 : 1
10	73%	6 : 1
15	78%	6 : 1
20	85%	6 : 1
30	97%	6 : 1

Conditions: 10 equiv naphthalene, 1 equiv  $[\text{Ph-Ir}^{\text{III}}\text{-Ph}]\text{BF}_4$ , X mol % PdI<sub>2</sub>, AcOH (0.1M) at 120 °C for 12 h, \*Based on uncorrected GC peak areas

Finally, we sought to investigate the effect of added base on the reaction. This necessitated the use of a solvent other than AcOH, and dichloroethane was chosen based on the study in **Table 4.14**. These reactions included 1 equiv of  $[\text{Ph-Ir}^{\text{III}}\text{-Ph}]\text{BF}_4$ , 10 equiv of naphthalene, 30 mol % of PdI<sub>2</sub>, and 2 equiv of added base in ClCH<sub>2</sub>CH<sub>2</sub>Cl at 120 °C for 12 h. From these experiments it was shown that added base increased the yield, with ZnO giving the most promising result of 92% yield. The ratio of regioisomers was again unaffected. This reaction proved to work as well as reactions in AcOH. However, since the theoretical maximum yield has been nearly reached, further experiments with a decreased catalyst loading will be necessary to determine the added benefit of base relative to the reaction in AcOH.

**Table 4.14:** Catalyst Loading Study for Naphthalene Phenylation.

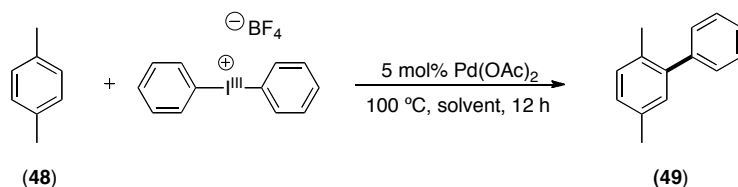
Base	GC Yield*	$\alpha : \beta$
NaHCO <sub>3</sub>	50%	ND
MgO	73%	5 : 1
ZnO	92%	5 : 1
Cs <sub>2</sub> CO <sub>3</sub>	5%	4 : 1
none	30%	ND

Conditions: 10 equiv naphthalene, 1 equiv [Ph-I<sup>III</sup>-Ph]BF<sub>4</sub>, 30 mol % PdI<sub>2</sub>, 2 equiv Base, ClCH<sub>2</sub>CH<sub>2</sub>Cl (0.1M) at 120 °C for 12 h, \*Based on uncorrected GC peak areas

An interesting analysis of the selectivity is to employ this transformation with arenes containing both benzylic C–H and aromatic C–H bonds. Previously, we have demonstrated that when directing groups are employed to attain site selective arylation, benzylic C–H bonds remain unaffected. However, Crabtree reported that the Pd-catalyzed C–H acetoxylation of toluene with PhI<sup>III</sup>(OAc)<sub>2</sub> resulted in the formation of both aromatic C–H acetoxylation products, and oxidation of a benzylic C–H bond to form benzaldehyde.

We chose to investigate this question by exploring the phenylation of *p*-xylene (48). Preliminary experiments began by completing a solvent screen using conditions similar to naphthalene phenylation. Reactions combined 1 equiv of *p*-xylene with 1.1 equiv of [Ph-I<sup>III</sup>-Ph]BF<sub>4</sub> and 5 mol % of Pd(OAc)<sub>2</sub> at 100 °C in several solvents (Table 4.15). Gratifyingly, in CH<sub>2</sub>Cl<sub>2</sub> a single phenylation product was formed in a 12% yield (as determined by GCMS based on uncorrected peak areas). Reactions in AcOH and CH<sub>3</sub>CN afforded only trace amounts of a phenylated product by GCMS. This result is interesting considering the reactivity of naphthalene in AcOH, and thus would merit further investigation. Employment of toluene as the solvent led to the observation of three peaks with a masses corresponding to phenylated toluene, with each peak presumably representing one of the three possible regioisomers.

**Table 4.15:** Phenylation of *p*-Xylene.



Solvent	GC Yield*
AcOH	1%
CH <sub>2</sub> Cl <sub>2</sub>	12%
Toluene	Toluene Phenylation
CH <sub>3</sub> CN	3%

Conditions: 1 equiv naphthalene, 1.1 equiv [Ph-I<sup>III</sup>-Ph]BF<sub>4</sub>, 5 mol % Pd(OAc)<sub>2</sub>, Solvent (0.1M) at 100 °C for 12 h, \*Based on uncorrected GC peak areas

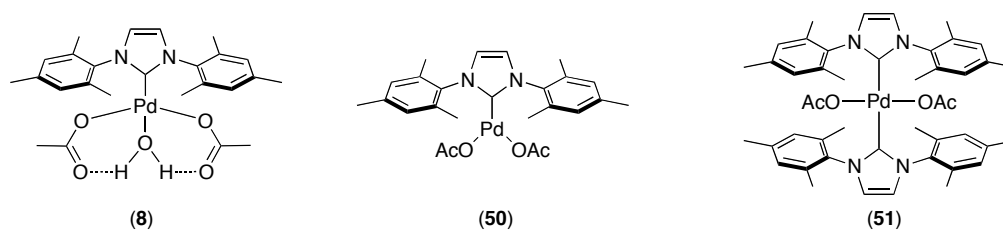
Next, the conditions described above with CH<sub>2</sub>Cl<sub>2</sub> as the solvent were then employed to evaluate this reaction with 5, 10, and 20 equiv of *p*-xylene relative to the oxidant. This resulted in the improved yields of 34%, 50%, and 100%, respectively. The isolation of the product of this reaction was attempted from the reaction with 20 equiv of *p*-xylene. Isolation of the product proved challenging due to the large excess of substrate required. Nevertheless the desired product was obtained in approximately 80% purity (based on GC). <sup>1</sup>H NMR analysis of this product revealed two aliphatic singlets with an integration of 1:1. This provides evidence that C–H arylation occurs at an aromatic position and not a benzylic site.

#### 4.8 Synthesis of the IMesPd(OAc)<sub>2</sub>•H<sub>2</sub>O Ligand

Several examples of Pd(OAc)<sub>2</sub> complexes bearing the IMes *N*-heterocyclic carbene ligands have been reported in the literature, including IMesPd(OAc)•H<sub>2</sub>O (**8**), IMesPd(OAc)<sub>2</sub> (**50**), and IMes<sub>2</sub>Pd(OAc)<sub>2</sub> (**51**).<sup>27-29</sup> Complex **8** was employed as the catalyst for many of the C–H arylations described above. Additionally, attempts were also made to synthesize catalyst **50**, but in our hands, afforded a different product than that reported in the literature.<sup>27</sup> Upon further investigation it was determined that the products obtained in the synthesis of **50**, were a mixture of Pd(OAc)<sub>2</sub> and complex **51**.<sup>29</sup>

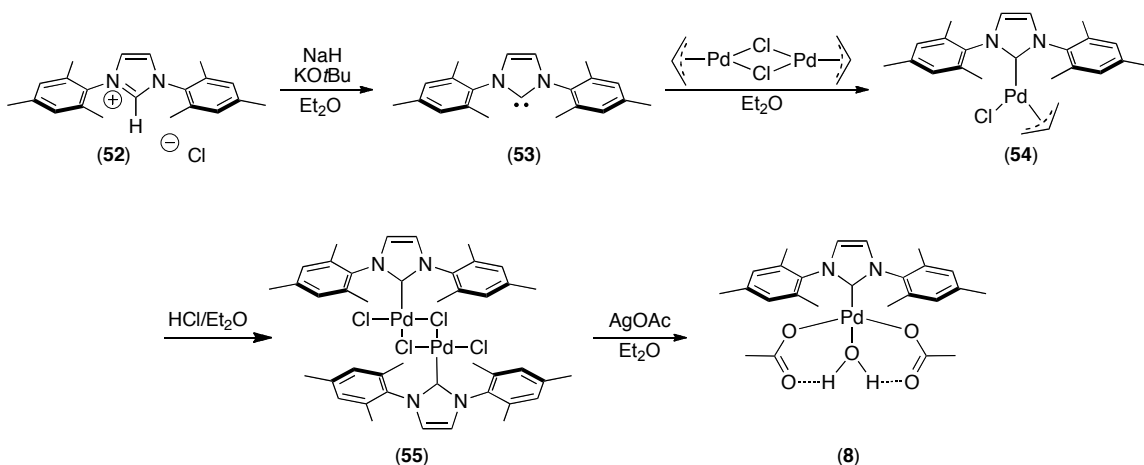


**Figure 4.2:** Pd(OAc)<sub>2</sub> Complexes Bearing IMes Ligands.



Catalyst **8** was synthesized according to a literature procedure. This was accomplished by combining 1 equiv of the imidazolium HCl salt **52** in Et<sub>2</sub>O with 2.2 equiv of NaH and 0.1 equiv NaOtBu to give the free carbene **53** (Scheme 4.15). The carbene was then metallated by combining 2.1 equiv of **53** with allyl palladium chloride in THF, to afford the palladium complex **54**.<sup>30</sup> The allyl group was then protonated by addition of HCl/Et<sub>2</sub>O, to give the chloride bridged palladium dimer **55**.<sup>30</sup> This complex was then combined with 1.1 equiv of AgOAc, resulting in an anion metathesis and yielding the desired catalyst **8**.<sup>30,31</sup> All intermediates as well as the final catalyst showed NMR spectra identical to those reported in the literature.

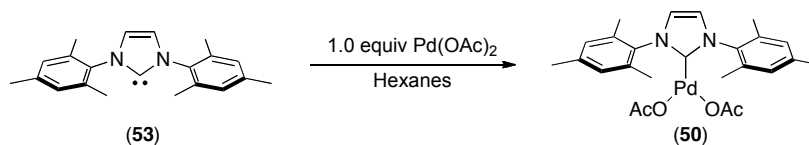
**Scheme 4.15:** Synthesis of IMesPd(OAc)•H<sub>2</sub>O.<sup>27</sup>



Next, the literature procedure for the synthesis of IMesPd(OAc)<sub>2</sub> (**50**) was followed (Scheme 4.16).<sup>28,32</sup> Synthesis of this catalyst involved the direct metallation of

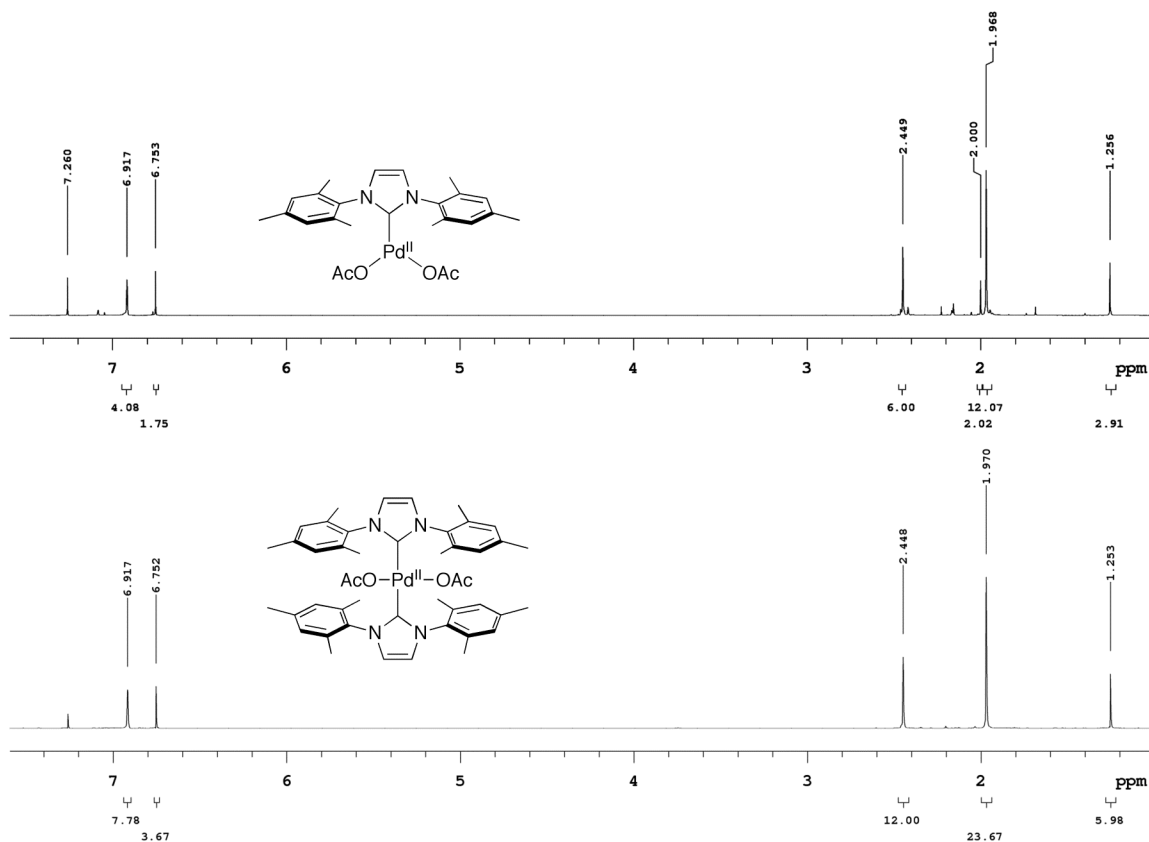
1 equiv of the free carbene **53** with 1 equiv of carefully purified Pd(OAc)<sub>2</sub> (recrystallized from dry benzene) in hexanes to afford a gray powder.

**Scheme 4.16:** Reported Synthesis of IMesPd(OAc)<sub>2</sub>.<sup>28</sup>



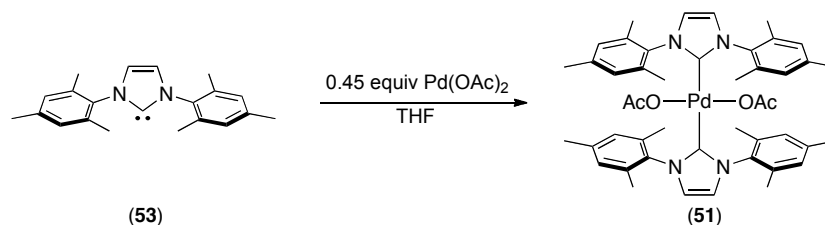
The <sup>1</sup>H NMR chemical shifts of the major product closely resemble the reported values in CDCl<sub>3</sub>, but with two key differences. First, the spectra contained several unidentified impurities in addition to the product, including a major singlet at 2.00 ppm (**Figure 4.3**). Second, the acetate methyl group and the *p*-Me of mesityl were expected to integrate 1:1 (2.45 ppm to 1.25 ppm). However our spectra revealed a 2:1 integration. To investigate the impurities, a <sup>1</sup>H NMR spectra of Pd(OAc)<sub>2</sub> was obtained and the chemical shift the Pd(OAc)<sub>2</sub> matched that of the unidentified singlet (2.00 ppm). Due to the presence of free Pd(OAc)<sub>2</sub>, it was reasoned that the remaining material was the bis-IMes complex **51**. However, the NMR data of the two complexes could not be directly compared based on the literature reports, since they were reported in different solvents.

**Figure 4.3:**  $^1\text{H}$  NMR Spectra of the Product Obtained in the Synthesis of **50** and **51** in  $\text{CDCl}_3$ .



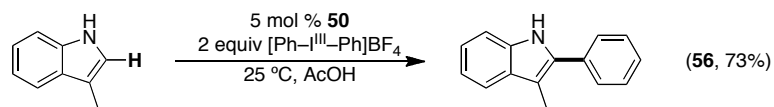
For comparison, synthesis of the bis carbene containing  $\text{IMes}_2\text{Pd}(\text{OAc})_2$  **51** was completed as reported by Stahl.<sup>29</sup> The IMes carbene **53** (2.1 equiv) was combined with 1 equiv of  $\text{Pd}(\text{OAc})_2$  (recrystallized from benzene) to afford the desired product **51**. The isolated product showed a  $^1\text{H}$  NMR spectrum identical to that reported in the literature in  $\text{C}_6\text{D}_6$ .<sup>29</sup> Additionally, the  $^1\text{H}$  NMR spectrum of **51** in  $\text{CDCl}_3$  matched exactly the chemical shifts reported by Nolan for **50**, but with the integration expected for **51** (Figure 4.3). Thus, in our hands, the products obtained using Nolan's procedure were a mixture of the bis-carbene complex **51** and  $\text{Pd}(\text{OAc})_2$ .

**Scheme 4.17:** Synthesis of  $\text{IMes}_2\text{Pd}(\text{OAc})_2$ .<sup>29</sup>

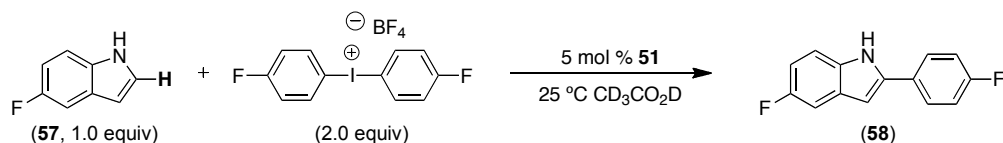


Interestingly however, **51** and the products obtained in the synthesis of **50** are viable catalysts for the arylation of indoles. First, the mixture of products obtained from synthesis of **50** was used for the phenylation of 1 equiv of 3-methylindole with 2.0 equiv of  $[\text{Ph}-\text{I}^{\text{III}}-\text{Ph}]\text{BF}_4$  and 5 mol % of **50** to obtain the phenylated product **56** in 73% yield (**Scheme 4.18**). Additionally, complex **51** was employed in the reaction of 1 equiv of 5-fluoroindole **57**, with 5 mol % of  $\text{IMes}_2\text{Pd}(\text{OAc})_2$  (**51**) and 2 equiv of  $[(p\text{-FC}_6\text{H}_4)_2\text{I}^{\text{III}}]\text{BF}_4$  in  $\text{CD}_3\text{CO}_2\text{D}$  at 25 °C to yield the phenylated product **58** (**Scheme 4.19**). This reaction afforded the desired product as confirmed by  $^{19}\text{F}$  NMR spectroscopy, as compared to an isolated sample employing  $\text{Pd}(\text{OAc})_2$  as the catalyst (40% isolated yield). Interestingly, no product appearance was observed after 3 h but the product was present after 6.5 h suggesting an induction period (*vide infra*).

**Scheme 4.18:** Utilization of the Products from Synthesis of **50** for Indole Arylation.



**Scheme 4.19:** Utilization of  $\text{IMes}_2\text{Pd}(\text{OAc})_2$  in Catalysis.

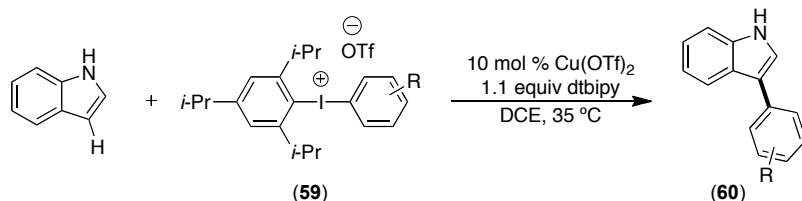


## 4.9 Subsequent Examples of Direct C–H Arylation

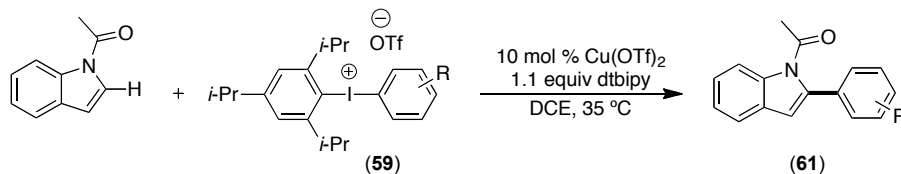
Following the publication of our palladium-catalyzed indole C–H arylation methodology, several related reports of indole arylation were published.<sup>1</sup> These examples of indole C–H arylations fall into three general categories: (1) arylation employing  $[\text{Ar}-\text{I}^{\text{III}}-\text{Ar}]^+$  oxidants with copper catalysts, (2) palladium catalyzed oxidative coupling, and (3) the use of  $\text{Ag}^+$  salts with  $\text{Ar}-\text{I}$ .

First, a report from the Gaunt group demonstrated regioselective indole arylation employing  $[\text{Ar}-\text{I}^{\text{III}}-\text{Ar}]\text{OTf}$  (**59**) oxidants and a copper catalyst.<sup>33</sup> It was demonstrated that indoles  $\text{N}-\text{H}$  and  $\text{N}-\text{Me}$  indoles reacted with the  $\text{I}^{\text{III}}$  reagent  $[\text{TRIP}-\text{I}^{\text{III}}-\text{Ar}]\text{OTf}$  (**59**,  $\text{TRIP} = 2,4,6\text{-tri-}i\text{-propylphenyl}$ ), the base dtbpy (2,6-di-*tert*-butylpyridine) and a copper catalyst to afford C3 indole arylation products like **60** in high selectivity under mild conditions (35 °C) (**Scheme 4.20**). When *N*-acetylindoles were employed at elevated temperatures (>60 °C), moderate selectivity (3:1 to 9:1) was achieved for C2 arylation to form **61** (**Scheme 4.21**). The change in selectivity is attributed to the presence of the *N*-acetyl group, which can act as a directing group for the copper to the C2 position.

**Scheme 4.20:** C3 Indole Arylation with a Cu Catalyst and  $[\text{Ar}-\text{I}^{\text{III}}-\text{Ar}]\text{OTf}$ .<sup>33</sup>



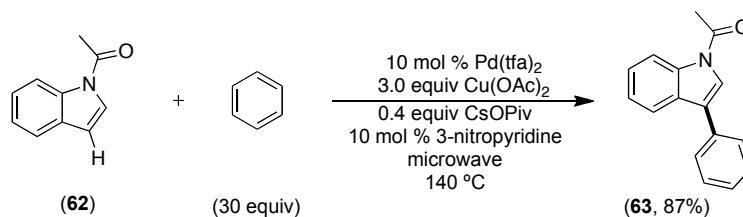
**Scheme 4.21:** C2 Indole Arylation with a Cu Catalyst and  $[\text{Ar}-\text{I}^{\text{III}}-\text{Ar}]\text{OTf}$ .<sup>33</sup>



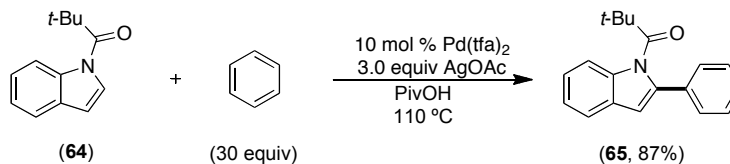
The second general category includes oxidative coupling of indoles with simple arenes.<sup>34-36</sup> Fagnou first demonstrated the C–H arylation of *N*-acetylindole **62** by combining this substrate with 30 equiv of benzene, 10 mol % of  $\text{Pd}(\text{tfa})_2$ , 10 mol % of 3-

nitropyridine, 0.4 equiv of CsOpiv, and a 3.0 equiv of a  $\text{Cu}(\text{OAc})_2$  oxidant, followed by subsection to microwave conditions to provide the C3 arylation product **63** in good yield and selectivity (87%, 9:1, **Scheme 4.22**).<sup>34</sup> He then demonstrated that this selectivity could be changed from C2 to C3 arylation by variation of the additives. By instead combining *N*-pivalylindole (**64**) with 60 equiv of benzene, 5 mol %  $\text{Pd}(\text{tfa})_2$ , and 2.0 equiv of  $\text{AgOAc}$  as an oxidant, and PivOH the C2 arylation product **65** was obtained in 84% yield and 25:1 selectivity (**Scheme 4.23**).<sup>35</sup> The nature of the observed selectivity is not clear, but the authors indicate work is ongoing to study this issue.

**Scheme 4.22:** C3 Indole Arylation Through Oxidative Coupling.<sup>34</sup>

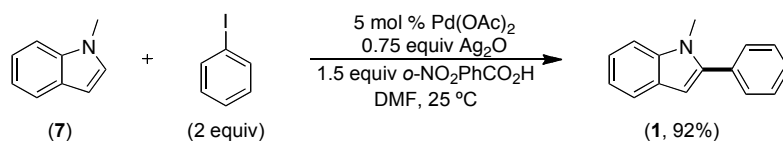


**Scheme 4.23:** C2 Indole Arylation Through Oxidative Coupling.<sup>35</sup>



Finally, methodology has been developed that affords indole C–H arylation using aryl iodides and a  $\text{AgOAc}$  additive.<sup>37</sup> Daugulis found that the combination of *N*-methylindole **7**, 5 mol % of  $\text{Pd}(\text{OAc})_2$ , 0.75 equiv of  $\text{Ag}_2\text{O}$  and 1.5 equiv of *o*-nitrobenzoic acid in DMF selectively provided the C2 arylation product in good yield at room temperature (**Scheme 4.24**). The authors propose that this reaction proceeds through a  $\text{Pd}^{0/\text{II}}$  catalytic cycle with the  $\text{Ag}^+$  acting to remove  $\text{I}^-$  from  $\text{Pd}^{\text{II}}$  thereby rendering it a more electrophilic catalyst for functionalization.

**Scheme 4.24:** C2 Indole Arylation Using  $\text{Ag}^+$  and  $\text{Ar-I}$ .<sup>37</sup>



## 4.10 Conclusions

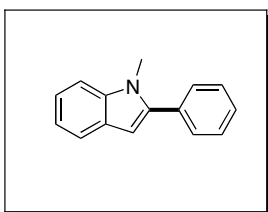
In summary we have developed a series of  $\text{Pd}^{\text{II}}$  catalyzed C–H arylation reactions, that employ  $[\text{Ar-I}^{\text{III}}\text{-Ar}]\text{BF}_4$  as terminal oxidant and are believed to proceed through a  $\text{Pd}^{\text{III/IV}}$  mechanism. The utility of this reaction has been demonstrated by the site selective C2 arylation of indoles. Additionally, we have achieved installation of a range of aryl groups with a broad functional group tolerance, which includes complimentary reactivity to  $\text{Pd}^{\text{0/II}}$  catalytic cycles. Next, investigations led to successful generation of  $[\text{Ar-I}^{\text{III}}\text{-Ar}]^+$  reagents *in situ*, followed by selective arylation of indoles. This methodology was preliminarily extended to the functionalization of other oxygen and sulfur containing heterocycles. Finally, preliminary investigations have also shown that these reactions can be applied to the arylation of simple arenes.

## 4.11 General Procedures and Materials and Methods

**General Procedures:** NMR spectra were obtained on a Varian Inova 400 (399.96 MHz for  $^1\text{H}$ ; 100.57 for  $^{13}\text{C}$ ) spectrometer unless otherwise noted.  $^1\text{H}$  NMR chemical shifts are reported in parts per million (ppm) relative to TMS, with the residual solvent peak used as an internal reference. Multiplicities are reported as follows: singlet (s), doublet (d), doublet of doublets (dd), doublet of doublets of doublets (ddd), triplet of doublets (td), quartet (q), multiplet (m), and broad resonances (br).

**Materials and Methods:** Substrates for products **1**, **2**, **10**, **13**, **15**, **16**, **20** and **21** were obtained from commercial sources and were used as received. Substrates for products **13**, and **21** were prepared by N-methylation of the corresponding indoles.<sup>3</sup> The Substrate for product **12** was prepared by reaction of 5-hydroxyindole with acetyl chloride (1.1 equiv) and  $\text{Et}_3\text{N}$  (1.1 equiv) in  $\text{CH}_2\text{Cl}_2$ . Substrate **9** was prepared according to a literature procedure.<sup>38</sup> Aryliodonium salts with  $\text{Ar} = \text{Ph}$ , *m*- $\text{CF}_3$ , *p*-F, *p*-Cl, *p*-Br, *p*-Me, *o*-Me, and

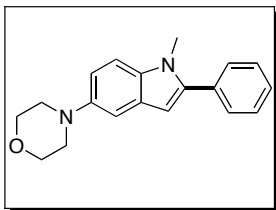
1-naphthyl were prepared in two steps – (i) conversion of the aryl iodide to the corresponding diacetoxyiodoarene<sup>39</sup> and (ii) reaction of  $\text{ArI}(\text{OAc})_2$  with  $\text{ArB}(\text{OH})_2$  in the presence of  $\text{BF}_3 \cdot \text{OEt}_2$ .<sup>40</sup> The arylodonium salt  $[(p\text{-MeOC}_6\text{H}_4)_2\text{I}]\text{BF}_4$  was prepared by the reaction of anisole and trifluoromethanesulfonic acid with  $p\text{-MeOC}_6\text{H}_4\text{I}(\text{OAc})_2$  according to a literature procedure.<sup>41</sup> Boronic acids were purchased from commercial sources and used as received. Other palladium catalysts were obtained from commercial sources (Strem or Pressure Chemicals) and used as received. Solvents were obtained from Fisher Chemical and used without further purification. Flash chromatography was performed on EM Science silica gel 60 (0.040-0.063 mm particle size, 230-400 mesh) and thin layer chromatography was performed on Merck TLC plates pre-coated with silica gel 60 F254. Control reactions (in the absence of Pd catalyst) were run for each substrate and generally showed no reaction under our standard conditions. GC yields were calculated from the peak area of the product divided by the total peak area of starting material and products, unless otherwise noted.



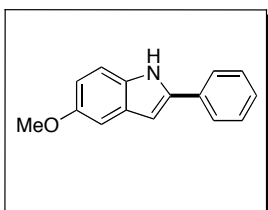
**Product 1:** 1-Methylindole (131.2 mg, 1.00 mmol, 1.0 equiv) and  $\text{IMesPd}(\text{OAc})_2 \cdot \text{H}_2\text{O}$  (26.5 mg, 0.05 mmol, 0.05 equiv) were dissolved in AcOH (10 mL), and the resulting solution was stirred at 25 °C for ~5 min.  $[\text{Ph}_2\text{I}]\text{BF}_4$  (735.4 mg, 2.0 mmol, 2.0 equiv) was added, and the reaction was stirred for 18 h at 25 °C. The reaction mixture was filtered through a plug of Celite and then evaporated to dryness. The resulting oil was dissolved in  $\text{CH}_2\text{Cl}_2$  (50 mL) and extracted with aqueous  $\text{NaHCO}_3$  (2 x 30 mL). The organic layer was dried with  $\text{MgSO}_4$ , concentrated, and the product was purified by chromatography on silica gel ( $R_f = 0.33$  in 96% hexanes/4% EtOAc). The product was obtained as a white solid (178 mg, 86% yield, average of three runs). Mp = 99-102 °C.  $^1\text{H}$  NMR (500 MHz,  $\text{CDCl}_3$ ):  $\delta$  7.65 (d,  $J = 7.9$  Hz, 1H), 7.53-7.51 (multiple peaks, 2H), 7.48 (t,  $J = 8.0$  Hz, 2H), 7.43-7.39 (m, 1H), 7.38 (d,  $J = 8.2$  Hz, 1H), 7.26 (td,  $J = 7.6, 1.4$  Hz, 1H), 7.15 (td,  $J = 7.9, 1.0$  Hz, 1H), 6.57 (s, 1H), 3.76 (s, 3H).  $^{13}\text{C}\{^1\text{H}\}$  NMR (125 MHz,  $\text{CDCl}_3$ ):  $\delta$



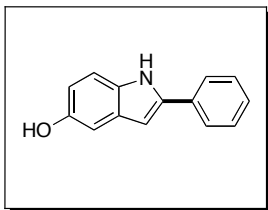
141.7, 138.5, 132.9, 129.5, 128.6, 128.1, 127.9, 121.8, 120.6, 120.0, 109.8, 101.8, 31.3.  
Anal. Calcd for C<sub>15</sub>H<sub>13</sub>N: C, 86.92, H, 6.32, N, 6.76; Found; C, 86.87, H, 6.54, N, 6.71.  
HRMS electrospray (m/z): [M<sup>+</sup>] calcd for C<sub>15</sub>H<sub>13</sub>N, 207.1048; found, 207.1044.



**Product 9:** 1-Methyl-5-morpholine-indole (175.0 mg, 0.81 mmol, 1.0 equiv) and IMesPd(OAc)<sub>2</sub>•H<sub>2</sub>O (42.8 mg, 0.81 mmol, 0.1 equiv) were dissolved in AcOH (8.1 mL), and the resulting solution was stirred at 25 °C for ~5 min. [Ph<sub>2</sub>I]BF<sub>4</sub> (893.3 mg, 2.43 mmol, 3.0 equiv) was added, and the reaction was stirred for 15 h at 60 °C. The reaction mixture was filtered through a plug of Celite and then evaporated to dryness. The resulting oil was dissolved in CH<sub>2</sub>Cl<sub>2</sub> (50 mL) and extracted with aqueous NaHCO<sub>3</sub> (2 x 30 mL). The organic layer was dried with MgSO<sub>4</sub>, concentrated, and the product was purified by chromatography on silica gel (R<sub>f</sub> = 0.25 in 70% hexanes/30% EtOAc). The product was obtained as a white solid (204 mg, 86% yield). Mp = 143-145 °C. <sup>1</sup>H NMR (400 MHz, C<sub>6</sub>D<sub>6</sub>): δ 7.27-7.32 (multiple peaks, 2H), 6.93-7.16 (multiple peaks, 6H), 6.57 (s, 1H), 3.63-3.67 (multiple peaks, 4H), 3.12 (s, 3H), 2.84-2.89 (multiple peaks, 4H). <sup>13</sup>C{<sup>1</sup>H} NMR (100 MHz, C<sub>6</sub>D<sub>6</sub>): δ 146.9, 141.8, 134.9, 133.6, 129.5, 129.2, 128.7, 115.3, 110.3, 107.9, 102.1, 67.4, 52.3, 30.7. Two carbon resonances are coincidentally overlapping. Anal. Calcd for C<sub>19</sub>H<sub>20</sub>N<sub>2</sub>O: C, 78.05, H, 6.89, N, 9.58; Found; C, 78.18, H, 7.03, N, 9.61. HRMS electrospray (m/z): [M<sup>+</sup>] calcd for C<sub>19</sub>H<sub>20</sub>N<sub>2</sub>O, 292.1576; found, 292.1575. Small amounts of product (~7% by GC) were observed in the control reaction (in the absence of Pd catalyst), which is believed to result from traces of palladium in the starting material (which was prepared via Pd catalyzed cross coupling).

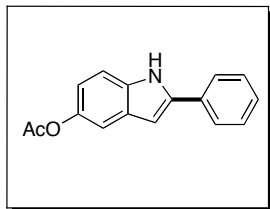


**Product 10:** 5-Methoxyindole (147.2 mg, 1.00 mmol, 1.0 equiv) and IMesPd(OAc)<sub>2</sub>•H<sub>2</sub>O (26.5 mg, 0.05 mmol, 0.05 equiv) were dissolved in AcOH (10 mL), and the resulting solution was stirred at 25 °C for ~5 min. [Ph<sub>2</sub>I]BF<sub>4</sub> (735.4 mg, 2.00 mmol, 2.0 equiv) was added, and the reaction was stirred for 15 h at 25 °C. The reaction mixture was filtered through a plug of Celite and then evaporated to dryness. The resulting oil was dissolved in CH<sub>2</sub>Cl<sub>2</sub> (50 mL) and extracted with aqueous NaHCO<sub>3</sub> (2 x 30 mL). The organic layer was dried with MgSO<sub>4</sub>, concentrated, and the product was purified by chromatography on silica gel (R<sub>f</sub> = 0.28 in 90% hexanes/10% EtOAc). The product was obtained as white solid (130 mg, 58% yield). Mp = 166-169 °C. δ <sup>1</sup>H NMR (400 MHz, CDCl<sub>3</sub>): δ 8.24 (br s, 1H), 7.65 (d, *J* = 7.2 Hz, 2H), 7.41-7.47 (multiple peaks, 2H), 7.25-7.36 (multiple peaks, 2H), 7.11 (d, *J* = 2.4 Hz, 1H), 6.88 (dd, *J* = 8.8, 2.4 Hz, 1H), 6.77 (d, *J* = 1.9 Hz, 1H), 3.88 (s, 3H). <sup>13</sup>C{<sup>1</sup>H} NMR (100 MHz, CDCl<sub>3</sub>): δ 154.4, 138.5, 132.4, 131.9, 129.7, 129.0, 127.6, 125.0, 112.6, 111.6, 102.2, 99.8, 55.8. Anal. Calcd for C<sub>15</sub>H<sub>13</sub>NO: C, 80.69, H, 5.87, N, 6.27; Found; C, 80.61, H, 5.93, N, 6.19. HRMS electrospray (m/z): [M<sup>+</sup>] calcd for C<sub>15</sub>H<sub>13</sub>NO, 223.0997; found, 223.0996.

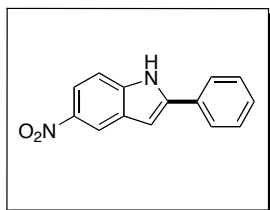


**Product 11:** 5-hydroxyindole (100.0 mg, 0.75 mmol, 1.0 equiv) and IMesPd(OAc)<sub>2</sub>•H<sub>2</sub>O (19.9 mg, 0.037 mmol, 0.05 equiv) were dissolved in AcOH (7.5 mL), and the resulting solution was stirred at 25 °C for ~5 min. [Ph<sub>2</sub>I]BF<sub>4</sub> (552 mg, 1.50 mmol, 2.0 equiv) was added, and the reaction was stirred for 15 h at 25 °C. The reaction mixture was filtered through a plug of Celite and then evaporated to dryness. The resulting oil was dissolved in CH<sub>2</sub>Cl<sub>2</sub> (50 mL) and extracted with aqueous NaHCO<sub>3</sub> (2 x 30 mL). The organic layer was dried with MgSO<sub>4</sub>, concentrated, and the product was purified by chromatography on silica gel (R<sub>f</sub> = 0.24 in 70% hexanes/30% EtOAc). The product was obtained as white solid (62 mg, 40% yield). δ <sup>1</sup>H NMR (400 MHz, DMSO-*d*<sub>6</sub>): δ 11.2 (br s, 1H), 8.67 (br s, 1H), 7.80 (d, *J* = 7.2 Hz, 2H), 7.43 (t, *J* = 7.4 Hz, 2H), 7.28 (t, *J* = 7.4 Hz, 2H), 7.18 (d, *J* = 8.7 Hz, 1H), 6.83 (d, *J* = 2.3 Hz, 1H), 6.71 (d, *J* = 1.5 Hz, 1H), 6.61 (dd, *J* = 8.6, 2.3

3H).  $^{13}\text{C}\{^1\text{H}\}$  NMR (100 MHz,  $\text{DMSO-}d_6$ ):  $\delta$  150.9, 137.8, 132.4, 131.7, 129.4, 128.8, 127.1, 124.7, 112.0, 111.6, 103.8, 98.0.

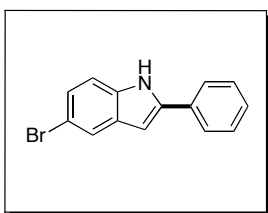


**Product 12:** 5-Acetoxyindole (100.0 mg, 0.57 mmol, 1.0 equiv) and  $\text{IMesPd}(\text{OAc})_2 \cdot \text{H}_2\text{O}$  (15.1 mg, 0.028 mmol, 0.05 equiv) were dissolved in AcOH (5.7 mL), and the resulting solution was stirred at 25 °C for ~5 min.  $[\text{Ph}_2\text{I}]\text{BF}_4$  (419.7 mg, 1.14 mmol, 2.0 equiv) was added, and the reaction was stirred for 15 h at 25 °C. The reaction mixture was filtered through a plug of Celite and then evaporated to dryness. The resulting oil was dissolved in  $\text{CH}_2\text{Cl}_2$  (50 mL) and extracted with aqueous  $\text{NaHCO}_3$  (2 x 30 mL). The organic layer was dried with  $\text{MgSO}_4$ , concentrated, and the product was purified by chromatography on silica gel ( $R_f = 0.22$  in 78% hexanes/22% EtOAc). The product was obtained as a light orange crystalline solid (101 mg, 71% yield).  $\text{Mp} = 170.7\text{-}172.2$  °C.  $^1\text{H}$  NMR (500 MHz,  $\text{CDCl}_3$ ):  $\delta$  8.39 (br s, 1H), 7.65 (d,  $J = 7.3$  Hz, 2H), 7.44 (t,  $J = 7.5$  Hz, 2H), 7.35-7.30 (multiple peaks, 3H), 6.89 (dd,  $J = 8.6, 2.2$  Hz, 1H), 6.79 (s, 1H), 2.33 (s, 3H).  $^{13}\text{C}\{^1\text{H}\}$  NMR (125 MHz,  $\text{CDCl}_3$ ):  $\delta$  170.6, 144.6, 139.3, 134.7, 132.1, 129.5, 129.1, 127.9, 125.2, 116.3, 112.6, 111.4, 100.1, 21.2. IR (KBr): 3392, 1742, 1371  $\text{cm}^{-1}$ . HRMS electrospray ( $m/z$ ):  $[\text{M}^+]$  calcd for  $\text{C}_{16}\text{H}_{13}\text{NO}_2$ , 251.0946; found, 251.0938.

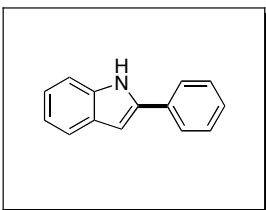


**Product 13:** 1-Methyl-5-nitroindole (150.0 mg, 0.85 mmol, 1.0 equiv) and  $\text{IMesPd}(\text{OAc})_2 \cdot \text{H}_2\text{O}$  (22.5 mg, 0.043 mmol, 0.05 equiv) were dissolved in AcOH (8.5 mL), and the resulting solution was stirred at 25 °C for ~5 min.  $[\text{Ph}_2\text{I}]\text{BF}_4$  (1.88 g, 5.11 mmol, 6.0 equiv) was added, and the reaction was stirred for 24 h at 60 °C. The reaction

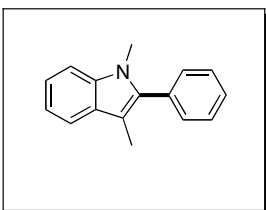
mixture was filtered through a plug of Celite and then evaporated to dryness. The resulting oil was dissolved in CH<sub>2</sub>Cl<sub>2</sub> (950 mL) and extracted with aqueous NaHCO<sub>3</sub> (2 x 30 mL). The organic layer was dried with MgSO<sub>4</sub>, concentrated, and the product was purified by chromatography on silica gel (R<sub>f</sub> = 0.2 in 92% hexanes/8% ethyl acetate). The product was obtained as a yellow powder (150 mg, 70% yield). Mp = 180-183 °C. <sup>1</sup>H NMR (500 MHz, CDCl<sub>3</sub>): δ 8.59 (d, *J* = 2.2 Hz, 1H), 8.16 (dd, *J* = 9.0, 2.2 Hz, 1H), 7.52-7.45 (multiple peaks, 5H), 7.38 (d, *J* = 9.0 Hz, 1H), 6.73 (s, 1H), 3.81 (s, 3H). <sup>13</sup>C{<sup>1</sup>H} NMR (100 MHz, CDCl<sub>3</sub>): δ 144.8, 141.8, 140.9, 131.4, 129.3, 128.8, 128.7, 127.1, 117.6, 117.3, 109.4, 103.8, 31.6. Anal. Calcd for C<sub>15</sub>H<sub>12</sub>N<sub>2</sub>O<sub>2</sub>: C, 71.42, H, 4.79, N, 11.10; Found; C, 71.63, H, 4.88, N, 10.85. HRMS electrospray (*m/z*): [M<sup>+</sup>] calcd for C<sub>15</sub>H<sub>12</sub>N<sub>2</sub>O<sub>2</sub>, 252.0899; found, 252.0894.



**Product 14:** 5-Bromoindole (117.6 mg, 0.60 mmol, 1.0 equiv) and IMesPd(OAc)<sub>2</sub>•H<sub>2</sub>O (15.8 mg, 0.03 mmol, 0.05 equiv) were dissolved in AcOH (6 mL), and the resulting solution was stirred at 25 °C for ~5 min. [Ph<sub>2</sub>I]BF<sub>4</sub> (441 mg, 1.20 mmol, 2.0 equiv) was added, and the reaction was stirred for 15 h at 60 °C. The reaction mixture was filtered through a plug of Celite and then evaporated to dryness. The resulting oil was dissolved in CH<sub>2</sub>Cl<sub>2</sub> (50 mL) and extracted with aqueous NaHCO<sub>3</sub> (2 x 30 mL). The organic layer was dried with MgSO<sub>4</sub>, concentrated, and the product was purified by chromatography on silica gel (R<sub>f</sub> = 0.13 in 90% hexanes/10% ethyl acetate). The product was obtained as a white solid (121 mg, 74% yield). Mp = 193-196 °C. <sup>1</sup>H NMR (300 MHz, DMSO-*d*<sub>6</sub>): δ 11.75 (s, 1H), 7.86 (d, *J* = 7.2 Hz, 2H), 7.71 (d, *J* = 1.9 Hz, 1H), 7.44-7.50 (multiple peaks, 2H), 7.31-7.38 (multiple peaks, 2H), 7.2 (dd, *J* = 8.6, 2.0 Hz, 1H), 6.89 (d, *J* = 1.4 Hz, 1H). <sup>13</sup>C{<sup>1</sup>H} NMR (100 MHz, DMSO-*d*<sub>6</sub>): δ 139.1, 135.7, 131.5, 130.4, 128.9, 127.8, 125.1, 123.9, 122.0, 113.1, 111.8, 98.2. Anal. Calcd for C<sub>14</sub>H<sub>10</sub>NBr: C, 61.79, H, 3.70, N, 5.15; Found; C, 61.86, H, 3.82, N, 5.10. HRMS electrospray (*m/z*): [M<sup>+</sup>] calcd for C<sub>14</sub>H<sub>10</sub>NBr, 270.9997; found, 270.9993.

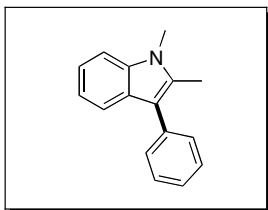


**Product 2:** Indole (117.2 mg, 1.00 mmol, 1.0 equiv) and IMesPd(OAc)<sub>2</sub>•H<sub>2</sub>O (26.5 mg, 0.05 mmol, 0.05 equiv) were dissolved in AcOH (10 mL), and the resulting solution was stirred at 25 °C for ~5 min. [Ph<sub>2</sub>I]BF<sub>4</sub> (735.4 mg, 2.00 mmol, 2.0 equiv) was added, and the reaction was stirred for 15 h at 25 °C. The reaction mixture was filtered through a plug of Celite and then evaporated to dryness. The resulting oil was dissolved in CH<sub>2</sub>Cl<sub>2</sub> (50 mL) and extracted with aqueous NaHCO<sub>3</sub> (2 x 30 mL). The organic layer was dried with MgSO<sub>4</sub>, concentrated, and the product was purified by chromatography on silica gel (R<sub>f</sub> = 0.1 in 96% hexanes/4% EtOAc). The product was obtained as a white solid (155.9 mg, 81% yield). Mp = 188-189 °C. <sup>1</sup>H NMR (400 MHz, CDCl<sub>3</sub>): δ 8.31 (br s, 1H), 7.65-7.69 (multiple peaks, 3H), 7.39-7.49 (multiple peaks, 3H), 7.35 (t, *J* = 7.4 Hz, 1H), 7.23 (ddd, *J* = 7.8, 7.0, 1.2 Hz, 1H), 7.16 (ddd, *J* = 7.7, 7.0, 1.0 Hz, 1H), 6.86 (s, 1H). <sup>13</sup>C{<sup>1</sup>H} NMR (100 MHz, CDCl<sub>3</sub>): δ 137.8, 136.7, 132.2, 129.2, 129.0, 127.7, 125.1, 122.3, 120.6, 120.2, 110.9, 99.9. Anal. Calcd for C<sub>14</sub>H<sub>11</sub>N: C, 87.01, H, 5.74, N, 7.25; Found; C, 87.03, H, 5.71, N, 7.16. HRMS electrospray (*m/z*): [M<sup>+</sup>] calcd for C<sub>14</sub>H<sub>11</sub>N, 193.0891; found, 193.0892.

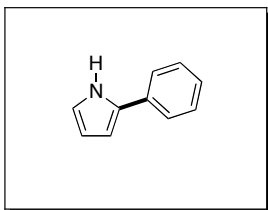


**Product 15:** 1,3-Dimethylindole (150.0 mg, 1.03 mmol, 1.0 equiv) and IMesPd(OAc)<sub>2</sub>•H<sub>2</sub>O (27.3 mg, 0.05 mmol, 0.05 equiv) were dissolved in AcOH (10 mL), and the resulting solution was stirred at 25 °C for ~5 min. [Ph<sub>2</sub>I]BF<sub>4</sub> (759.7 mg, 2.00 mmol, 2.0 equiv) was added, and the reaction was stirred for 15 h at 25 °C. The reaction mixture was filtered through a plug of Celite and then evaporated to dryness. The resulting oil was dissolved in CH<sub>2</sub>Cl<sub>2</sub> (50 mL) and extracted with aqueous NaHCO<sub>3</sub> (2 x

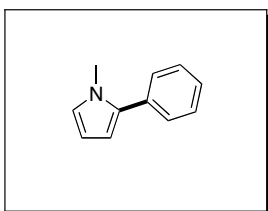
30 mL). The organic layer was dried with MgSO<sub>4</sub>, concentrated, and the product was purified by chromatography on silica gel ( $R_f = 0.2$  in 98% hexanes/2% EtOAc). The product was obtained as a light yellow viscous oil (203 mg, 89% yield). <sup>1</sup>H NMR (500 MHz, CDCl<sub>3</sub>): δ 7.61 (d,  $J = 7.84$  Hz, 1H), 7.50 (t,  $J = 7.93$  Hz, 2H), 7.44-7.40 (multiple peaks, 3H), 7.34 (d,  $J = 8.2$  Hz, 1H), 7.28-7.25 (m, 1H), 7.16 (td,  $J = 7.0, 1.0$  Hz, 1H), 3.62 (s, 3H), 2.29 (s, 3H). <sup>13</sup>C{<sup>1</sup>H} NMR (125 MHz, CDCl<sub>3</sub>): δ 137.6, 137.2, 132.1, 130.6, 128.4, 128.3, 127.7, 121.7, 119.1, 118.8, 109.2, 108.5, 30.9, 9.3. Anal. Calcd for C<sub>16</sub>H<sub>15</sub>N: C, 86.84, H, 6.83, N, 6.33; Found; C, 86.71, H, 6.92, N, 6.33. HRMS electrospray (m/z): [M<sup>+</sup>] calcd for C<sub>16</sub>H<sub>15</sub>N, 221.1204; found, 221.1202.



**Product 16:** 2-Methylindole (150 mg, 1.03 mmol, 1.0 equiv) and IMesPd(OAc)<sub>2</sub>•H<sub>2</sub>O (27.3 mg, 0.05 mmol, 0.05 equiv) were dissolved in AcOH (10 mL), and the resulting solution was stirred at 25 °C for ~5 min. [Ph<sub>2</sub>I]BF<sub>4</sub> (758 mg, 2.07 mmol, 2.0 equiv) was added, and the reaction was stirred for 15 h at 25 °C. The reaction mixture was filtered through a plug of Celite and then evaporated to dryness. The resulting oil was taken up in CH<sub>2</sub>Cl<sub>2</sub> and extracted with aqueous NaHCO<sub>3</sub> (2 x 30 mL). The organic layer was dried with MgSO<sub>4</sub>, concentrated, and the product was purified by chromatography on silica gel in 80% hexanes/20% benzene ( $R_f = 0.25$ ) followed by a second column in 97.5% hexanes/2.5% EtOAc ( $R_f = 0.18$ ). The two columns were required to remove a high molecular weight side product ( $R_f = 0.18$  in 80% hexanes/20% benzene) as well as unreacted starting material ( $R_f = 0.22$  in 97.5% hexanes/2.5% EtOAc). The product was obtained as a white solid (66 mg, 29% yield). Mp = 108.9-111.2 °C. <sup>1</sup>H NMR (400 MHz, CDCl<sub>3</sub>) δ 7.71 (d,  $J = 7.9$  Hz, 1H), 7.55-7.49 (multiple peaks, 4H), 7.37-7.33 (multiple peaks, 2H), 7.25 (t,  $J = 8.1$  Hz, 1H), 7.15 (t,  $J = 7.9$  Hz, 1H), 3.77 (s, 3H), 2.53 (s, 3H). <sup>13</sup>C{<sup>1</sup>H} NMR (125 MHz, CDCl<sub>3</sub>): δ 136.5, 135.7, 133.3, 129.7, 128.4, 126.9, 125.6, 121.1, 119.6, 118.7, 113.9, 108.7, 29.6, 11.0. HRMS electrospray (m/z): [M<sup>+</sup>] calcd for C<sub>16</sub>H<sub>15</sub>N, 221.1204; found, 221.1201.

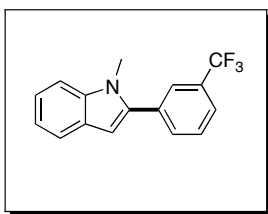


**Product 20:** Pyrrole (939 mg, 14.0 mmol, 10 equiv) and IMesPd(OAc)<sub>2</sub>•H<sub>2</sub>O (37.0 mg, 0.07 mmol, 0.05 equiv) were dissolved in AcOH (13 mL), and the resulting solution was stirred at 25 °C for ~5 min. [Ph<sub>2</sub>I]BF<sub>4</sub> (515 mg, 1.40 mmol, 1.0 equiv) was added, and the reaction was stirred for 15 h at 25 °C. The reaction mixture was filtered through a plug of Celite and then evaporated to dryness. The resulting oil was dissolved in CH<sub>2</sub>Cl<sub>2</sub> (50 mL) and extracted with aqueous NaHCO<sub>3</sub> (2 x 30 mL). The organic layer was dried with MgSO<sub>4</sub>, concentrated, and the product was purified by chromatography on silica gel (R<sub>f</sub> = 0.20 in 95% hexanes/5% EtOAc). The product was obtained as a white solid (137 mg, 69% yield). Mp = 125-128 °C. <sup>1</sup>H NMR (400 MHz, CDCl<sub>3</sub>): δ 8.45 (br s, 1H), 7.48 (d, *J* = 7.3 Hz, 2H), 7.34-7.40 (multiple peaks, 2H), 7.21 (t, *J* = 7.3 Hz, 1H), 6.88 (m, 1H), 6.54 (m, 1H), 6.31 (td, *J* = 3.5, 2.6 Hz, 1H). <sup>13</sup>C{<sup>1</sup>H} NMR (100 MHz, DMSO-*d*<sub>6</sub>): δ 132.7, 132.0, 128.8, 126.1, 123.8, 118.8, 110.0, 105.9. HRMS electrospray (*m/z*): [M<sup>+</sup>] calcd for C<sub>10</sub>H<sub>9</sub>N, 143.0735; found, 143.0735.



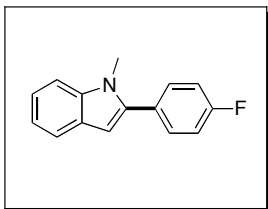
**Product 21:** 1-Methylpyrrole (1.136 g, 14.0 mmol, 10 equiv) and IMesPd(OAc)<sub>2</sub>•H<sub>2</sub>O (37.0 mg, 0.07 mmol, 0.05 equiv) were dissolved in AcOH (14 mL), and the resulting solution was stirred at 25 °C for ~5 min. [Ph<sub>2</sub>I]BF<sub>4</sub> (515 mg, 1.40 mmol, 1.0 equiv) was added, and the reaction was stirred for 15 h at 25 °C. The reaction mixture was filtered through a plug of Celite and then evaporated to dryness. The resulting oil was dissolved in CH<sub>2</sub>Cl<sub>2</sub> (50 mL) and extracted with aqueous NaHCO<sub>3</sub> (2 x 30 mL). The organic layer was dried with MgSO<sub>4</sub>, concentrated, and the product was purified by chromatography on silica gel (R<sub>f</sub> = 0.27 in 82% hexanes/18% benzene). The product was obtained as a white

solid (148 mg, 67% yield, 0.94 mmol) which was 96% pure by GC analysis. This product was inseparable from 4% of the corresponding diphenylated product 1-methyl-2,5-diphenylindole (6.6 mg, 0.028 mmol). Mp = 45-48 °C.  $^1\text{H}$  NMR (400 MHz,  $\text{CDCl}_3$ ):  $\delta$  7.37-7.50 (multiple peaks, 4H), 7.27-7.34 (m, 1H), 6.72 (t,  $J = 2.0$  Hz, 1H), 6.19-6.26 (multiple peaks, 2H), 3.67 (s, 3H).  $^{13}\text{C}\{^1\text{H}\}$  NMR (100 MHz,  $\text{CDCl}_3$ ):  $\delta$  134.5, 133.3, 128.5, 128.2, 126.6, 123.6, 108.6, 107.7, 34.9. HRMS electrospray ( $m/z$ ):  $[\text{M}^+]$  calcd for  $\text{C}_{11}\text{H}_{11}\text{N}$ , 157.0891; found, 157.0888.

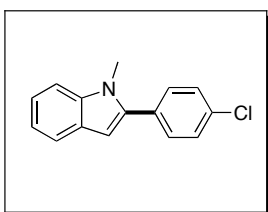


**Product 22:** 1-Methylindole (78.7 mg, 0.60 mmol, 1.0 equiv) and  $\text{IMesPd}(\text{OAc})_2 \cdot \text{H}_2\text{O}$  (15.9 mg, 0.03 mmol, 0.05 equiv) were dissolved in AcOH (6 mL), and the resulting solution was stirred at 25 °C for ~5 min.  $[(m\text{-CF}_3\text{C}_6\text{H}_5)_2\text{I}]\text{BF}_4$  (604.8 mg, 1.2 mmol, 2.0 equiv) was added, and the reaction was stirred for 15 h at 25 °C. The reaction mixture was filtered through a plug of Celite and then evaporated to dryness. The resulting oil was dissolved in  $\text{CH}_2\text{Cl}_2$  (50 mL) and extracted with aqueous  $\text{NaHCO}_3$  (2 x 30 mL). The organic layer was dried with  $\text{MgSO}_4$ , concentrated, and the product was purified by chromatography on silica gel ( $R_f = 0.26$  in 90% hexanes/10% benzene). The product was obtained as a pale yellow oil (106 mg, 64% yield).  $^1\text{H}$  NMR (400 MHz,  $\text{CDCl}_3$ ):  $\delta$  7.82 (s, 1H), 7.67-7.74 (multiple peaks, 3H), 7.59-7.65 (multiple peaks, 1H), 7.39-7.43 (m, 1H), 7.32 (ddd,  $J = 8.2, 7.0, 1.2$  Hz, 1H), 7.21 (ddd,  $J = 7.9, 7.0, 1.1$  Hz, 1H), 6.66 (s, 1H), 3.78 (s, 3H).  $^{13}\text{C}\{^1\text{H}\}$  NMR (100 MHz,  $\text{CDCl}_3$ ):  $\delta$  139.7, 138.6, 133.6, 132.4 (q,  $^4J_{\text{CF}_3} = 1.2$  Hz), 131.0 (q,  $^2J_{\text{CF}_3} = 32$  Hz), 129.0, 127.8, 125.9 (q,  $^3J_{\text{CF}_3} = 3.9$  Hz), 124.4 (q,  $^3J_{\text{CF}_3} = 3.8$  Hz), 124.0 (q,  $^1J_{\text{CF}_3} = 273$  Hz), 122.2, 120.7, 120.1, 109.7, 102.6, 31.1. Anal. Calcd for  $\text{C}_{16}\text{H}_{12}\text{F}_3\text{N}$ : C, 69.81, H, 4.39, N, 5.09; Found; C, 69.89, H, 4.46, N, 5.05. HRMS electrospray ( $m/z$ ):  $[\text{M}^+]$  calcd for  $\text{C}_{16}\text{H}_{12}\text{F}_3\text{N}$ , 275.0922; found, 275.0920.



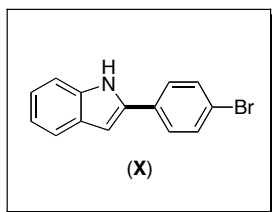


**Product 23:** 1-Methylindole (131.2 mg, 1.00 mmol, 1.0 equiv) and IMesPd(OAc)<sub>2</sub>•H<sub>2</sub>O (26.5 mg, 0.05 mmol, 0.05 equiv) were dissolved in AcOH (10 mL), and the resulting solution was stirred at 25 °C for ~5 min. [(*p*-FC<sub>6</sub>H<sub>5</sub>)<sub>2</sub>I]BF<sub>4</sub> (808.0 mg, 2.00 mmol, 2.0 equiv) was added, and the reaction was stirred for 15 h at 25 °C. The reaction mixture was filtered through a plug of Celite and then evaporated to dryness. The resulting oil was dissolved in CH<sub>2</sub>Cl<sub>2</sub> (50 mL) and extracted with aqueous NaHCO<sub>3</sub> (2 x 30 mL). The organic layer was dried with MgSO<sub>4</sub>, concentrated, and the product was purified by chromatography on silica gel (R<sub>f</sub> = 0.43 in 90% hexanes/10% benzene). The product was obtained as a light orange solid (180 mg, 80% yield). Mp = 119-122 °C. <sup>1</sup>H NMR (400 MHz, CD<sub>3</sub>OD): δ 7.51-7.57 (multiple peaks, 3H), 7.36 (d, *J* = 8.3 Hz, 1H), 7.15-7.25 (multiple peaks, 3H), 7.05 (ddd, *J* = 7.8, 7.0, 1.0 Hz, 1H), 6.48 (s, 1H), 3.71 (s, 3H). <sup>13</sup>C{<sup>1</sup>H} NMR (100 MHz, CDCl<sub>3</sub>): δ 162.4 (d, <sup>1</sup>*J*<sub>F</sub> = 247 Hz), 140.3, 138.2, 130.9 (d, <sup>3</sup>*J*<sub>F</sub> = 7.4 Hz), 128.8 (d, <sup>4</sup>*J*<sub>F</sub> = 4.4 Hz), 127.8, 121.7, 120.4, 119.9, 115.4 (d, <sup>2</sup>*J*<sub>F</sub> = 22 Hz), 109.6, 101.6, 30.9. Anal. Calcd for C<sub>15</sub>H<sub>12</sub>FN: C, 79.98, H, 5.37, N, 6.22; Found; C, 80.33, H, 5.43, N, 6.26. HRMS electrospray (*m/z*): [M<sup>+</sup>] calcd for C<sub>15</sub>H<sub>12</sub>FN, 225.0954; found, 225.0953.

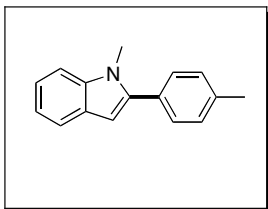


**Product 24:** 1-Methylindole (131.2 mg, 1.00 mmol, 1.0 equiv) and IMesPd(OAc)<sub>2</sub>•H<sub>2</sub>O (26.5 mg, 0.05 mmol, 0.05 equiv) were dissolved in AcOH (10 mL), and the resulting solution was stirred at 25 °C for ~5 min. [(*p*-ClC<sub>6</sub>H<sub>5</sub>)<sub>2</sub>I]BF<sub>4</sub> (873.6 mg, 2.00 mmol, 2.0 equiv) was added, and the reaction was stirred for 15 h at 25 °C. The reaction mixture was filtered through a plug of Celite and then evaporated to dryness. The resulting oil was dissolved in CH<sub>2</sub>Cl<sub>2</sub> (50 mL) and extracted with aqueous NaHCO<sub>3</sub> (2 x 30 mL). The

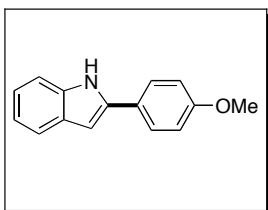
organic layer was dried with MgSO<sub>4</sub>, concentrated, and the product was purified by chromatography on silica gel (R<sub>f</sub> = 0.25 in 98% hexanes/2% ethyl acetate). The product was obtained as white solid (219 mg, 90% yield). Mp = 115-118 °C. <sup>1</sup>H NMR (400 MHz, CDCl<sub>3</sub>): δ 7.65 (d, *J* = 7.8 Hz, 1H), 7.38-7.45 (m, 4H), 7.35 (d, *J* = 7.9 Hz, 1H), 7.27 (ddd, *J* = 8.2, 7.0, 1.2 Hz, 1H), 7.17 (ddd, *J* = 7.9, 6.9, 1.1 Hz, 1H), 6.56 (s, 1H), 3.69 (s, 3H). <sup>13</sup>C{<sup>1</sup>H} NMR (100 MHz, CDCl<sub>3</sub>): δ 140.1, 138.4, 133.8, 131.2, 130.4, 128.7, 127.8, 121.9, 120.5, 120.0, 109.6, 101.9, 31.1. Anal. Calcd for C<sub>15</sub>H<sub>12</sub>ClN: C, 74.53, H, 5.00, N, 5.79; Found; C, 74.23, H, 5.00, N, 5.61. HRMS electrospray (m/z): [M<sup>+</sup>] calcd for C<sub>15</sub>H<sub>12</sub>ClN, 241.0658; found, 241.0655.



**Product 25:** Indole (88.1 mg, 0.75 mmol, 1.00 equiv) and IMesPd(OAc)<sub>2</sub>•H<sub>2</sub>O (19.8 mg, 0.037 mmol, 0.05 equiv) were dissolved in AcOH (7.5 mL), and the resulting solution was stirred at 25 °C for ~5 min. [(*p*-BrC<sub>6</sub>H<sub>5</sub>)<sub>2</sub>I]BF<sub>4</sub> (788.6 mg, 1.50 mmol, 2.0 equiv) was added, and the reaction was stirred for 15 h at 80 °C. The reaction mixture was filtered through a plug of Celite and then evaporated to dryness. The resulting oil was dissolved in CH<sub>2</sub>Cl<sub>2</sub> (50 mL) and extracted with aqueous NaHCO<sub>3</sub> (2 x 30 mL). The organic layer was dried with MgSO<sub>4</sub>, concentrated, and the product was purified by chromatography on silica gel (R<sub>f</sub> = 0.13 in 95% hexanes/5% ethyl acetate). The product was obtained as a white solid (135 mg, 66% yield). Mp = 208-212 °C. <sup>1</sup>H NMR (400 MHz, DMSO-*d*<sub>6</sub>): δ 11.59 (s, 1H), 7.82 (d, *J* = 8.6 Hz, 2H), 7.65 (d, *J* = 8.6 Hz, 2H), 7.54 (d, *J* = 7.9 Hz, 1H), 7.40 (d, *J* = 8.0 Hz, 1H), 7.11 (ddd, *J* = 8.1, 7.0, 1.1 Hz, 1H), 7.00 (ddd, *J* = 7.8, 7.0, 1.0 Hz, 1H), 6.94 (d, *J* = 0.9 Hz, 1H). <sup>13</sup>C{<sup>1</sup>H} NMR (100 MHz, DMSO-*d*<sub>6</sub>): δ 137.1, 136.3, 131.7, 131.4, 128.4, 126.8, 121.8, 120.2, 120.1, 119.4, 111.3, 99.2. Anal. Calcd for C<sub>14</sub>H<sub>10</sub>BrN: C, 61.79, H, 3.70, N, 5.15; Found; C, 61.59, H, 3.77, N, 5.07. HRMS electrospray (m/z): [M<sup>+</sup>] calcd for C<sub>14</sub>H<sub>10</sub>BrN, 270.9997; found, 271.0002.

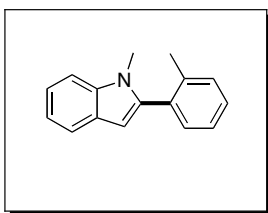


**Product 26:** 1-Methylindole (131.2 mg, 1.00 mmol, 1.0 equiv) and IMesPd(OAc)<sub>2</sub>•H<sub>2</sub>O (26.5 mg, 0.05 mmol, 0.05 equiv) were dissolved in AcOH (10 mL), and the resulting solution was stirred at 25 °C for ~5 min. [(*p*-CH<sub>3</sub>C<sub>6</sub>H<sub>5</sub>)<sub>2</sub>I]BF<sub>4</sub> (791.9 mg, 2.00 mmol, 2.0 equiv) was added, and the reaction was stirred for 15 h at 25 °C. The reaction mixture was filtered through a plug of Celite and then evaporated to dryness. The resulting oil was dissolved in CH<sub>2</sub>Cl<sub>2</sub> (50 mL) and extracted with aqueous NaHCO<sub>3</sub> (2 x 30 mL). The organic layer was dried with MgSO<sub>4</sub>, concentrated, and the product was purified by chromatography on silica gel (R<sub>f</sub> = 0.21 in 90% hexanes/10% benzene). The product obtained was a white solid (155 mg, 70% yield). Mp = 96-98 °C. <sup>1</sup>H NMR (400MHz, CDCl<sub>3</sub>): δ 7.65 (d, *J* = 7.8Hz, 1H), 7.43 (d, *J* = 8.2 Hz, 2H), 7.38 (d, *J* = 8.2 Hz, 1H), 7.31-7.24 (multiple peaks, 3H), 7.16 (td, *J* = 8.0, 1.0 Hz, 1H), 6.55 (s, 1H), 3.76 (s, 3H), 2.45 (s, 3H). <sup>13</sup>C{<sup>1</sup>H} NMR (100 MHz, CDCl<sub>3</sub>): δ 141.5, 138.2, 137.6, 129.8, 129.2, 129.1, 127.9, 121.4, 120.3, 119.7, 109.5, 101.2, 31.0, 21.2. Anal. Calcd for C<sub>16</sub>H<sub>15</sub>N: C, 86.84, H, 6.83, N, 6.33; Found; C, 86.69, H, 6.89, N, 6.40. HRMS electrospray (*m/z*): [M<sup>+</sup>] calcd for C<sub>16</sub>H<sub>15</sub>N, 221.1204; found, 221.1197.

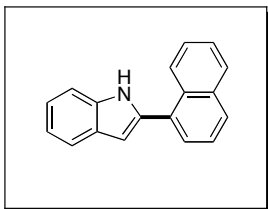


**Product 27:** 1-Methylindole (111 mg, 0.84 mmol, 1.0 equiv) and IMesPd(OAc)<sub>2</sub>•H<sub>2</sub>O (22.3 mg, 0.042 mmol, 0.05 equiv) were dissolved in AcOH (8.5 mL), and the resulting solution was stirred at 25 °C for ~5 min. [(*p*-OMeC<sub>6</sub>H<sub>5</sub>)<sub>2</sub>I]BF<sub>4</sub> (721 mg, 1.68 mmol, 2.0 equiv) was added, and the reaction was stirred for 15 h at 60 °C. The reaction mixture was filtered through a plug of Celite and then evaporated to dryness. The resulting oil was dissolved in CH<sub>2</sub>Cl<sub>2</sub> (50 mL) and extracted with aqueous NaHCO<sub>3</sub> (2 x 30 mL). The organic layer was dried with MgSO<sub>4</sub>, concentrated, and the product was purified by

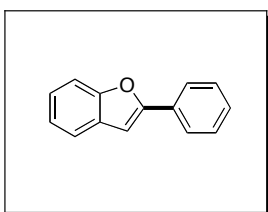
chromatography on silica gel ( $R_f = 0.23$  in 70% hexanes/30% benzene). The product was obtained as a light brown solid (161 mg, 80% yield). Mp = 117-120 °C.  $^1\text{H}$  NMR (400 MHz,  $\text{CDCl}_3$ ):  $\delta$  7.76 (d,  $J = 7.8$  Hz, 1H), 7.54 (d,  $J = 8.8$  Hz, 2H), 7.45 (d,  $J = 8.2$  Hz, 1H), 7.36 (ddd,  $J = 7.9, 7.0, 1.1$  Hz, 1H), 7.27 (ddd,  $J = 7.7, 6.9, 1.0$  Hz, 1H), 7.10 (d,  $J = 8.8$  Hz, 2H), 6.63 (s, 1H), 3.95 (s, 3H), 3.80 (s, 3H).  $^{13}\text{C}\{^1\text{H}\}$  NMR (100 MHz,  $\text{CDCl}_3$ ):  $\delta$  59.3, 141.3, 138.1, 130.5, 127.9, 125.1, 121.3, 120.2, 119.7, 113.9, 109.5, 100.9, 55.2, 30.9. Anal. Calcd for  $\text{C}_{16}\text{H}_{15}\text{NO}$ : C, 80.98, H, 6.37, N, 5.90; Found; C, 80.95, H, 6.37, N, 5.92. HRMS electrospray (m/z):  $[\text{M}^+]$  calcd for  $\text{C}_{16}\text{H}_{15}\text{NO}$ , 237.1154; found, 237.1151.



**Product 28:** 1-Methylindole (116 mg, 0.88 mmol, 1.0 equiv) and  $\text{IMesPd}(\text{OAc})_2 \cdot \text{H}_2\text{O}$  (23.4 mg, 0.044 mmol, 0.05 equiv) were dissolved in AcOH (8.5 mL), and the resulting solution was stirred at 25 °C for ~5 min.  $[(o\text{-MeC}_6\text{H}_5)_2\text{I}]\text{BF}_4$  (700 mg, 1.77 mmol, 2.0 equiv) was added, and the reaction was stirred for 15 h at 60 °C. The reaction mixture was filtered through a plug of Celite and then evaporated to dryness. The resulting oil was dissolved in  $\text{CH}_2\text{Cl}_2$  (50 mL) and extracted with aqueous  $\text{NaHCO}_3$  (2 x 30 mL). The organic layer was dried with  $\text{MgSO}_4$ , concentrated, and the product was purified by chromatography on silica gel ( $R_f = 0.17$  in 95% hexanes/5% benzene). The product was obtained as a light orange solid (121 mg, 62% yield). Mp = 90-92 °C.  $^1\text{H}$  NMR (400 MHz,  $\text{CDCl}_3$ ):  $\delta$  7.66 (d,  $J = 7.8$  Hz, 1H), 7.23-7.40 (multiple peaks, 6H), 7.16 (ddd,  $J = 7.8, 6.9, 1.0$  Hz, 1H), 6.45 (s, 1H), 3.53 (s, 3H), 2.22 (s, 3H).  $^{13}\text{C}\{^1\text{H}\}$  NMR (100 MHz,  $\text{CDCl}_3$ ):  $\delta$  140.5, 138.0, 137.3, 132.5, 131.1, 130.0, 128.6, 128.0, 125.5, 121.2, 120.4, 119.6, 109.4, 101.5, 30.3, 20.0. Anal. Calcd for  $\text{C}_{16}\text{H}_{15}\text{N}$ : C, 86.84, H, 6.83, N, 6.33; Found; C, 86.57, H, 6.87, N, 6.26. HRMS electrospray (m/z):  $[\text{M}^+]$  calcd for  $\text{C}_{16}\text{H}_{15}\text{N}$ , 221.1204; found, 221.1198.

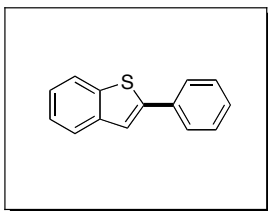


**Product 29:** Indole (94 mg, 0.80 mmol, 1.0 equiv) and IMesPd(OAc)<sub>2</sub>•H<sub>2</sub>O (21.2 mg, 0.04 mmol, 0.05 equiv) were dissolved in AcOH (8.0 mL) and the resulting solution was stirred at 25 °C for ~5 min. [(1-Naphthyl)<sub>2</sub>I]BF<sub>4</sub> (749 mg, 1.60 mmol, 2.0 equiv) was added, and the reaction was stirred for 15 h at 60 °C. The reaction mixture was filtered through a plug of Celite and then evaporated to dryness. The resulting oil was dissolved in CH<sub>2</sub>Cl<sub>2</sub> (50 mL) and extracted with aqueous NaHCO<sub>3</sub> (2 x 30 mL). The organic layer was dried with MgSO<sub>4</sub>, concentrated, and the product was purified by chromatography on silica gel (R<sub>f</sub> = 0.20 in 95% hexanes/5% ethyl acetate). The product was obtained as a white solid (131 mg, 67% yield). Mp = 99-102 °C. <sup>1</sup>H NMR (400 MHz, DMSO-*d*<sub>6</sub>): δ 11.59 (s, 1H), 8.31-8.37 (m, 1H), 7.96-8.05 (multiple peaks, 2H), 7.72 (dd, *J* = 7.1, 1.2 Hz, 1H), 7.56-7.65 (multiple peaks, 4H), 7.47 (d, *J* = 8.1 Hz, 1H), 7.16 (ddd, *J* = 8.0, 7.0, 1.2 Hz, 1H), 7.07 (ddd, *J* = 7.8, 7.0, 1.0 Hz, 1H), 6.75 (d, *J* = 2.1 Hz, 1H). <sup>13</sup>C{<sup>1</sup>H} NMR (100 MHz, CDCl<sub>3</sub>): δ 136.7, 136.4, 133.5, 130.9, 130.7, 128.3, 128.0, 127.2, 126.6, 126.0, 125.4, 121.3, 120.0, 119.2, 111.3, 102.4. Note: two of the <sup>13</sup>C peaks for this compound appear to be coincidentally overlapping. HRMS electrospray (*m/z*): [M<sup>+</sup>] calcd for C<sub>18</sub>H<sub>13</sub>N, 243.1048; found, 243.1042.



**Product 42:** Benzofuran (118.1 mg, 1.0 mmol, 1.0 equiv), [Ph-I<sup>III</sup>-Ph]BF<sub>4</sub> (735.4 mg, 2.0 mmol, 2.0 equiv) and Pd(tfa)<sub>2</sub> (16.6 mg, 0.05 mmol, 0.05 equiv) were combined in AcOH (10 mL) then the vial was then sealed with a Teflon-lined cap, and heated to 100 °C for 12 hours. The reaction mixture was filtered through a plug of Celite and rinsed with CH<sub>2</sub>Cl<sub>2</sub>, and the solvent was then removed under vacuum. The residue was taken up in CH<sub>2</sub>Cl<sub>2</sub> and extracted with saturated aqueous NaHCO<sub>3</sub> (3 × 30 mL). The organic layer

was then dried over MgSO<sub>4</sub>, filtered, and concentrated onto silica gel for purification by column chromatography (125.3 mg, 65% yield, R<sub>f</sub> = 0.26 in 99% hexanes/1% CH<sub>2</sub>Cl<sub>2</sub>). <sup>1</sup>H NMR (CDCl<sub>3</sub>): δ 7.84 (d, *J* = 7.6, 2H), 7.56 (d, *J* = 7.6, 1H), 7.50 (d, *J* = 8 Hz, 1H), 7.43 (t, *J* = 7.6 Hz, 2H), 7.33 (t, *J* = 7.4 Hz, 1H), 7.29-7.18 (multiple peaks, 2H), 7.01 (s, 1H).



**Product 44:** Benzothiophene (134.2 mg, 1.0 mmol, 1.0 equiv), [Ph-I<sup>III</sup>-Ph]BF<sub>4</sub> (735.4 mg, 2.0 mmol, 2.0 equiv) and IMesPd(OAc)<sub>2</sub>•H<sub>2</sub>O (26.5 mg, 0.05 mmol, 0.05 equiv) were combined in nitrobenzene (10 mL) then the vial was then sealed with a Teflon-lined cap, and heated to 120 °C for 12 hours. The reaction mixture was filtered through a plug of Celite and rinsed with CH<sub>2</sub>Cl<sub>2</sub>, and the solvent was then removed under vacuum. The residue was concentrated onto silica gel for purification by column chromatography and found to be 95% pure by gas chromatography (100.7 mg, 65% yield, R<sub>f</sub> = 0.45 in 100% hexanes). <sup>1</sup>H NMR (CDCl<sub>3</sub>): δ 7.97-7.90 (multiple peaks, 2H), 7.62-7.59 (multiple peaks, 2H), 7.52-7.46 (multiple peaks, 2H), 7.46-7.38 (multiple peaks 4H). <sup>1</sup>H NMR (*d*<sub>6</sub>-acetone): δ 8.20-7.99 (multiplet, 1H), 7.90-7.96 (multiplet, 1H), 7.64-7.59 (multiple peaks, 3H) 7.51 (t, *J* = 7.6, 2H), 7.46-7.39 (multiple peaks, 3H). <sup>13</sup>C{<sup>1</sup>H} NMR (*d*<sub>6</sub>-acetone): δ 141.57, 138.65, 138.57, 136.70, 129.60, 129.34, 128.73, 125.33, 125.27, 124.61, 123.79, 123.45.

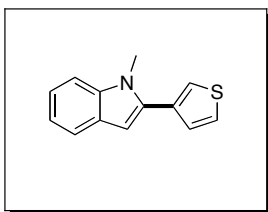
### ***In Situ* Oxidant Gereneration:**

**General Procedure for *in situ* Oxidant Generation for 1 and 26.** Pd(OAc)<sub>2</sub> (8.5 mg, 0.04 mmol, 0.05 equiv), ArI(OAc)<sub>2</sub> (1.52 mmol, 2 equiv) and ArB(OH)<sub>2</sub> (1.52 mmol, 2 equiv) were combined in AcOH (7.6 mL). The resulting mixture was stirred for 15 min at room temperature. 1-Methylindole (100 mg, 0.76 mmol, 1 equiv) was then added and the reaction was stirred for 12 h at room temperature. The reactions were worked up and

purified as described above for products **1** and **26** to afford the corresponding 2-arylindoles in 80% and 81% isolated yields, respectively.

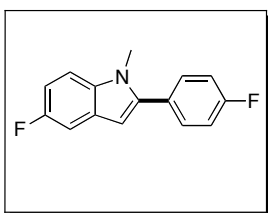
**General Procedure for *in situ* Oxidant Generation for **24**.** Pd(OAc)<sub>2</sub> (8.5 mg, 0.04 mmol, 0.05 equiv), *p*-ClC<sub>6</sub>H<sub>4</sub>I(OAc)<sub>2</sub> (1.09 g, 3.05 mmol, 4 equiv) and *p*-ClC<sub>6</sub>H<sub>4</sub>B(OH)<sub>2</sub> (477 mg, 3.05 mmol, 4 equiv) were combined in AcOH (7.6 mL). The resulting mixture was stirred for 15 min at room temperature. 1-Methylindole (100 mg, 0.76 mmol, 1 equiv) was then added and the reaction was stirred for 12 h at room temperature. The reaction was worked up and purified as described above for product **24**, to afford the corresponding product in 67% isolated yield.

**General Procedure for *in situ* Oxidant Generation with MesI(OAc)<sub>2</sub>.** Pd(OAc)<sub>2</sub> (1.7 mg, 0.008 mmol, 0.05 eq), MesI(OAc)<sub>2</sub> (114 mg, 0.31 mmol, 2.0 equiv) and ArB(OH)<sub>2</sub> (0.31 mmol, 2.0 equiv) were combined in AcOH (1.56 mL), and the resulting mixture was stirred for 15 min at room temperature. 1-Methylindole (20.5 mg, 0.16 mmol, 1 equiv) was then added and the reaction was stirred for 12 h at room temperature. The reactions were analyzed by GC, and yields were determined by integration relative to an internal standard. Products **1**, **24** and **26**, were obtained in 44%, 39% and 62% GC yields respectively.



**Product 39:** Iodomesitylene diacetate (728.4 mg, 2.0 mmol, 2.0 equiv), and 3-thiophene boronic acid (256.0 mg, 2.0 mmol, 2.0 equiv) were combined in AcOH (10 mL) and stirred for 15 minutes in a 20 mL scintillation vial. Then *N*-methylindole (131.2 mg, 1.0 mmol, 1.0 equiv) and Pd(OAc)<sub>2</sub> (11.2 mg, 0.05 mmol, 0.05 equiv) were added to the reaction mixture. The vial was then sealed with a Teflon-lined cap, and heated to 100 °C for 12 hours. The reaction mixture was filtered through a plug of Celite and rinsed with CH<sub>2</sub>Cl<sub>2</sub>, and the solvent was then removed under vacuum. The residue was taken up in

CH<sub>2</sub>Cl<sub>2</sub> and extracted with saturated aqueous NaHCO<sub>3</sub> (3 × 30 mL). The organic layer was then dried over MgSO<sub>4</sub>, filtered, and concentrated onto silica gel for purification by column chromatography (43.9 mg, 20% yield, R<sub>f</sub> = 0.13 in 100% hexanes. <sup>1</sup>H NMR (CDCl<sub>3</sub>): δ 7.67 (d, *J* = 6.4 Hz, 1H), 7.46 (dd, *J* = 4.0, 2.0 Hz, 1H), 7.43 (dd, *J* = 2.0, 1.0 Hz, 1H), 7.39 (d, *J* = 6.4 Hz, 1H), 7.33 (dd, *J* = 4.0, 1.0 Hz, 1H), 7.28 (td, *J* = 6.0, 1Hz, 1H), 7.19 (t, *J* = 6.4 Hz, 1H), 6.64 (s, 1H), 3.82 (s, 3H). <sup>13</sup>C{<sup>1</sup>H} NMR (CDCl<sub>3</sub>): δ 138.04, 136.33, 133.33, 128.41, 127.75, 125.82, 123.16, 121.64, 120.37, 119.81, 109.42, 101.40.



**Product 58:** 5-fluoroindole (75.0 mg, 0.56 mmol, 1.0 equiv) and Pd(OAc)<sub>2</sub> (6.3 mg, 0.028 mmol, 0.05 equiv) were dissolved in AcOH (10 mL), and the resulting solution was stirred at 25 °C for ~5 min. [(*p*-FC<sub>6</sub>H<sub>4</sub>)<sub>2</sub>I]BF<sub>4</sub> (448.3 mg, 1.11 mmol, 2.0 equiv) was added, and the reaction was stirred for 15 h at 25 °C. The reaction mixture was filtered through a plug of Celite and then evaporated to dryness. The resulting oil was dissolved in CH<sub>2</sub>Cl<sub>2</sub> (50 mL) and extracted with aqueous NaHCO<sub>3</sub> (2 x 30 mL). The organic layer was dried with MgSO<sub>4</sub>, concentrated, and the product was purified by chromatography on silica gel (R<sub>f</sub> = 0.15 in 96% hexanes/4% EtOAc). The product was obtained as white solid (51.7 mg, 40% yield). δ <sup>1</sup>H NMR (400 MHz, CD<sub>3</sub>CO<sub>2</sub>D): δ 7.90 (dd, *J* = 8.4, 5.2 Hz, 2H), 7.34 (dd, *J* = 8.8, 4.4 Hz, 1H), 7.26-7.12 (multiple peaks, 3H), 6.89 (dt, *J* = 9.2, 2.4, 1H), 6.76 (s, 1H). The resonance at 6.76 ppm for the C3 H disappears over time due to H/D exchange with the solvent. <sup>19</sup>F NMR (376 MHz, CD<sub>3</sub>CO<sub>2</sub>D): δ -115.60 (multiplet, 1F), -125.92 (multiplet, 1F)



## 4.12 References

1. Joucla, L.; Djakovitch, L. *Adv. Synth. Catal.* **2009**, *351*, 673-714.
2. Alberico, D.; Scott, M. E.; Lautens, M. *Chem. Rev.* **2007**, *107*, 174-238.
3. Lane, B. S.; Sames, D. *Org. Lett.* **2004**, *6*, 2897-2900.
4. Lane, B. S.; Brown, M. A.; Sames, D. *J. Am. Chem. Soc.* **2005**, *127*, 8050-8057.
5. Bellina, F.; Cauteruccio, S.; Rossi, R. *Eur. J. Org. Chem.* **2006**, 1379-1382.
6. Bayler, A.; Canty, A. J.; Ryan, J. H.; Skelton, B. W.; White, A. H. *Inorg. Chem. Commun.* **2000**, *3*, 575-578.
7. Canty, A. J.; Rodemann, T. *Inorg. Chem. Commun.* **2003**, *6*, 1382-1384.
8. Canty, A. J.; Patel, J.; Rodemann, T.; Ryan, J. H.; Skelton, B. W.; White, A. H. *Organometallics* **2004**, *23*, 3466-3473.
9. Canty, A. J.; Rodemann, T.; Skelton, B. W.; White, A. H. *Inorg. Chem. Commun.* **2005**, *8*, 55-57.
10. Canty, A. J.; Rodemann, T.; Skelton, B. W.; White, A. H. *Organometallics* **2006**, *25*, 3996-4001.
11. Chaudhuri, P. D.; Guo, R.; Malinakova, H. C. *J. Organomet. Chem.* **2008**, *693*, 567-573.
12. Lagunas, M.-C.; Gossage, R. A.; Spek, A. L.; van Koten, G. *Organometallics* **1998**, *17*, 731-741.
13. Dick, A. R.; Kampf, J. W.; Sanford, M. S. *J. Am. Chem. Soc.* **2005**, *127*, 12790-12791.
14. Whitfield, S. R.; Sanford, M. S. *J. Am. Chem. Soc.* **2007**, *129*, 15142-15143.
15. Racowski, J. M.; Dick, A. R.; Sanford, M. S. *J. Am. Chem. Soc.* **2009**, *131*, 10974-10983.
16. Deprez, N. R.; Sanford, M. S. *Inorg. Chem.* **2007**, *46*, 1924-1935.
17. Deprez, N. R.; Sanford, M. S. *J. Am. Chem. Soc.* **2009**, *131*, 11234-11241.
18. Kalyani, D.; Deprez, N. R.; Desai, L. V.; Sanford, M. S. *J. Am. Chem. Soc.* **2005**, *127*, 7330-7331.
19. Yang, S.-D.; Sun, C.-L.; Fang, Z.; Li, B.-J.; Li, Y.-Z.; Shi, Z.-J. *Angew. Chem., Int. Ed.* **2008**, *47*, 1473-1476.

20. Kashulin, I. A.; Nifant'ev, I. E. *J. Org. Chem.* **2004**, *69*, 5476-5479.
21. Yang, F.; Wu, Y.; Li, Y.; Wang, B.; Zhang, J. *Tetrahedron* **2009**, *65*, 914-919.
22. Weiss, R.; Seubert, J. *Angew. Chem., Int. Ed. Engl.* **1994**, *33*, 891-893.
23. Zhdankin, V. V.; Kuposov, A. Y.; Yashin, N. V. *Tetrahedron Lett.* **2002**, *43*, 5735-5737.
24. Ochiai, M.; Suefuji, T.; Miyamoto, K.; Shiro, M. *Chem. Commun.* **2003**, 1438-1439.
25. Suefuji, T.; Shiro, M.; Yamaguchi, K.; Ochiai, M. *Heterocycles* **2006**, *67*, 391-397.
26. Yoneyama, T.; Crabtree, R. H. *J. Mol. Catal. A: Chem.* **1996**, *108*, 35-40.
27. Campeau, L.-C.; Thansandote, P.; Fagnou, K. *Org. Lett.* **2005**, *7*, 1857-1860.
28. Singh, R.; Viciu, M. S.; Kramareva, N.; Navarro, O.; Nolan, S. P. *Org. Lett.* **2005**, *7*, 1829-1832.
29. Konnick, M. M.; Guzei, I. A.; Stahl, S. S. *J. Am. Chem. Soc.* **2004**, *126*, 10212-10213.
30. Jensen, D. R.; Sigman, M. S. *Org. Lett.* **2003**, *5*, 63-65.
31. Jensen, D. R.; Schultz, M. J.; Mueller, J. A.; Sigman, M. S. *Angew. Chem., Int. Ed.* **2003**, *42*, 3810-3813.
32. Viciu, M. S.; Stevens, E. D.; Petersen, J. L.; Nolan, S. P. *Organometallics* **2004**, *23*, 3752-3755.
33. Phipps, R. J.; Grimster, N. P.; Gaunt, M. J. *J. Am. Chem. Soc.* **2008**, *130*, 8172-8174.
34. Stuart, D. R.; Fagnou, K. *Science* **2007**, *316*, 1172-1175.
35. Stuart, D. R.; Villemure, E.; Fagnou, K. *J. Am. Chem. Soc.* **2007**, *129*, 12072-12073.
36. Dwight, T. A.; Rue, N. R.; Charyk, D.; Josselyn, R.; DeBoef, B. *Org. Lett.* **2007**, *9*, 3137-3139.
37. Lebrasseur, N.; Larrosa, I. *J. Am. Chem. Soc.* **2008**, *130*, 2926-2927.
38. Wolfe, J. P.; Tomori, H.; Sadighi, J. P.; Yin, J.; Buchwald, S. L. *J. Org. Chem.* **2000**, *65*, 1158-1174.
39. McKillop, A.; Kemp, D. *Tetrahedron* **1989**, *45*, 3299-3306.

40. Chen, D.-W.; Ochiai, M. *J. Org. Chem.* **1999**, *64*, 6804-6814.
41. Shah, A.; Pike, V. W.; Widdowson, D. A. *J. Chem. Soc., Perkin Trans. 1* **1997**, 2463-2465.

## Chapter 5

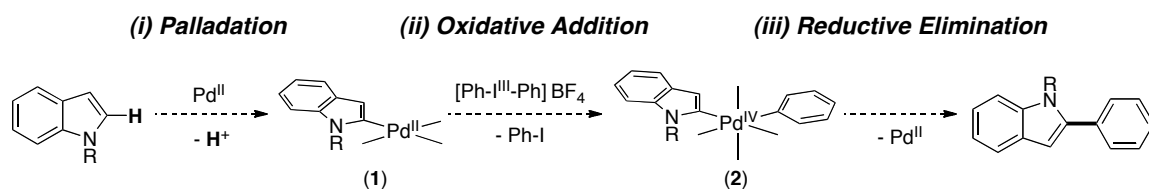
### Initial Mechanistic Investigations of Palladium-Catalyzed C–H Arylation of Indole

#### 5.1 Background and Significance

After exploring the scope of palladium-catalyzed indole C–H arylation (*Chapter 4*), we next sought to investigate the mechanism of the reaction for two purposes. First, a mechanistic understanding could allow us to achieve a number of goals for indole arylation. These include: (1) understanding the differences between catalysts, (2) resolving mass balance issues, (3) employing other  $I^{III}$  reagents, (4) improving the *in situ* oxidant generation, and (5) achieving lower catalyst loadings. Second, insight gained from understanding the mechanism of indole arylation may lead to more efficient C–H arylation reactions of simple unactivated arenes such as naphthalene.

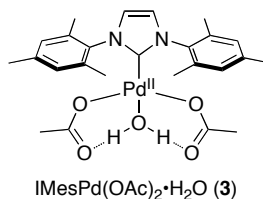
We initially proposed a  $Pd^{II/IV}$  mechanism for this arylation reaction (**Scheme 5.1**) by analogy to mechanistic studies performed by Sames' with a similar transformation proceeding through a  $Pd^{0/II}$  catalytic cycle (*Chapter 4*).<sup>1</sup> The proposed mechanism consists of the following: (i) palladation of the indole at  $Pd^{II}$  resulting in intermediate **1**, (ii) oxidation of the electron rich  $\sigma$ -indole- $Pd^{II}$  species **1** by  $[Ph-I^{III}-Ph]BF_4$  to afford  $Pd^{IV}$  intermediate **2**, and (iii) C–C bond forming reductive elimination to generate the C2 phenylated product and release  $Pd^{II}$ .

**Scheme 5.1:** Proposed Mechanism of Non-Directed Arylation with  $[\text{Ph-I}^{\text{III}}-\text{Ph}]\text{BF}_4$ .



We now sought to obtain evidence in support of the proposed  $\text{Pd}^{\text{II/IV}}$  mechanism, by conducting several key kinetic experiments including reaction order studies, Hammett studies, and kinetic isotope effect studies. As described in *Chapter 4*, a dramatic difference in product yield and mass balance was observed between the two catalysts  $\text{Pd}(\text{OAc})_2$  and  $\text{IMesPd}(\text{OAc})_2 \cdot \text{H}_2\text{O}$  (**3**, IMes = 1,3-Bis(2,4,6-trimethylphenyl)imidazole). For this reason we undertook these kinetic experiments with both catalysts using  $^{19}\text{F}$  NMR spectroscopy to monitor the reactions.

**Figure 5.1:**  $\text{IMesPd}(\text{OAc})_2 \cdot \text{H}_2\text{O}$  Catalyst.



## 5.2 Development of Collection Method

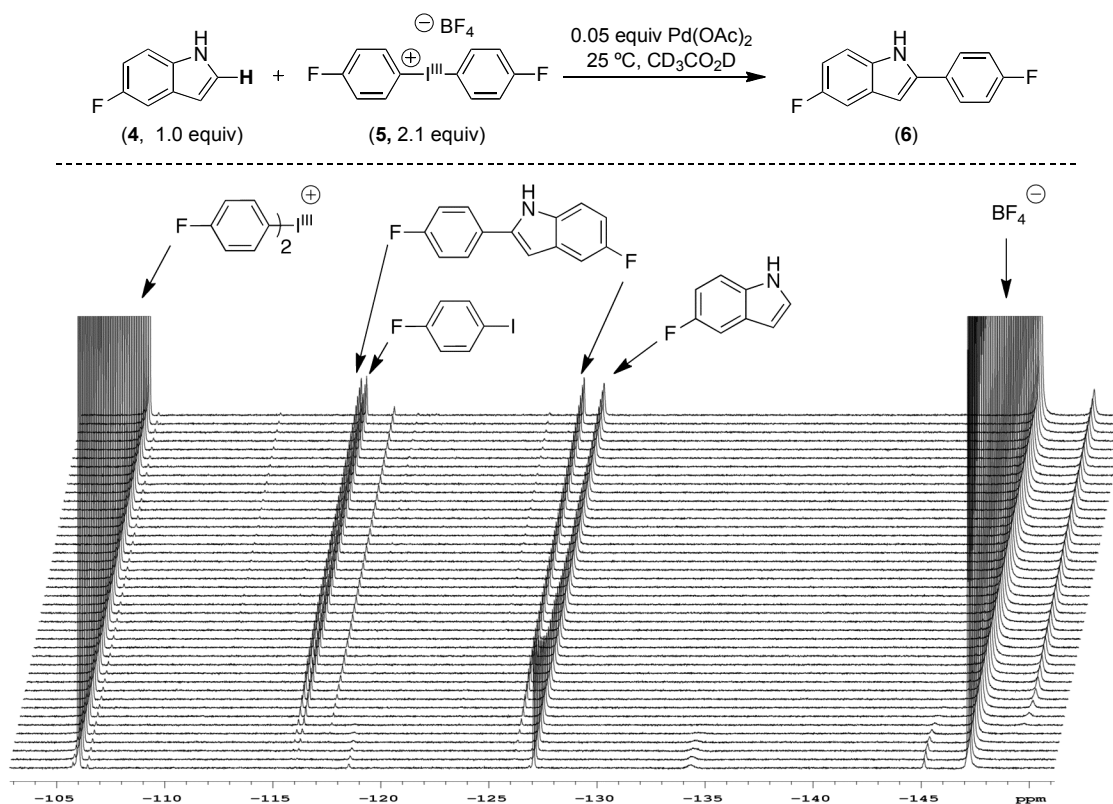
Investigations to probe the mechanism of this reaction focused on exploring kinetics using the method of initial rates. We wanted to choose an analysis strategy that would enable us to compare several catalysts and probe the origin of the dramatic catalyst effects. Due to the fast reaction rate observed with  $\text{Pd}(\text{OAc})_2$ , gas chromatography was avoided because of difficulty obtaining the necessary time points in a short time period (<2 min). For example, the phenylation of *N*-methylindole proceeded to 49% yield in 5 min at rt with  $\text{Pd}(\text{OAc})_2$  (note – cooling not possible due to solvent).  $^1\text{H}$ -NMR analysis also proved to be challenging due to overlapping resonances of the starting material and product. We circumvented these challenges by instead placing fluorine substituents on

both starting material and product and monitoring the reaction progress by  $^{19}\text{F}$  NMR spectroscopy (**Figure 5.2**).

$\text{Pd}(\text{OAc})_2$  was initially examined as a catalyst for two reasons. First,  $\text{IMesPd}(\text{OAc})_2\cdot\text{H}_2\text{O}$  (**3**) is a more precious catalyst and thus is undesirable to use for exploratory chemistry. Second, the reaction rate is faster with this  $\text{Pd}(\text{OAc})_2$ , so optimizing this method would ensure the ability to compare with the slower  $\text{IMesPd}(\text{OAc})_2\cdot\text{H}_2\text{O}$  reactions.

The reaction of 1 equiv of 5-fluoroindole **4** with 2.1 equiv of  $[(p\text{-FC}_6\text{H}_4)_2\text{-I}^{\text{III}}]\text{BF}_4$  (**5**) and 5 mol % of  $\text{Pd}(\text{OAc})_2$  in  $\text{CD}_3\text{CO}_2\text{D}$  was followed by  $^{19}\text{F}$  NMR spectroscopy, and an arrayed series of spectra is displayed in **Figure 5.2**. During data collection the relaxation delay was set to 1 s. The number of transients per spectrum was 8, and each spectrum represents one data point. Additionally, there was no delay between collections of each spectrum. In these spectra, disappearance of the indole starting material ( $\delta = -126.8$  ppm) and oxidant ( $\delta = -105.8, -147.0$  ppm) can be observed. Also, the appearance of phenylated product ( $\delta = -114.8, -115.5$  ppm), and the  $p\text{-FC}_6\text{H}_4\text{I}$  reaction byproduct ( $\delta = -115.8$  ppm) can be monitored. Additional resonances were also observed at  $-117.2$  and  $-149.6$  ppm, that are as of yet unidentified.

**Figure 5.2:** Arrayed  $^{19}\text{F}$  NMR Spectra of Indole Arylation.



This strategy allows for the determination of reaction rate based on both starting material disappearance and product appearance. Plotting the relative integration of product ( $-125.5$  ppm) versus time (s) reveals the presence of an induction period (**Figure 5.3**). A plot of relative integration of starting material ( $-126.8$  ppm) versus time (s) showed a similar induction period (**Figure 5.4**). Typically, an induction period signifies the conversion of a pre-catalyst to an active catalyst prior to the reaction that generates the desired product.

**Figure 5.3:** Induction Period Based on Product Appearance.

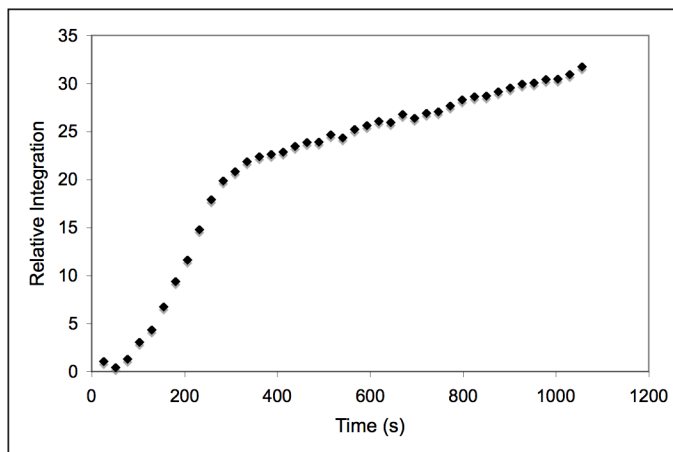
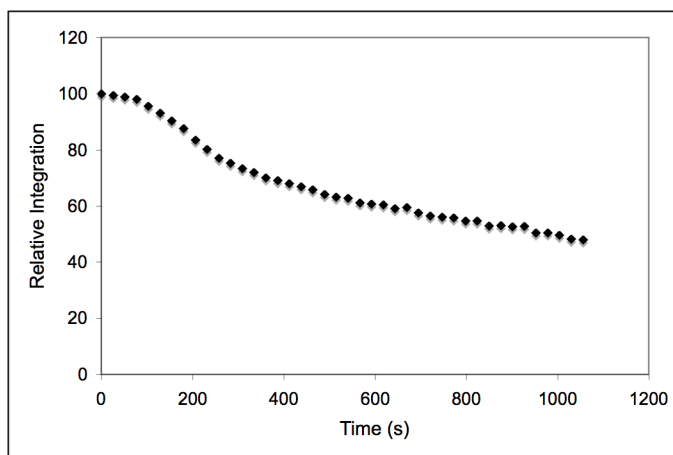


**Figure 5.4:** Induction Period Based on Starting Material Disappearance.



This presented a challenge for determining the initial reaction rates, and unless the induction period can be avoided, such analysis is not possible. To eliminate the induction period a method must be developed to form the active catalyst prior to initiating the desired reaction. It was reasoned that initial addition of a 0.1 equiv of a sacrificial substrate and 0.1 equiv of catalyst with excess oxidant in solution would allow for the formation of the active catalyst (**Scheme 5.2**). This was done by combining 0.1 equiv of *N*-methylindole **7** with 2.1 equiv of  $[(p\text{-FC}_6\text{H}_4)_2\text{-I}^{\text{III}}]\text{BF}_4$  and 0.1 equiv of  $\text{Pd}(\text{OAc})_2$  in  $\text{CD}_3\text{CO}_2\text{D}$  in an NMR tube and agitating the tube for 2 min. The length of the induction period (2 min in this example) was determined by following the reaction without the



sacrificial indole, and this was the method for determining the induction period in all future examples. Next, a solution containing 5-fluoroindole (**4**, 1.0 equiv) was added to the NMR tube, and data acquisition commenced. During data collection the relaxation delay was set to 1 s. The number of transients per spectrum was 8, and each spectrum represents one data point. Additionally, there was no delay between collections of each spectrum. A plot of the relative integration of product versus time (s) revealed that the induction period had been eliminated (**Figure 5.5**). This was corroborated by analysis of the relative integration of starting material versus time (**Figure 5.6**).

**Scheme 5.2:** Strategy for Eliminating the Induction Period Using a Sacrificial Substrate.

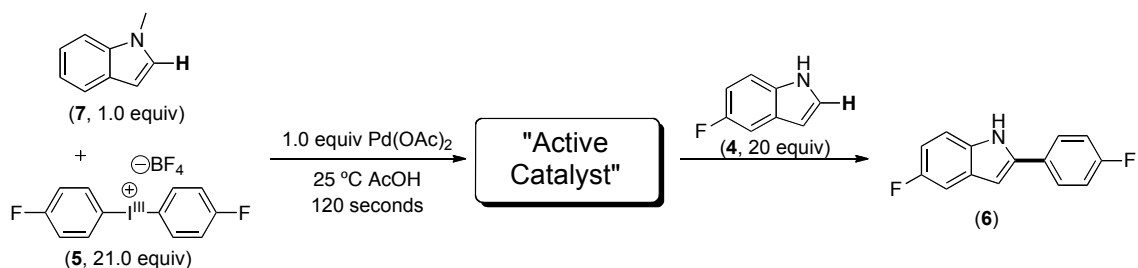


**Figure 5.5:** Product Appearance After Eliminating the Induction Period.

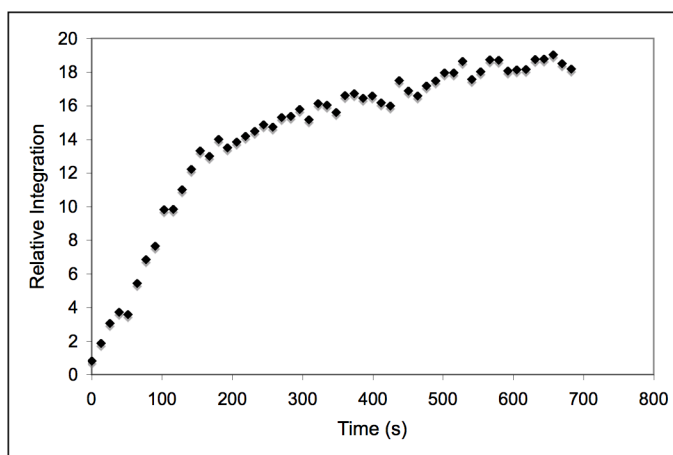
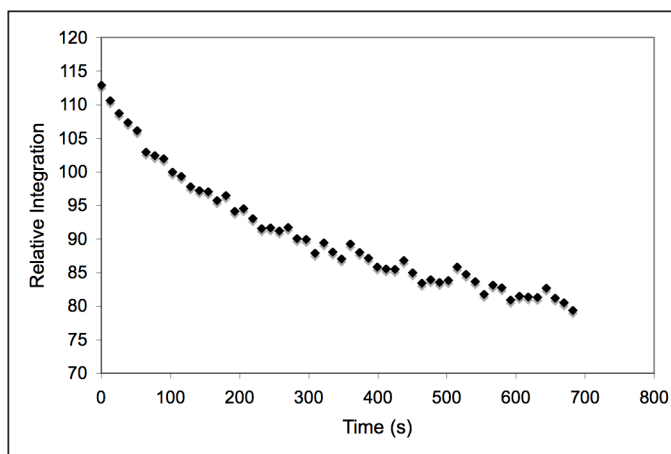


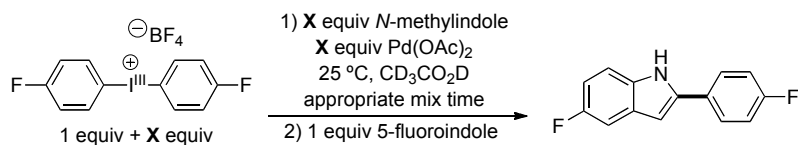
**Figure 5.6:** Starting Material Disappearance After Eliminating the Induction Period.



### 5.3 Mechanistic Investigations with Pd(OAc)<sub>2</sub>

With a method developed for determining initial rates by <sup>19</sup>F NMR spectroscopy, the reaction order in [Pd<sup>II</sup>] was determined. This was accomplished by obtaining the initial reaction rate at several different [Pd<sup>II</sup>] under conditions where the induction period was eliminated. In these reactions, solutions with varying concentrations of Pd(OAc)<sub>2</sub> (0.025–0.10 equiv) were combined with *N*-methyl indole **7** (0.025–0.10 equiv) and [(*p*-FPh)<sub>2</sub>-I<sup>III</sup>]BF<sub>4</sub> (1.025–1.10 equiv) in CD<sub>3</sub>CO<sub>2</sub>D. These solutions were allowed to mix in an NMR tube for the predetermined induction period for that [Pd<sup>II</sup>]. Next, a solution of 5-fluoroindole (**4**, 1.0 equiv) was added to the NMR tube and acquisition of the arrayed spectra was initiated. For data collection, the relaxation delay was set to 1 s. The number of transients per spectrum was 8, and each spectrum represents one data point. Also, there was no delay between collections of each spectrum. For reproducibility, this procedure was completed three times at each [Pd<sup>II</sup>]. The relative initial rate of product appearance and of starting material disappearance, as well as the mixing time (induction period) for each [Pd<sup>II</sup>] are shown in **Table 5.1**. A plot of the initial rate of product appearance versus [Pd<sup>II</sup>] showed a linear relationship suggesting a first order dependence (**Figure 5.7**). This conclusion is also supported by the linearity of the plot of starting material disappearance versus [Pd<sup>II</sup>] (**Figure 5.8**).

**Table 5.1:** Kinetic Order in Pd(OAc)<sub>2</sub>.



X = [Pd <sup>II</sup> ] (M)	Relative Rate (Product)	Relative Rate (Starting Material)	Mix time (s)
1.0 × 10 <sup>-3</sup>	1 ± 0.07	1 ± 0.1	60
2.1 × 10 <sup>-3</sup>	1.8 ± 0.2	2.5 ± 0.7	210
3.2 × 10 <sup>-3</sup>	2.9 ± 0.5	4.2 ± 0.5	3600
4.2 × 10 <sup>-3</sup>	3.1 ± 0.8	6 ± 2	6000

**Figure 5.7:** Kinetic Order in Pd(OAc)<sub>2</sub> Based on Product Appearance.

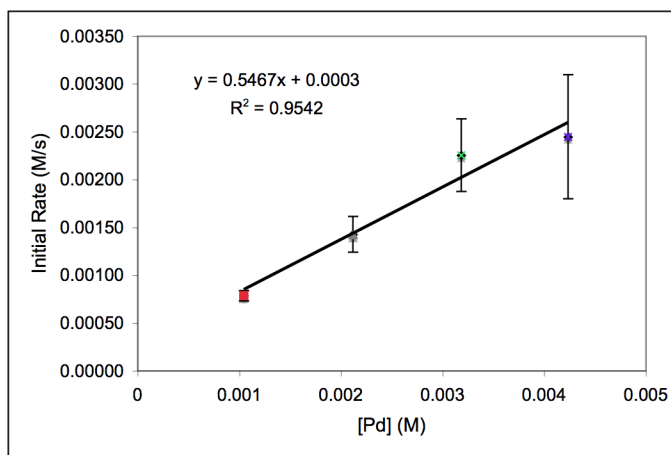
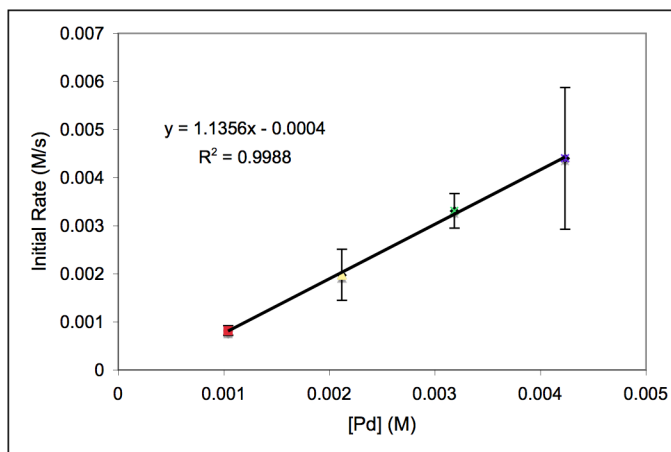


**Figure 5.8:** Kinetic Order in Pd(OAc)<sub>2</sub> Based on Starting Material Disappearance.



From the observed 1<sup>st</sup> order dependence on [Pd<sup>II</sup>], we can conclude that the catalyst is involved at or before the rate-limiting step of the reaction. Notably, this is somewhat different than the directed C–H arylation where a second order dependence on catalyst was observed.<sup>2</sup> It was also found that the induction period was dependant upon the [Pd<sup>II</sup>].

However, it was expected that relative initial rate for the appearance of product and the disappearance of starting material would be the same. Clearly this is not the case, which may indicate this is not an accurate representation of the kinetics. A first possible explanation for the discrepancy in initial rates is that the relaxation delay for the acquisition is too short (1 s), and there is no delay between spectra, not allowing for the nuclei to completely relax and leading to inaccurate integrations. Unfortunately, since the reaction rates are very fast, increasing the relaxation delay is problematic because it also increases the length of time to acquire each spectrum and limits the number of data points that can be taken. This same problem is encountered if the delay between acquiring spectra is increased. To test this hypothesis, an array should be collected where a single transient represents each data point with a long relaxation delay (~10 s) between each acquisition. The second possible explanation is that the unidentified peaks (–117.1 and –149.6 ppm) result from the formation of a byproduct, however, analyzing the integration of these peaks did not completely account for the observed discrepancy.

Next, the order in substrate **4** using was probed using Pd(OAc)<sub>2</sub> as the catalyst. The same method for the determination of the catalyst order with Pd(OAc)<sub>2</sub> was employed by combining *N*-methylindole **7** (0.05 equiv) with Pd(OAc)<sub>2</sub> (0.05 equiv) and [(*p*-FPh)<sub>2</sub>-I<sup>III</sup>]<sub>2</sub>BF<sub>4</sub> (**5**, 1.05 equiv) in CD<sub>3</sub>CO<sub>2</sub>D and agitating in an NMR tube for 6 min. After this time, a solution of 5-fluoroindole (**4**, 0.25–1.0 equiv) was added to this solution and acquisition of the array was begun (**Table 5.2**). During data collection the relaxation delay was set to 1 s. The number of transients per spectrum was 8, and each spectrum represents one data point. Additionally, there was no delay between collections of each spectrum. Additionally, there was no delay between collections of each spectrum. Several pieces of information can be drawn from this data. First, it was determined that the induction period is independent of substrate concentration. Second, a plot of the initial

rate based on product appearance versus time show a non-linear relationship (**Figure 5.9**). A plot of initial rate of starting material disappearance versus time is also not linear (**Figure 5.10**). Third, Preliminary analysis suggests that when  $[5] > [4]$  the reaction is zero order in substrate, and when  $[5] < [4]$  the reaction is first order or greater in substrate, with the change in order occurring near  $[5] = [4]$ . However, more data is necessary to support this assertion. Fourth, the relative reaction rate based on product appearance and starting material disappearances again do not agree.

**Table 5.2:** Order in Substrate **4** with  $\text{Pd}(\text{OAc})_2$ .

[X] (M)	Relative Rate (Product)	Relative Rate (Starting Material)
$2.1 \times 10^{-2}$	$1.1 \pm 0.1$	$1.3 \pm 0.2$
$3.1 \times 10^{-2}$	$1.0 \pm 0.1$	$1.2 \pm 0.3$
$4.2 \times 10^{-2}$	$1.00 \pm 0.09$	$1.1 \pm 0.1$
$6.2 \times 10^{-2}$	$1.2 \pm 0.2$	$2.1 \pm 0.5$
$8.3 \times 10^{-2}$	$2.2 \pm 0.3$	$5 \pm 1$

**Figure 5.9:** Order in **4** with  $\text{Pd}(\text{OAc})_2$  based on Product Appearance.

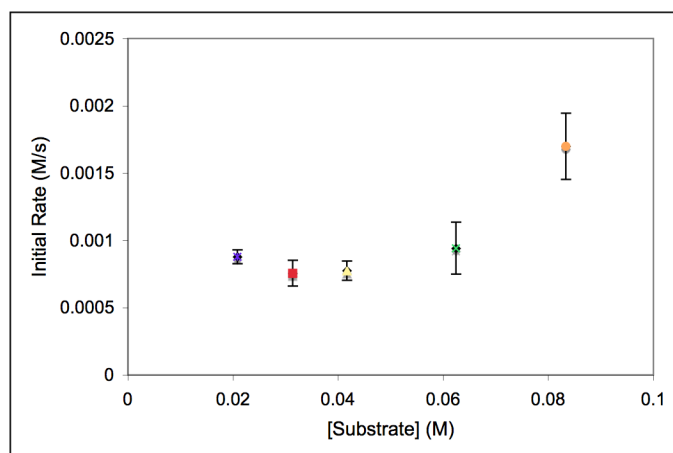
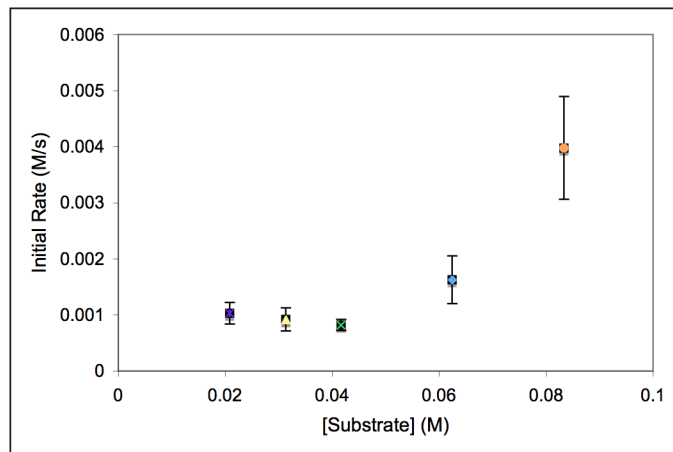


**Figure 5.10:** Order in **4** with Pd(OAc)<sub>2</sub> based on Starting Material Disappearance.



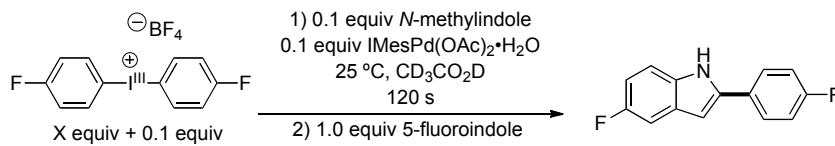
Due to the apparent change in order when  $[5] = [4]$  we next investigated whether the substrate and the oxidant are interacting. It is known that basic functional groups can coordinate to  $I^{III}$  reagents, and it was reasoned that this may lead to inhibition by substrate, similar to what has been observed in related systems.<sup>2</sup> To study this 1 equiv of 5-fluoroindole was combined with 0, 1, and 2 equiv of  $[(p\text{-FC}_6\text{H}_4)_2\text{-I}^{III}]\text{BF}_4$  in  $\text{CD}_3\text{CO}_2\text{D}$  and the resulting solutions were analyzed by  $^1\text{H}$  and  $^{19}\text{F}$  NMR spectroscopy. No change in any chemical shifts was observed, suggesting that there is not an interaction between the substrate and the oxidant.

Finally, the reaction order in oxidant with Pd(OAc)<sub>2</sub> as the catalyst has not yet been determined. These studies should include the determination of oxidant order where  $[5] > [4]$  and  $[5] < [4]$ . These conditions should be chosen due to the apparent change in substrate order discussed above, which may indicate a change in rate-limiting step or mechanism. For this same reason, catalyst order studies also need to be repeated where  $[5] > [4]$  and  $[5] < [4]$  since the initial studies were completed under conditions where the substrate order changes from zero to higher order ( $[5] = [4]$ ).

## 5.4 Mechanistic Investigations with IMesPd(OAc)<sub>2</sub>•H<sub>2</sub>O

Due to the challenges associated with mass balance and the unclear kinetic results with Pd(OAc)<sub>2</sub>, we also investigated the mechanism with IMesPd(OAc)<sub>2</sub>•H<sub>2</sub>O as the catalyst. Preliminary kinetic studies employing IMesPd(OAc)<sub>2</sub>•H<sub>2</sub>O focused on determining the order in oxidant. As was previously described with Pd(OAc)<sub>2</sub>, an induction period was observed, prompting the use of a sacrificial indole to eliminate the induction period. These experiments were completed by combining *N*-methylindole (7, 0.10 equiv) with IMesPd(OAc)<sub>2</sub>•H<sub>2</sub>O (3, 0.1 equiv) and [(*p*-FC<sub>6</sub>H<sub>4</sub>)<sub>2</sub>-I<sup>III</sup>]BF<sub>4</sub> (5, 1.1–3.1 equiv) in CD<sub>3</sub>CO<sub>2</sub>D. The solutions were agitated in an NMR tube for 2 min. Then a solution of 5-fluoroindole (1.0 equiv) was added and data acquisition was begun (Table 5.3). During data collection the relaxation delay was set to 1 s. The number of transients per spectrum was 16, and each spectrum represents one data point. Additionally, there was no delay between collections of each spectrum. A plot of the initial rate of product appearance versus time resulted in a linear relationship, and suggests a first order dependence on [I<sup>III</sup>] (Figure 5.11). Furthermore, a linear relationship was also observed upon plotting the initial rate of starting material disappearance versus time, corroborating this first order dependence on [I<sup>III</sup>] (Figure 5.12). Additionally, it was found that the induction period was independent of [I<sup>III</sup>]. Determination of kinetic order in both catalyst and substrate under these conditions have not been completed, but are necessary for a more thorough analysis.

**Table 5.3:** Order in Oxidant with IMesPd(OAc)<sub>2</sub>•H<sub>2</sub>O.



[X] (M)	Relative Rate (Product)	Relative Rate (Starting Material)
4.2 x 10 <sup>-2</sup>	1.0 ± 0.4	1.4 ± 0.5
6.2 x 10 <sup>-2</sup>	1.75 ± 0.01	2.4 ± 0.2
8.4 x 10 <sup>-2</sup>	2.6 ± 0.2	3.6 ± 0.2
10.4 x 10 <sup>-2</sup>	3.3 ± 0.3	3.6 ± 0.3

**Figure 5.11:** Oxidant Order with  $\text{IMesPd}(\text{OAc})_2 \cdot \text{H}_2\text{O}$  based on Product Appearance.

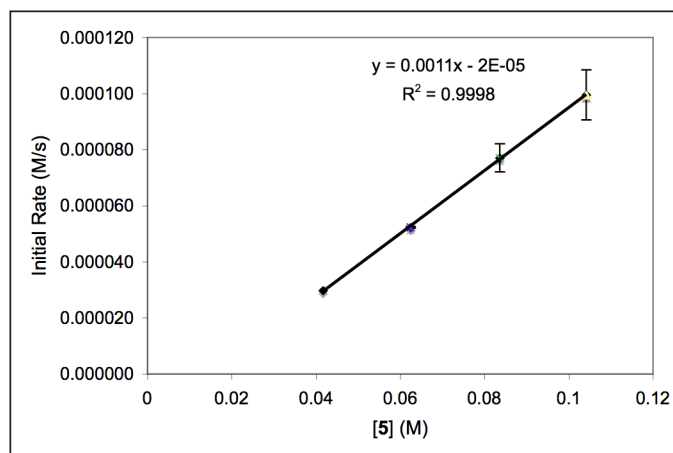
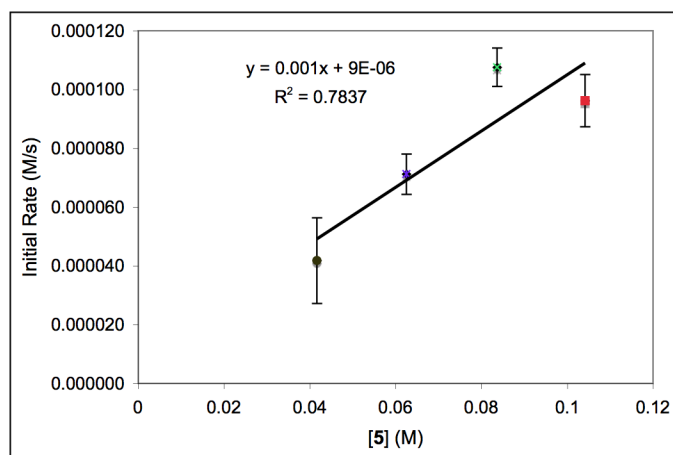


**Figure 5.12:** Oxidant order with  $\text{Pd}(\text{OAc})_2$  based on Starting Material Disappearance.



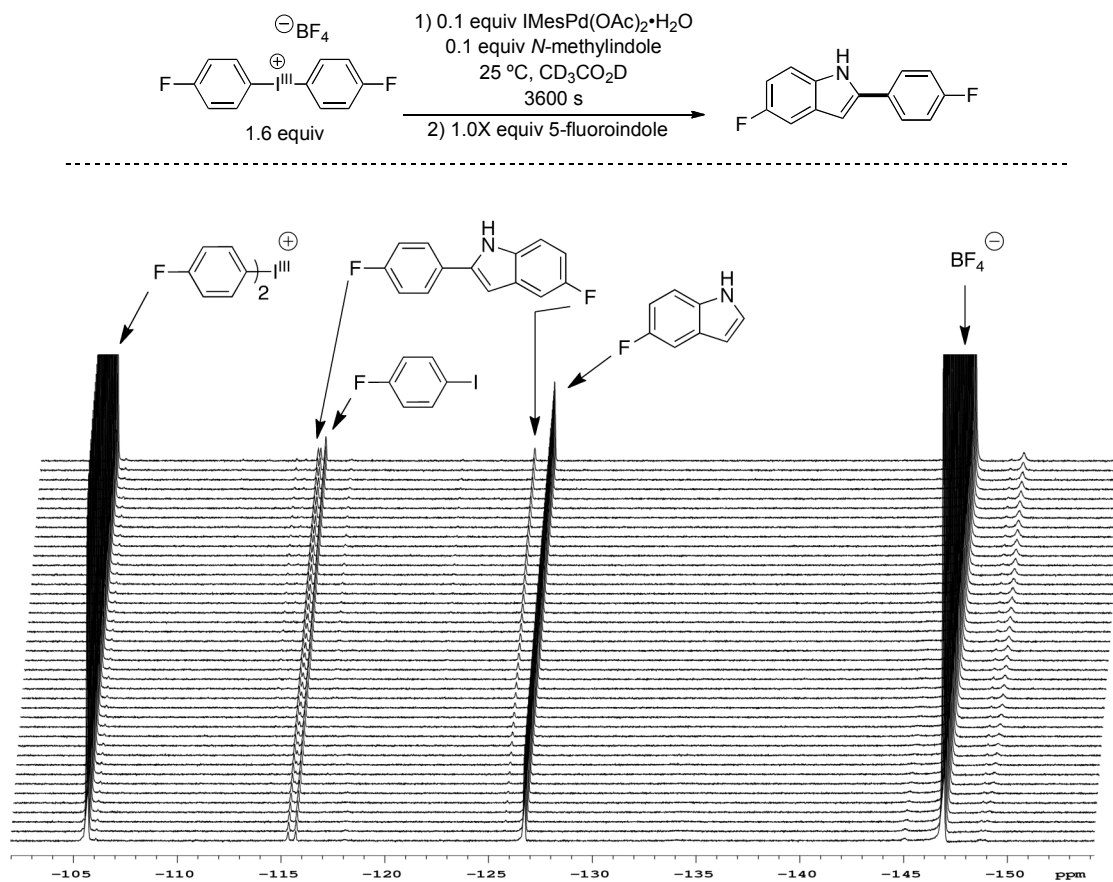
## 5.5 Comparison of $\text{Pd}(\text{OAc})_2$ and $\text{IMesPd}(\text{OAc})_2 \cdot \text{H}_2\text{O}$

Several tentative conclusions can be made based upon the data with  $\text{Pd}(\text{OAc})_2$  and  $\text{IMesPd}(\text{OAc})_2 \cdot \text{H}_2\text{O}$ . A first order dependence on oxidant suggests that it is involved at or before the rate-limiting step of the reaction. Next, preliminary qualitative experiments have suggested that  $\text{Pd}(\text{OAc})_2$  catalyzes arylation at faster rate than  $\text{IMesPd}(\text{OAc})_2 \cdot \text{H}_2\text{O}$ , which was confirmed by these kinetic results. The initial rate of arylation with 5-fluoroindole (1 equiv) with  $[(p\text{-FPh})_2\text{I}]\text{BF}_4$  (1 equiv) and 10 mol % of  $[\text{Pd}^{\text{II}}]$  is eight times faster with  $\text{Pd}(\text{OAc})_2$  than  $\text{IMesPd}(\text{OAc})_2 \cdot \text{H}_2\text{O}$ . Furthermore, using  $\text{IMesPd}(\text{OAc})_2 \cdot \text{H}_2\text{O}$ ,



the discrepancy between product appearance and starting material difference is negligible. This difference between catalysts may be related to the unidentified resonance at  $-117.2$  ppm observed with  $\text{Pd}(\text{OAc})_2$ , but not with  $\text{IMesPd}(\text{OAc})_2 \cdot \text{H}_2\text{O}$ . Notably however, the unidentified resonance at  $-149.6$  ppm also appeared with both catalysts (Figure 5.13 compared to Figure 5.2).

**Figure 5.13:** Example  $^{19}\text{F}$  NMR Spectra of Indole Arylation Kinetics with  $\text{IMesPd}(\text{OAc})_2 \cdot \text{H}_2\text{O}$ .



Finally, it is important to note that the length of the induction period using  $\text{IMesPd}(\text{OAc})_2 \cdot \text{H}_2\text{O}$  differed between batches of the catalyst synthesized. The kinetic data described above was obtained using cleanly isolated  $\text{IMesPd}(\text{OAc})_2 \cdot \text{H}_2\text{O}$ . Employing catalyst that contained unidentified impurities, did not provided the product within the same time period as clean  $\text{IMesPd}(\text{OAc})_2 \cdot \text{H}_2\text{O}$  (<45 min). It was found that the impure catalyst does provided product after 3 h. This was determined by periodically

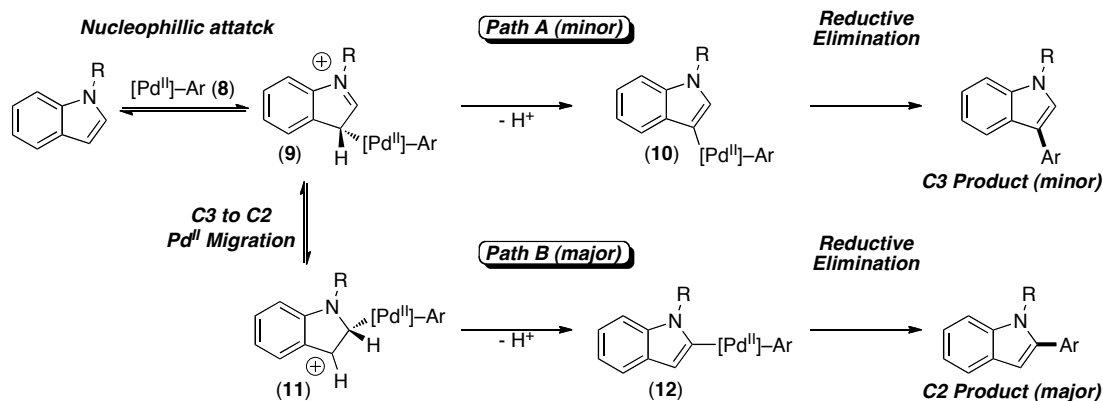
analyzing these reactions by  $^{19}\text{F}$  NMR spectroscopy. This indicated that these catalysts are viable, but displays a long induction period. This is possibly due to difficulty in attaining clean catalyst required for reliable kinetics and highlights the necessity for a more reproducible catalyst synthesis.

## 5.6 Possible Mechanisms for Indole Arylation

A general mechanism involving a  $\text{Pd}^{\text{II/IV}}$  catalytic cycle was proposed in **Scheme 5.1**. However, the details of the palladation step of this reaction remain unclear. Three detailed mechanisms for this transformation can be envisioned that would proceed through a  $\text{Pd}^{\text{II/IV}}$  catalytic cycle.<sup>3</sup> These include (1) nucleophilic palladation at the C3 position of the indole followed by migration to C2, (2) direct palladation of the indole C2 position, and (3) an olefin insertion mechanism.

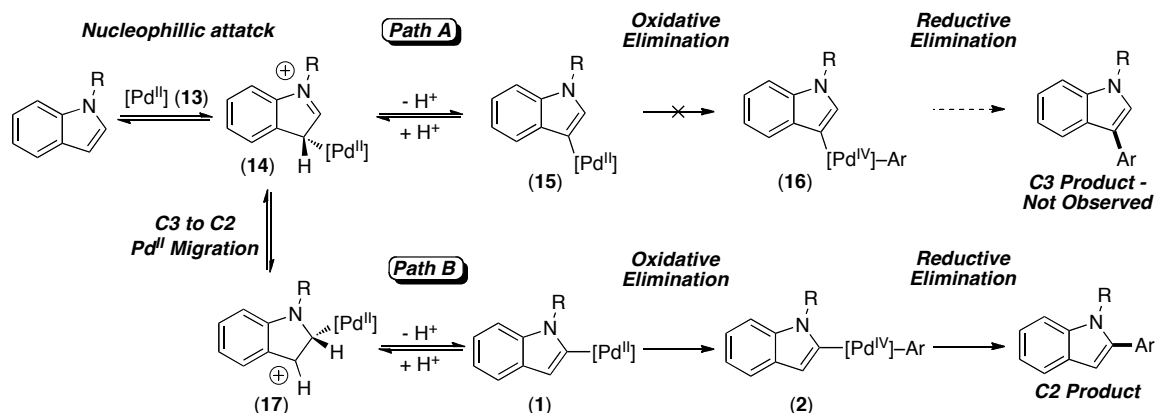
The first pathway would involve a similar mechanism to Sames'  $\text{Pd}^{0/\text{II}}$  transformation, as summarized in **Scheme 5.3**.<sup>1,4,5</sup> He provided evidence that his reaction proceeds through initial oxidative addition of  $\text{Pd}^0$  to an Ar-I to afford **8**, then nucleophilic attack of the Ar-Pd<sup>II</sup> by the indole to yield the proposed intermediate **9**. This Ar-Pd<sup>II</sup>-indole intermediate **9** can rearomatize to generate intermediate **10**, followed by direct reductive elimination to afford the C3 arylation product (Path A). Alternatively, the palladium in intermediate **9** can migrate from C3 to C2 to yield intermediate **11**. Rearomatization to the  $\sigma$ -indole-Pd<sup>II</sup> intermediate **12**, and final reductive elimination leads to the C2 arylation product (Path B). Migration to the C2 position is thermodynamically favorable due to inductive stabilization provided by the adjacent heteroatom. Notably, the authors reasoned that the decreased selectivity when employing ortho substituted aryl iodides was due a decreased rate of C3 to C2 palladium migration leading to competitive formation of C3 arylation products.

**Scheme 5.3:** Proposed Palladation Mechanism for a Pd<sup>0/II</sup> C–H Arylation.



With this precedent, a mechanism involving a similar pathway can be proposed for a transformation involving a Pd<sup>II/IV</sup> catalytic cycle (**Scheme 5.4**, Path B). The palladation mechanism would initiate by nucleophilic attack of the indole on the [Pd<sup>II</sup>] (**13**) to yield intermediate **14**. Next, the Pd<sup>II</sup> in intermediate **14** migrates from the C3 to the C2 position to afford intermediate **17** (Path B). This intermediate can then undergo rearomatization to afford the C2 indole-Pd<sup>II</sup> (**1**). Oxidative addition by [Ar-I<sup>III</sup>-Ar]BF<sub>4</sub> affords the Ar-Pd<sup>IV</sup>-indole species **2**, and final reductive elimination results in the C2 arylation product. Notably, a C3 arylation mechanism can be proposed proceeding through Path A, however these products are not observed under our reaction conditions.

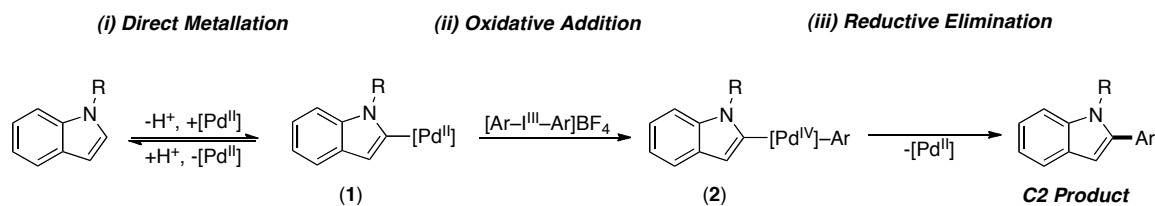
**Scheme 5.4:** Proposed Palladation Mechanism for a Pd<sup>II/IV</sup> C–H Arylation.



There are several key differences in this Pd<sup>II/IV</sup> and Sames Pd<sup>0/II</sup> mechanism. First, [Pd<sup>II</sup>] (13) does not have an aryl ligand and is more electrophilic, as compared to the Ar–Pd<sup>II</sup> (8) in the Pd<sup>II/0</sup> mechanism. Second, slow oxidative addition of [Ar–I<sup>III</sup>–Ar]BF<sub>4</sub> allows for equilibration of Pd<sup>II</sup> from intermediate 14 to the more thermodynamically favored C2 palladation intermediate (17). This agrees with the observed selectivity for exclusively C2 arylation products, which differs significantly from that observed by Sames. Additionally, cursory evidence for this is given by the low yielding, yet productive reaction with a 2-substituted indole in which intermediate 1 cannot be attained due to the substitution.

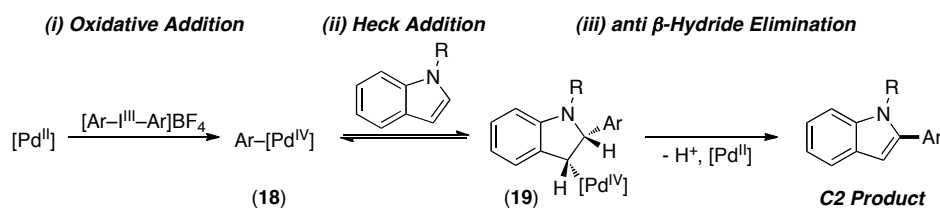
The second possible mechanism involves direct palladation of the C2 position of the indole (Scheme 5.5).<sup>3</sup> This mechanism proceeds through (i) direct metallation to give intermediate 1, via either nucleophilic attack on Pd<sup>II</sup> at the C2 position or through a  $\sigma$  bond metathesis mechanism; (ii) oxidative addition of the Pd<sup>II</sup> to [Ar–I<sup>III</sup>–Ar]BF<sub>4</sub> to afford the Ar–Pd<sup>IV</sup> intermediate 2; and (iii) reductive elimination results in the observed C2 arylated product. It has been well documented that substitution by electrophiles at the C3 position of an indole is strongly favored over the C2 position.<sup>6</sup> Direct palladation at the C2 position of indoles has been observed previously, however this required the presence of strong a directing group that is not present in this chemistry.<sup>7,8</sup> Thus it seems unlikely that in the absence of a directing group palladation at the C2 position would occur through nucleophilic attack. However, a direct  $\sigma$  bond metathesis mechanism to yield intermediate 1 cannot be ruled out.

**Scheme 5.5:** Pd<sup>II/IV</sup> Direct C2 Metallation Mechanism for Arylation.



Finally, arylation through an olefin insertion mechanism can also be envisioned (**Scheme 5.6**).<sup>3</sup> This would proceed through (i) initial oxidative addition of Pd<sup>II</sup> to yield a Ar-Pd<sup>IV</sup> **18**, (ii) syn addition of Ar-Pd<sup>IV</sup> to the indole to afford intermediate **19**, and (iii) anti  $\beta$ -hydride elimination to give the C2 arylated product. Notably this mechanism requires an unprecedented olefin insertion into an Ar-Pd<sup>IV</sup> bond, followed by an unusual anti  $\beta$ -hydride elimination.<sup>9-11</sup> Additionally, oxidative addition occurs at an electron poor Pd(OAc)<sub>2</sub>, rather than the more electron rich indole  $\sigma$ -indole-Pd<sup>II</sup> as proposed in the alternative mechanisms (**1**).

**Scheme 5.6:** Pd<sup>II/IV</sup> Olefin Insertion Mechanism for Arylation.

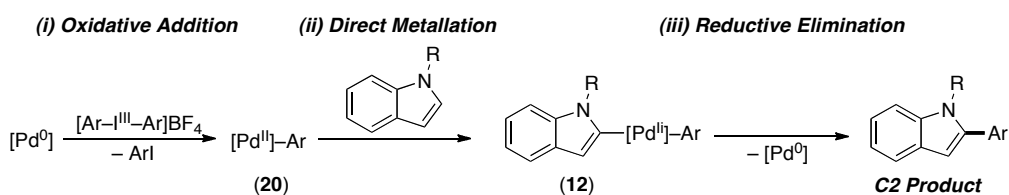


Considering these mechanisms, a Pd<sup>II/IV</sup> pathway involving C3 palladation followed by migration to C2 is most plausible based on Sames work. The latter two mechanisms are less likely due to the lack of precedent for the individual steps. It is also necessary to consider Pd<sup>0/II</sup> mechanisms since coupling reactions employing this reaction manifold with diaryl iodonium salts are known.<sup>12</sup> There are three Pd<sup>0/II</sup> mechanisms to be considered that are similar to the Pd<sup>II/IV</sup> pathways discussed above. All would require

initial reduction of Pd<sup>II</sup> to Pd<sup>0</sup>. First is the Pd<sup>0/II</sup> mechanism involving a Pd<sup>II</sup> C3 to C2 migration analogous to Sames mechanism in **Scheme 5.2**.

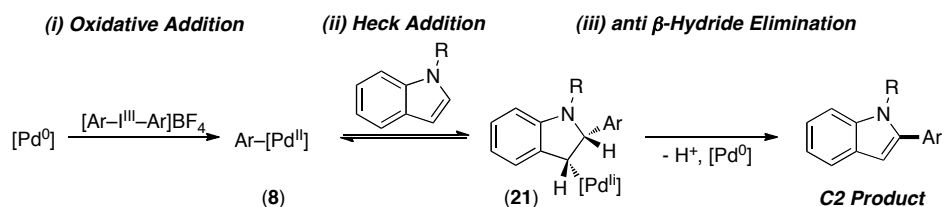
The second possible Pd<sup>0/II</sup> mechanism is a direct C2 metallation (**Scheme 5.7**). This mechanism occurs via (i) oxidative addition of Pd<sup>0</sup> to [Ar-I<sup>III</sup>-Ar]BF<sub>4</sub> to give Ar-[Pd<sup>II</sup>] (**20**), (ii) direct C2 metallation of indole by this intermediate to provide **12**, and (iii) reductive elimination to afford the C2 arylated product and Pd<sup>0</sup>. The mechanism of metallation may proceed via direct C2 palladation or  $\sigma$ -bond metathesis as discussed in the context of the Pd<sup>II/IV</sup> catalytic cycle involving direct metallation.

**Scheme 5.7:** Pd<sup>0/II</sup> Direct C2 Metallation Mechanism for Arylation.



The third possibility is a Pd<sup>0/II</sup> olefin insertion mechanism (**Scheme 5.8**). This mechanism involves (i) oxidative addition of Pd<sup>0</sup> to [Ar-I<sup>III</sup>-Ar]BF<sub>4</sub> to afford **8**, followed by (ii) insertion of Ar-[Pd<sup>II</sup>] into the olefin of indole to provide **21**, and lastly (iii)  $\beta$ -hydride elimination to afford the C2 arylation product. As previously discussed for the Pd<sup>II/IV</sup> olefin insertion mechanism (**Scheme 5.6**), this mechanism also involves an unusual anti  $\beta$ -hydride elimination.

**Scheme 5.8:** Pd<sup>0/II</sup> Olefin Insertion Mechanism for Arylation.



Each of these Pd<sup>0/II</sup> pathways are unlikely based on the observed tolerance of aryl halides, which are known to be reactive toward the low valent palladium required for

these mechanism. Nevertheless, they warrant consideration, and the experiments discussed for exploration of the directed chemistry (*Chapter 3*, section 5.2) would be useful. These include the Hg drop test to test for palladium nano particles, as well as substitution of the diaryliodonium oxidant with Ph-I and Ph-OTf to determine if these are viable electrophiles for this transformation. Finally, radical pathways cannot be ruled out without conducting these reactions in the presence of free radical inhibitors.

## 5.7 Conclusions

In summary, attempts have been made to obtain mechanistic information about the palladium-catalyzed C-H arylation of indoles. A method to obtain kinetic data has been developed employing fluorine labeled starting materials and oxidants. This labeling allows for the reaction to be monitored by  $^{19}\text{F}$  NMR spectroscopy. There is an induction period observed in these reactions, which is likely associated with the formation of an active intermediate. This induction period can be eliminated with the addition of a sacrificial substrate. Using this approach, we examined the catalyst order and substrate order when employing  $\text{Pd}(\text{OAc})_2$  as the catalyst. We also explored the oxidant order with  $\text{IMesPd}(\text{OAc})_2 \cdot \text{H}_2\text{O}$ . The results from these studies are preliminary and can lead to no final conclusion about the details of this mechanism, but present a method to further study this reaction.

## 5.8 General Procedures and Materials and Methods

**General Procedures:** NMR spectra were obtained on a Varian Inova 400 (399.96 MHz for  $^1\text{H}$ , 376 MHz for  $^{19}\text{F}$ ) spectrometer.  $^1\text{H}$ -NMR chemical shifts are reported in parts per million (ppm) relative to TMS, with the residual solvent peak used as an internal reference.

**Materials and Methods:** Substrates **4**, **7** and palladium sources were obtained commercially and were used as received. Diaryliodonium salt  $[(p\text{-FC}_6\text{H}_4)_2\text{-I}]\text{BF}_4$  were prepared by (i) conversion of the aryl iodide to the corresponding diacetoxyiodoarene<sup>13</sup> and (ii) reaction of  $p\text{-FC}_6\text{H}_4\text{I}(\text{OAc})_2$  with  $p\text{-FC}_6\text{H}_4\text{B}(\text{OH})_2$  in the presence of  $\text{BF}_3 \cdot \text{OEt}_2$ .<sup>14</sup>

Catalysts were synthesized as outline in Chapter 4. Solvents were obtained from Cambridge Isotopes and used without further purification.

**Order in [Pd] with Pd(OAc)<sub>2</sub>:** [(*p*-FC<sub>6</sub>H<sub>4</sub>)<sub>2</sub>-I<sup>III</sup>]<sub>2</sub>BF<sub>4</sub> (0.02563–0.02754 mmol, 1.025–1.10 equiv) was diluted in a 0.2 mL stock solution of CD<sub>3</sub>CO<sub>2</sub>D containing Pd(OAc)<sub>2</sub> (0.000625–0.00254 mmol, 0.025–0.10 equiv). This was combined with 0.2 mL of a stock solution of *N*-methyl indole **7** (0.000625–0.00254 mmol, 0.025–0.10 equiv) and 10 μL of trifluorotoluene was added as an internal standard. This solution transferred to the NMR tube via pipette was then mixed by rotating the NMR tube for the appropriate time based on the length of the induction period time. Finally 0.2 mL of a stock solution of 5-fluoroindole (0.025 mmol, 1 equiv) was added to the NMR tube. The tube was then placed in the NMR spectrometer, which has already been shimmed to a blank sample, and acquisition of the <sup>19</sup>F NMR array was begun. During data collection the relaxation delay was set to 1 s. The number of transients per spectrum was 8, and each spectrum represents one data point. Additionally, there was no delay between collections of each spectrum. The initial rate (M/s) for each data point was determined based on the initial concentration of 5-fluoroindole and normalized based on the internal standard. Each data point was repeated three times and the rate was taken as the average of those two points with the error being the standard deviation.

**Table 5.4:** Rate Data for [Pd] Order Study with Pd(OAc)<sub>2</sub>.

[Pd <sup>II</sup> ] (M)	rate (M/s) (Product)	rate (M/s) (Starting Material)	Mix time (s)
1.0 × 10 <sup>-3</sup>	7.9 ± 0.5 × 10 <sup>-4</sup>	7.9 ± 0.5 × 10 <sup>-4</sup>	60
2.1 × 10 <sup>-3</sup>	14 ± 2 × 10 <sup>-4</sup>	20 ± 5 × 10 <sup>-4</sup>	210
3.2 × 10 <sup>-3</sup>	23 ± 4 × 10 <sup>-4</sup>	33 ± 4 × 10 <sup>-4</sup>	3600
4.2 × 10 <sup>-3</sup>	24 ± 6 × 10 <sup>-4</sup>	44 ± 1 × 10 <sup>-4</sup>	6000

**Order in Substrate with Pd(OAc)<sub>2</sub>:** [(*p*-FPh)<sub>2</sub>-I<sup>III</sup>]<sub>2</sub>BF<sub>4</sub> (0.0263 mmol, 1.05 equiv) was diluted in 0.2 mL of a stock solution of CD<sub>3</sub>CO<sub>2</sub>D containing Pd(OAc)<sub>2</sub> (0.00127 mmol, 0.05 equiv). This was combined with 0.2 mL of a stock solution of *N*-methyl indole (0.00126 mmol, 0.05 equiv) and 10 μL of trifluorotoluene was added as an internal standard. This solution transferred to the NMR tube via pipette was then mixed by



rotating the NMR tube for the appropriate time based on the length of the induction period time. Finally 0.2 mL of a stock solution containing varying equivalents of 5-fluoroindole (0.0125–0.05 mmol, 0.5–2 equiv) was added to the NMR tube. The tube was then placed in the NMR spectrometer, which has already been shimmed to a blank sample, and acquisition of the  $^{19}\text{F}$  NMR array was begun. During data collection the relaxation delay was set to 1 s. The number of transients per spectrum was 8, and each spectrum represents one data point. Additionally, there was no delay between collections of each spectrum. The initial rate (M/s) for each data point was determined based on the initial concentration of 5-fluoroindole and normalized based on the internal standard. Each data point was repeated two times and the rate was taken as the average of those two points with the error being the standard deviation.

**Table 5.5:** Rate Data for Substrate Order Study with  $\text{Pd}(\text{OAc})_2$ .

[4] (M)	rate (M/s) (Product)	rate (M/s) (Starting Material)
$2.1 \times 10^{-2}$	$8.8 \pm 0.5 \times 10^{-4}$	$10 \pm 2 \times 10^{-4}$
$3.1 \times 10^{-2}$	$7 \pm 1 \times 10^{-4}$	$9 \pm 2 \times 10^{-4}$
$4.2 \times 10^{-2}$	$7.7 \pm 0.7 \times 10^{-4}$	$8 \pm 1 \times 10^{-4}$
$6.2 \times 10^{-2}$	$9 \pm 2 \times 10^{-4}$	$16 \pm 4 \times 10^{-4}$
$8.3 \times 10^{-2}$	$17 \pm 3 \times 10^{-4}$	$40 \pm 9 \times 10^{-4}$

**Order in Oxidant with  $\text{IMesPd}(\text{OAc})_2 \cdot \text{H}_2\text{O}$ :** Varying amounts of  $[(p\text{-FC}_6\text{H}_4)_2\text{-I}^{\text{III}}]\text{BF}_4$  (0.041–0.0775 mmol, 1.1–3.1 equiv) were diluted in 0.2 mL of a stock solution of  $\text{CD}_3\text{CO}_2\text{D}$  containing  $\text{IMesPd}(\text{OAc})_2 \cdot \text{H}_2\text{O}$  (0.0025 mmol, 0.1 equiv). This was combined with 0.2 mL of a stock solution of *N*-methyl indole (0.0025 mmol, 0.1 equiv). This solution transferred to the NMR tube via pipette was then mixed by rotating the NMR tube for the appropriate time based on the length of the induction period time. Finally 0.2 mL of a stock solution of 5-fluoroindole (0.025 mmol, 1 equiv) was added to the NMR tube. The tube was then placed in the NMR spectrometer, which has already been shimmed to a blank sample, and acquisition of the  $^{19}\text{F}$  NMR array was begun. During data collection the relaxation delay was set to 1 s. The number of transients per spectrum was 16, and each spectrum represents one data point. Additionally, there was no delay between collections of each spectrum. The initial rate (M/s) for each data point was determined based on the initial concentration of 5-fluoroindole; in this case no internal

standard was employed. Each data point was repeated twice and the rate was taken as the average of those two points with the error being the standard deviation.

**Table 5.6:** Rate Data for Oxidant Order Study with IMesPd(OAc)<sub>2</sub>•H<sub>2</sub>O.

[5] (M)	Rate (M/s) (Product)	Rate (M/s) (Starting Material)
4.2 x 10 <sup>-2</sup>	3 ± 2 x 10 <sup>-5</sup>	4 ± 2 x 10 <sup>-5</sup>
6.2 x 10 <sup>-2</sup>	5.23 ± 0.03 x 10 <sup>-5</sup>	7.1 ± 0.7 x 10 <sup>-5</sup>
8.4 x 10 <sup>-2</sup>	7.7 ± 0.5 x 10 <sup>-5</sup>	10.8 ± 0.7 x 10 <sup>-5</sup>
10.4 x 10 <sup>-2</sup>	10.0 ± 0.9 x 10 <sup>-5</sup>	9.6 ± 0.9 x 10 <sup>-5</sup>

## 5.9 References

1. Lane, B. S.; Brown, M. A.; Sames, D. *J. Am. Chem. Soc.* **2005**, *127*, 8050-8057.
2. Deprez, N. R.; Sanford, M. S. *J. Am. Chem. Soc.* **2009**, *131*, 11234-11241.
3. Alberico, D.; Scott, M. E.; Lautens, M. *Chem. Rev.* **2007**, *107*, 174-238.
4. Lane, B. S.; Sames, D. *Org. Lett.* **2004**, *6*, 2897-2900.
5. Bellina, F.; Cauteruccio, S.; Rossi, R. *Eur. J. Org. Chem.* **2006**, 1379-1382.
6. Jackson, A. H.; Lynch, P. P. *J. Chem. Soc., Perkin Trans. 2* **1987**, 1215-1219.
7. Tollari, S.; Demartin, F.; Cenini, S.; Palmisano, G.; Raimondi, P. *J. Organomet. Chem.* **1997**, *527*, 93-102.
8. Nonoyama, M.; Nakajima, K. *Polyhedron* **1998**, *18*, 533-543.
9. Glover, B.; Harvey, K. A.; Liu, B.; Sharp, M. J.; Tymoschenko, M. F. *Org. Lett.* **2003**, *5*, 301-304.
10. Ikeda, M.; El Bialy, S. A. A.; Yakura, T. *Heterocycles* **1999**, *51*, 1957-1970.
11. Lautens, M.; Fang, Y.-Q. *Org. Lett.* **2003**, *5*, 3679-3682.
12. Deprez, N. R.; Sanford, M. S. *Inorg. Chem.* **2007**, *46*, 1924-1935.
13. McKillop, A.; Kemp, D. *Tetrahedron* **1989**, *45*, 3299-3306.
14. Chen, D.-W.; Ochiai, M. *J. Org. Chem.* **1999**, *64*, 6804-6814.